Theory overview of forward physics at the LHC and EIC

Kazuhiro Watanabe
(Tohoku Univ, JP)

Go-Forward 2025@Nagasaki, JP, 02/27/2025

TOHOKU UNIVERSITY

Outline

1. Background
2. High-energy QCD
3. CGC EFT
4. Phenomenology

This talk

A. Diffraction and UPC
B. TMD and CGC
C. Other Cold Nuclear Effects
D. CGC calculations at NLO
E. Introduction to EIC physics

Appendices, input for discussion

Our goal

❖ What is the origin of this universe?

- ❑ Extreme matter in the early universe
- ❑ "Big-bang" at labs (LHC, RHIC)

❖ What is the origin of cosmic rays?

- ❑ High-energy cosmic neutrinos (messengers)
- ❑ Air-shower (IceCube), Accelerators (LHCf, FASER)

❖ What are the building blocks of visible matter?

- ❑ Strong interaction and confinement
- ❑ Femtoscopes (EIC, JLab, COMPASS)

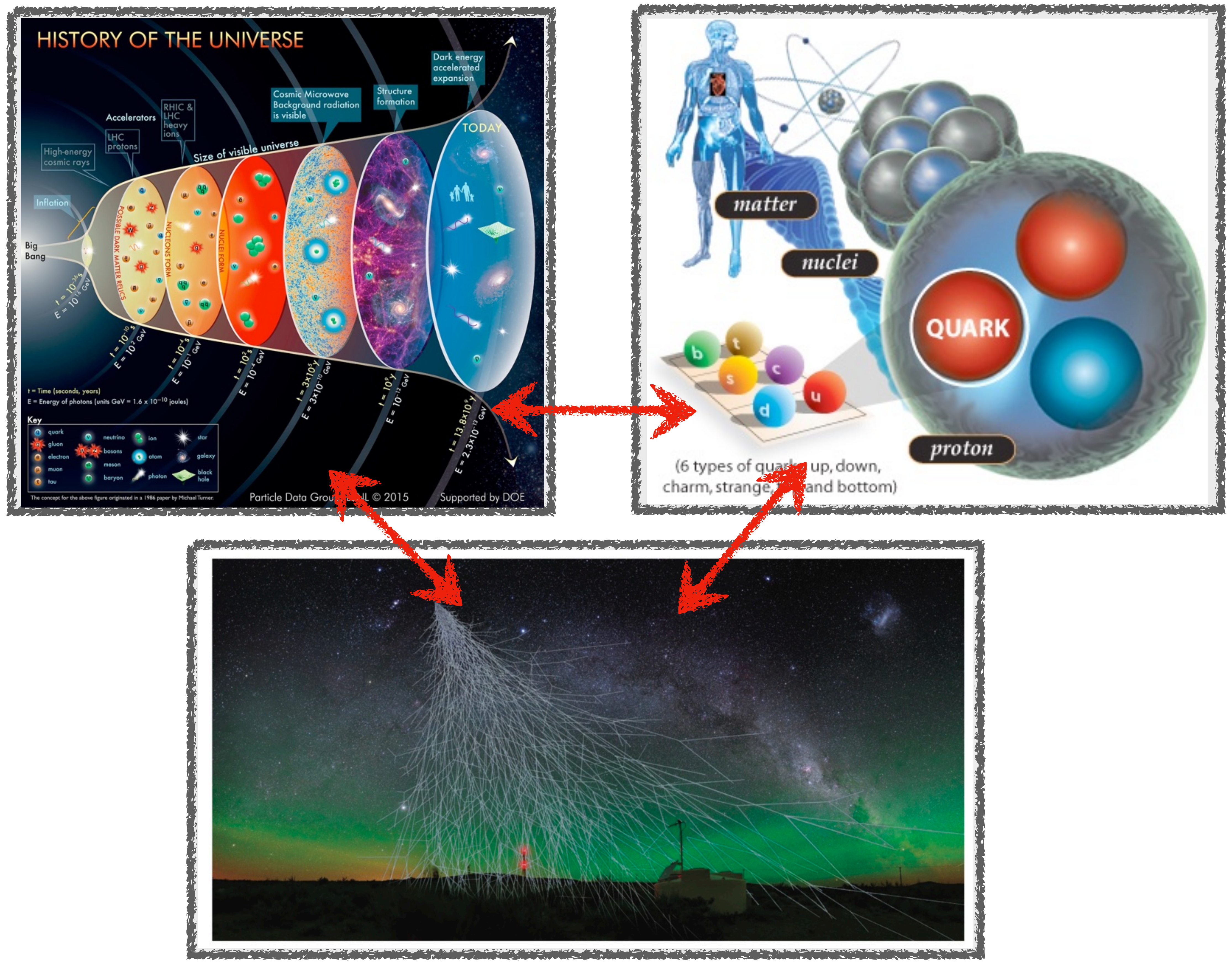

→ Need to study high and low-energy (also hard and soft) QCD extensively.

Part I:
Background

From LHC-CMS

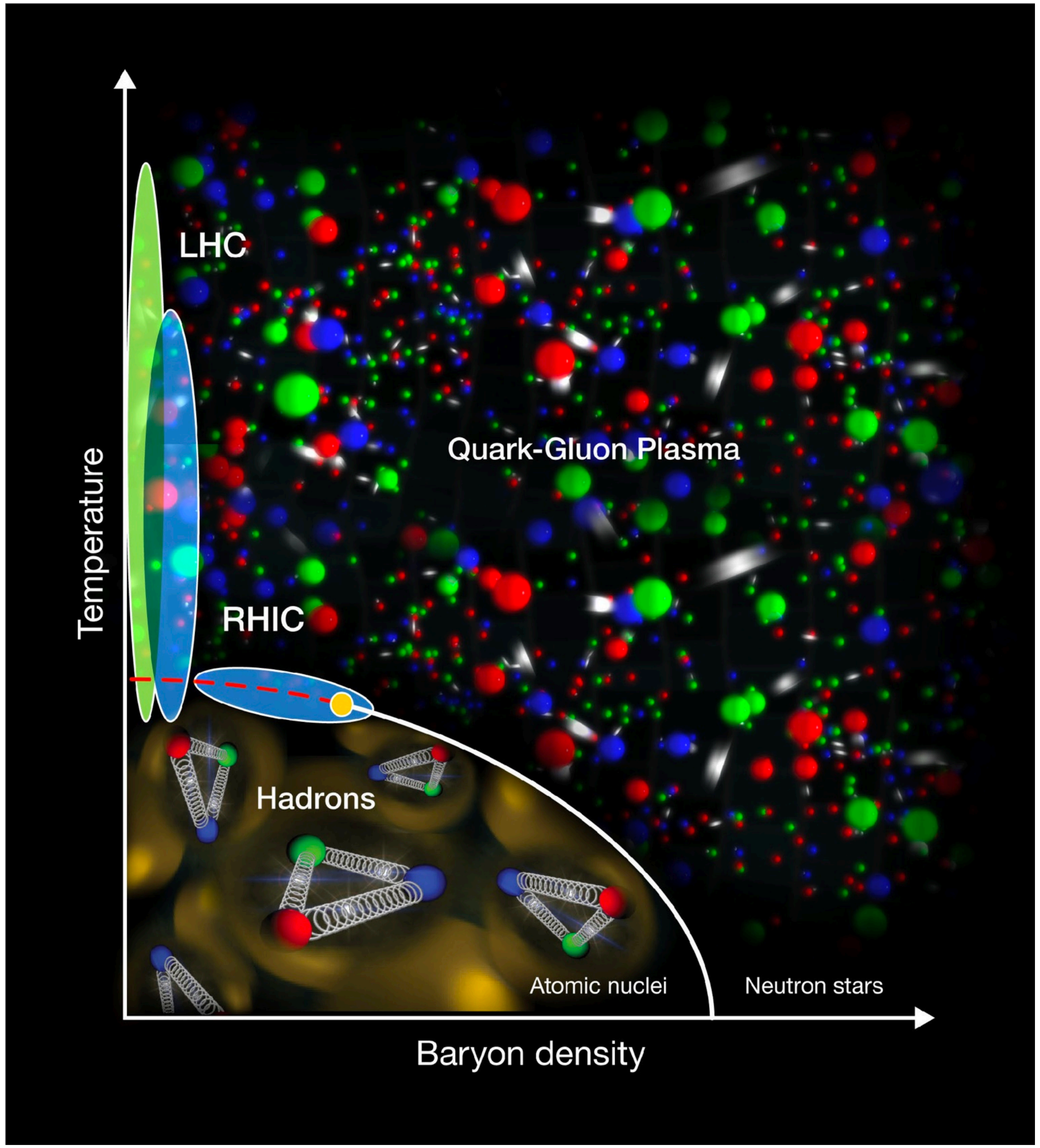

From CEA

Initial condition of Heavy-Ion Collisions

https://u.osu.edu/vishnu/2015/07/22/photon-emission-from-relativistic-heavy-ion-collisions/

The structure of incoming nuclei (embodied in their wave-functions) affects all physical observables at the last stage!

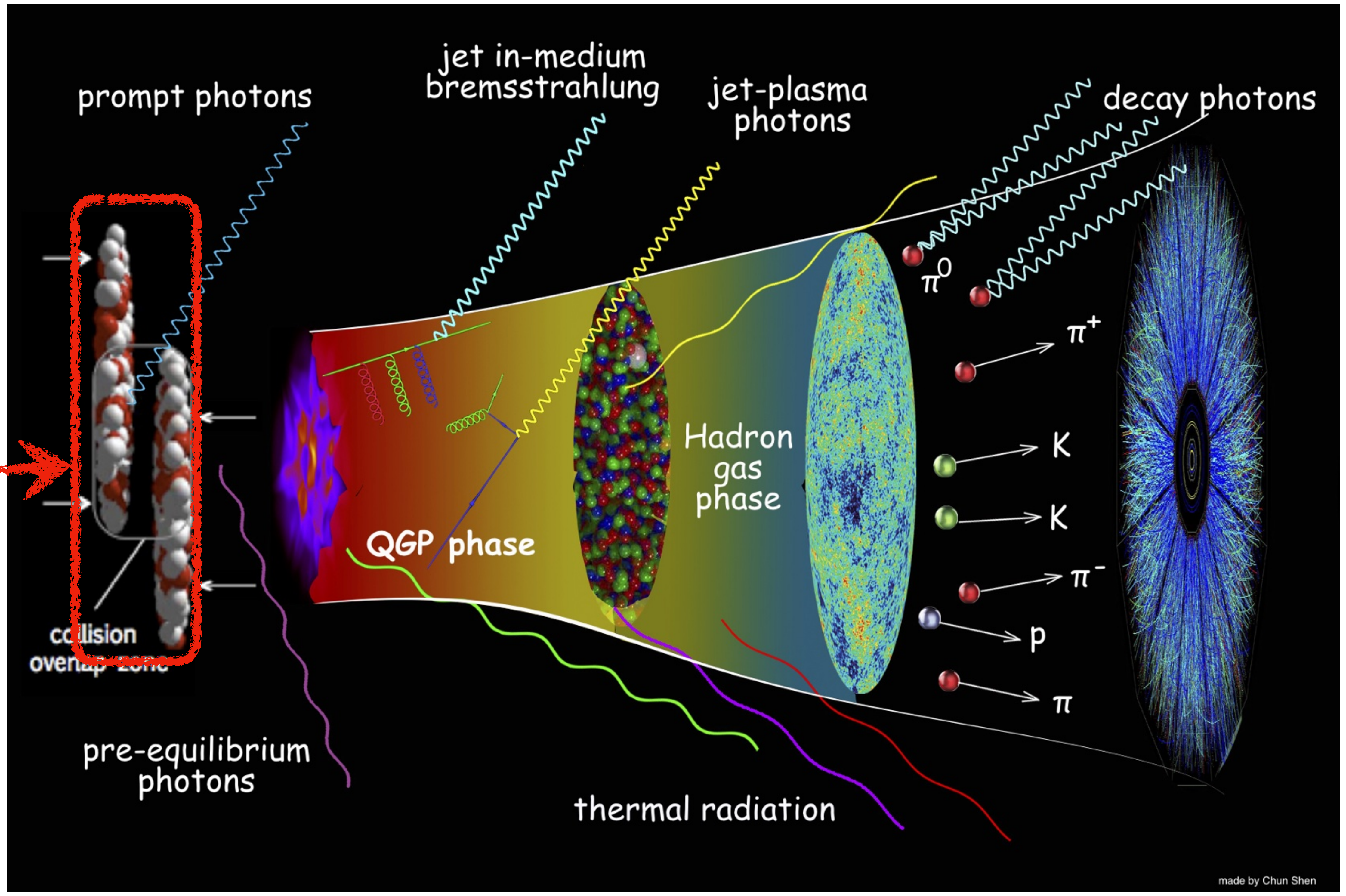

Fig from P. Achenbach, et al. Nucl. Phys. A 1047, 122874 (2024)

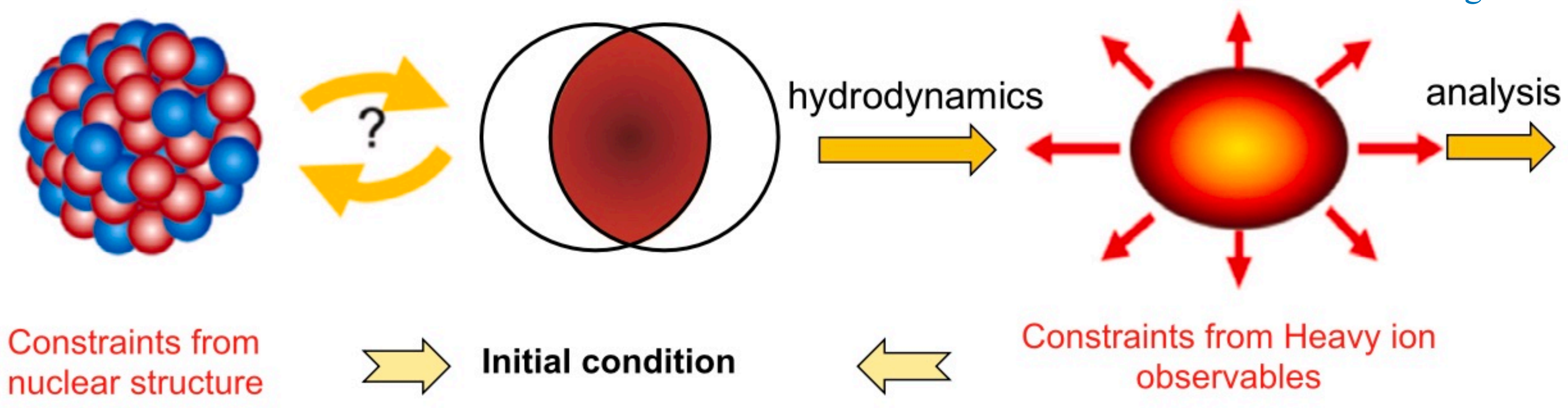

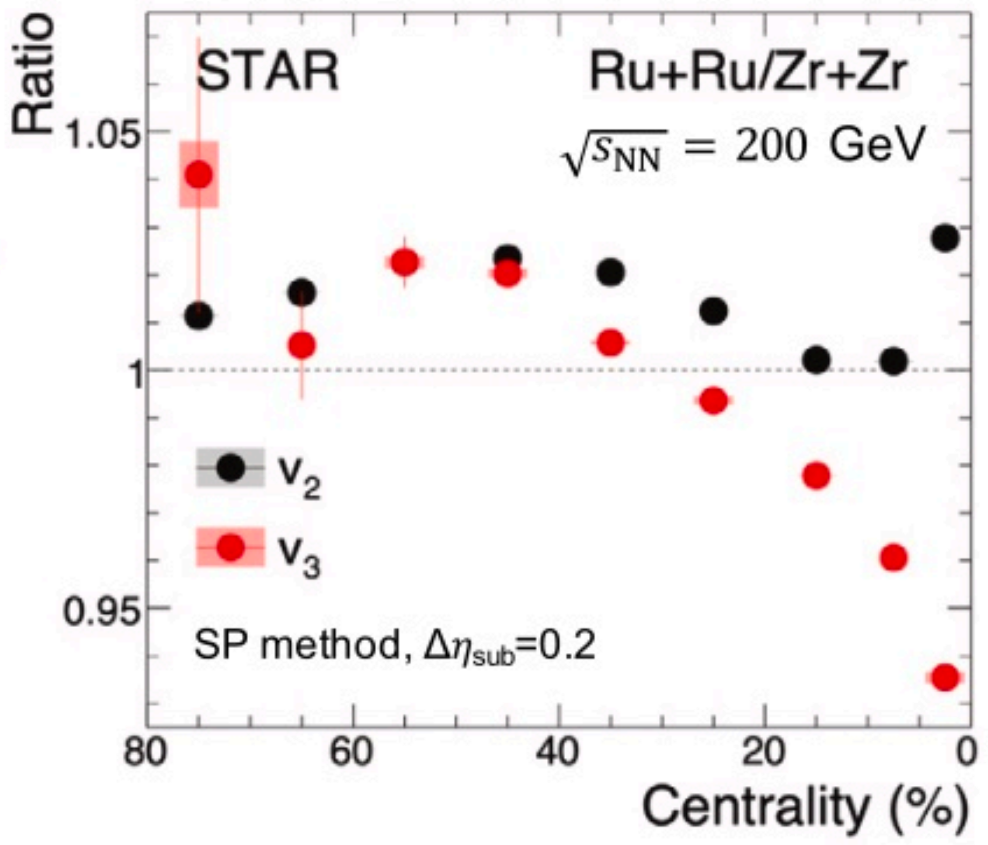

Probing high-energy nuclei

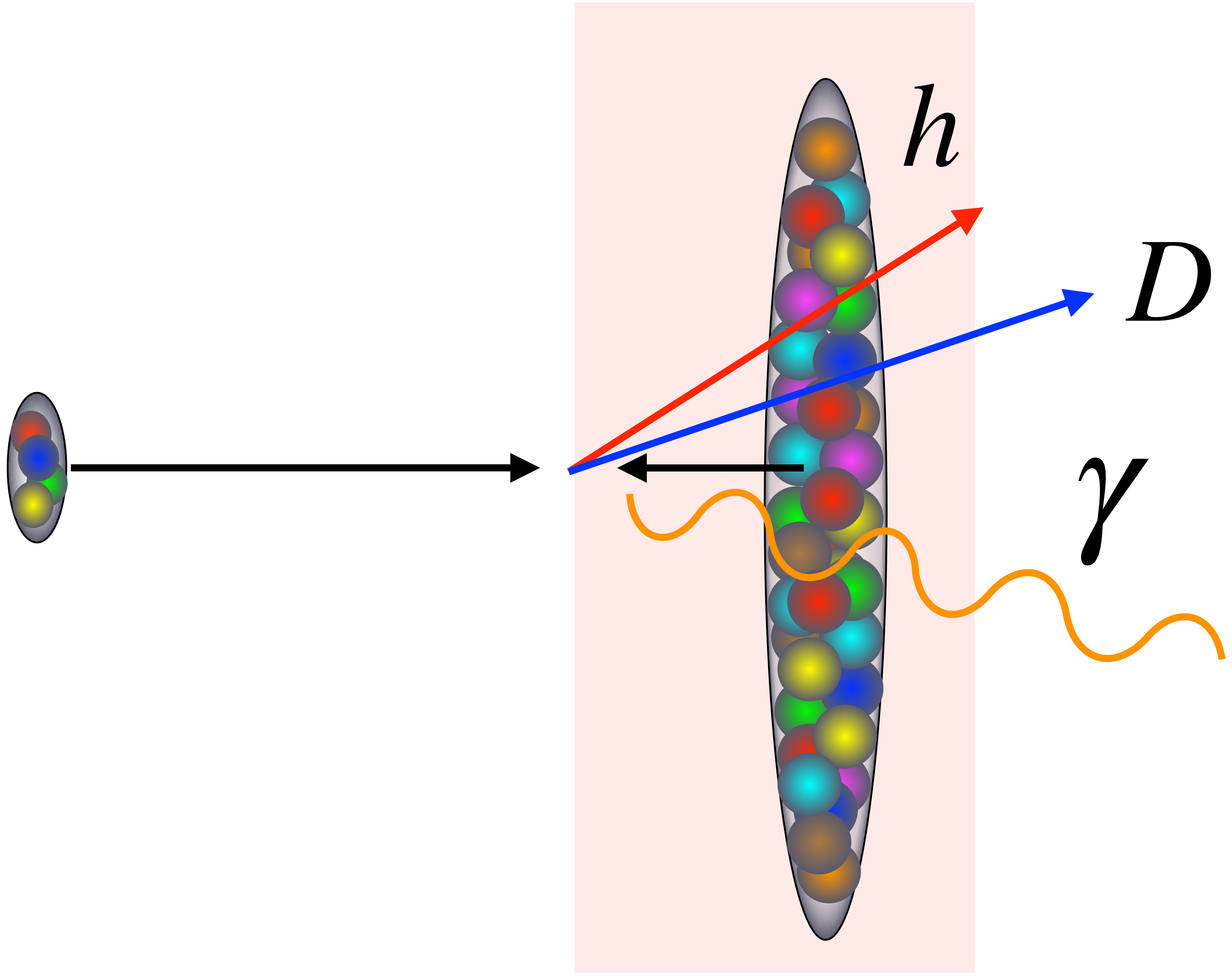

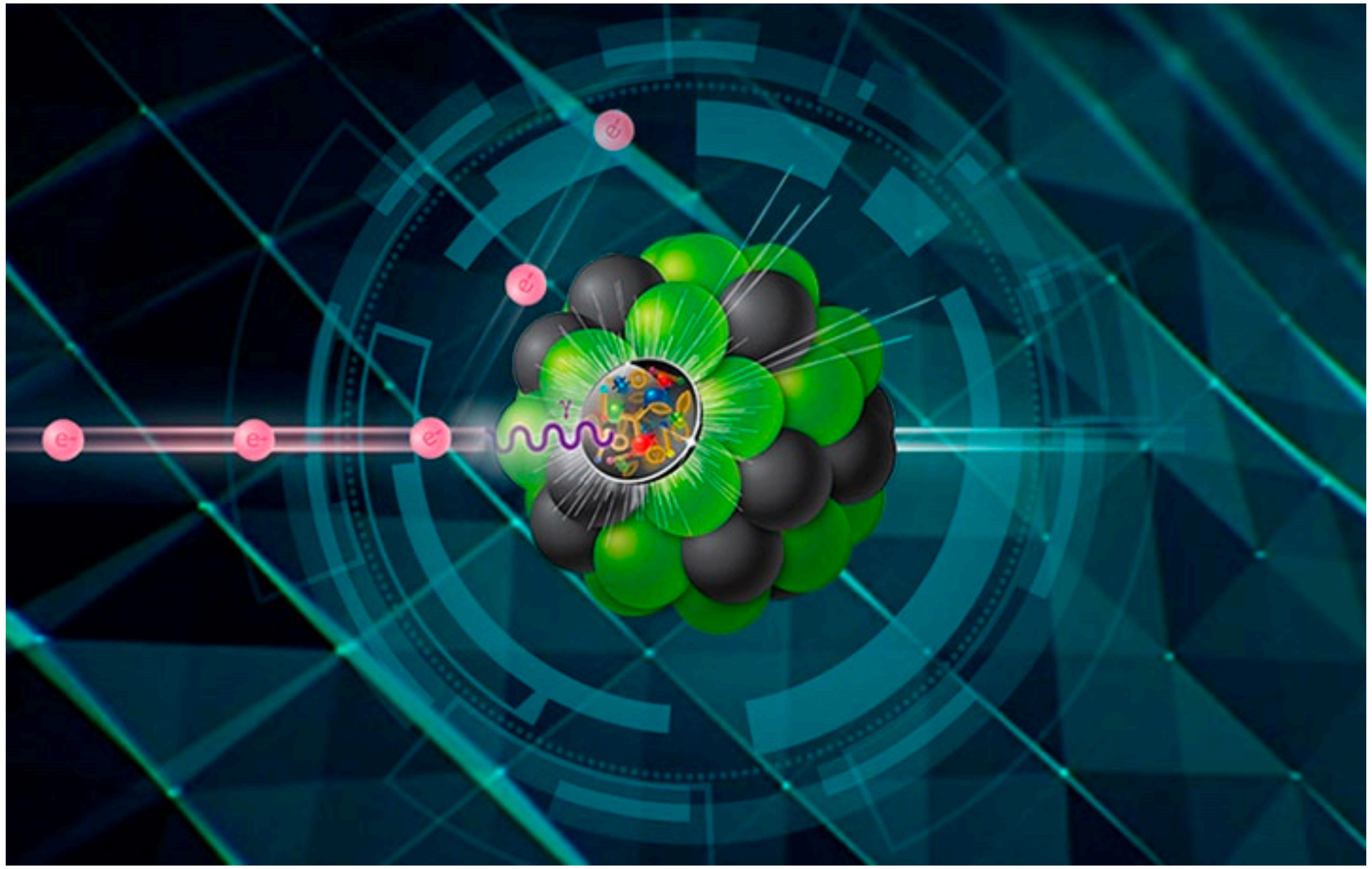

❖ Proton-nucleus (pA) and electron-nucleus (eA) collisions are pivotal playgrounds for studying the initial condition and cold nuclear effects.

❖ Proton-proton is also a fundamental reference collision.

Target kinematic regions

From FPF white paper, J. Phys. G50, no.3, 030501 (2023)

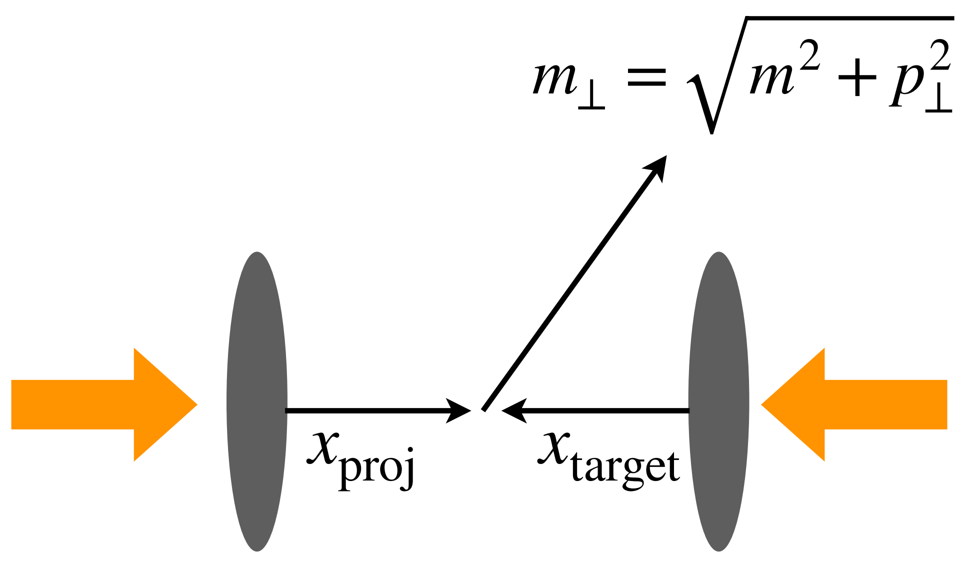

$$x_{proj} \propto \frac{m_\perp}{\sqrt{s}} e^{+y}$$

$$x_{target} \propto \frac{m_\perp}{\sqrt{s}} e^{-y}$$

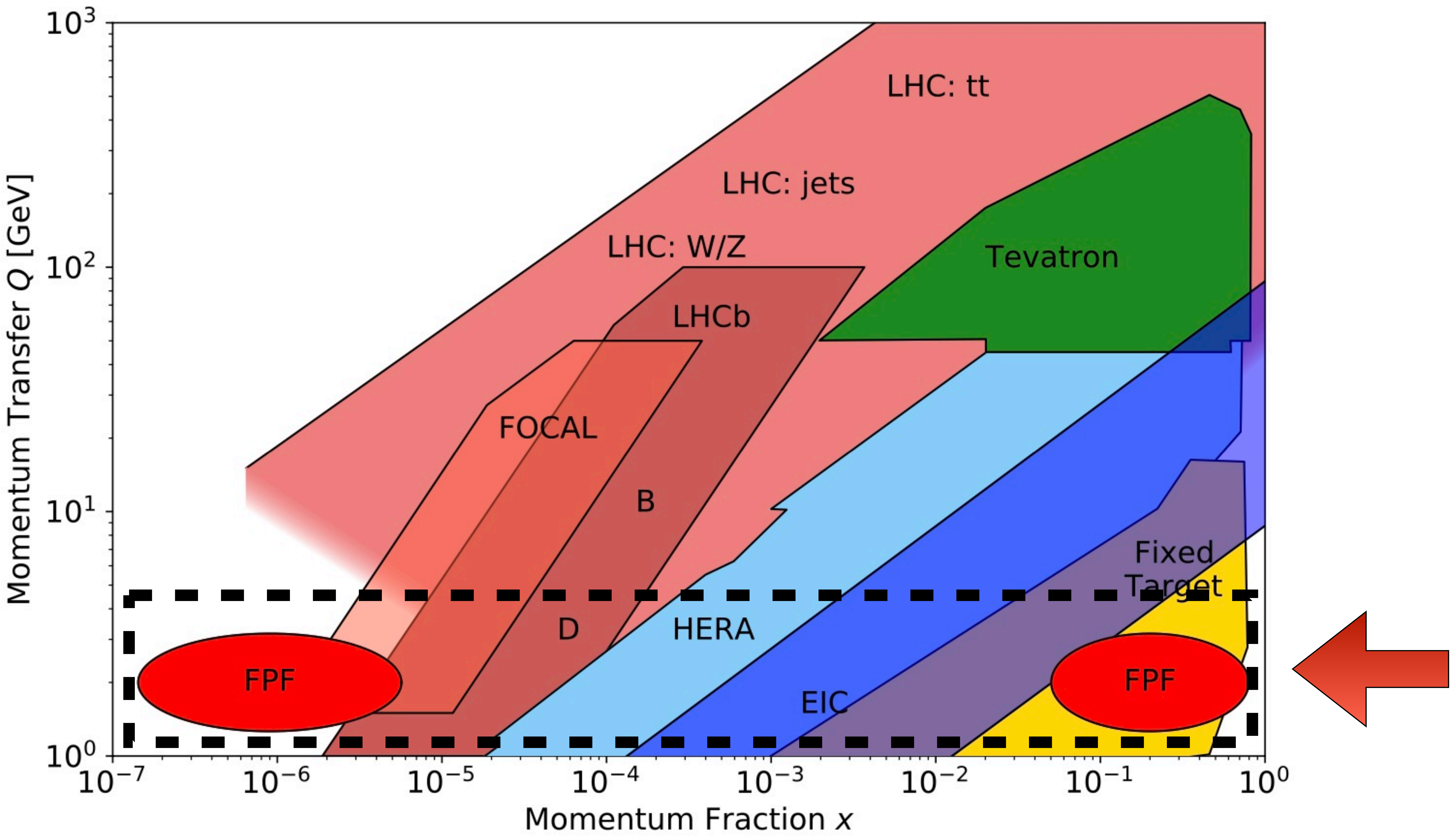

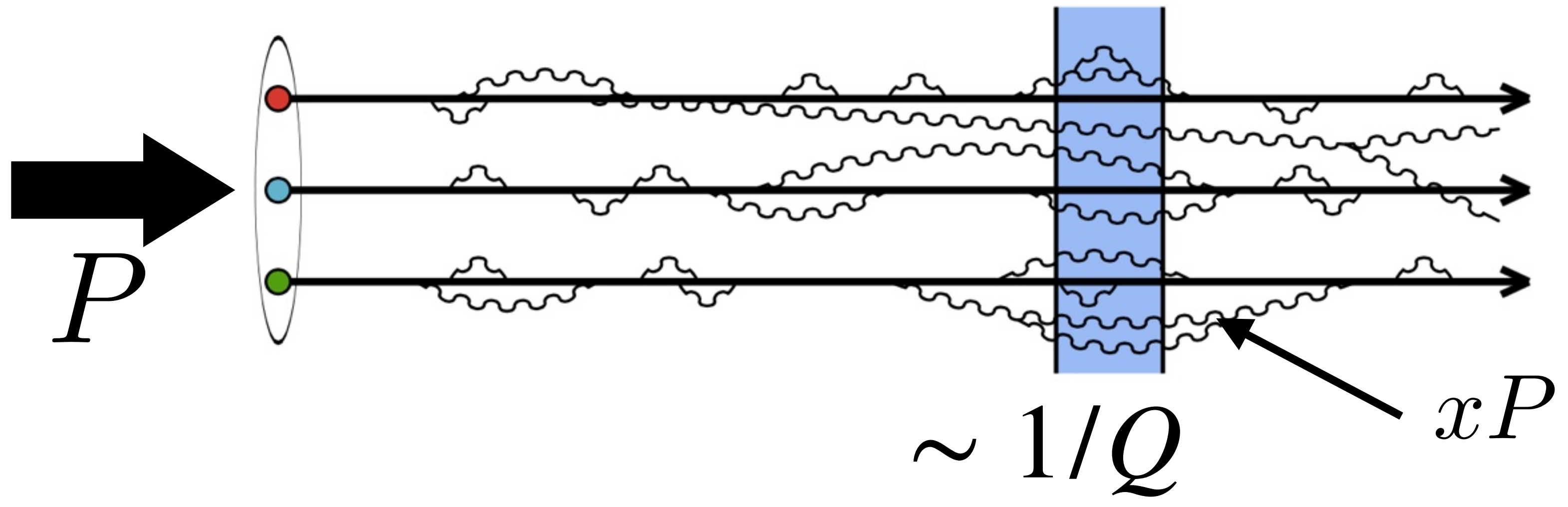

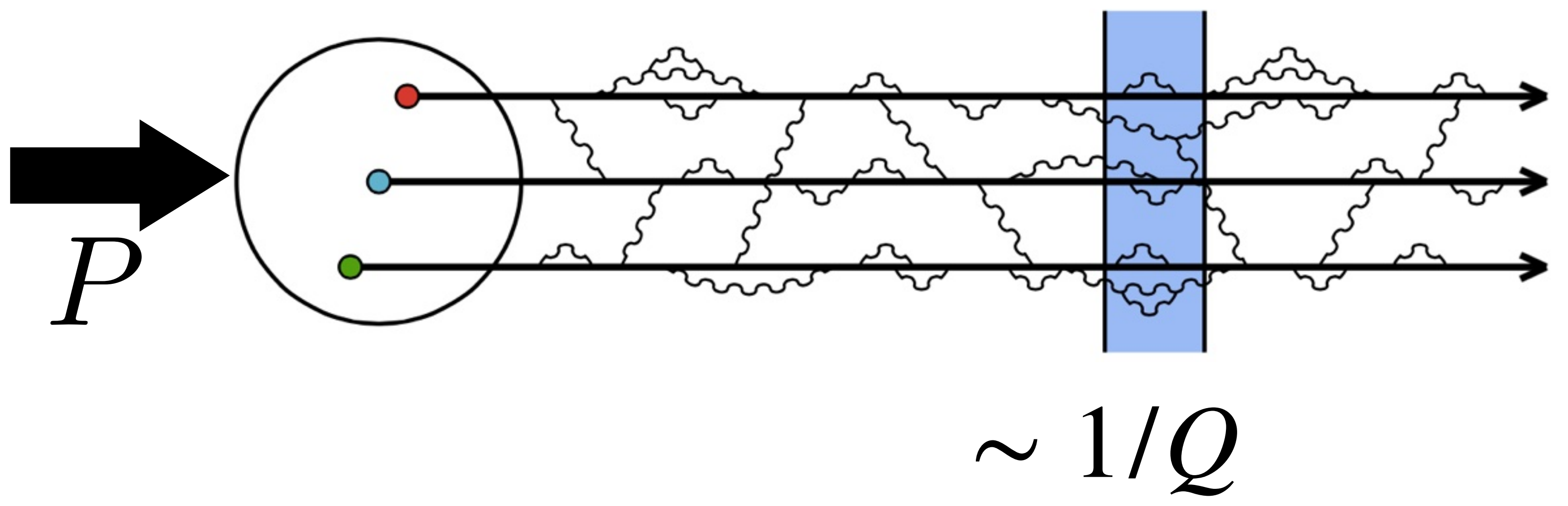

Forward particle production and dense systems

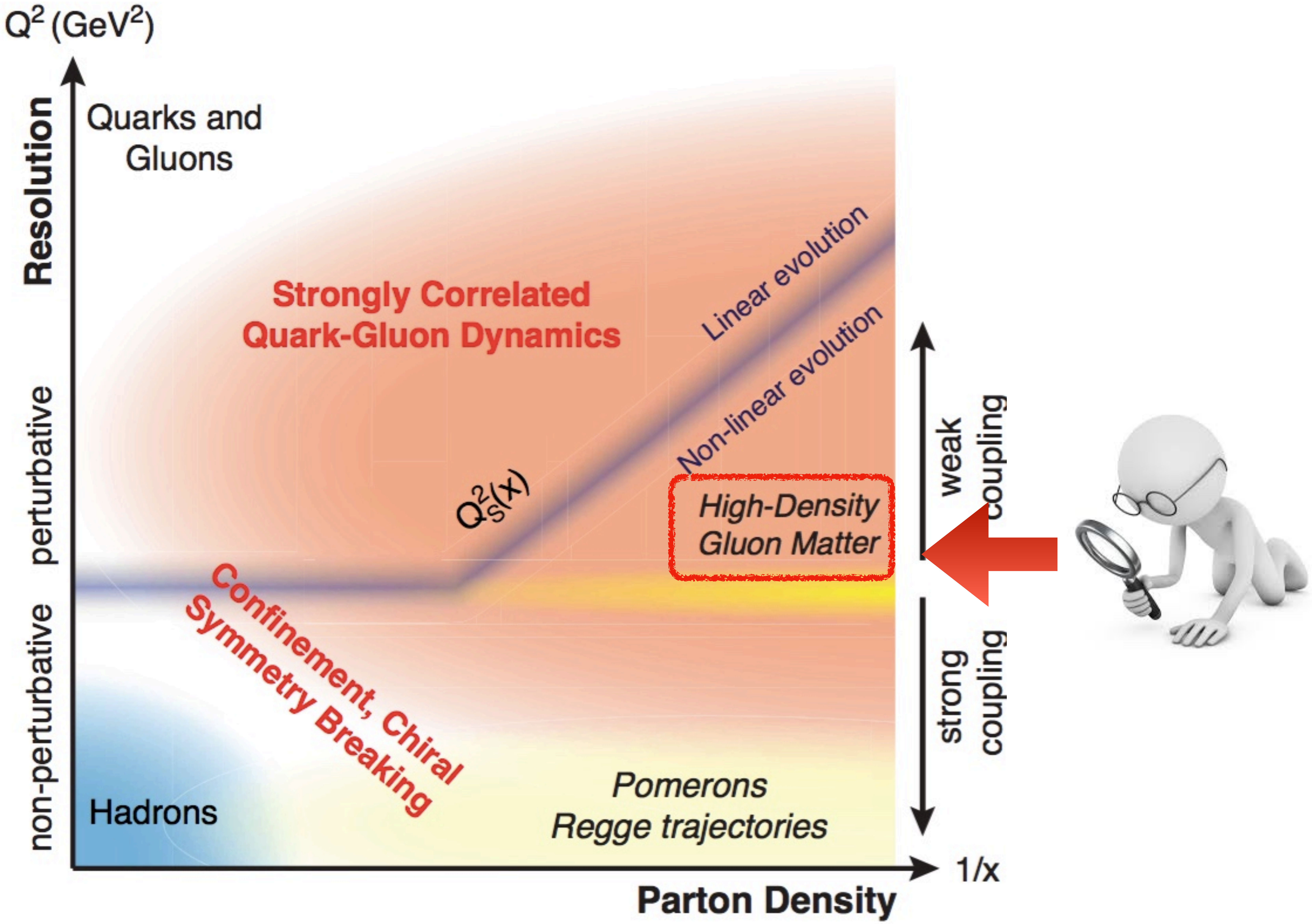

Atmospheric Neutrinos

J. Albrecht, *et al.,* Astrophys. Space Sci. 367, no.3, 27 (2022)

Nucleon-nucleon collisions energy

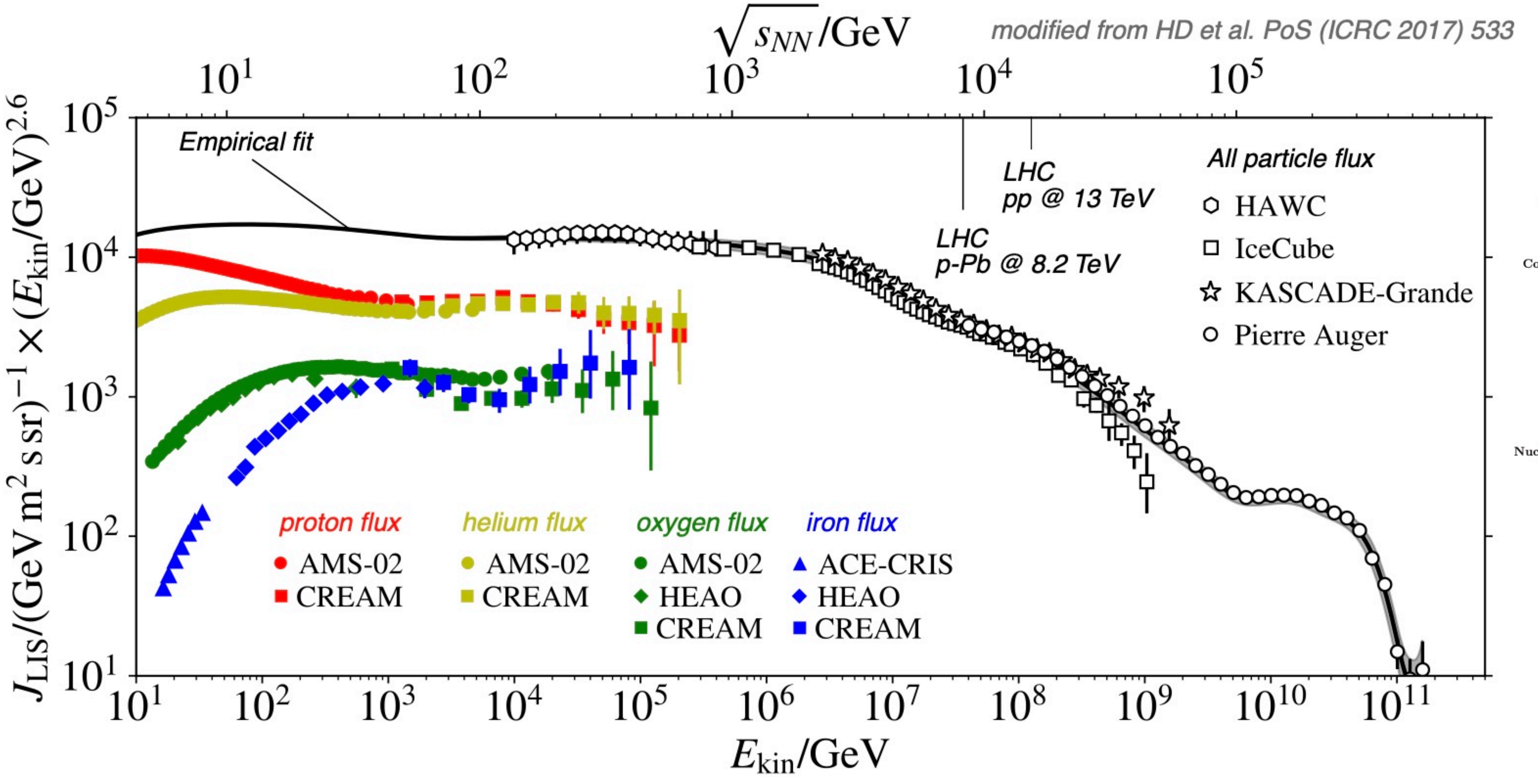

Cosmic ray's kinetic energy

Goncalves, Maciula and Szczurek, Eur. Phys. J. C 82, no.3, 236 (2022)

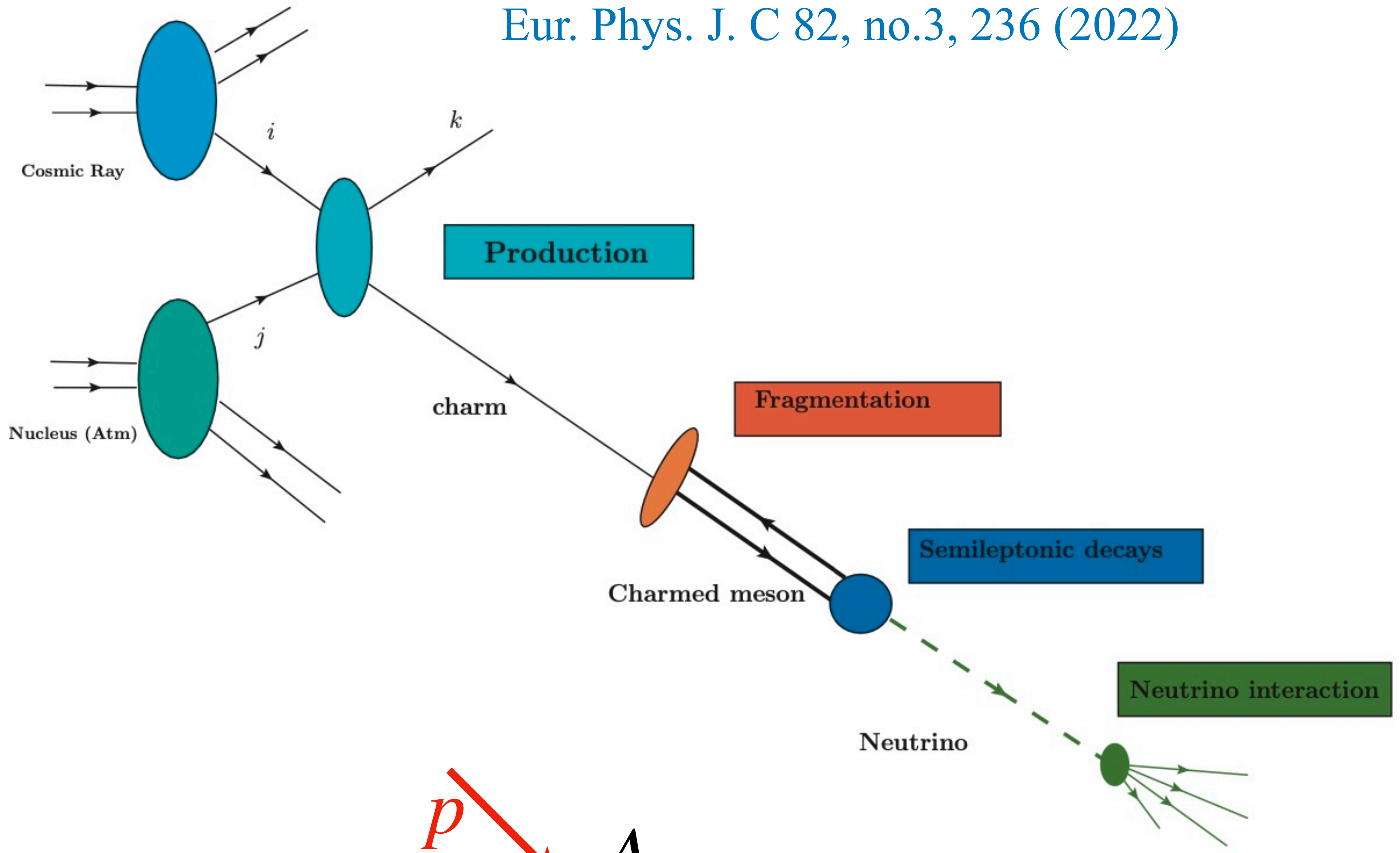

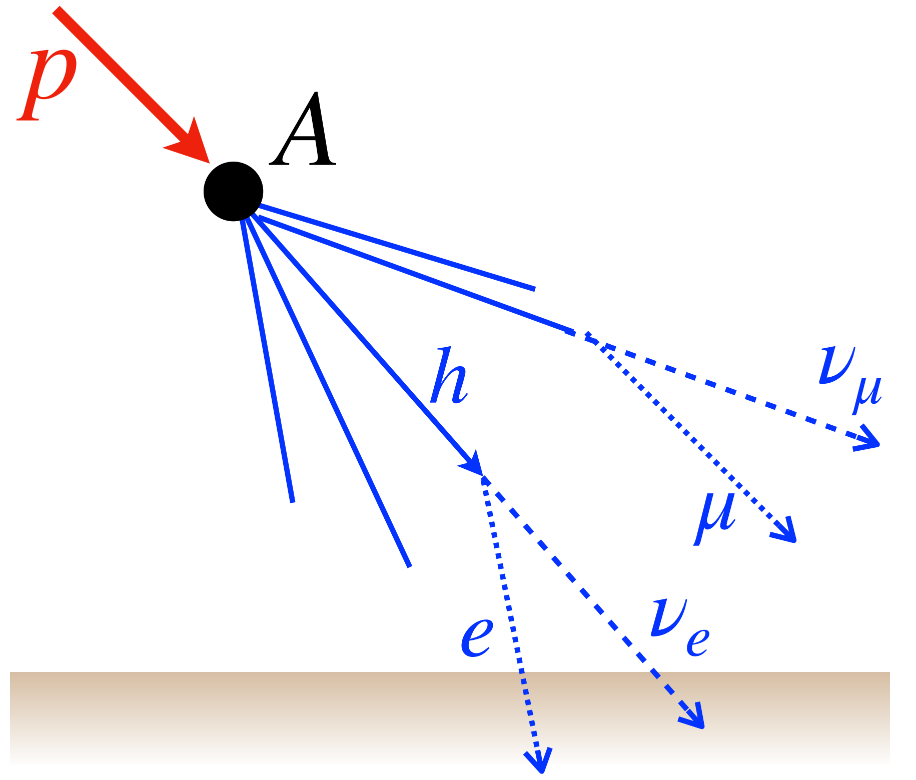

Understanding forward hadron production at the LHC should help us deepen our insights into the origin of cosmic rays.

Our theory: QCD

$$\mathscr{L}_{\rm QCD} = \bar{\psi}(iD^\mu\gamma_\mu - m_q)\psi - \frac{1}{4}F^a_{\mu\nu}F^{a\mu\nu}$$

Quarks and **Gluon** carry **color charges**. At short distances $r < 1\,\text{fm}$, they behave like quasi-free particles.

The Nobel Prize in Physics 2004

Politzer, Gross, Wilczek

Strong coupling constant $\alpha_s = g^2/(4\pi)$

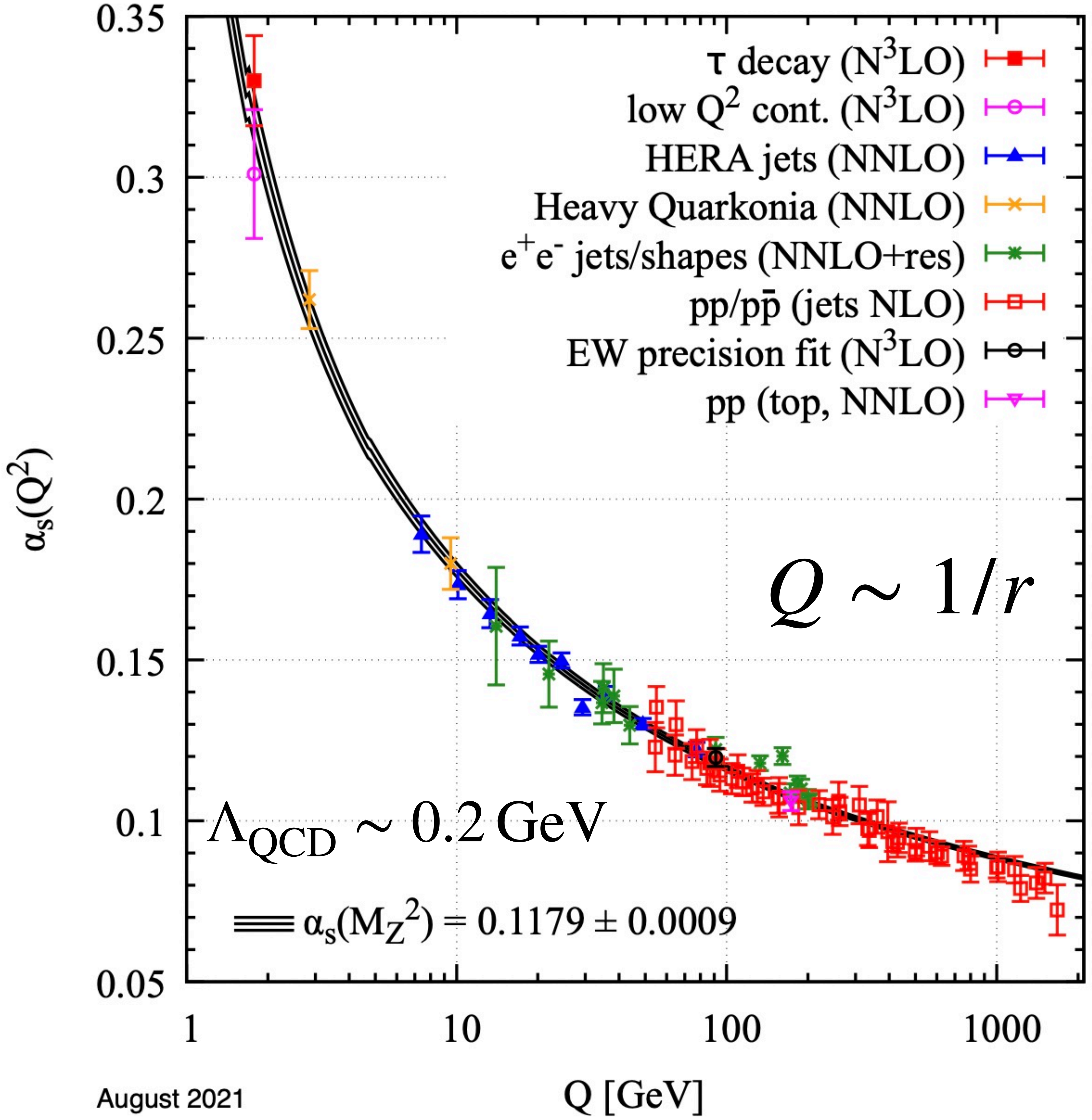

❖ Hard probes ($Q \gg \Lambda_{\rm QCD}$) enable us to look at quarks and gluons inside hadrons using QCD perturbation theory as $\alpha_s(Q) < 1$.

Hard scale : $Q \gg \Lambda_{\rm QCD}$

Soft scale : $Q = \mathcal{O}(\Lambda_{\rm QCD})$

Standard pQCD cannot describe…

S. Acharya *et al.* [ALICE], PLB845, 137730 (2023)

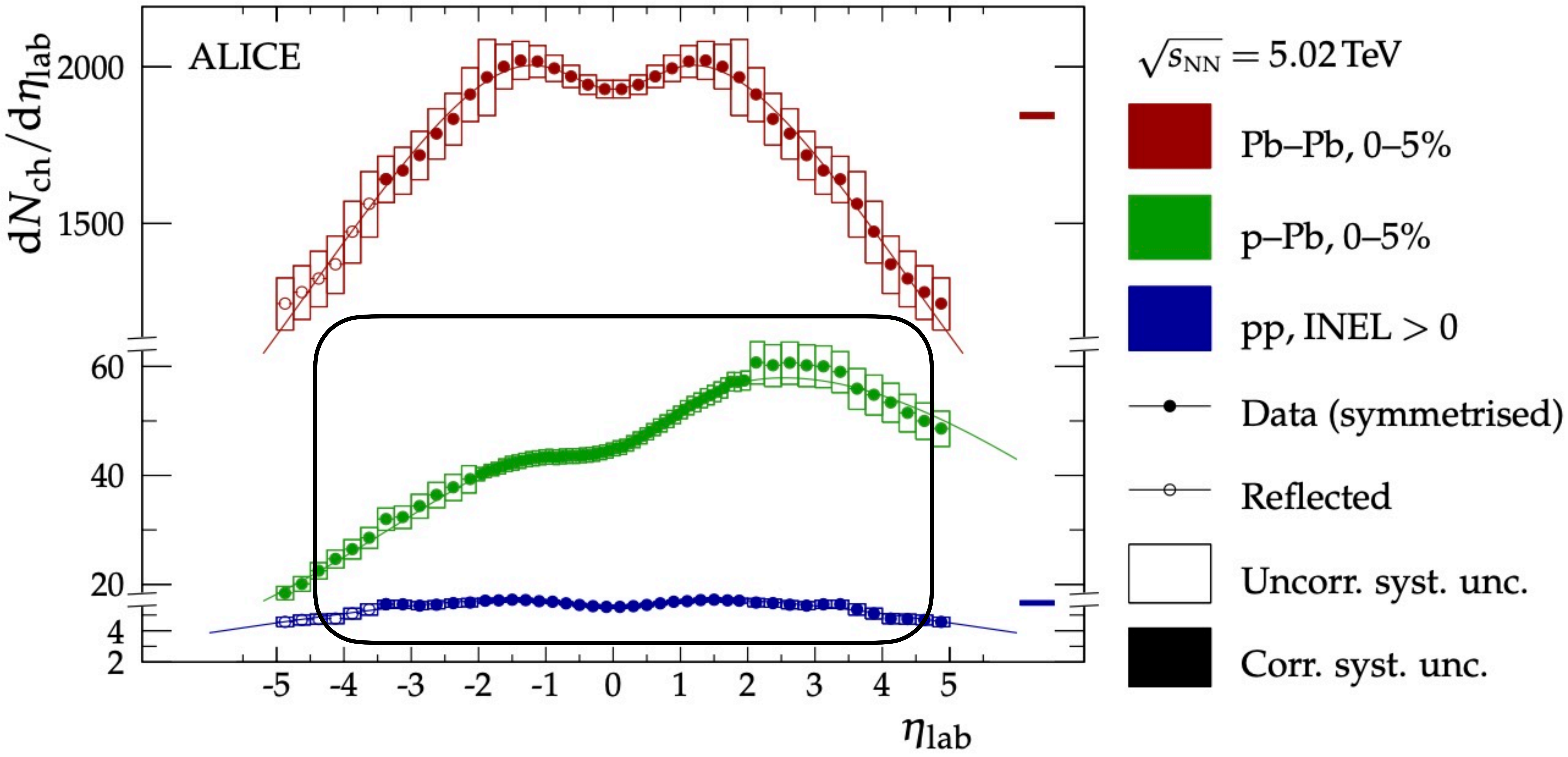

❖ How do we describe bulk particle production of low p_T?

❖ We need an alternate framework!

Gluons at extremely small values of x

f : the number density of **partons** with longitudinal momentum fraction x.

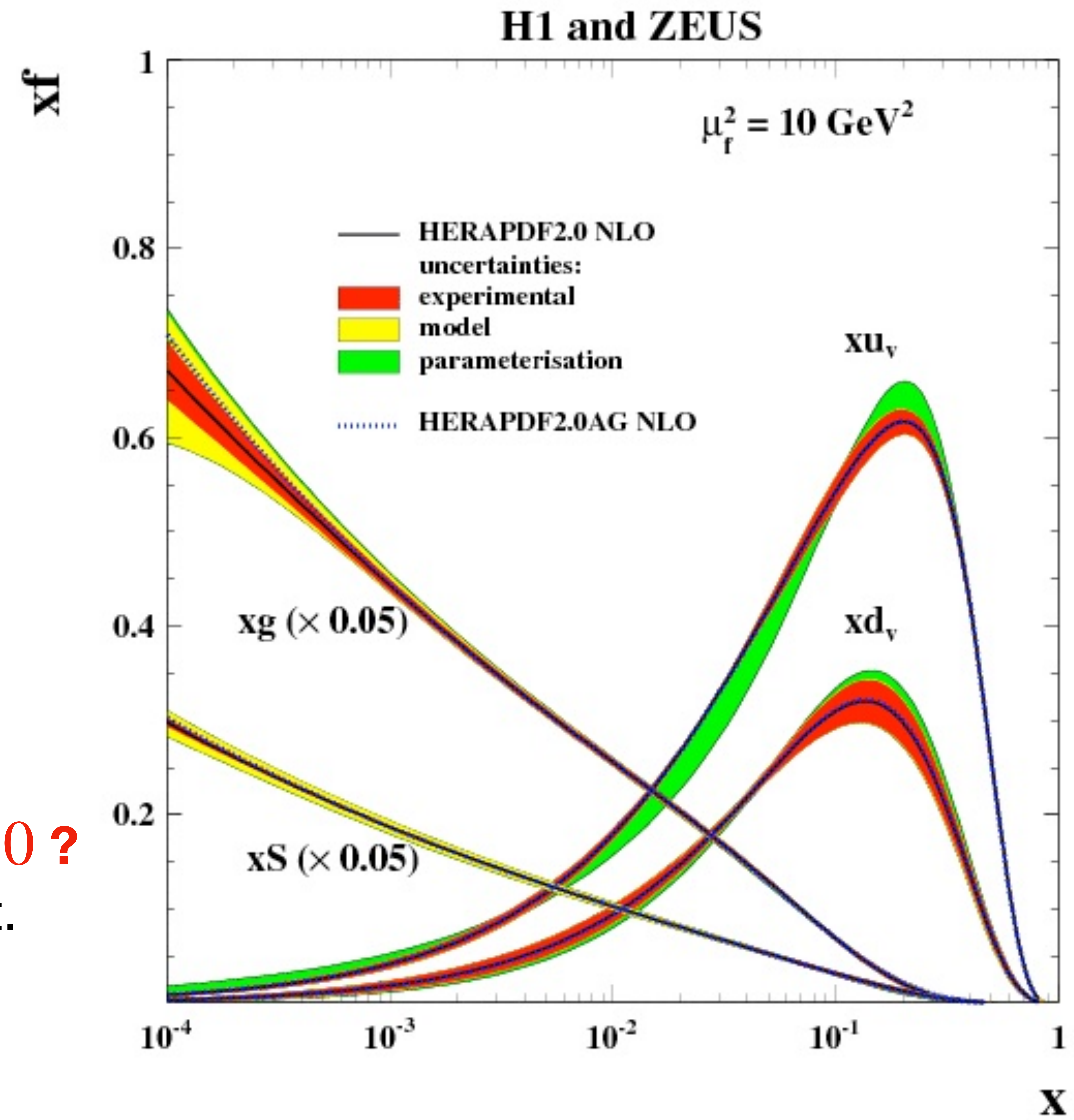

What happens inside hadrons as $x \to 0$?

Dense gluons require a paradigm shift.

What this talk will recap:

- ❖ QCD predicts that **ANY** hadrons and nuclei become a dense gluonic state, the so-called **Color-Glass Condensate (CGC)**, at extremely high energy.

- ❖ In the CGC state, the gluon density inside nuclei saturates, resulting in the gluon saturation phenomenon.

- ❖ CGC Effective Field Theory (weak coupling theory) systematically describe gluon saturation.

- ❖ Clear experimental evidence of gluon saturation or CGC has not been discovered yet, so we need new experiments: FoCal, FASER, EIC.

- ❖ Gluon saturation, an inevitable consequence of QCD, is a scientific truth we must grapple with in our pursuit of knowledge.

Part II:
Résumé of QCD at high energy

1. Bjorken limit: fixed x with $Q^2, s \to \infty$
2. Regge-Gribov limit: fixed Q^2 with $s \to \infty, x \to 0$

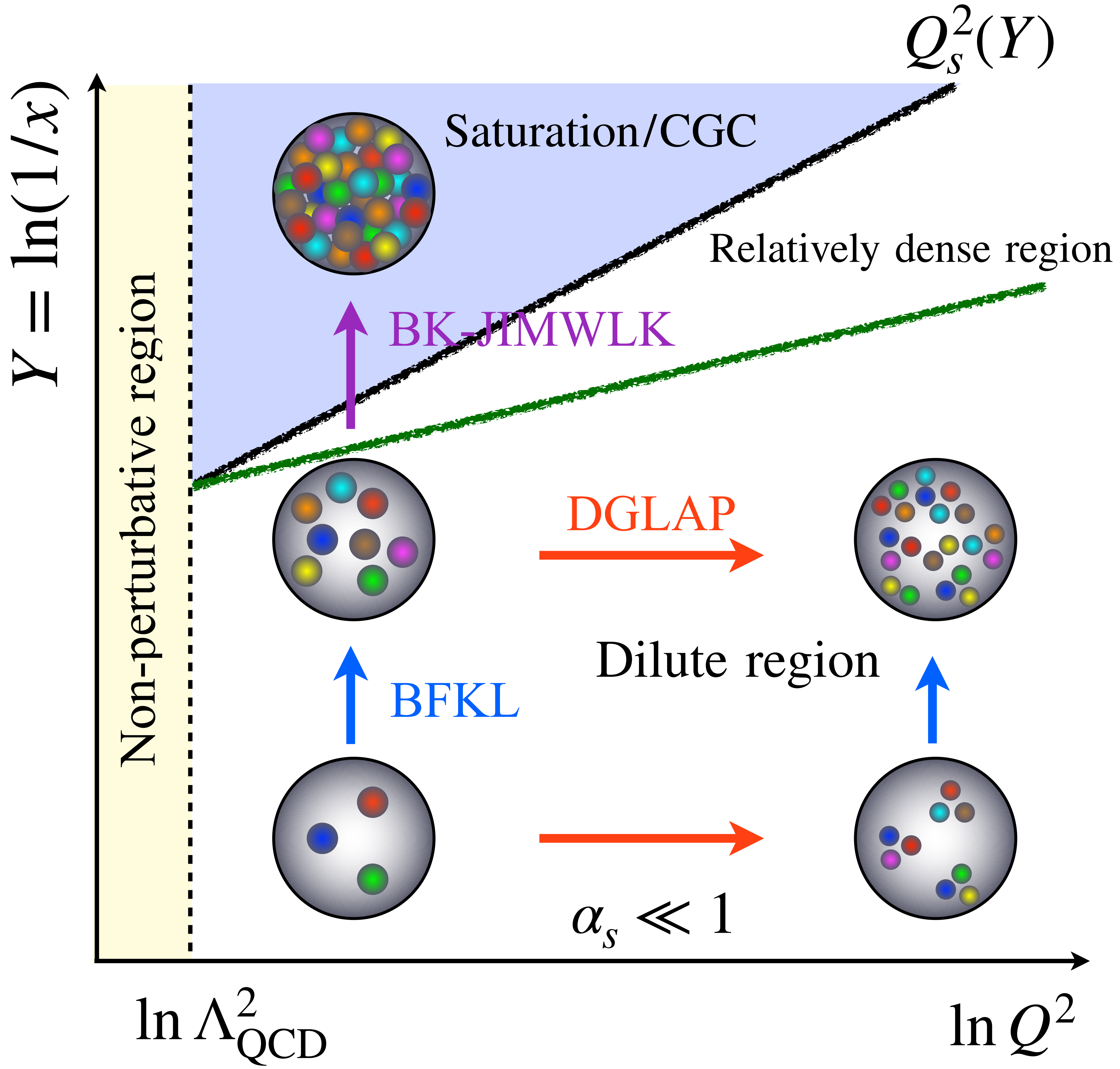

Reference frame

❖ Hadron rest frame: $P^\mu = (M,0,0,0)$

❖ Infinite momentum frame (IMF): $P \gg M \Longrightarrow P^\mu = (P,0,0,P)$

In IMF, partonic picture is manifest. PDFs are number densities.

❖ Light-cone coordinate: $x^\pm = (t \pm z)/\sqrt{2}$

❖ Light-cone momentum: $p^\pm = (E \pm p_z)/\sqrt{2}$

❖ Rapidity: $y = \frac{1}{2}\ln\left(\frac{p^+}{p^-}\right)$

❖ "Longitudinal" momentum fraction: $x = k^+/P^+$

In IMF, $P^\mu \to (P^+,0^-,0_\perp)$

If $P^\mu = (P,0,0,-P)$, $P^\mu \to (0^+,P^-,0_\perp)$

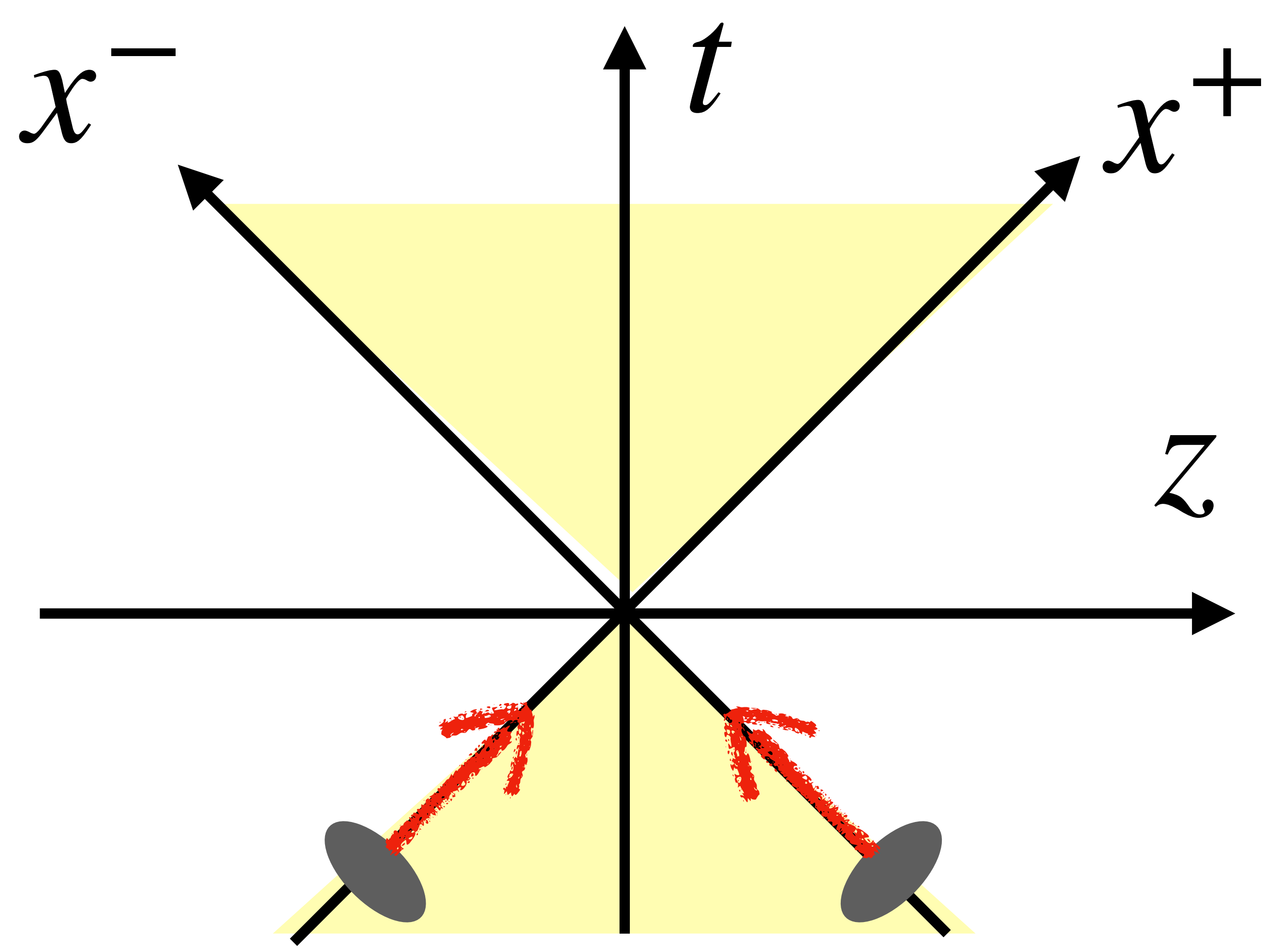

We will discuss scatterings in the light-cone coordinate.

Electromagnetic probe

Inclusive DIS ($e + p \to e' + X$) with a large momentum transfer $Q \gg \Lambda_{\rm QCD}$:

- ❖ dominated by the scattering of the lepton off an active quark/gluon (parton)
- ❖ not sensitive to the dynamics at a hadronic scale $\sim \Lambda_{\rm QCD} \sim 1/{\rm fm}$
- ❖ **QCD factorization** provides a probe to "see" quarks, gluons and their dynamics indirectly.

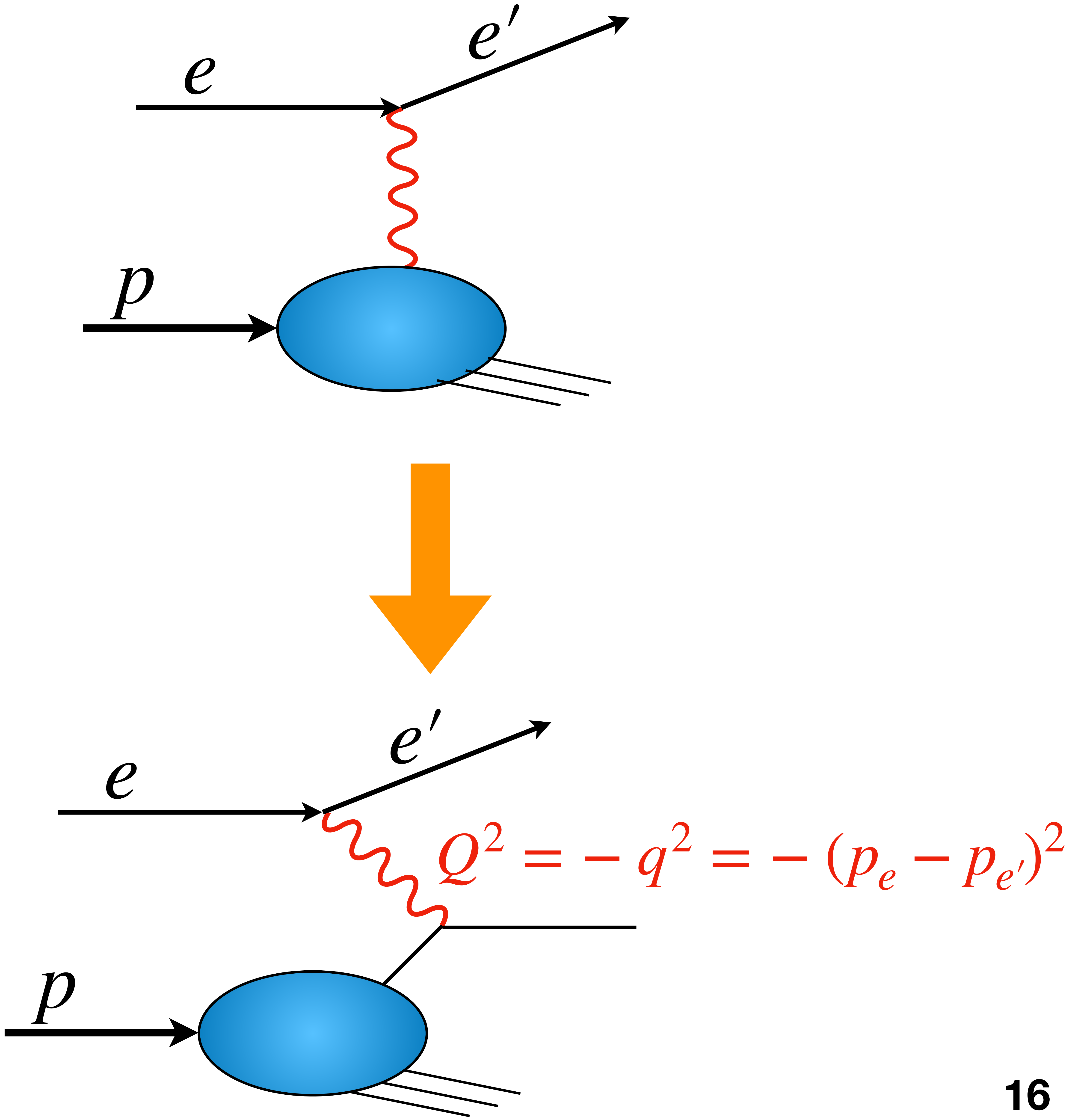

Two characteristic scales

Image resolution

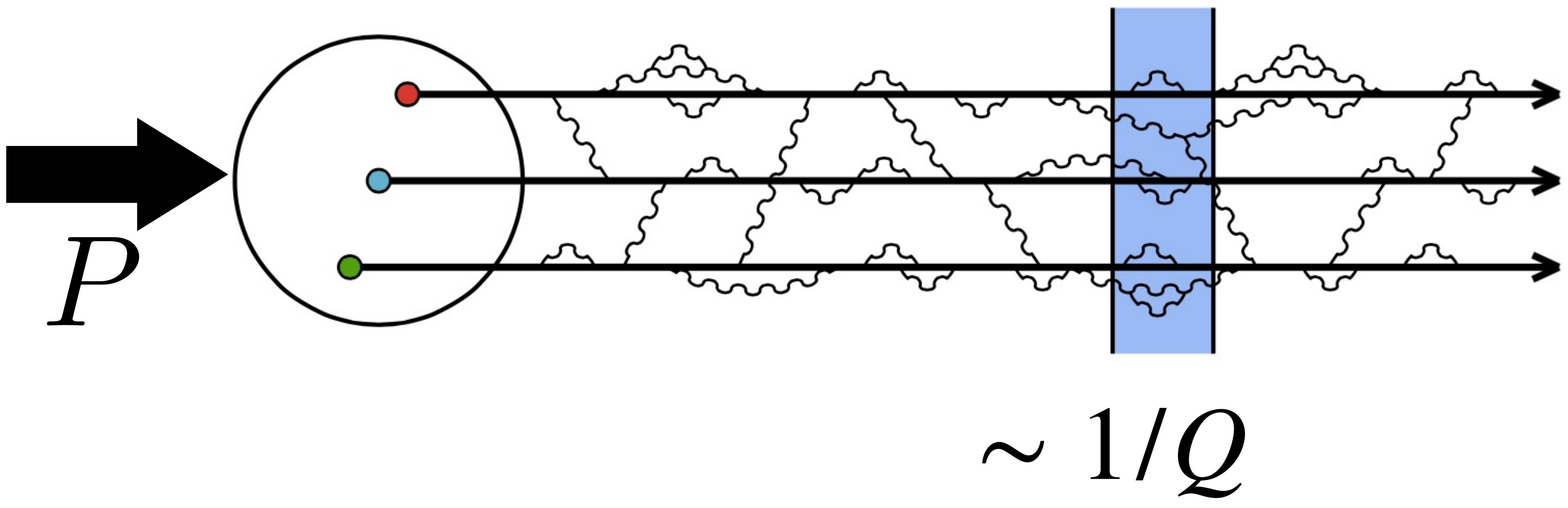

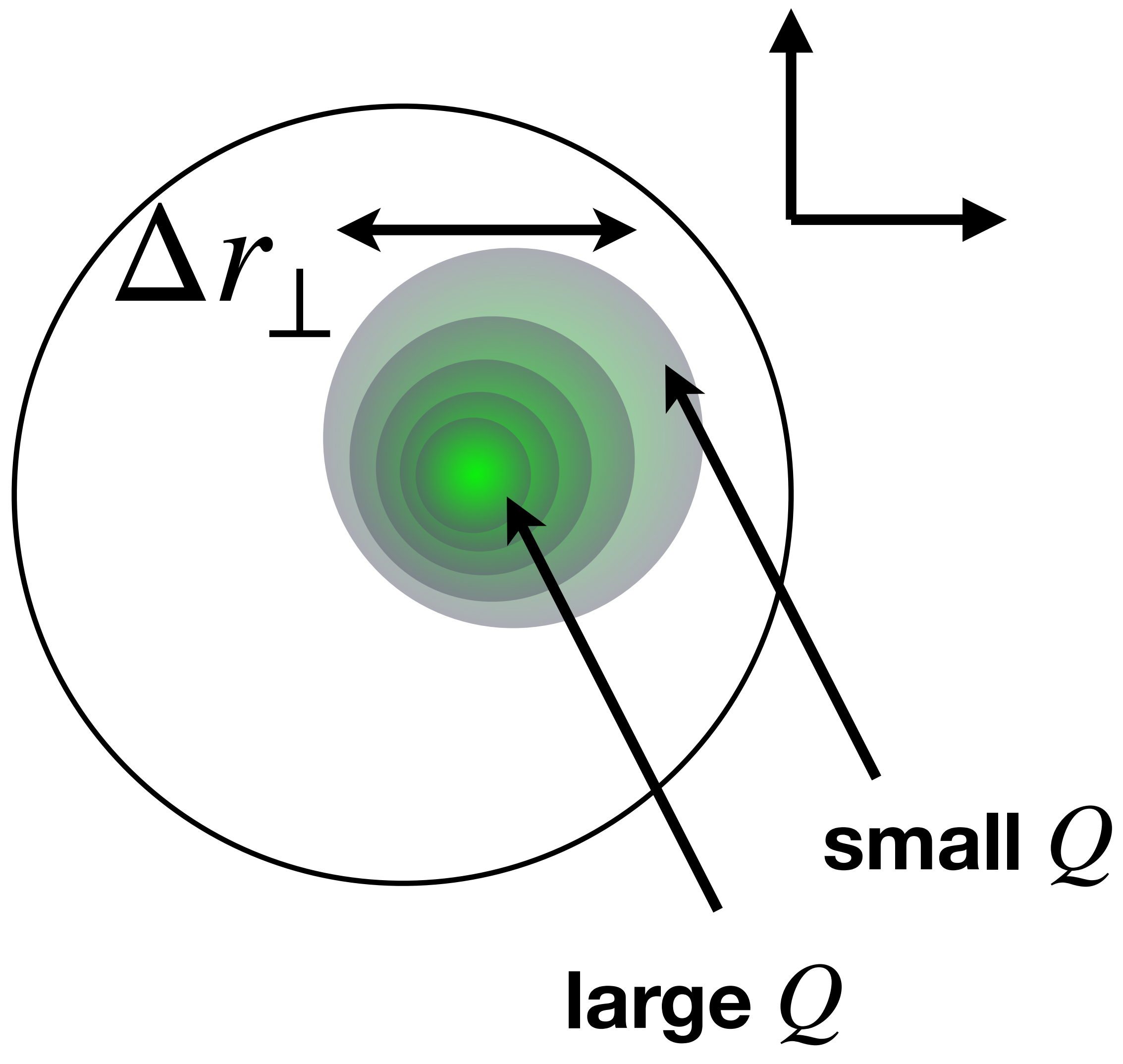

Localized probe $\Delta r_\perp \propto 1/Q$: spatial resolution in transverse plane

Exposure time

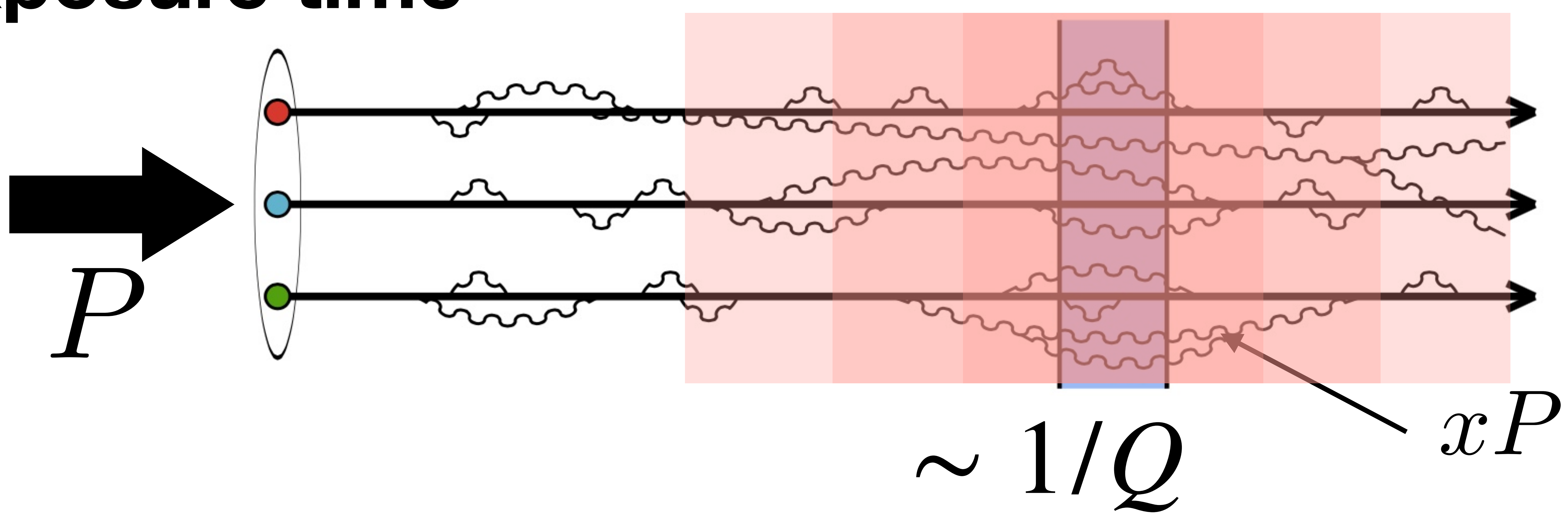

lifetime of a parton in IMF:

$$\Delta t \sim \Delta x^+ \sim k^- = \frac{k_T^2}{2k^+} = \frac{k_T^2}{2xP^+}$$

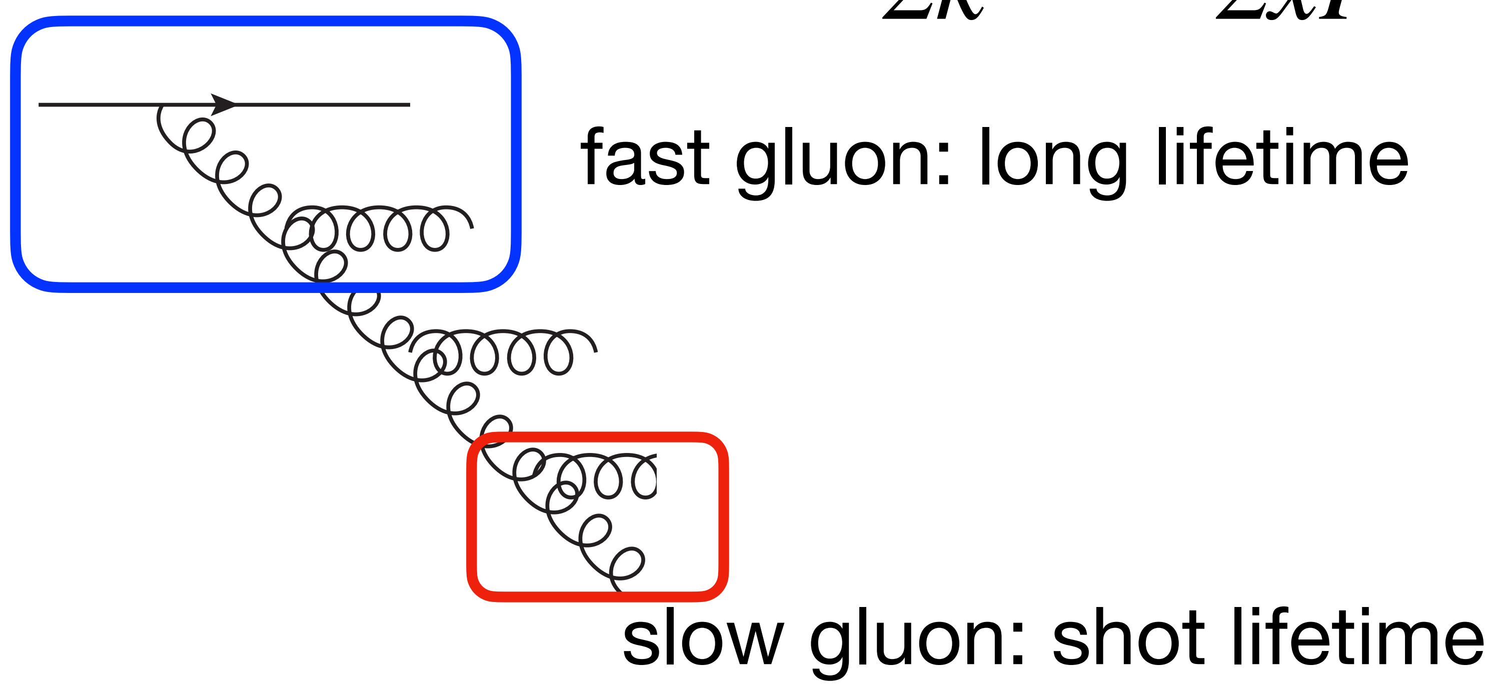

Ioffe time $\Delta t \propto 1/x$: fluctuation in longitudinal direction

Extracting PDFs

The lepton's energy loss:

$$y = \frac{q \cdot P}{k \cdot P}$$

Center-of-mass energy:

$$s = (P + p)^2$$

Momentum transfer:

$$Q^2 = -q^2$$

Bjorken-x: $x = \frac{P \cdot k}{P \cdot p} \propto \frac{1}{s}$

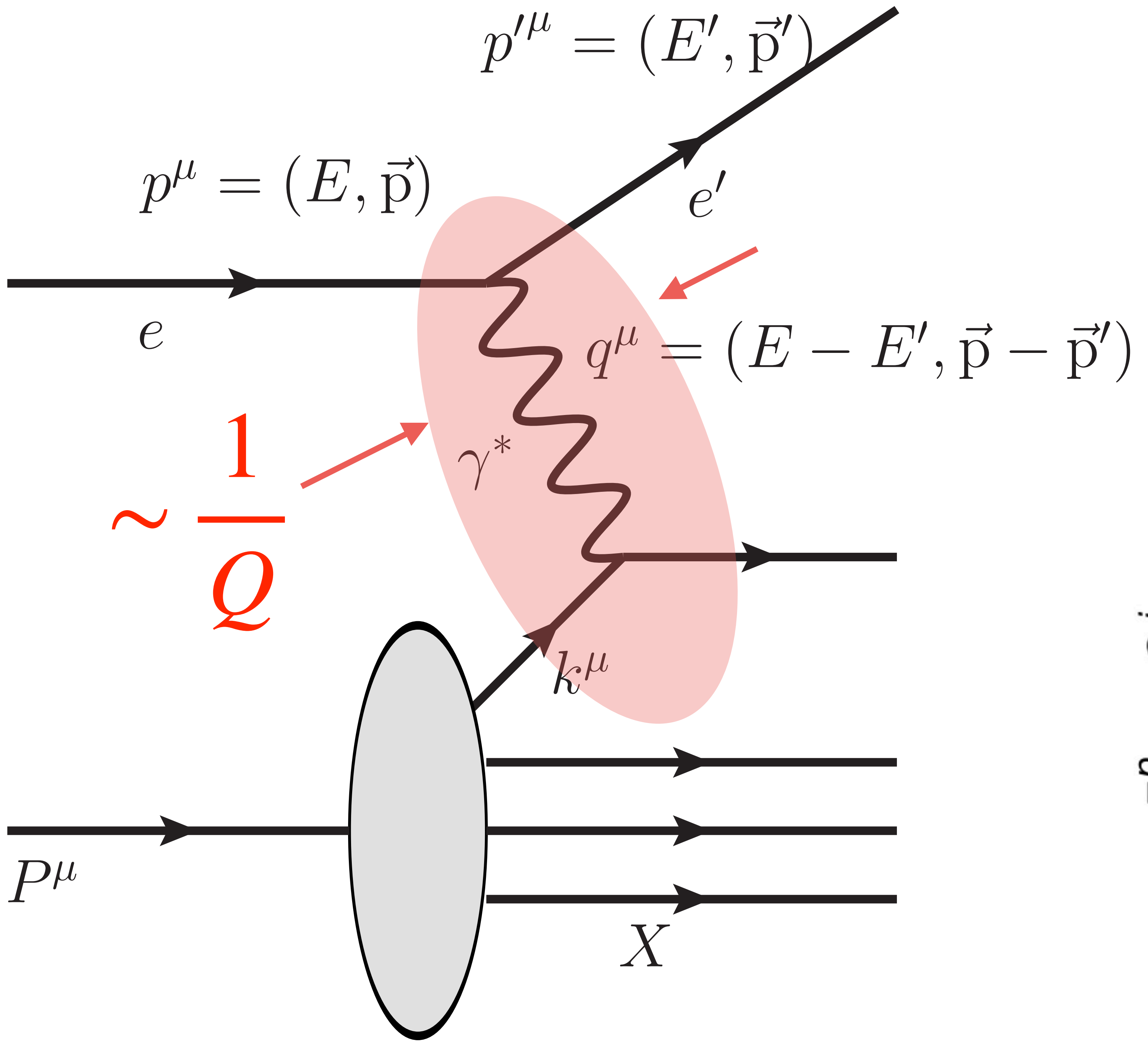

$$\frac{d^2\sigma_{\text{DIS}}}{dxdy} \approx \frac{4\pi\alpha_{\text{EM}}^2}{xyQ^2}\left[\left(1-y\right)F_2 + y^2 xF_1\right]$$

Structure functions $F_i \approx \sum_a C_i^a \otimes f_a$ ← Global data fitting

Perturbatively calculable

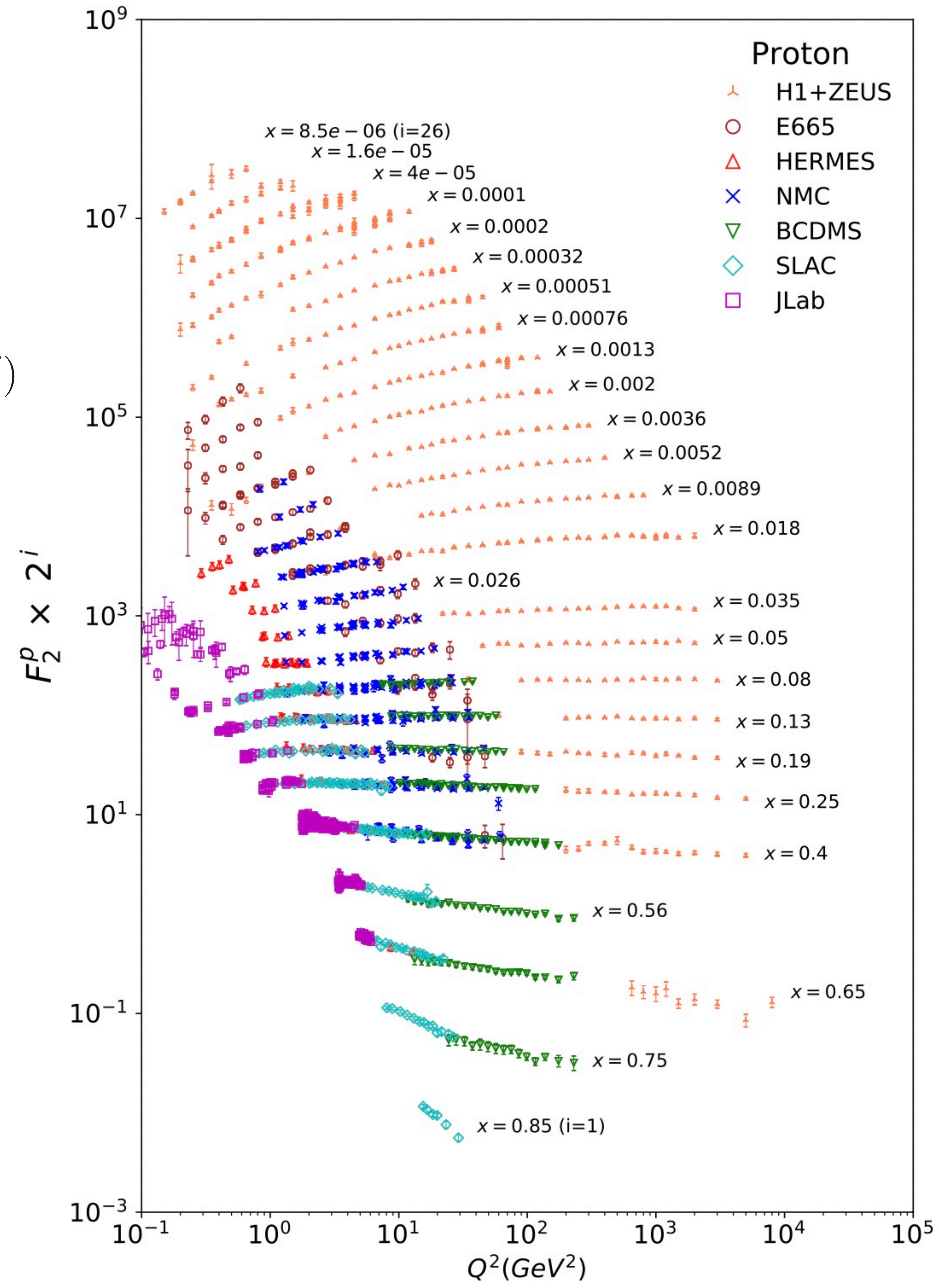

Dokshitzer–Gribov–Lipatov–Altarelli–Parisi evolution

$$\frac{\partial}{\partial \ln \mu^2}\begin{pmatrix} f_{q_i}(z,\mu) \\ f_g(z,\mu) \end{pmatrix} = \frac{\alpha_s(\mu)}{2\pi}\int_z^1 \frac{dz'}{z'} \sum_{q_j,\bar{q}_j} \begin{pmatrix} P_{q_i\to q_j}(z/z') & P_{q_j\to g}(z/z') \\ P_{g\to q_i}(z/z') & P_{g\to g}(z/z') \end{pmatrix} \begin{pmatrix} f_{q_j}(z',\mu) \\ f_g(z',\mu) \end{pmatrix}$$

In the small-x limit, the gluon density is high so that we just consider the gluon distribution.

$$F_2(x,\mu^2) = \sum_q e_q^2 \left[x f_{q/p}(x,\mu^2) + x f_{\bar{q}/p}(x,\mu^2) \right]$$

$$x \ll 1$$

$$\frac{\partial F_2(x,\mu^2)}{\partial \ln \mu^2} \approx \frac{10\alpha_s}{27\pi} G(2x,\mu^2), \quad G(x,\mu^2) \equiv x f_{g/p}(x,\mu^2)$$

K. Prytz, Phys. Lett. B 311, 286-290 (1993)

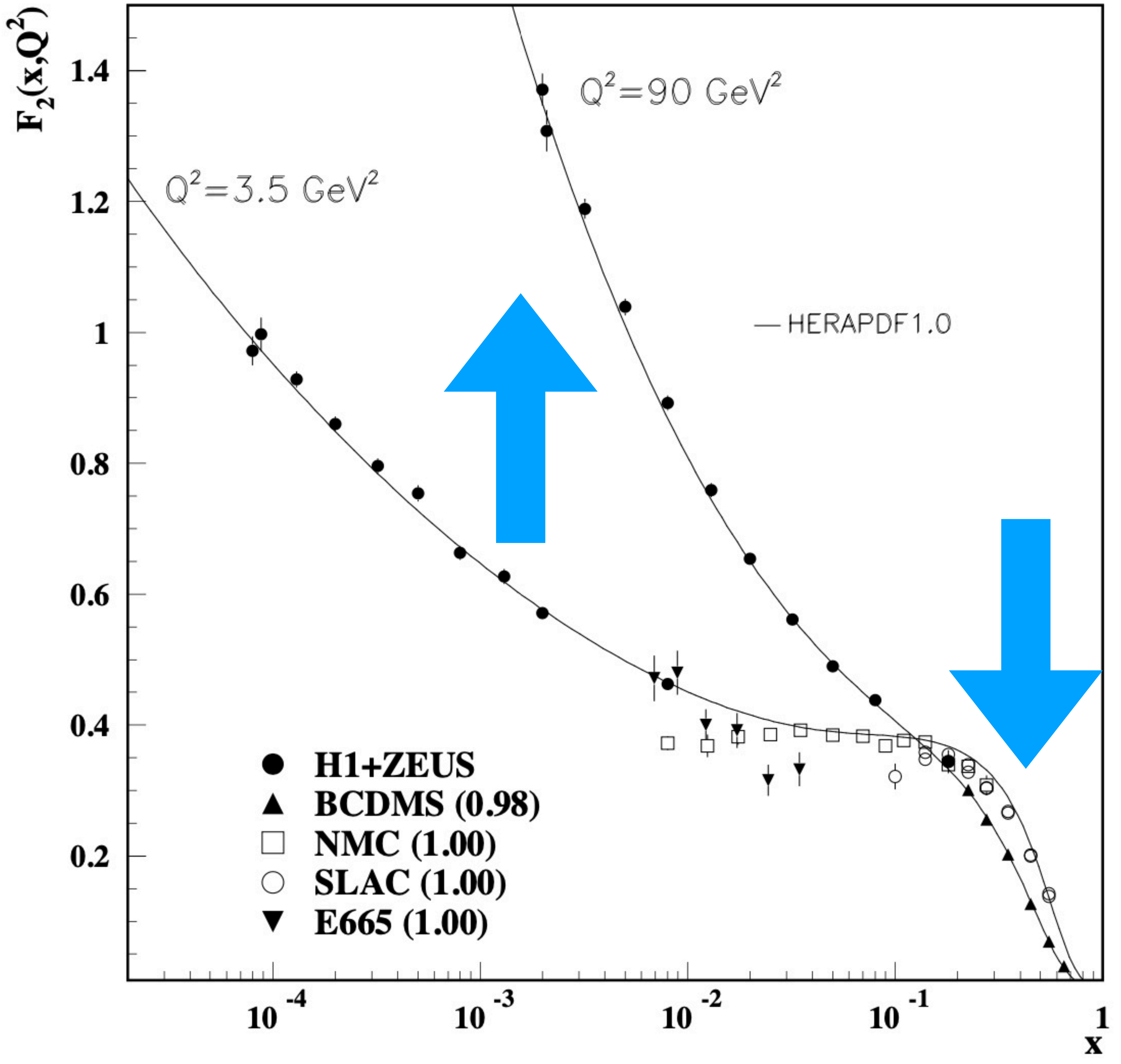

Scale evolution of PDFs in Bjorken limit

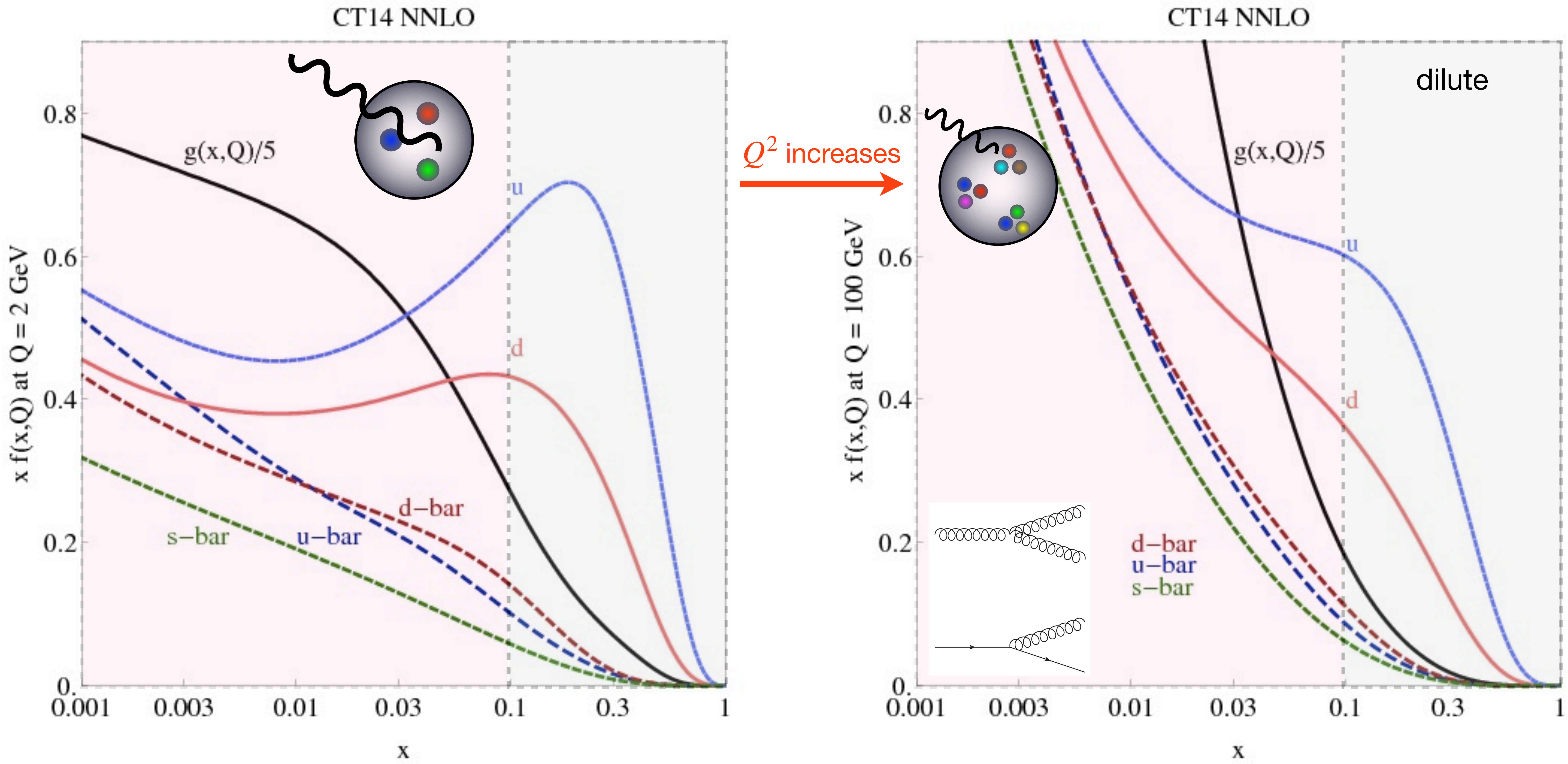

❖ DGLAP equations resum $\alpha_s \ln(Q^2)$-type enhanced corrections. (x is fixed)

❖ The double logs approximation of DGLAP equations at small-x can be solved analytically: $xf_g \sim e^{\sqrt{\ln(1/x)\ln(Q^2)}}$

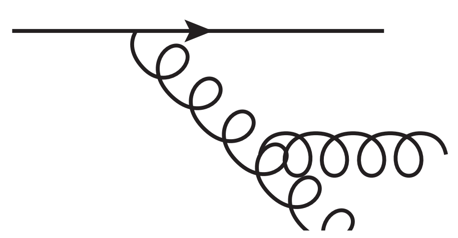

$$\alpha_s \int_{\Lambda^2}^{Q^2} \frac{dk_T^2}{k_T^2} = \alpha_s \ln(Q^2/\Lambda^2)$$

Validity of perturbative expansion

Let us think about LO splitting functions of DGLAP evolution:

Important channels in the small-x limit

$$P_{q\to g} \propto \frac{1}{x}$$

$$P_{g\to g} \propto \frac{1}{x}$$

Important channels in the large-x limit

$$P_{q\to q} \propto \frac{1}{1-x}$$

$$P_{g\to g} \propto \frac{1}{1-x}$$

❖ Even if $\alpha_s \ll 1$, perturbative calculations are unreliable at the edge of phase space: $x \sim 0$ or $x \sim 1$.

❖ In addition to higher-order corrections, one must consider resummations: small-x resummation and threshold resummation (**not considered now**).

❖ Power corrections are also important (**will be discussed later**).

Regge-Grobov limit

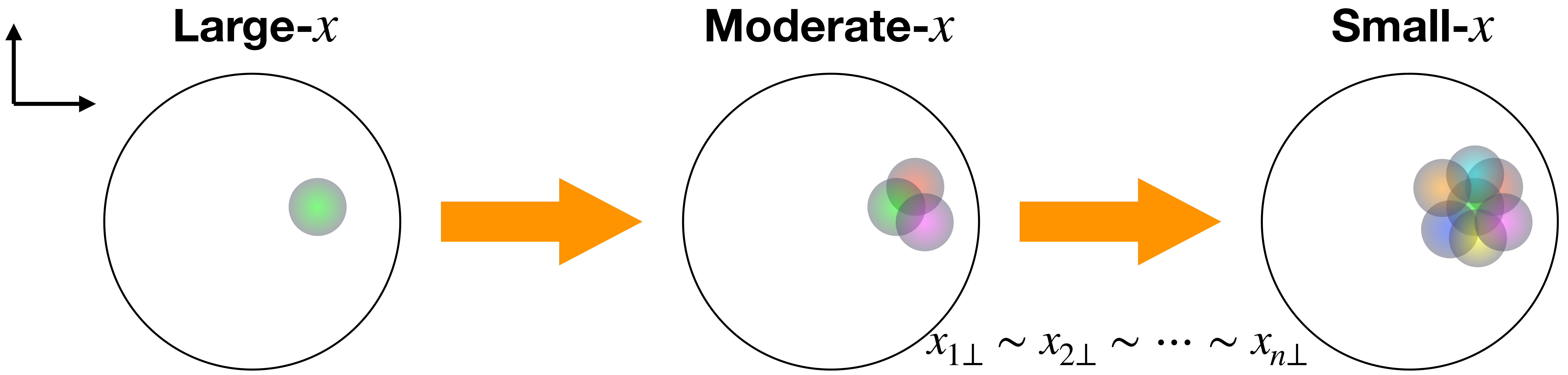

- ❖ The number of partons increases due to the increased longitudinal phase space as $x \to 0$.
- ❖ The radiated gluons are of the same transverse size ($x_\perp \sim 1/Q$).
- ❖ BFKL equation resums large $\alpha_s \ln(1/x)$-type corrections.
- ❖ Hadron/nucleus becomes dense. A quasi-free parton picture is not so useful.

Resummations

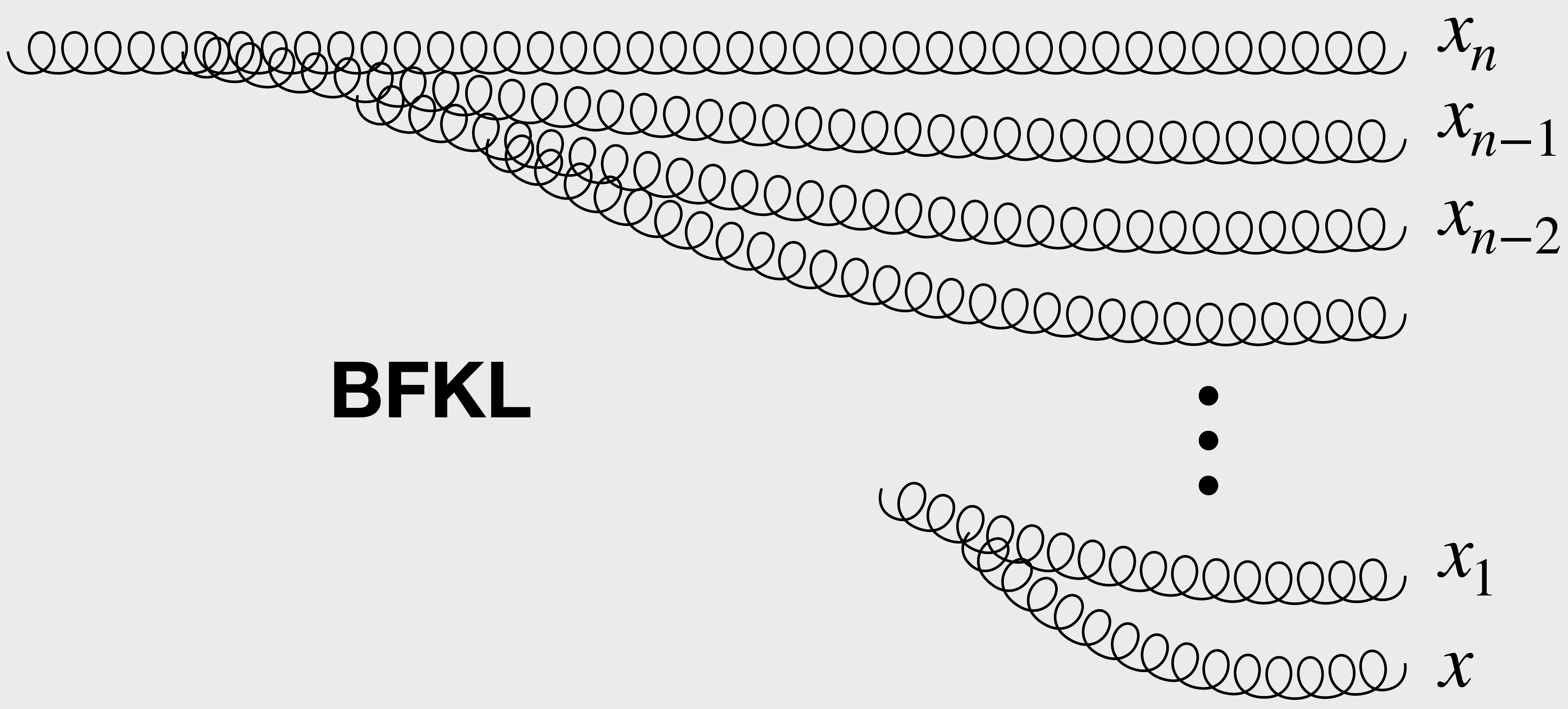

BFKL

Strong ordering in longitudinal momenta:

$$x \ll x_1 \ll x_2 \ll \cdots \ll x_{n-1} \ll x_n$$

Leading log resummation: $\left(\dfrac{\alpha_s}{2\pi}\ln\dfrac{1}{x}\right)^n$

Logs of energy as $x \propto 1/E$

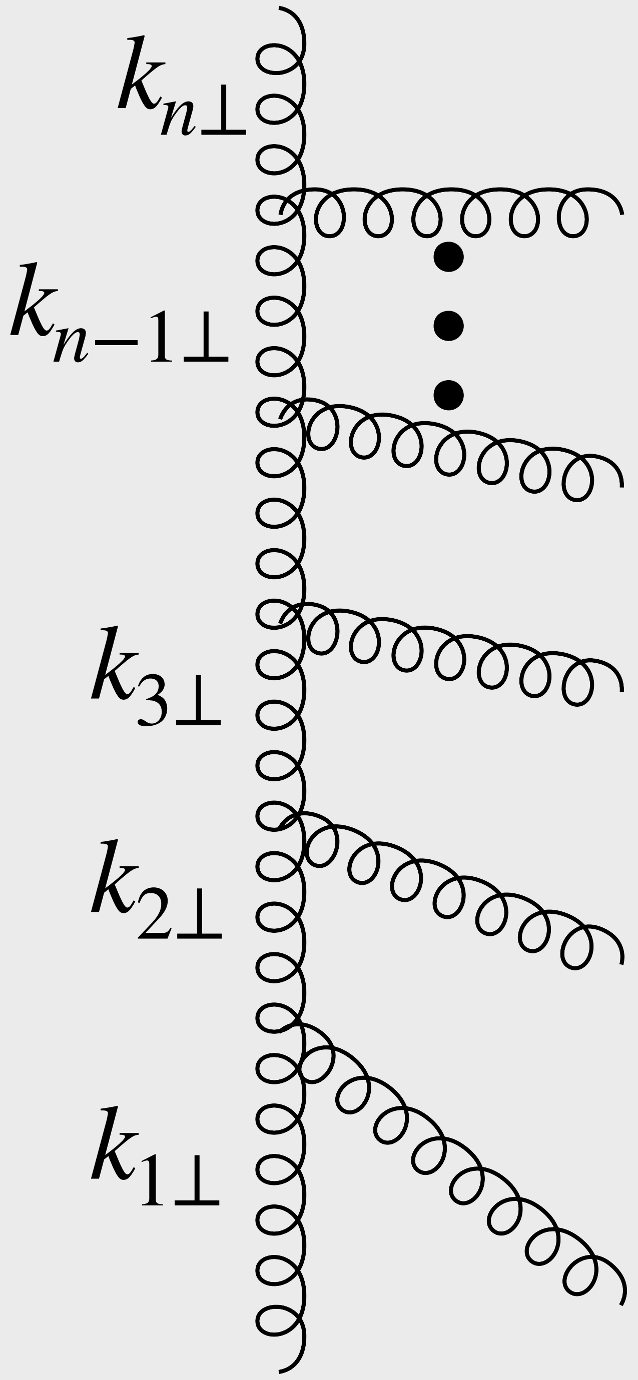

DGLAP

Strong ordering in transverse momenta:

$$Q^2 \gg k_{1\perp}^2 \gg k_{2\perp}^2 \gg \cdots k_{n-1\perp}^2 \gg k_{n\perp}^2$$

Leading log resummation: $\left(\dfrac{\alpha_s}{2\pi}\ln\dfrac{Q^2}{\mu_0^2}\right)^n$

Logs of relative scale

Balitsky-Fadin-Kuraev-Lipatov evolution

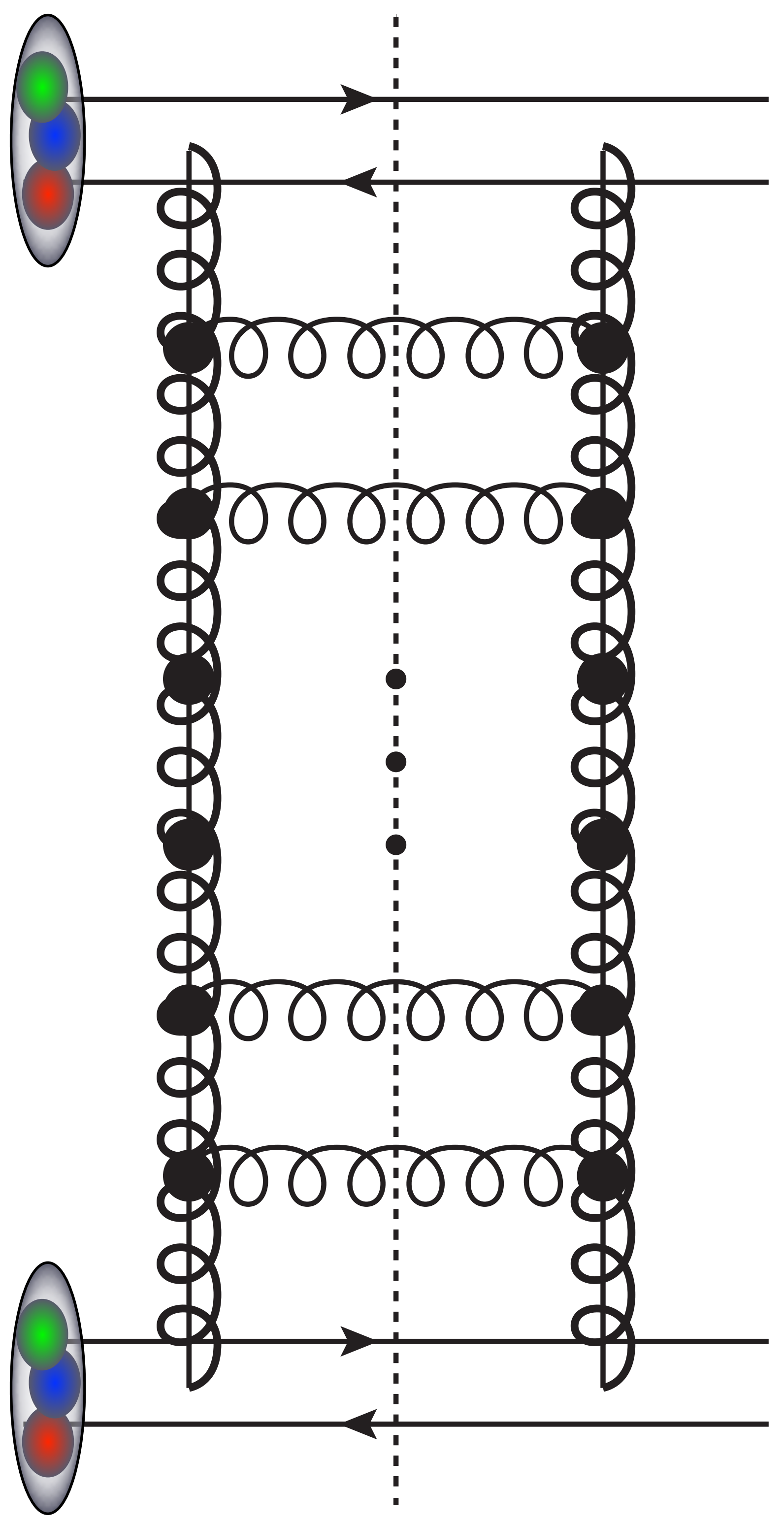

Unintegrated gluon distribution $\phi(x, Q^2) = \partial x f_g(x, Q^2)/\partial Q^2$ obeys BFKL equation:

$$\frac{\partial \phi(x, k_\perp)}{\partial \ln(1/x)} = \frac{\alpha_s N_c}{\pi^2} \int \frac{d^2 q_\perp}{(k_\perp - q_\perp)^2} \left[\phi(x, q_\perp) - \frac{k_\perp^2}{2q_\perp^2} \phi(x, k_\perp) \right]$$

$$\phi(x, k_\perp) \sim e^{(\alpha_P - 1)Y} \sim \left(\frac{1}{x}\right)^{\alpha_P - 1}$$

A choice, different from the standard definition in the com frame.

❖ Intercept of the BFKL perturbative pomeron: $\alpha_P - 1 = \frac{4\alpha_s N_c}{\pi} \ln 2 \sim 0.79 \quad (\alpha_s = 0.3)$

❖ QCD factorization + resum of $\ln(x)$: CCFM evolution (Catani-Ciafaloni-Fiorani-Marchesini)

M. Ciafaloni, Nucl. Phys. B 296, 49 (1988). S. Catani, F. Fiorani, and G. Marchesini, Phys. Lett. B234, 339 (1990). S. Catani, F. Fiorani, and G. Marchesini, Nucl. Phys.B 336, 18 (1990). G. Marchesini, Nucl. Phys. B 445, 49 (1995).

Importance of resummation at small-x

xFitter Developers' Team, EPJC78, no.8, 621 (2018)

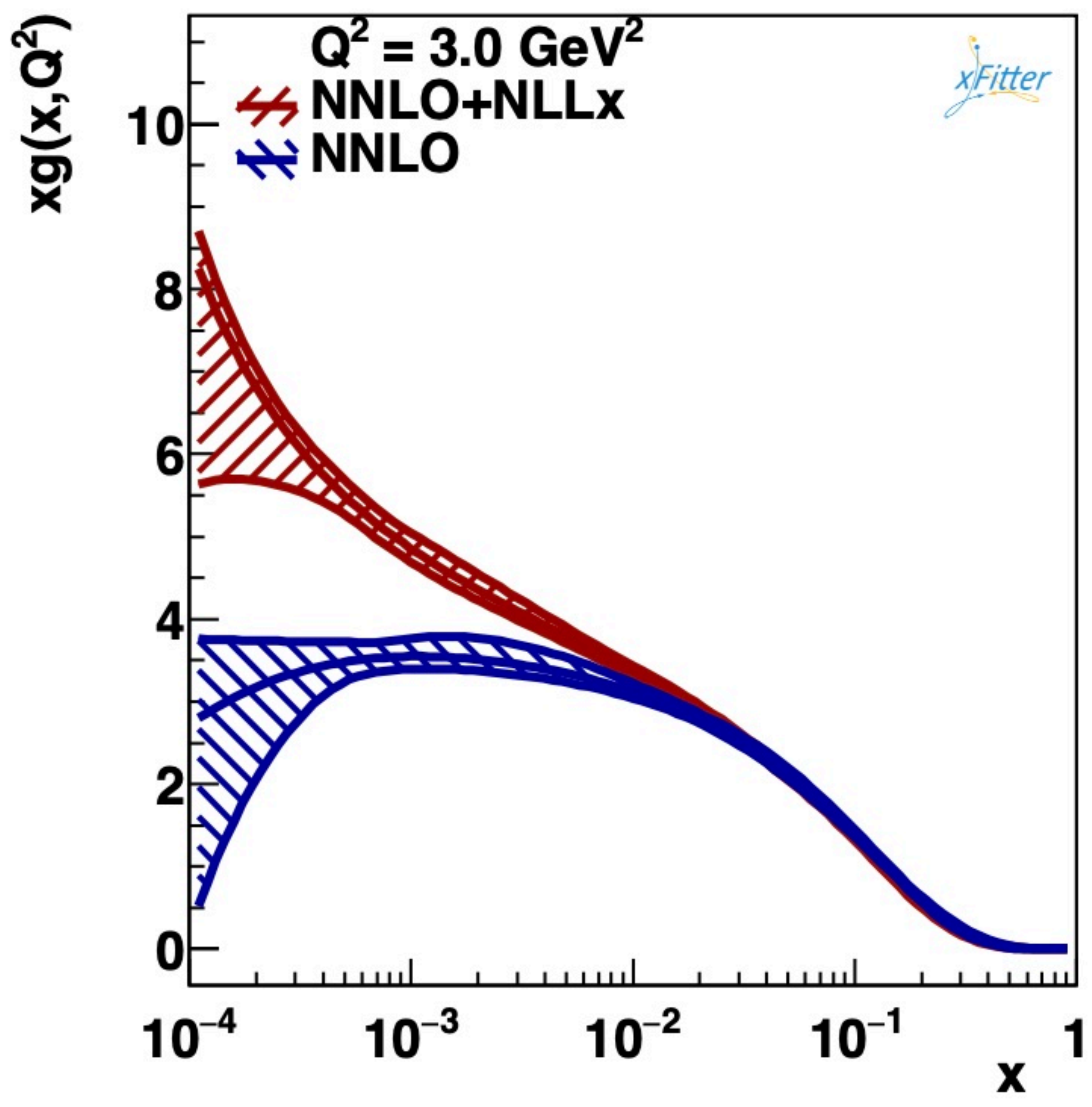

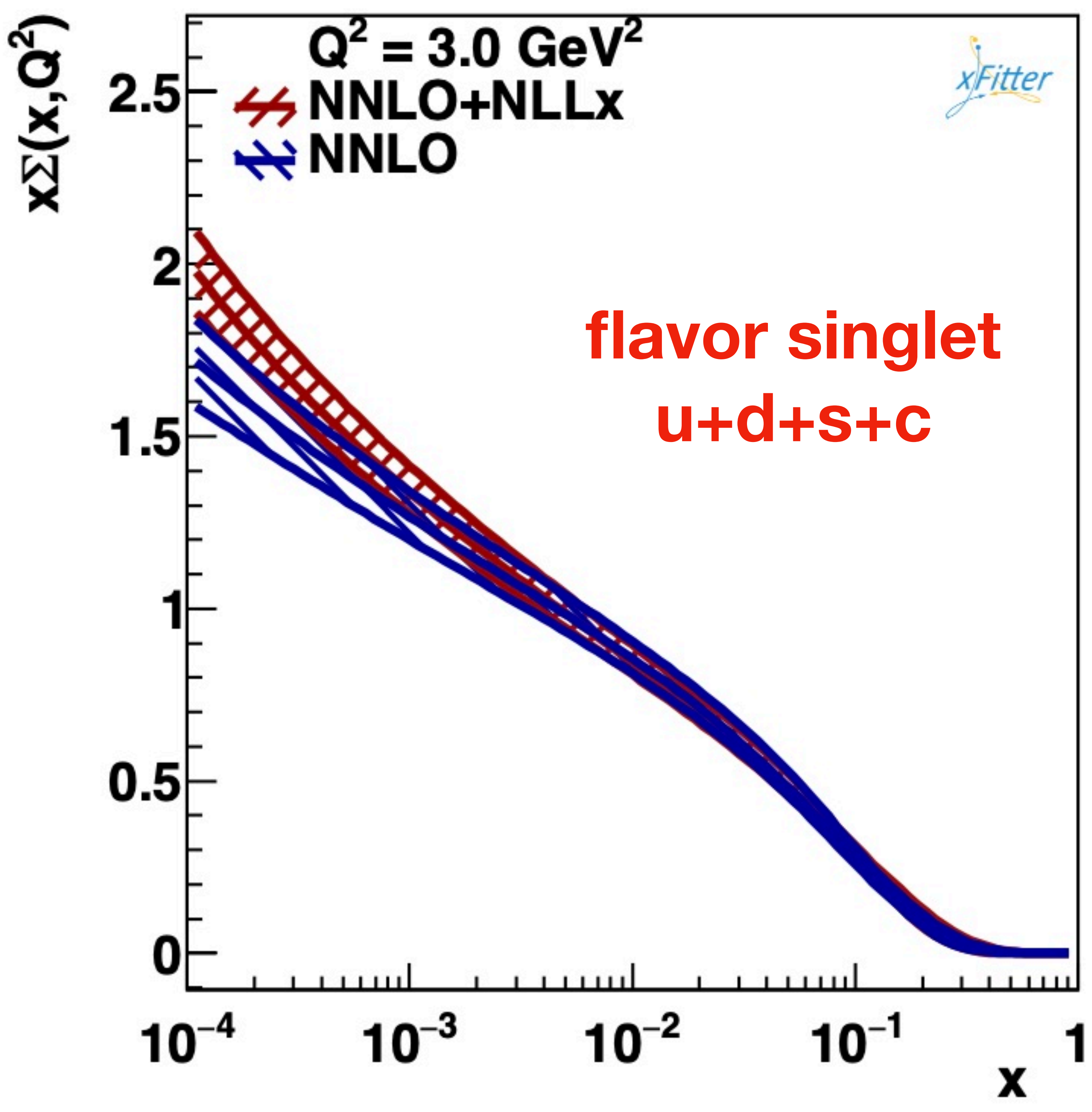

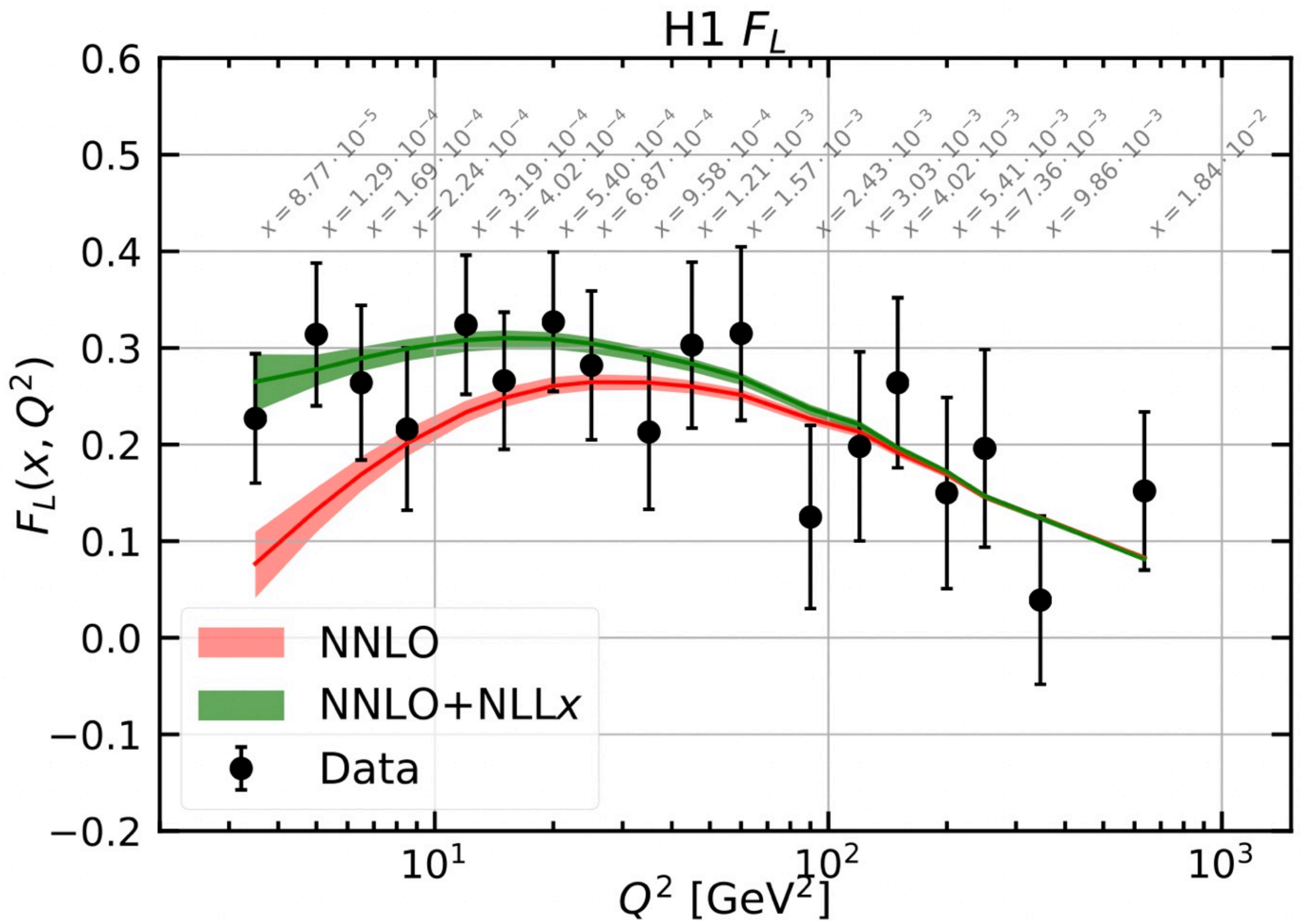

For NLLx, see [Bonvini, Marzani and Peraro,Eur. Phys. J. C76, no.11, 597 (2016)]

- ❖ **NLLx (next-to-leading-log accuracy in** $\ln(1/x)$**) :** $P^{\rm NNLO} + P^{\rm NLLx}$ and $C^{\rm NNLO}_{\rm DIS} + C^{\rm NLLx}_{\rm DIS}$
- ❖ Fixed order calculations are unstable and can lead to negative gluon density, cured by the resummation at small-x.
- ❖ Near the charm mass threshold, the cham PDF impacts on the gluon PDF.

DIS in Dipole frame at high energy

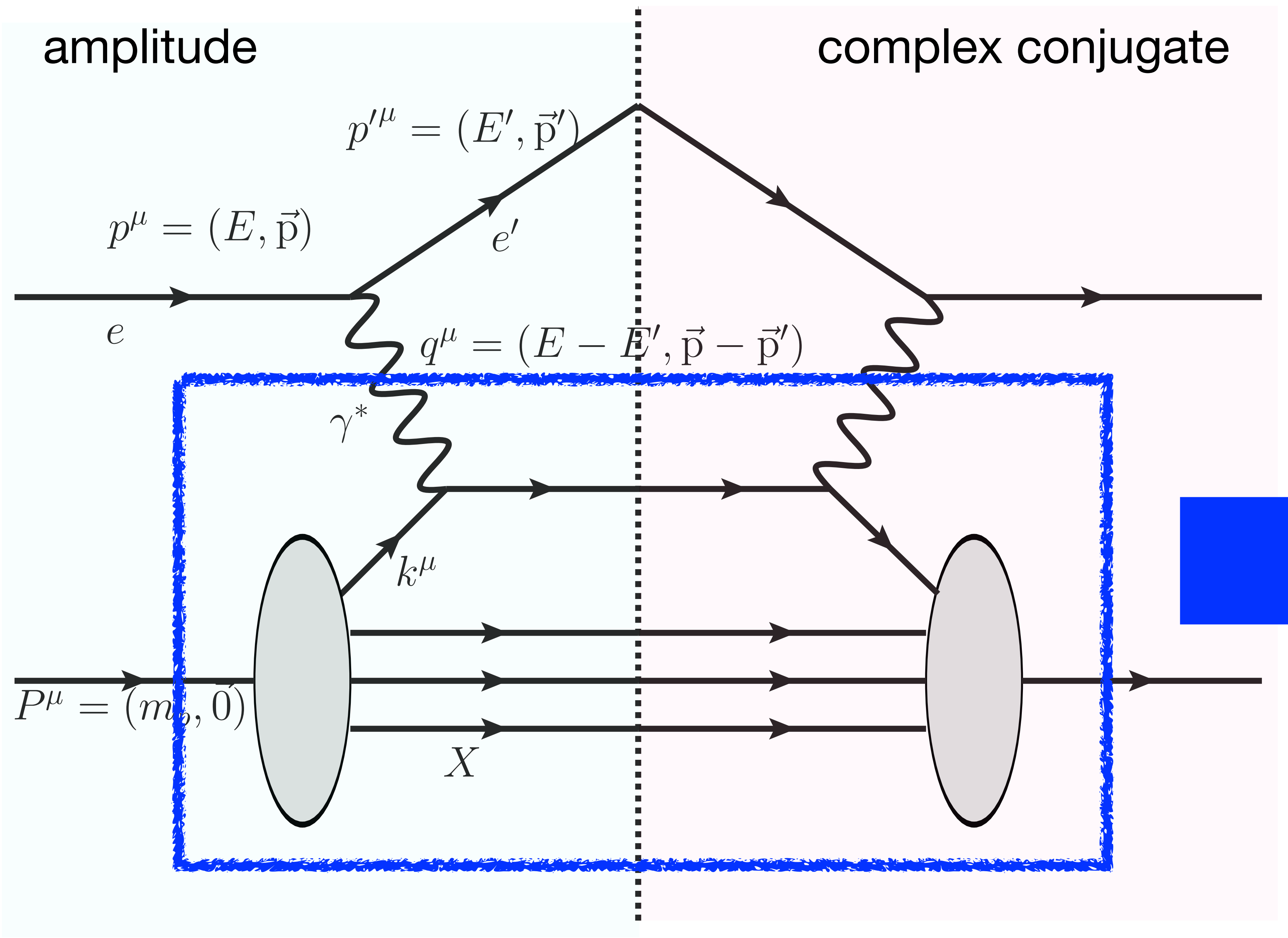

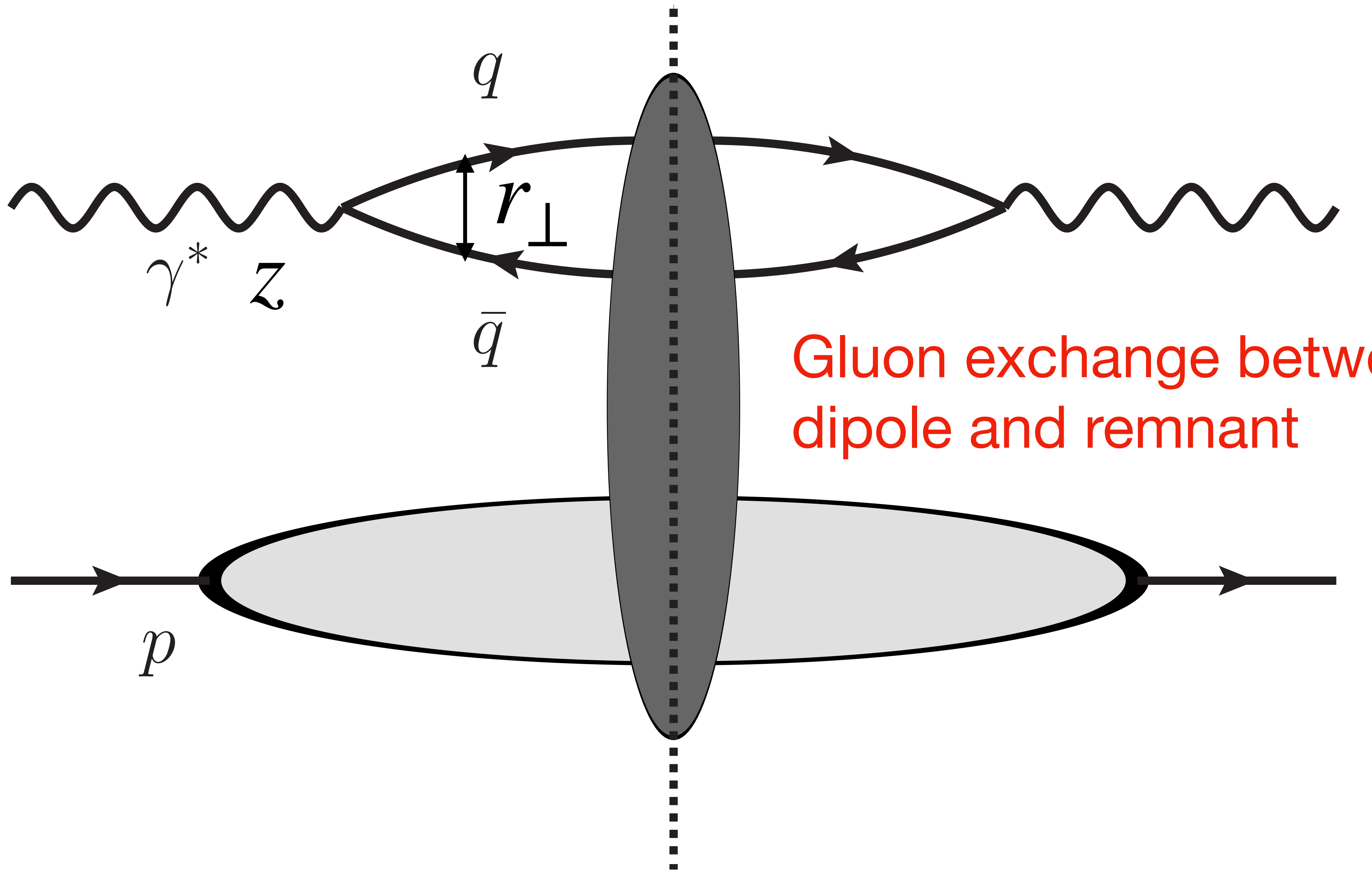

- Both the proton and photon move along the z-axis in opposite directions.
- The standard partonic picture is no longer valid.

Factorization at high s

$$\sigma_{tot}^{\gamma^* A}(x, Q^2) = \int d^2 r_\perp \int_0^1 dz \left| \Psi^{\gamma^* \to q\bar{q}}(r_\perp, z, Q^2) \right| \hat{\sigma}_{tot}^{q\bar{q}A}(r_\perp, x)$$

QED part: calculable in light-cone perturbation theory

QCD part: the dipole amplitude

BFKL evolution in Dipole frame

Mueller's dipole model: Mueller (1994)

q

$\bar{q}$

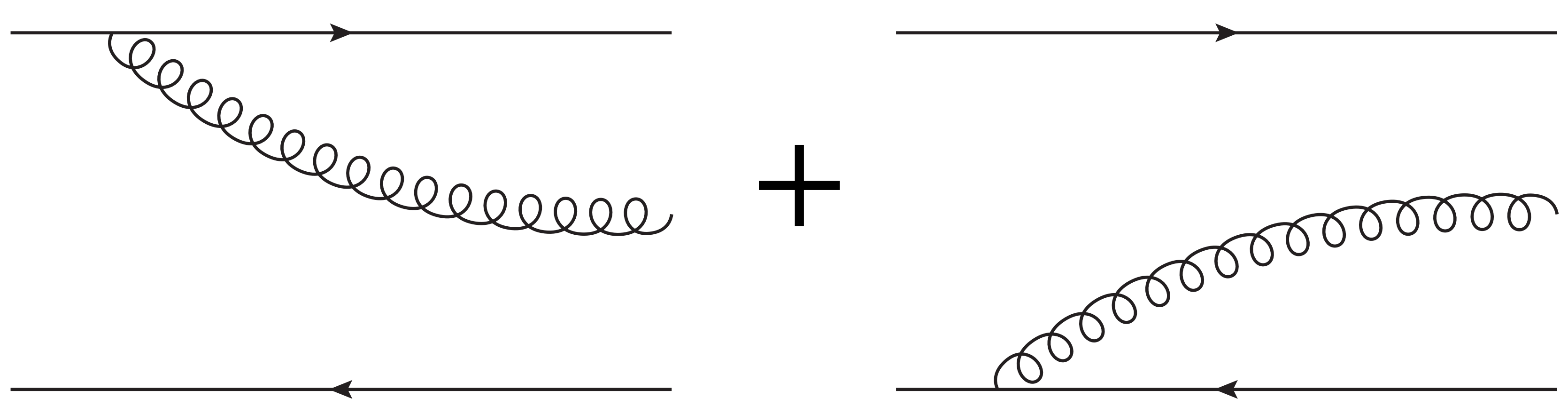

large-Nc

$$C_F = \frac{N_c^2 - 1}{2N_c} \to \frac{N_c}{2}$$

$$Y = \ln(z_1/z_0)$$

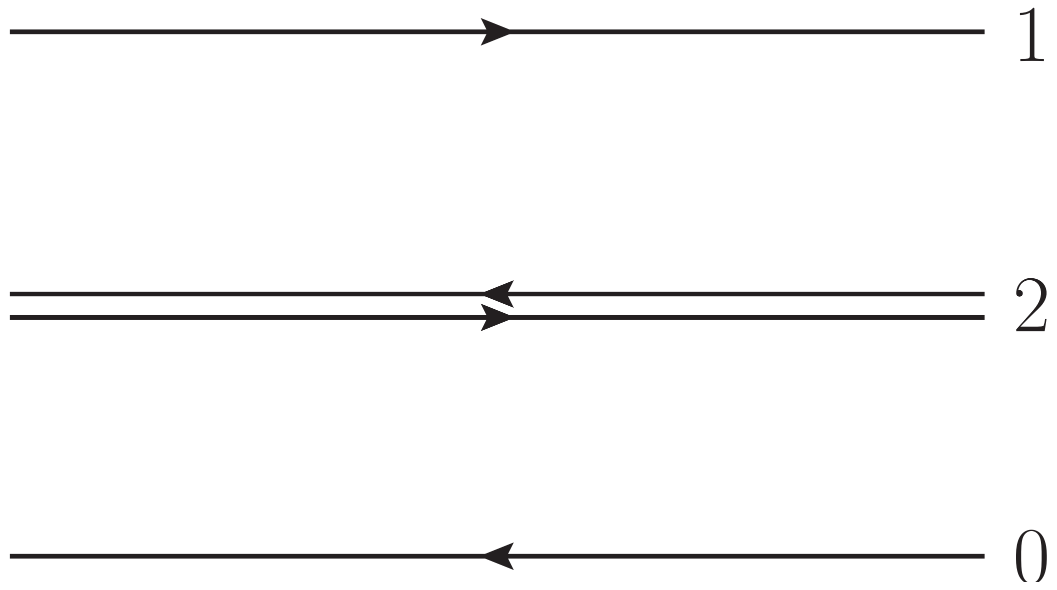

$z_1 = k_1^+/p^+$

$\gg$

$z_2 = k_2^+/p^+$

$\gg$

$z_0 = k_0^+/p^+$

Two daughter dipoles (Real)

$$\frac{\partial}{\partial Y} N(x_{10}, Y) = \frac{\alpha_s N_c}{2\pi^2} \int d^2 x_2 \frac{x_{10}^2}{x_{20}^2 x_{21}^2} \left[N(x_{12}, Y) + N(x_{20}, Y) - N(x_{10}, Y) \right]$$

Parent dipole

Absorption (Imaginary)

Parent dipole's size

$$x_{10} = |\vec{x}_{1\perp} - \vec{x}_{0\perp}|$$

Daughter dipole's size

$$x_{21} = |\vec{x}_{2\perp} - \vec{x}_{1\perp}| \qquad x_{20} = |\vec{x}_{2\perp} - \vec{x}_{0\perp}|$$

Problems of BFKL evolution

❖ Problem 1: Total x-section in hadronic collisions

➡ BFKL evolution gives $\sigma_{tot} \sim s^{\alpha_P - 1}$ (Hard pomeron)

➡ Data fit gives $\sigma_{tot} \sim s^{0.1}$ (soft pomeron)

A. Donnachie and P. V. Landshoff, PLB727, 500-505 (2013) [erratum: PLB750, 669-669 (2015)]

➡ $\sigma_{tot} \sim s^{\alpha_P - 1}$ can violate the unitarity (Froissart-Martin bound) $\sigma_{tot} \propto \ln^2 s$ at an extreme high s, which may be higher than the highest collider energies.

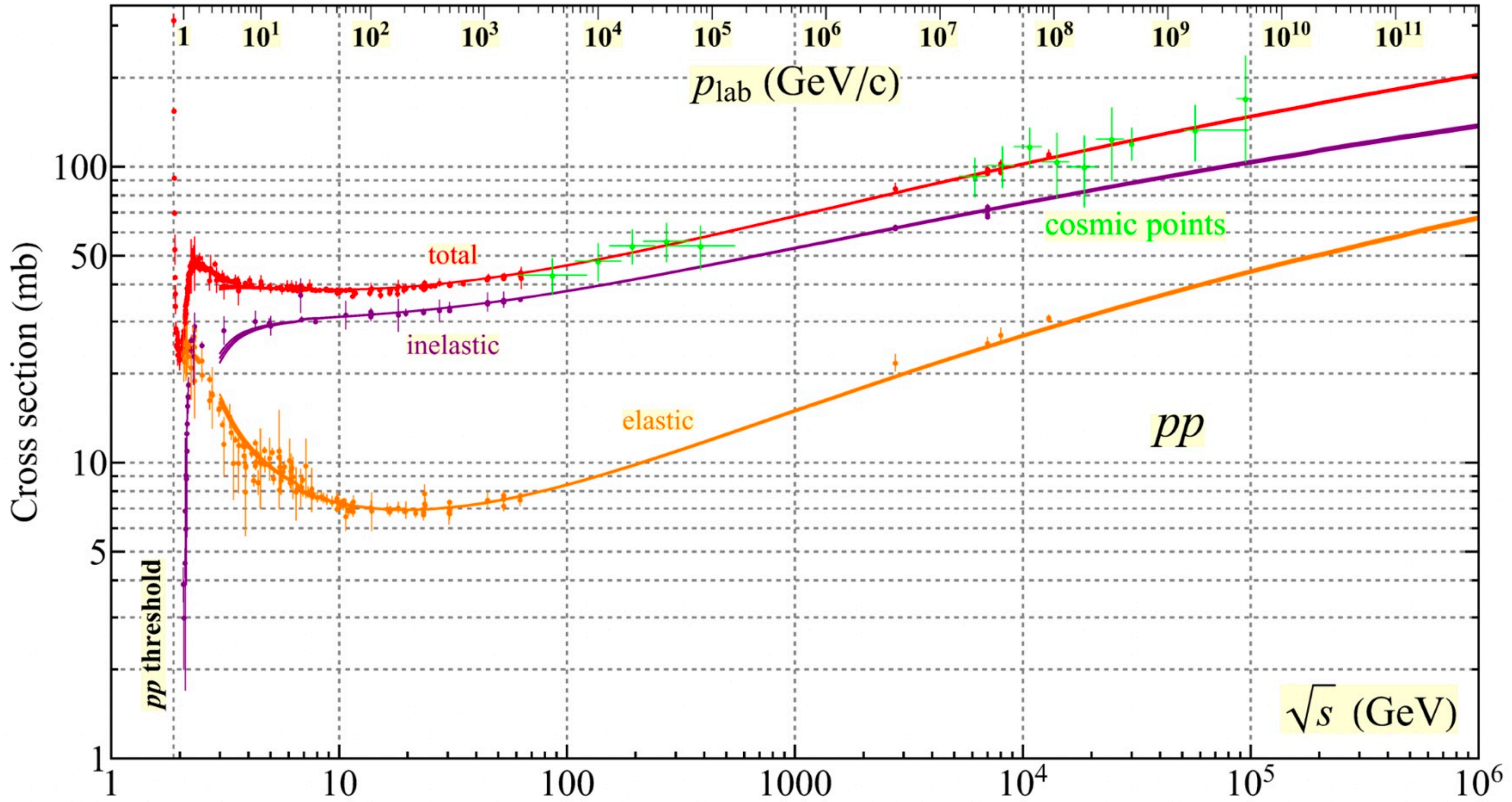

❖ Problem 2: Infrared gluons

Diffusion of the gluon **ladder** in the BFKL equation happens, so perturbative gluons could go to the Infrared regime.

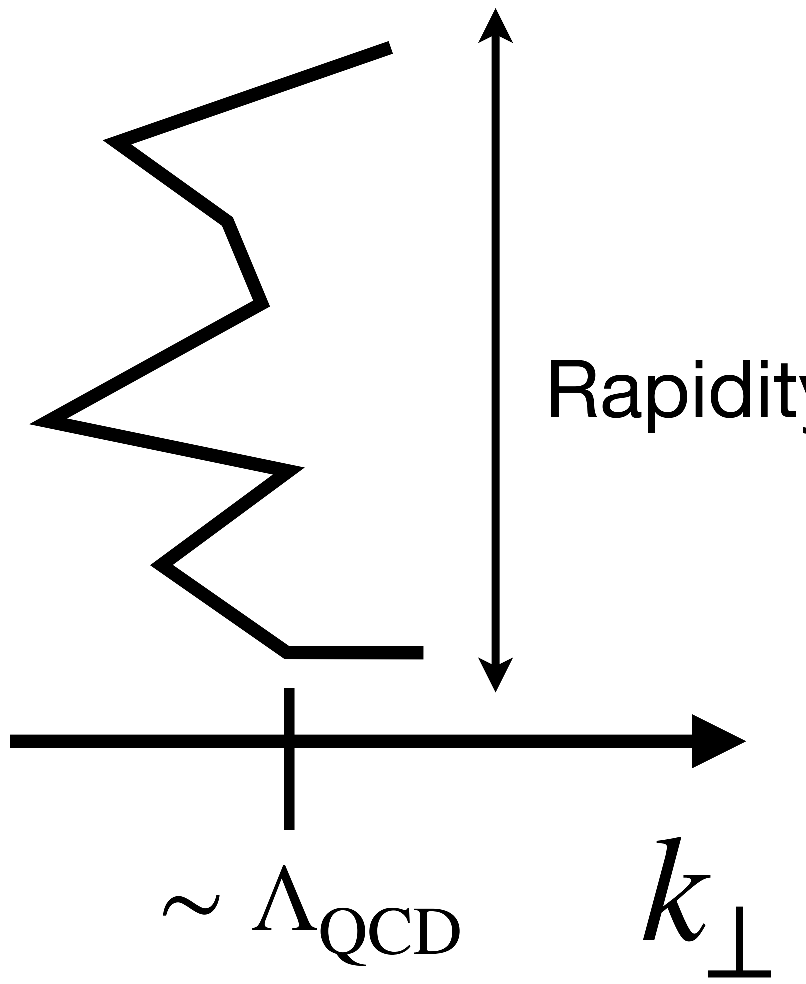

Gluon recombination

Gribov, Levin and Ryskin, Phys. Rept. 100, 1 (1983)
Mueller and Qiu, NPB268, 427 (1986), Qiu, NPB291, 746 (1987)

Modified DGLAP (GLV-MQ) equation at small-x:

$$\frac{\partial xf_g}{\partial \ln(1/x)\,\partial \ln \mu^2} = \frac{\alpha_s N_c}{\pi}\left(xf_g\right) - \frac{1}{\mu^2}\frac{\alpha_s^2 N_c \pi}{2C_F S_\perp}\left(xf_g\right)^2$$

$$xf_g(x,Q^2) = \int^{Q^2} dk_\perp^2\, \phi(x,k_\perp)$$

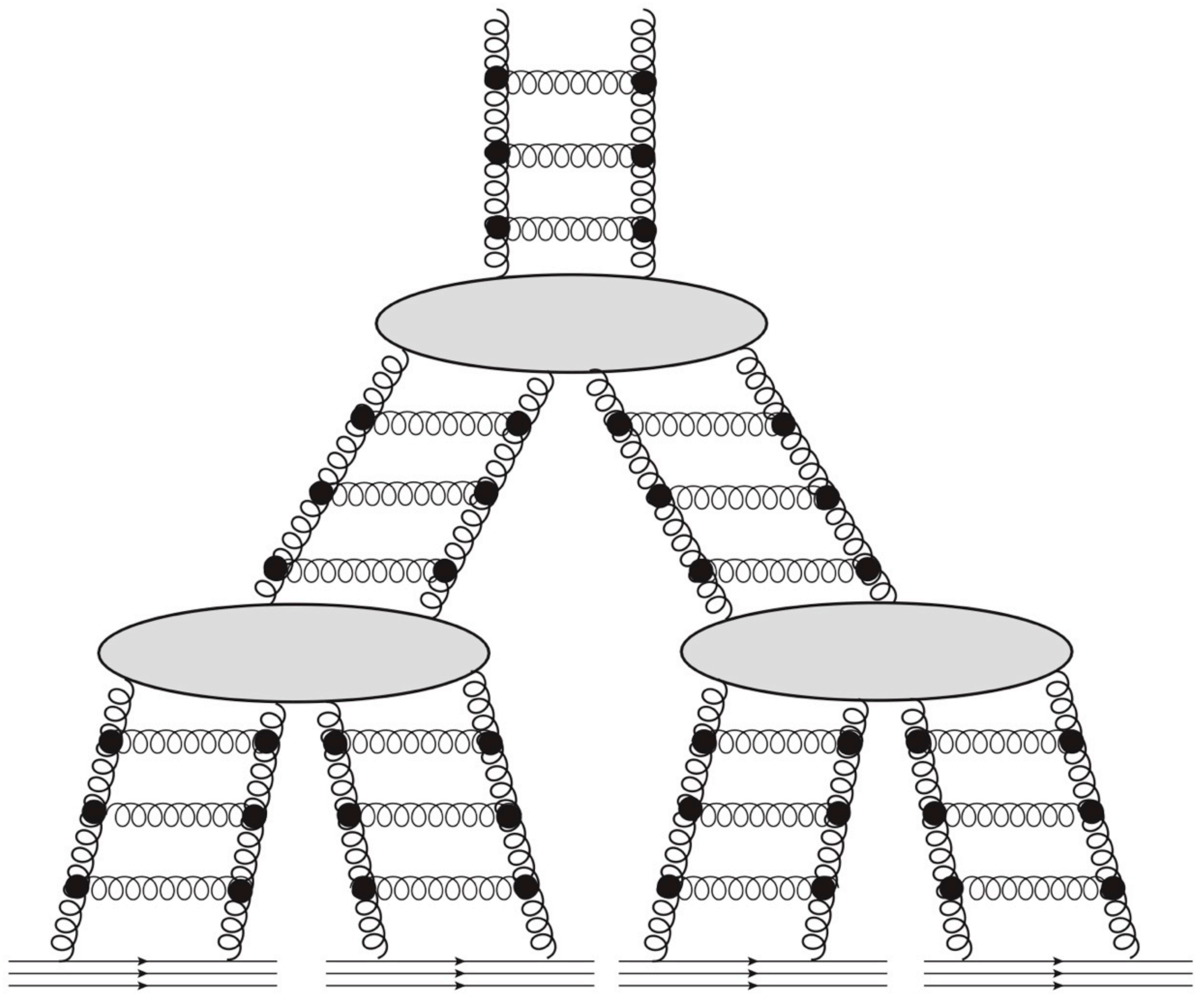

- Gluon recombination slows down the small-x evolution.
- The nonlinear term is a higher twist correction, suppressed by $1/\mu^2$, but remains to be significant even at high μ^2.
- All-twist contributions are equally important at small-x (**Wilson line**).

$$\frac{\partial xf_g}{\partial \ln(1/x)\,\partial \ln \mu^2} = 0 \longrightarrow Q_s^2 \sim \mu^2 = \frac{\alpha_s \pi^2 xf_g}{2C_F S_\perp}$$

large occupation number : strong field

$$N_g \sim \frac{xf_g}{S_\perp Q_s^2} \sim \frac{1}{\alpha_s}$$

The gluon density can be “saturated”.

Geometric Scaling from HERA

DIS total cross section ($\sigma_{tot}^{\gamma^* p}$) is the function of only one dimensionless variable τ:

$$\tau \sim \frac{Q^2}{Q_0^2}\left(\frac{x}{x_0}\right)^{\lambda}$$

$$Q_0 = 1\,\mathrm{GeV}, \quad \lambda = 0.288, \quad x_0 = 3.04 \times 10^{-4}$$

- ❖ The scaling is seen at $x \leq 0.01$ even at high Q^2.
- ❖ $\lambda \sim 0.3$: a slower x-dependence and consistent with running coupling BK eq. (**later**)

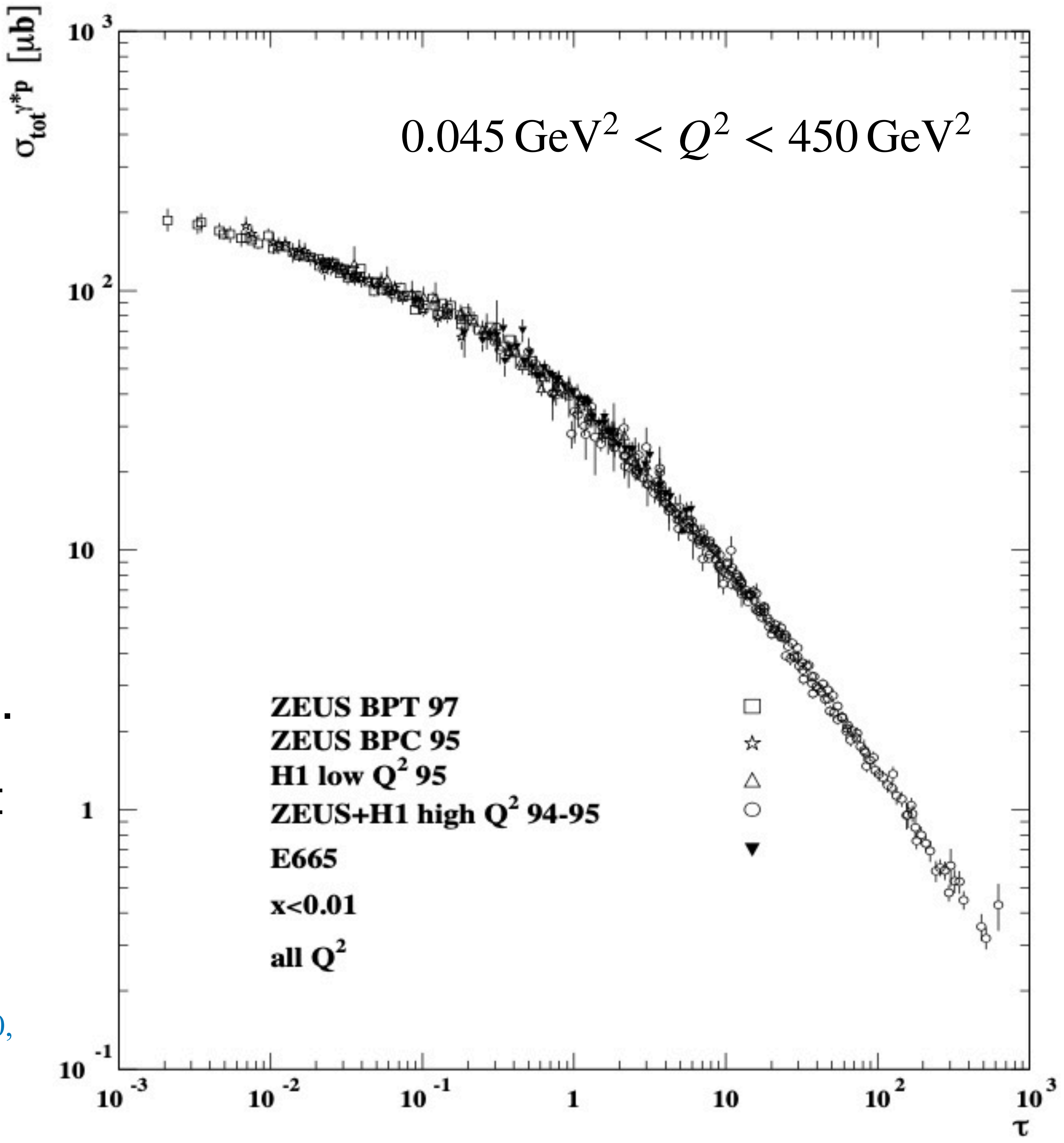

Golec-Biernat and Wusthoff, PRD59, 014017 (1998), PRD60, 114023 (1999)
Stasto, Golec-Biernat and Kwiecinski, PRL86, 596 (2001)

Color Glass Condensate (CGC): Gluonic matter

Color: Quarks and gluons carry color charges.

Glass: Small-x gluons evolve slowly. A loose analogy to "Spin Glass".

Condensate: High gluon density. A loose analogy to "Bose Condensate".

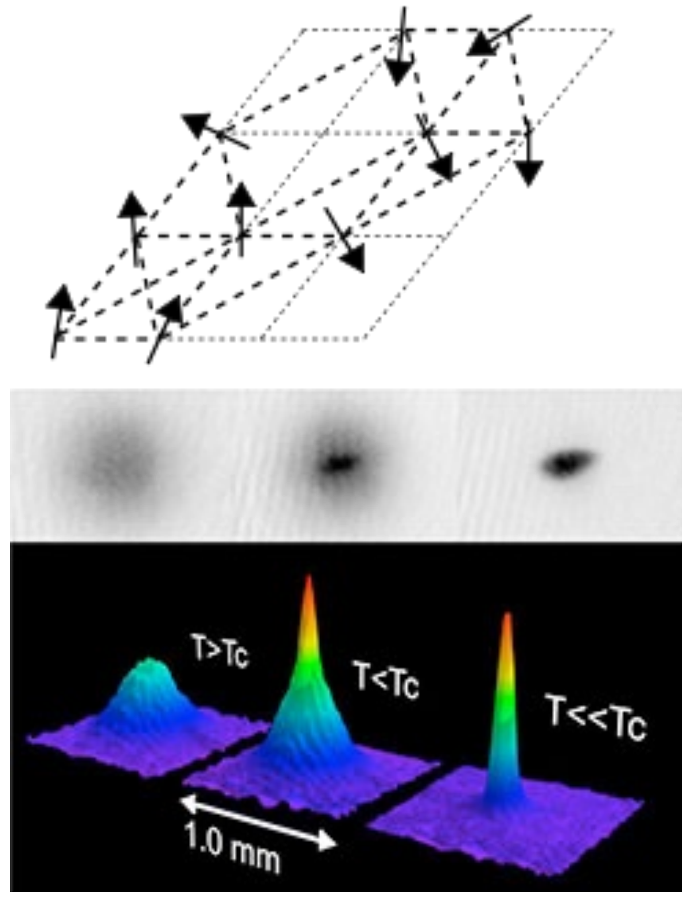

https://coldatomlab.jpl.nasa.gov/sciencebackground/

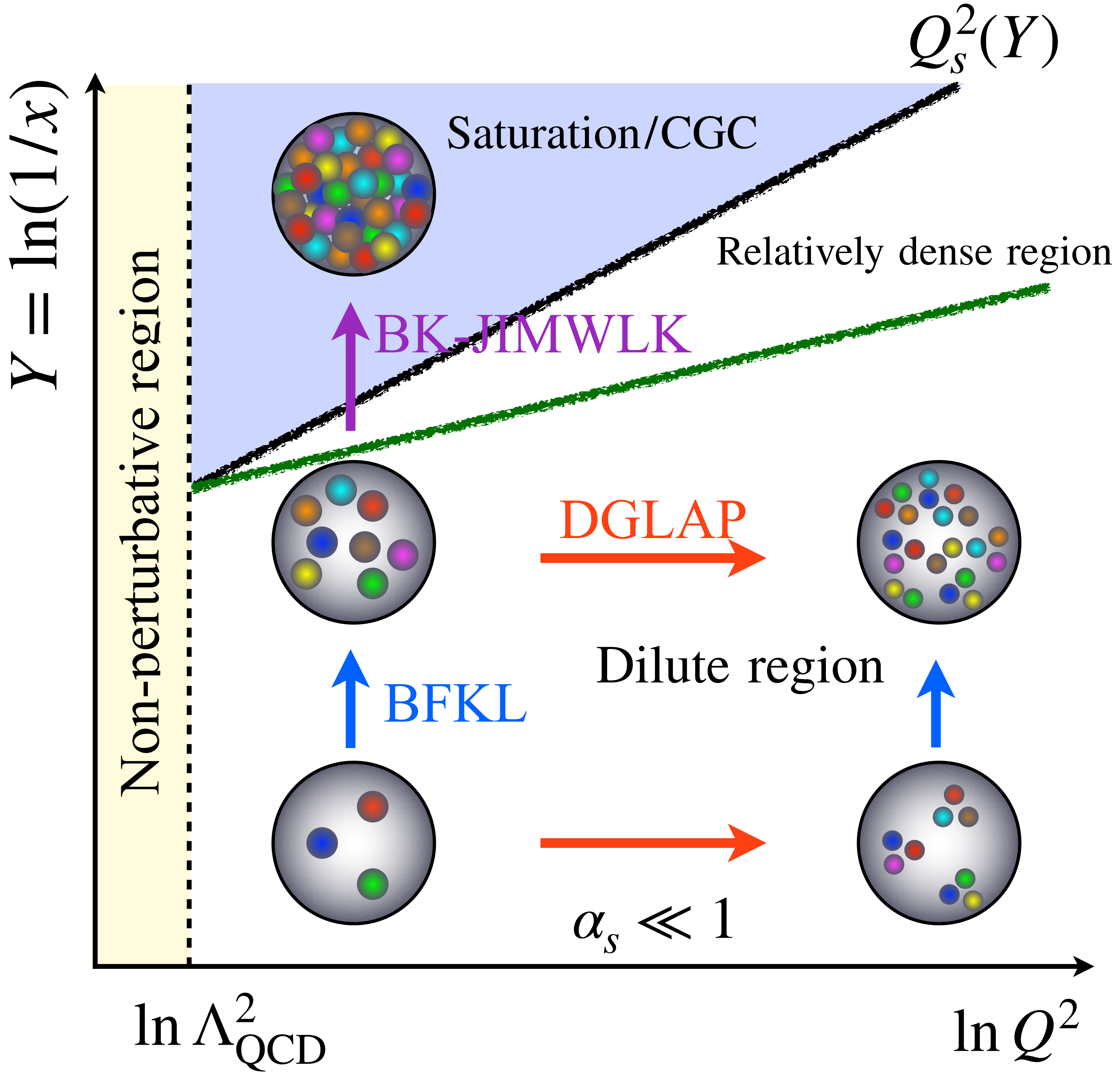

- Gluons per unit area: $\rho \propto \dfrac{Axf_g}{\pi R_A^2}$
- Recombination: $\sigma_{gg\to g} \propto \dfrac{\alpha_s}{Q^2}$
- Saturation starts when $\rho\sigma_{gg\to g} \sim \mathcal{O}(1)$ leading to $Q_s^2 \propto A^{1/3}x^{-\lambda} \gg \Lambda^2_{QCD}$
- Weak-coupling theory ($\alpha_s(Q_s^2) \ll 1$) describes bulk soft particle production: **new paradigm**.

Part III:
Color-Glass-Condensate EFT

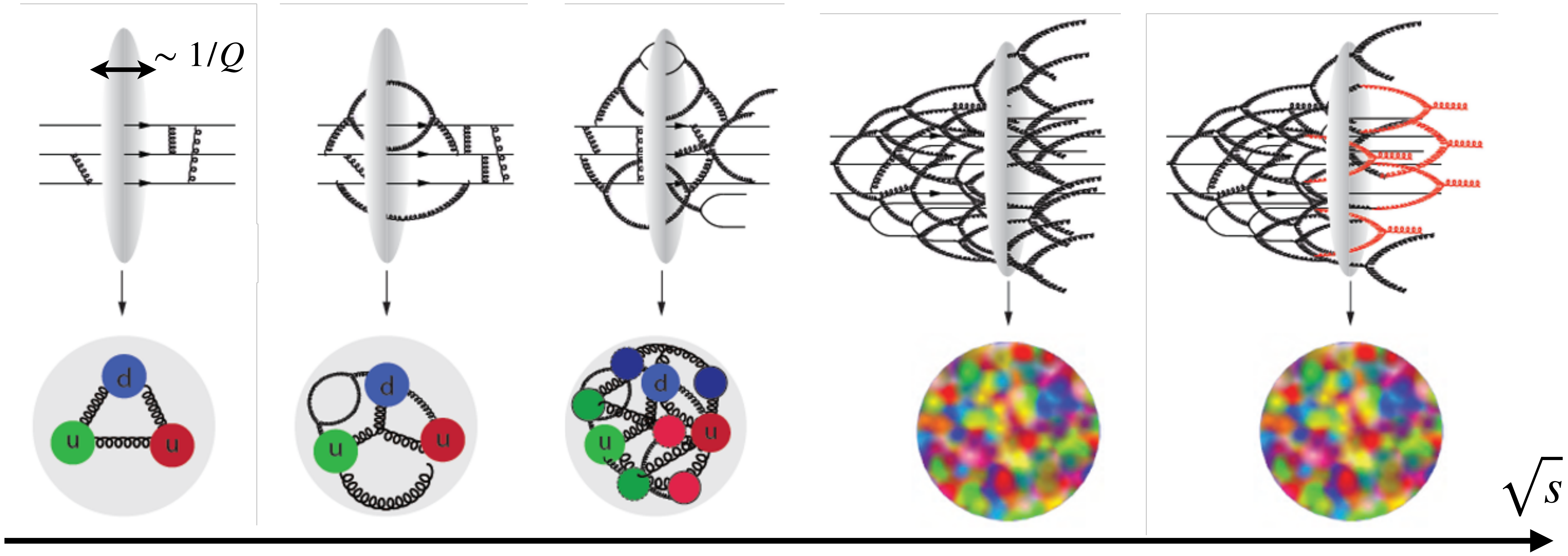

Wilson line in dipole amplitude

Interaction with background gauge field in Eikonal approximation: gauge (phase) rotation

- The quark's trajectory inside the shockwave can be frozen: Eikonal approximation.
- The interaction of the quark with the shockwave (gauge rotation) will be described by a gauge factor ordered along this segment of a straight line → Wilson line

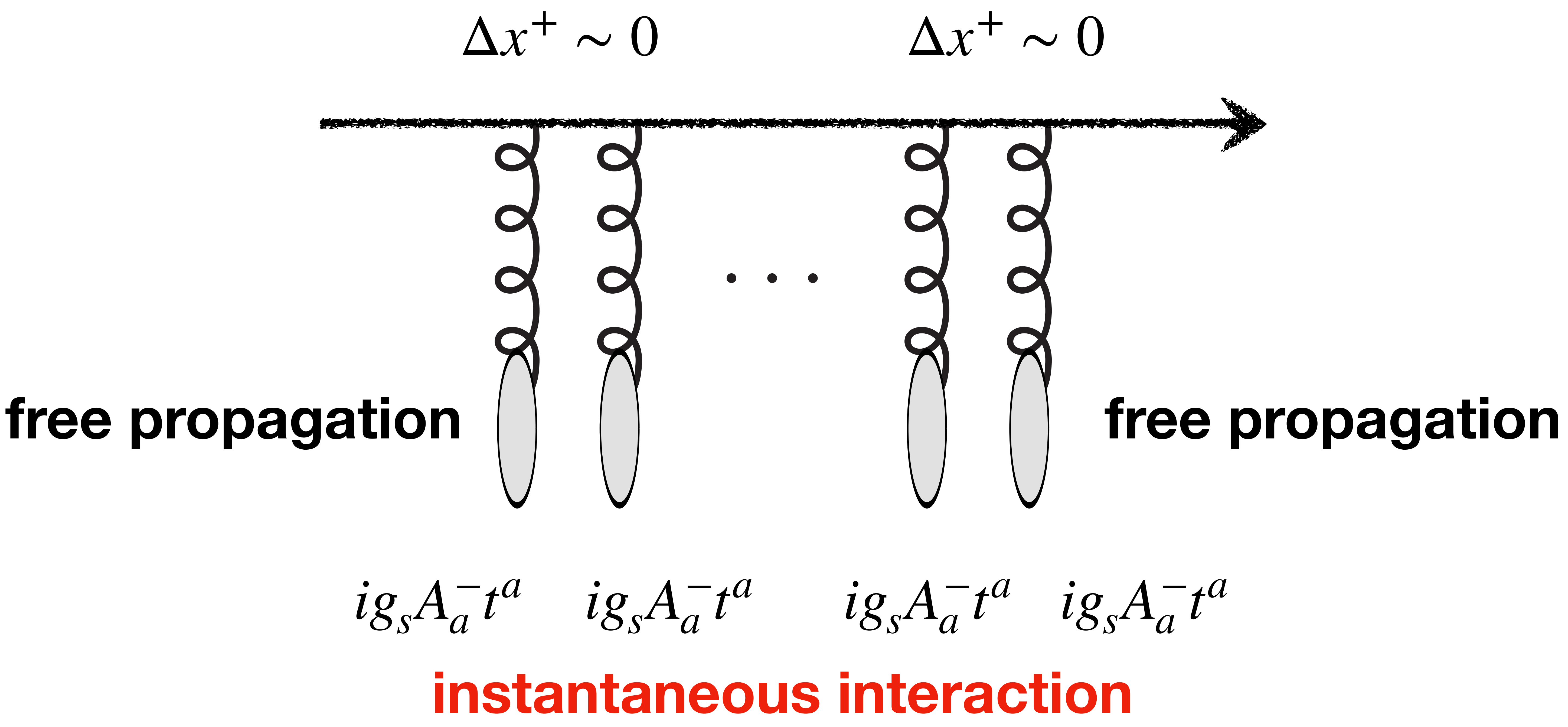

Quark and gluon receive different gauge rotations (fundamental or adjoint reps.) when traversing the shockwave.

$$U_r = \mathscr{P} \exp \left[ig_s \int_{-\infty}^{\infty} \mathrm{d}x^+ A_a^-(x^+, r) t^a \right]$$

Shockwave approximation

Background field becomes a shockwave "wall"

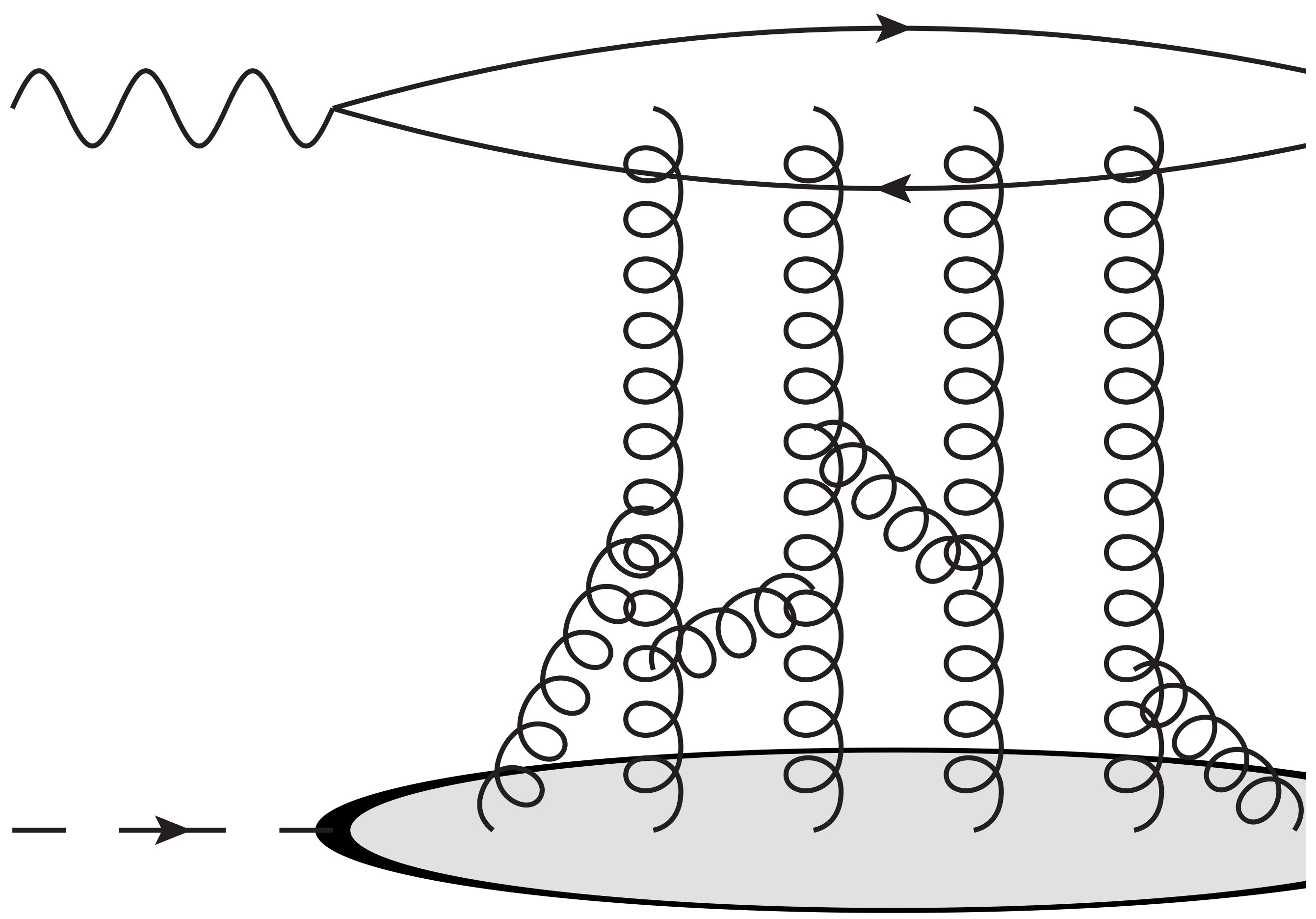

Lorentz boost

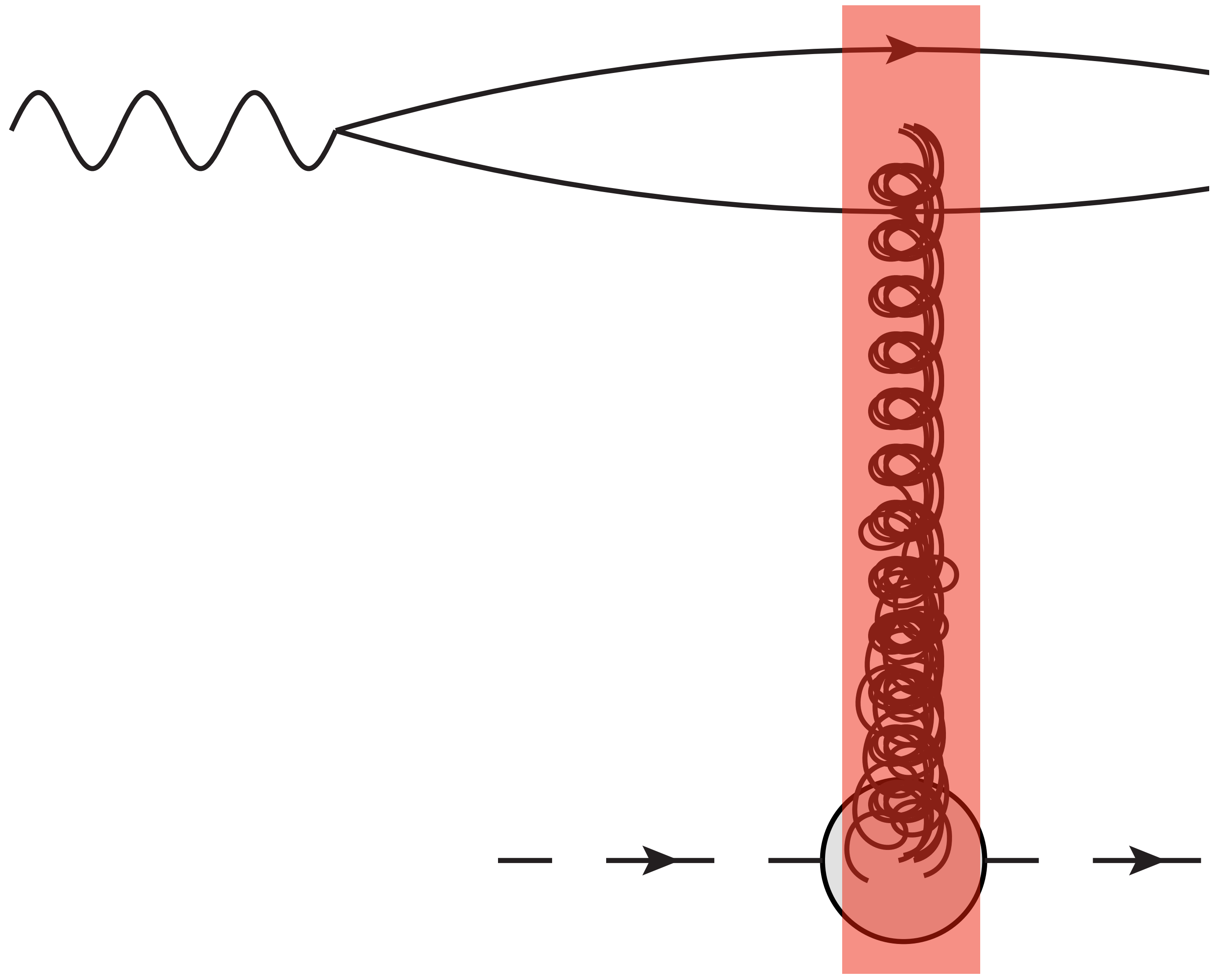

- The shockwave is very thin: coherent interaction
- The quark has no time to deviate in the transverse direction.

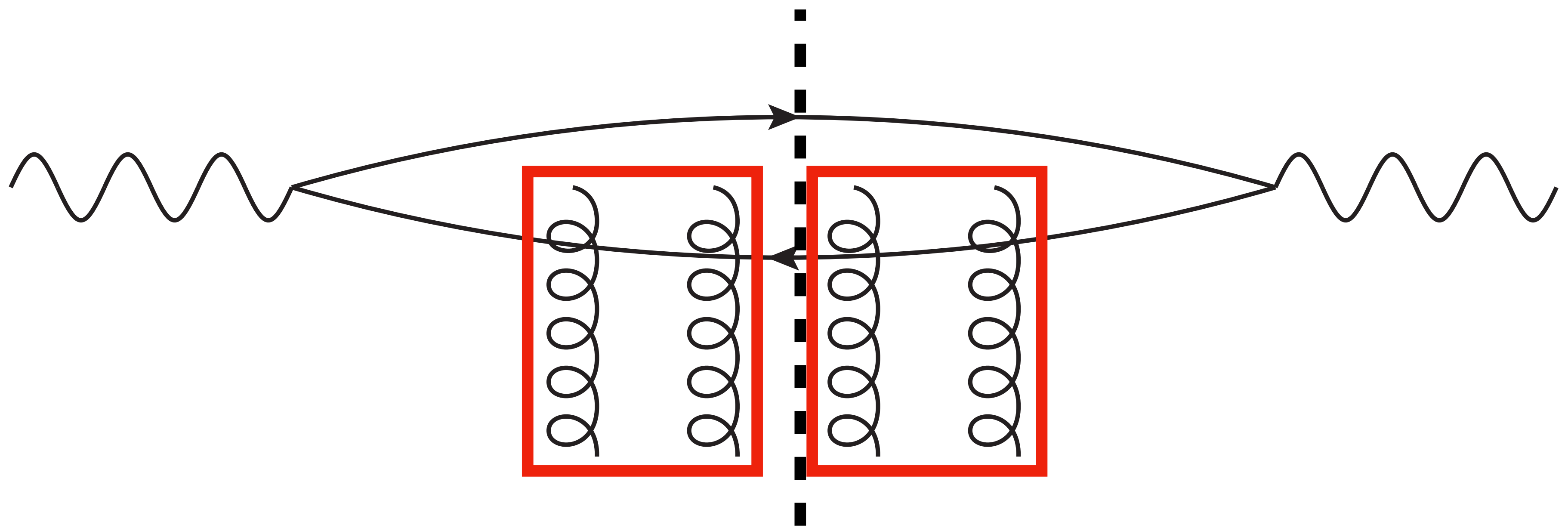

$$S(r_\perp = x_{01}) = \frac{1}{N_c}\langle \mathrm{Tr}\left[U^\dagger(x_0)U(x_1)\right]\rangle$$

Dipole amplitude and saturation

$$S(r_\perp = x_{01}) = \frac{1}{N_c}\langle \mathrm{Tr}\left[U^\dagger(x_0)U(x_1)\right]\rangle$$

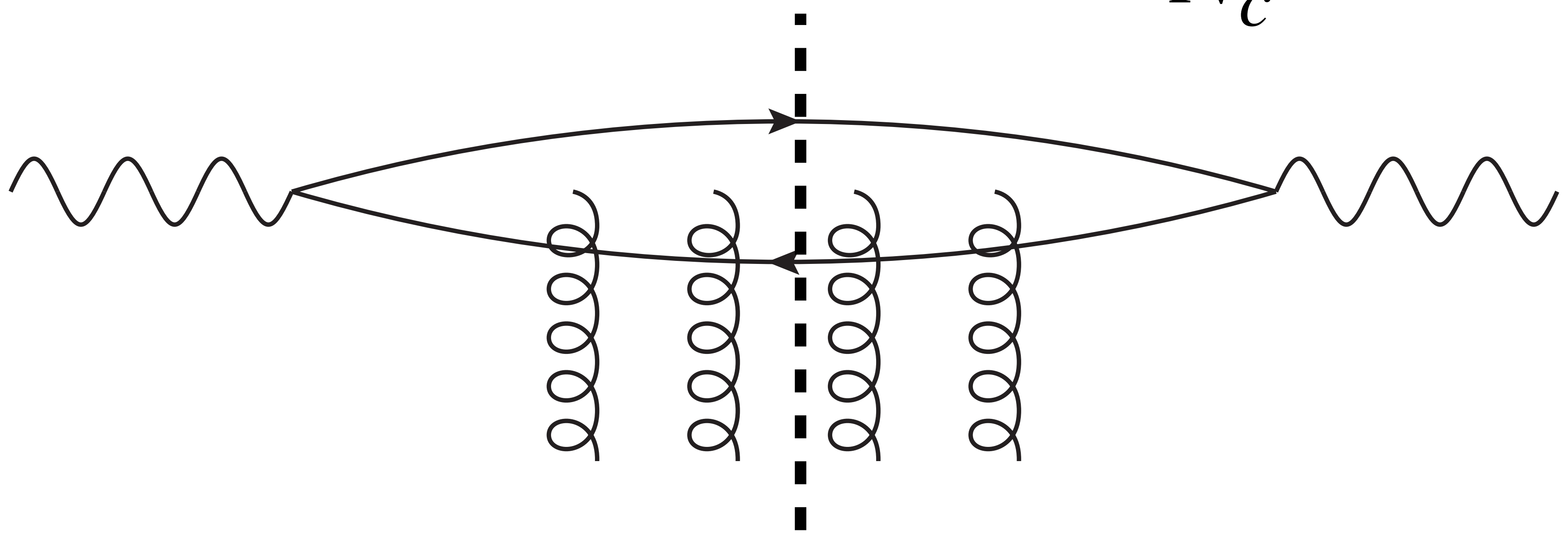

$$\sigma_{q\bar{q}N}(r_\perp, x) = 2\int d^2b_\perp N(r_\perp, x) = \sigma_0\left[1 - e^{-r_\perp^2 Q_s^2(x)}\right]$$

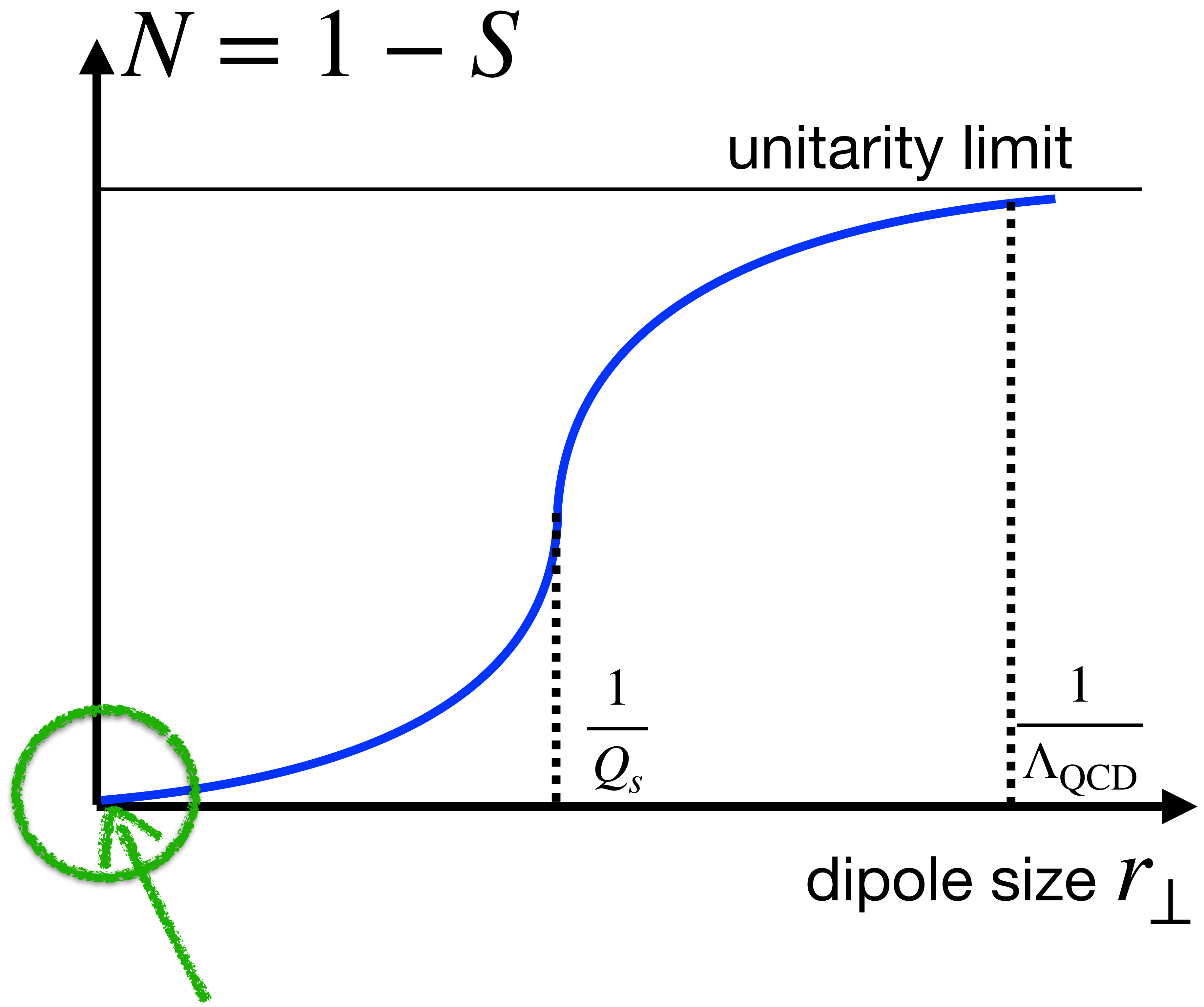

- ❖ Bjorken frame (IMF): Saturation is the limit of parton's number density.
- ❖ Dipole frame: Patonic picture is no longer manifest. Saturation is the unitarity limit for scatterings.

As $r_\perp \to 0$, the color charges of the quark and the antiquark cancel each other

$\Longrightarrow$ the disappearance of interactions with the target (Color Transparency)

Color Glass Condensate Effective Field Theory

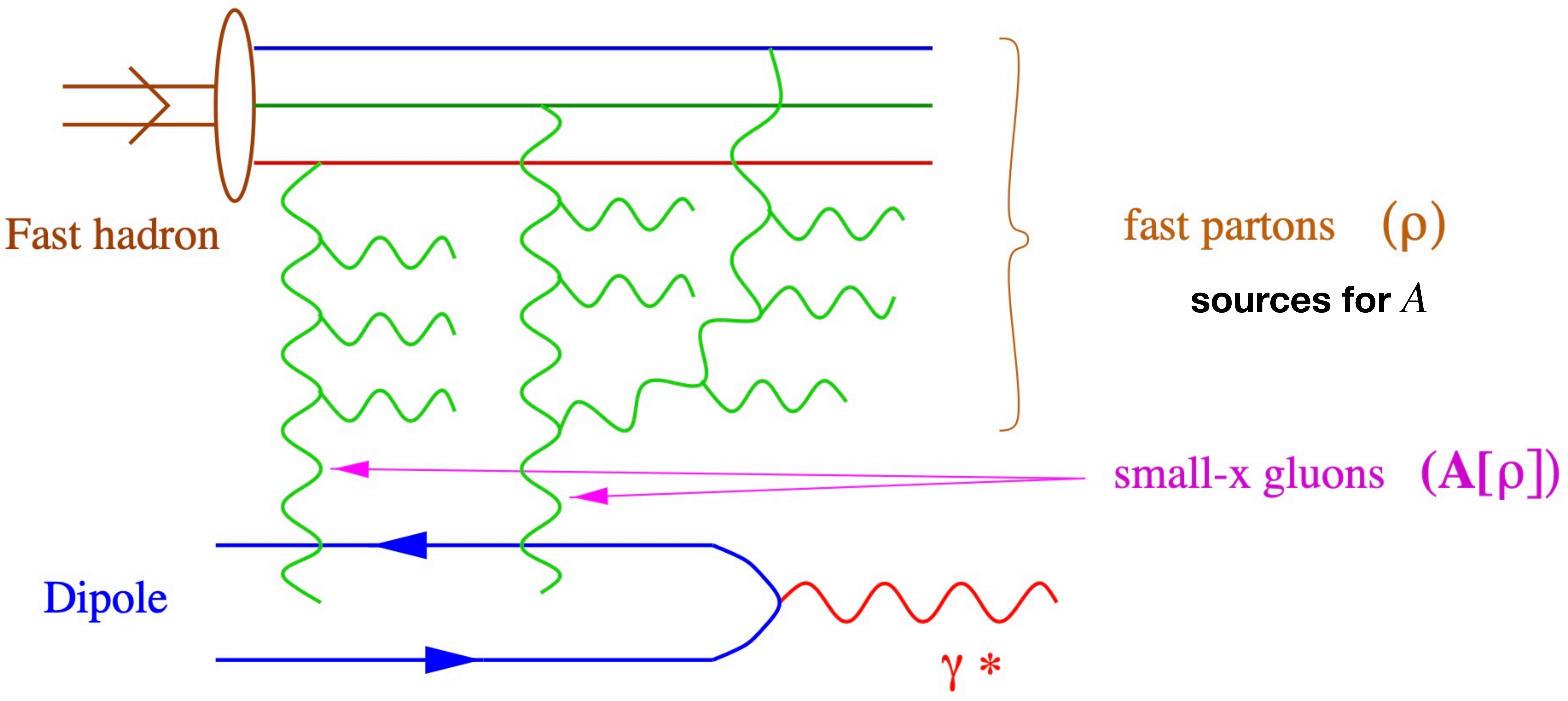

- ❖ Static and strong $(1/g)$ color charge ρ
- ❖ Universal statistical distribution $W[\rho]$ (c.f. PDFs in Bjorken limit)
- ❖ Color current $J_a^\mu = \delta^{+\mu}\rho^a$

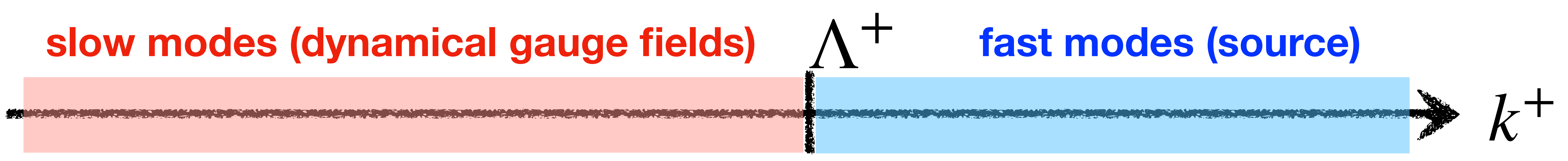

JIMWLK renormalization group equation describes the separation between fast modes ($k^+ > \Lambda^+$) and slow modes ($k^+ < \Lambda^+$).

Dynamical gauge field

- ❖ Hadron wave function = collection of static color sources ρ (classical random variable)
- ❖ Hard and soft modes are coupled via Yang-Mills equations at LO (classical equations of motion):

$$[\mathscr{D}_\mu, F^{\mu\nu}] = J^\nu \quad \text{with} \quad J^\nu = \delta^{+\nu}\rho$$

The occupation numbers are large, so the generated classical fields are strong: $A \sim \dfrac{1}{g}$

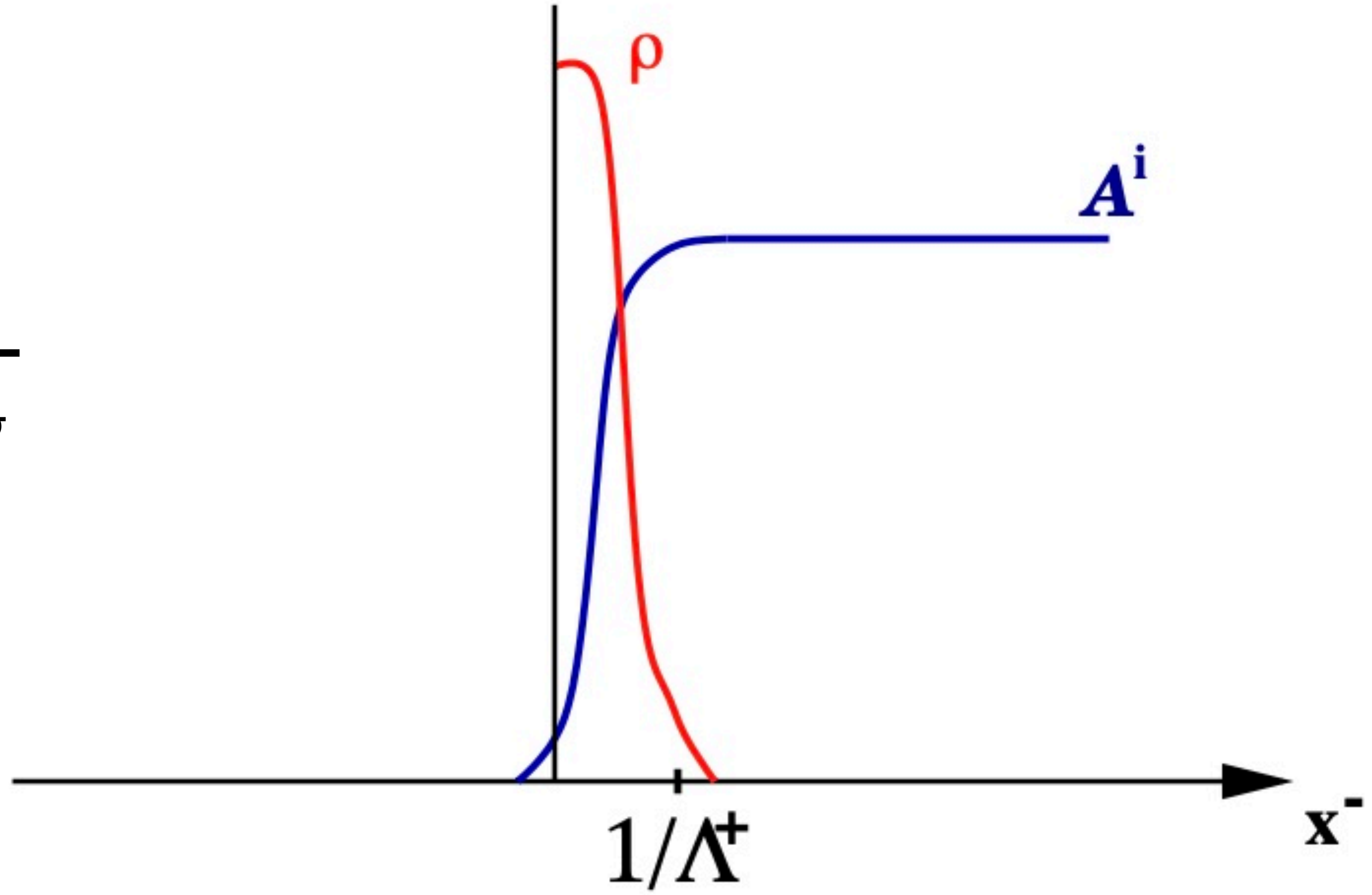

CGC expectation value

$$\langle \mathcal{O} \rangle_{\Lambda^+} = \frac{\int [\mathcal{D}\rho] W_{\Lambda^+}[\rho] \mathcal{O}[\rho]}{\int [\mathcal{D}\rho] W_{\Lambda^+}[\rho]}$$

n-point Wilson line correlators

- ✓ gauge invariant
- ✓ probability of a configuration ρ
- ✓ in the saturation regime, $\rho = \mathcal{O}(1/g)$
- ✓ normalization: $\int [\mathcal{D}\rho] W_{\Lambda^+}[\rho] = 1$

The requirement that physical quantities (the expectation value of the operator) do not depend on the choice of the cutoff Λ^+, leading to the Jalilian–Marian–Iancu–McLerran–Weigert–Leonidov–Kovner (JIMWLK) equation for $W_{\Lambda^+}[\rho]$:

$$\frac{\partial W_Y[\rho]}{\partial Y} = -\mathcal{H}_{\mathrm{JIMWLK}} W_Y[\rho]$$

resums all powers of $\alpha_s Y$

$$\Rightarrow \quad \frac{\partial \langle \mathcal{O} \rangle_Y}{\partial Y} = \langle \mathcal{H}_{\mathrm{JIMWLK}} \mathcal{O} \rangle_Y$$

Customary notation:

$\Lambda^+ \leftrightarrow x = \Lambda^+/P^+$

$x \leftrightarrow Y = \ln(1/x)$

B-JIMWLK evolution

Let us consider S-matrix $\mathcal{O} = S(x_{10}) = \frac{1}{N_c}\mathrm{Tr}[U^\dagger(x_1)U(x_0)]$ as an example:

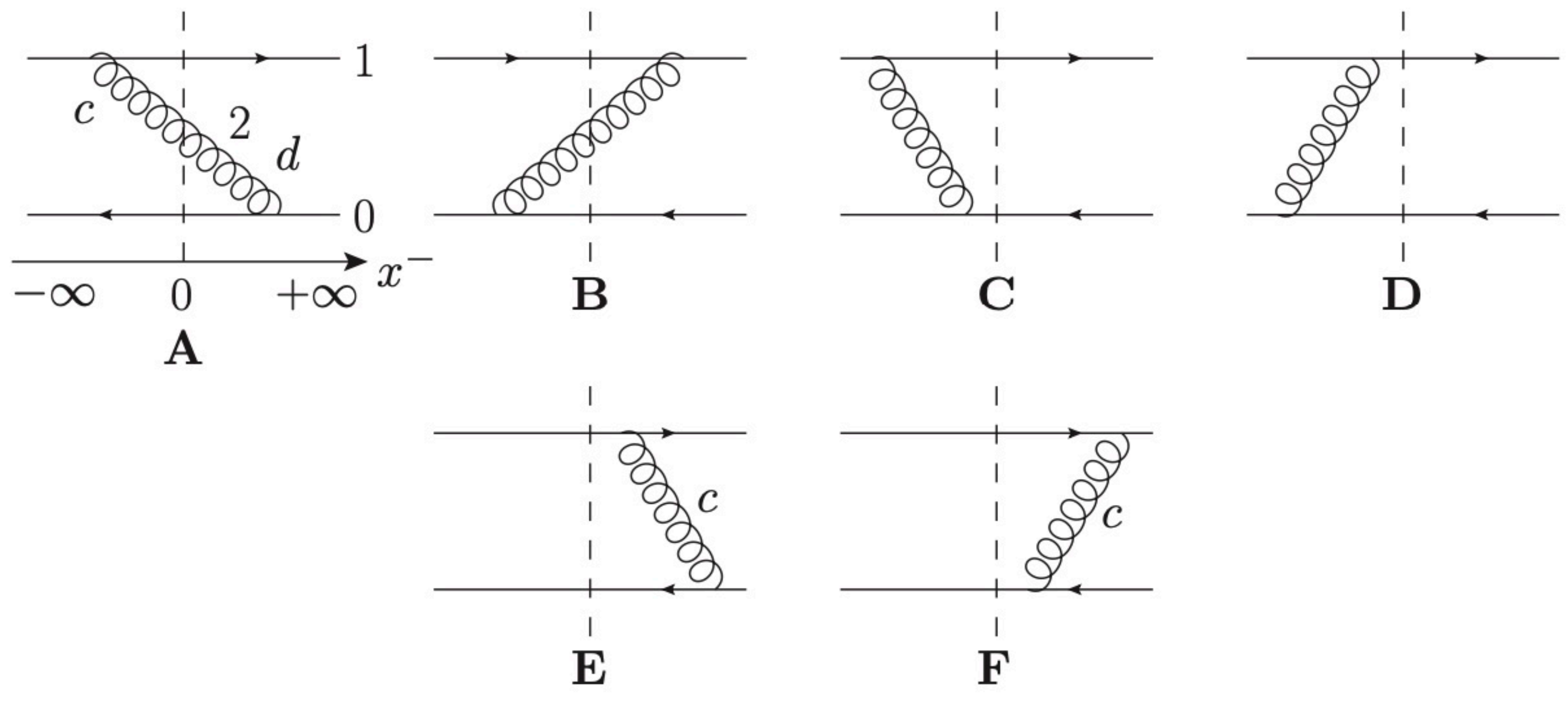

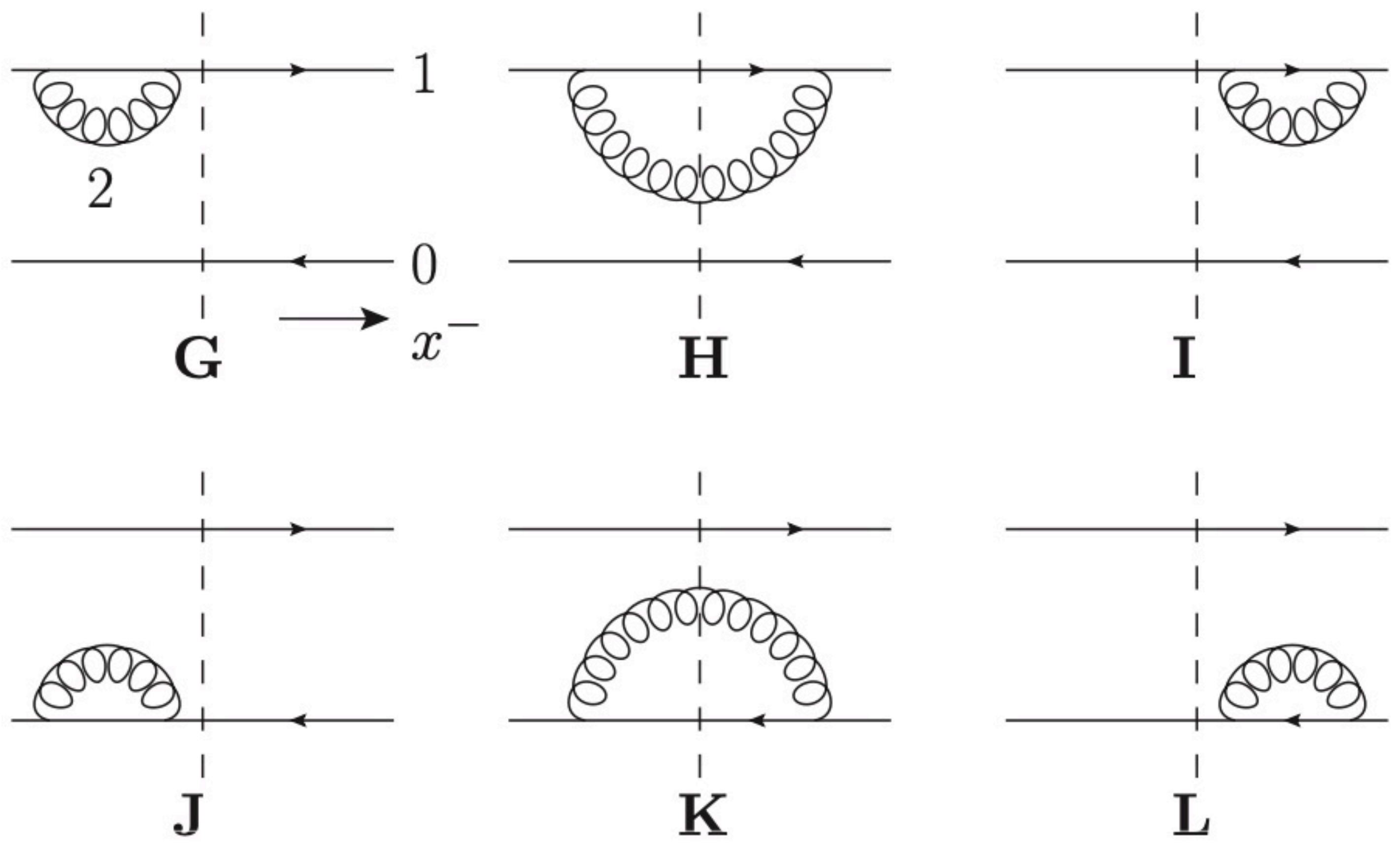

Balitsky hierarchy: an infinite set of evolution equations could be obtained; the evolution of n-Wilson line correlators can be derived from $(n+2)$-Wilson line correlators.

I. Balitsky, NPB463, 99-160 (1996)

$$\frac{\partial}{\partial Y}\langle S(x_{10})\rangle_Y = \frac{\alpha_s N_c}{2\pi^2}\int d^2x_2 \frac{x_{10}^2}{x_{20}^2 x_{21}^2}\left[\langle S(x_{12})S(x_{20})\rangle_Y - \langle S(x_{10})\rangle_Y\right]$$

$$\frac{\partial}{\partial Y}\langle S(x_{12})S(x_{20})\rangle_Y = \cdots$$

Not a closed-equation.
No analytic solutions.

Large-N_c limit and BK evolution

$$\langle S(x_{12})S(x_{20})\rangle_Y = \langle S(x_{12})\rangle_Y \langle S(x_{20})\rangle_Y + \mathcal{O}\left(\frac{1}{N_c}\right)$$

- ❖ Naive estimation of the $1/N_c$ corrections to BK equation: $1/N_c^2 \approx 11\,\%$
- ❖ However, the $1/N_c$ corrections are more suppressed due to the saturation effect.
- ❖ BK eq. can be a good approximation as long as IC. does not contain strong $1/N_c$ corrections

K. Rummukainen and H. Weigert, NPA739, 183-226 (2004)
Y. V. Kovchegov, J. Kuokkanen, K. Rummukainen and H. Weigert, NPA823, 47-82 (2009)

"nonplanner"

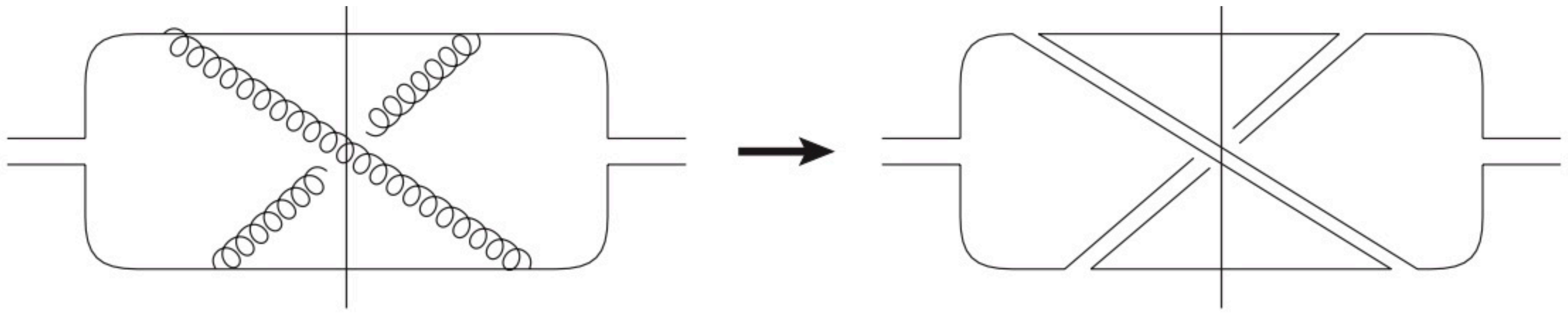

$\sim \mathcal{O}\left(\frac{1}{N_c^2}\right)$

"planner"

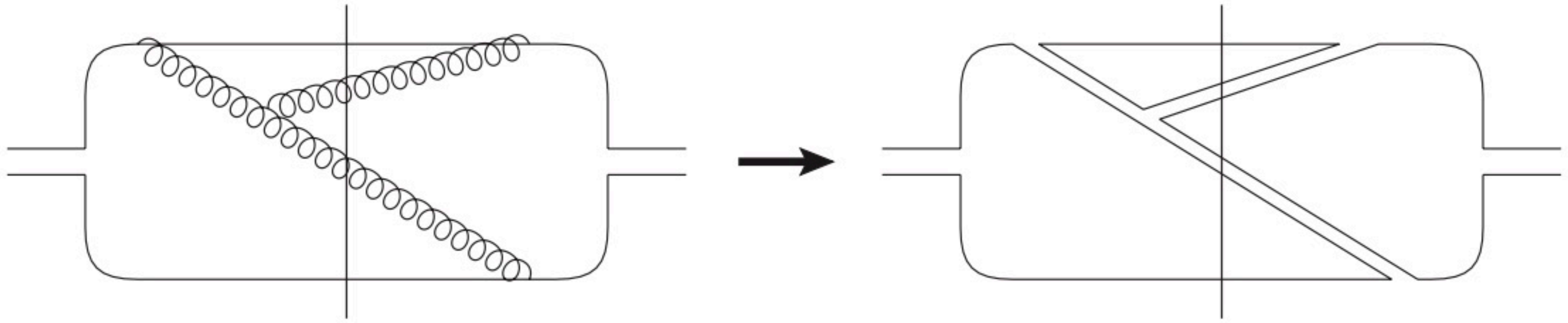

Balitsky-Kovchegov equation

I. Balitsky, NPB463 (1996),99
Y. Kovchegov, PRD60(1999), 034008

In terms of the dipole scattering amplitude $N = S - 1$:

$$\frac{\partial}{\partial Y} N(x_{10}, Y) = \frac{\alpha_s N_c}{2\pi^2} \int d^2x_2 \frac{x_{10}^2}{x_{20}^2 x_{21}^2} \left[N(x_{12}, Y) + N(x_{20}, Y) - N(x_{10}, Y) - N(x_{12}, Y) N(x_{20}, Y) \right]$$

Bremsstrahlung (BFKL) **Recombination**

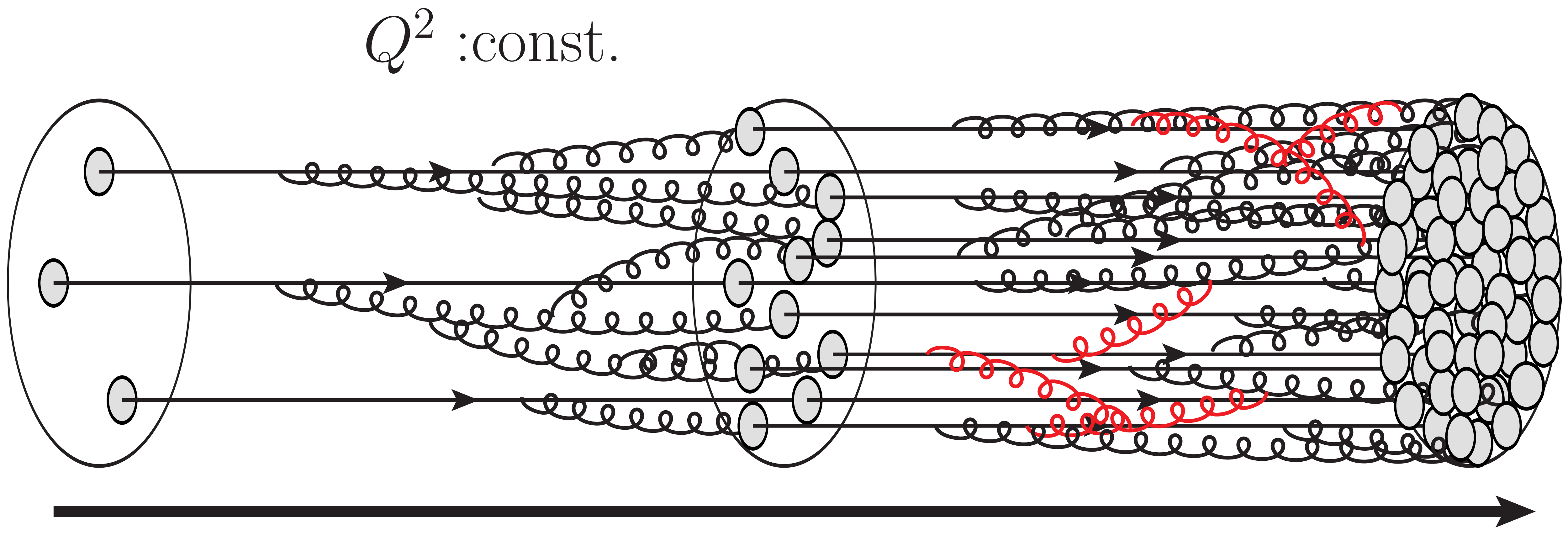

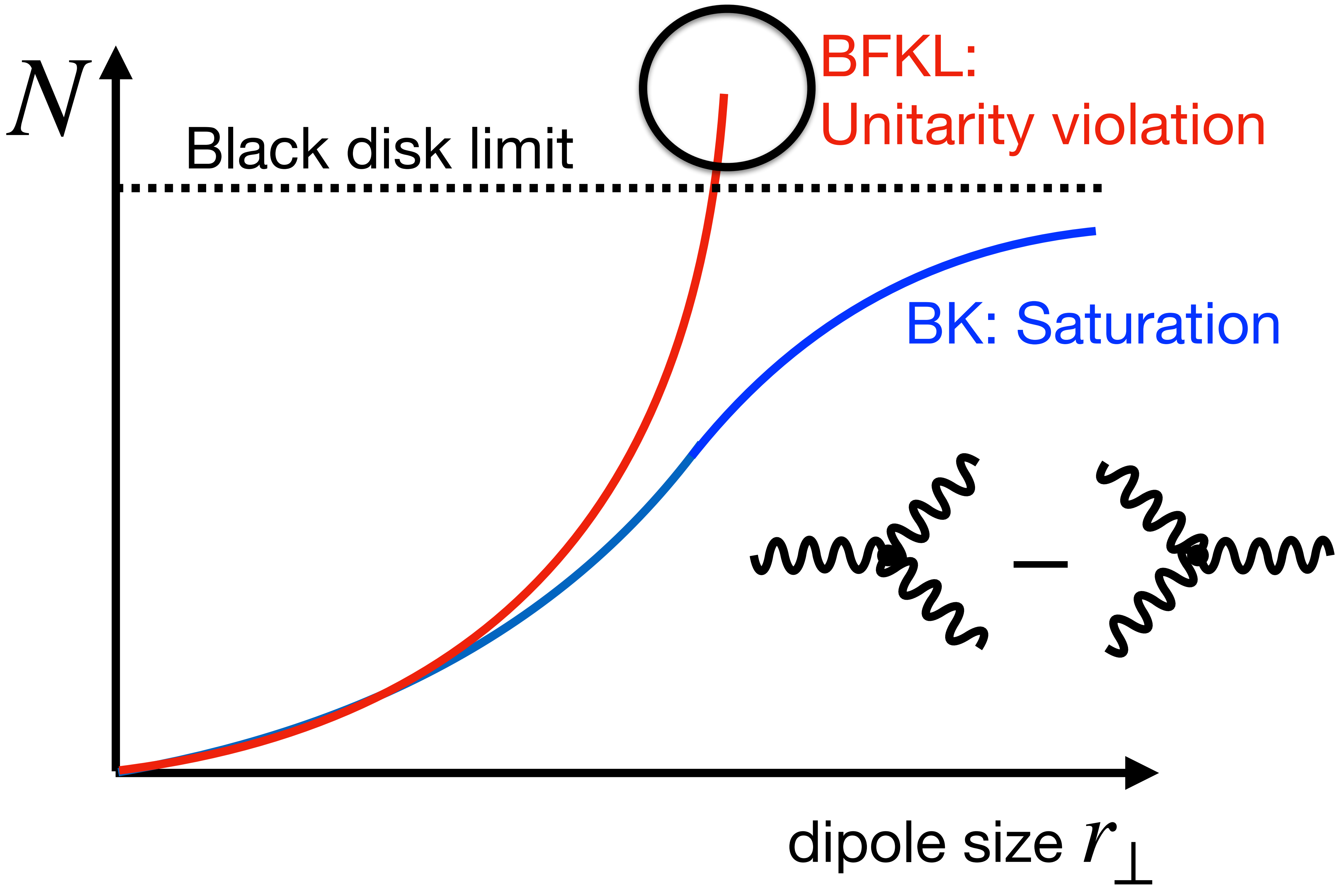

Nonlinear gluon fusion (two dipoles merging) slows down the quantum evolution speed and results in the saturation of the gluon density.

McLerran-Venugopalan model

L.McLerran and R. Venugopalan, Phys. Rev. D49 (1994) 2233; ibid. 49 (1994) 3352; ibid. 50 (1994) 2225

In a large nucleus, a probe of small-x does not resolve the longitudinal extent of the nucleus when $Q^2 \ll \Lambda^2_{\rm QCD} A^{1/3}$:

$$W_{Y_0}[\rho] = \exp\left[-\int d^2x_\perp \frac{\rho^a(x_\perp)\rho^a(x_\perp)}{2\mu_A^2(x_\perp)} \right]$$

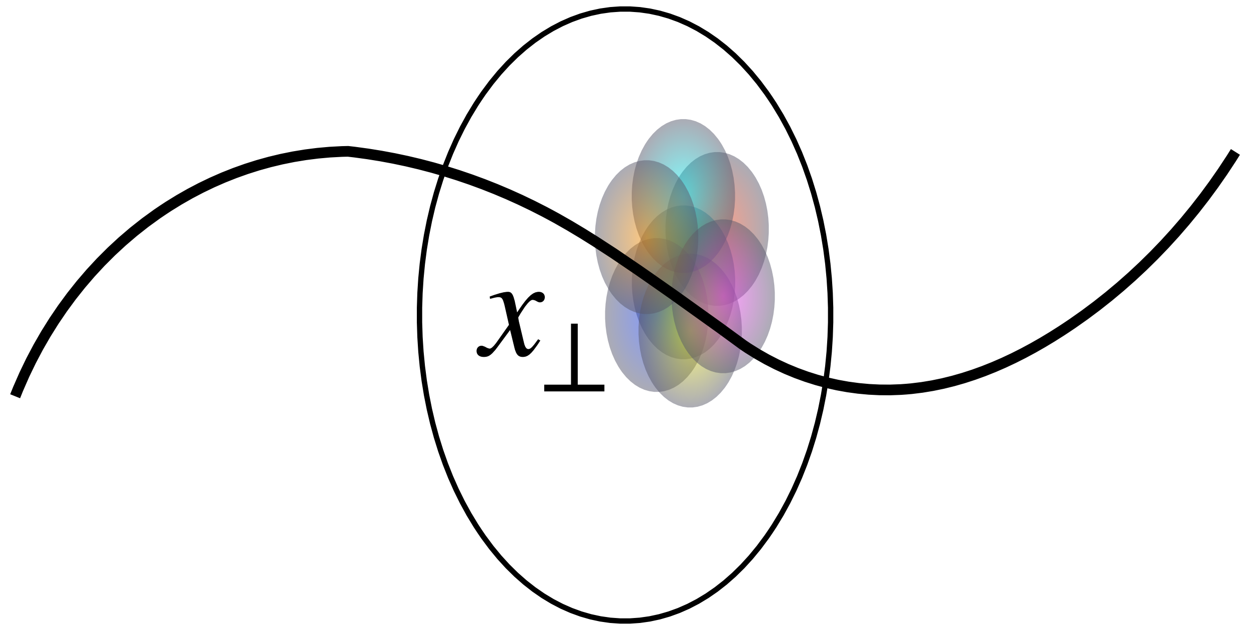

For $A \gg 1,\, \mu_A^2 \sim Q^2_{sA} \propto A^{1/3} \gg \Lambda^2_{\rm QCD}$

Here we assume that $\langle \rho \rangle = 0$ and higher point functions vanish.

❖ **The main idea:** the color charge per unit area, $\rho(x_\perp)$, is the sum of the color charges of the partons that sit at approximately the same impact parameter $x_\perp$.

❖ There are local correlations at $x_\perp$ as a consequence of confinement: color charges separated by more than the nucleon size cannot be correlated!

Schematic view of the quantum evolution

Proton

Nucleus

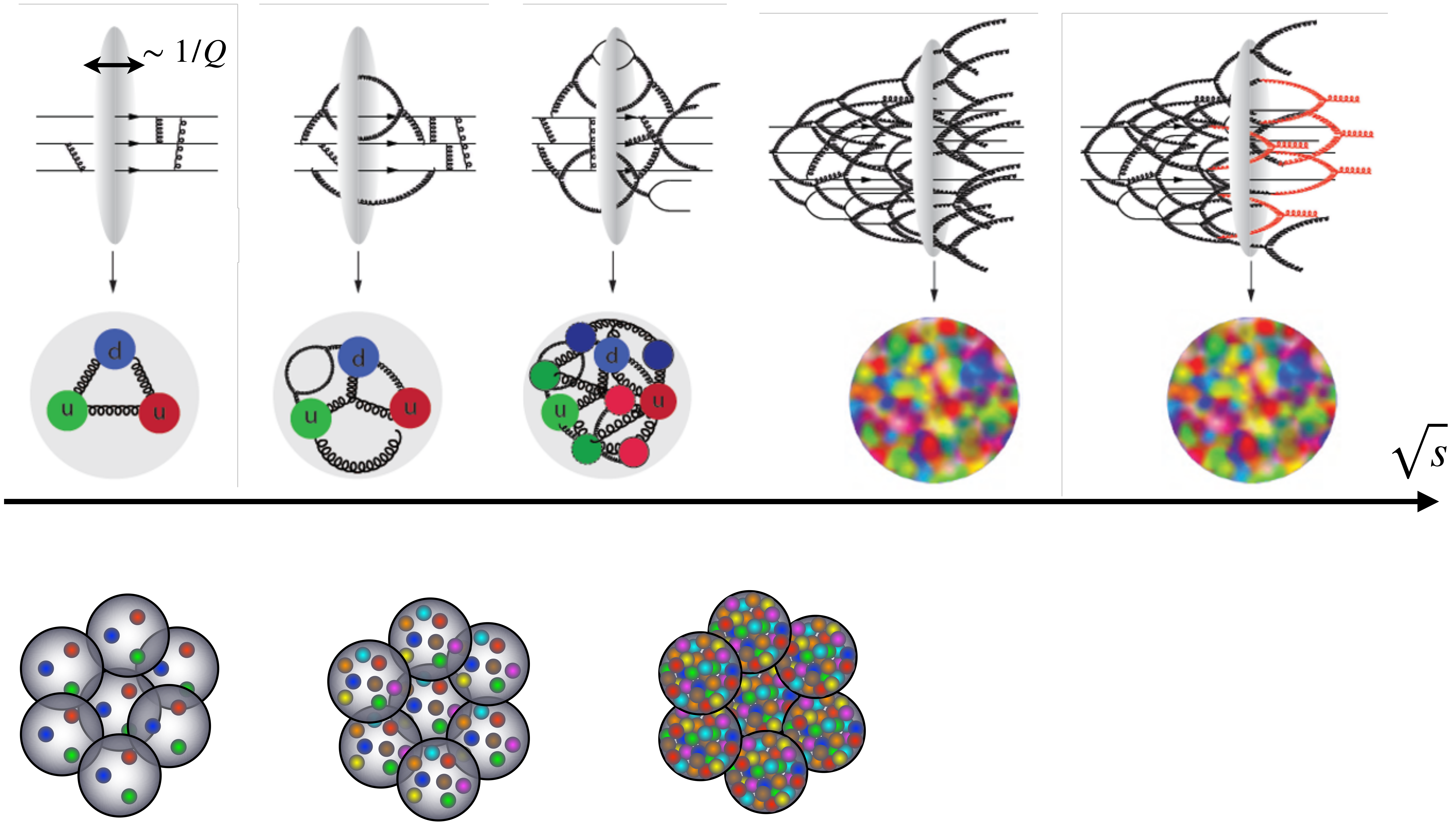

Part IV:

Phenomenology

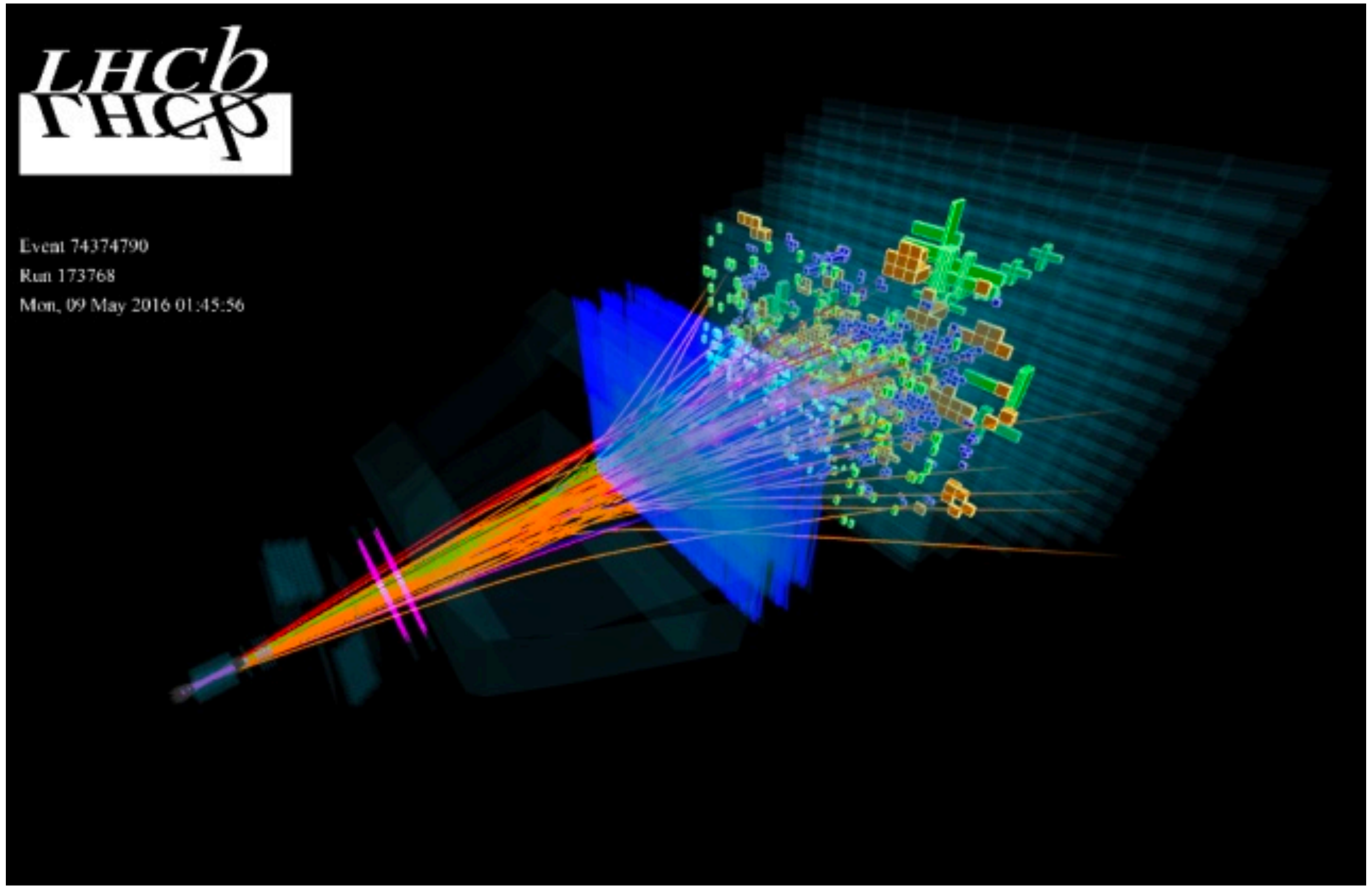

Rapidity evolution of the dipole amplitude

Parameters in the MV initial condition can be fitted by HERA inclusive data for $x \leq 0.01$.

$$\varphi_{p,Y}(k_\perp) = \pi R_p^2 \frac{N_c k_\perp^2}{4\alpha_s} \mathcal{N}_Y^A(k_\perp)$$

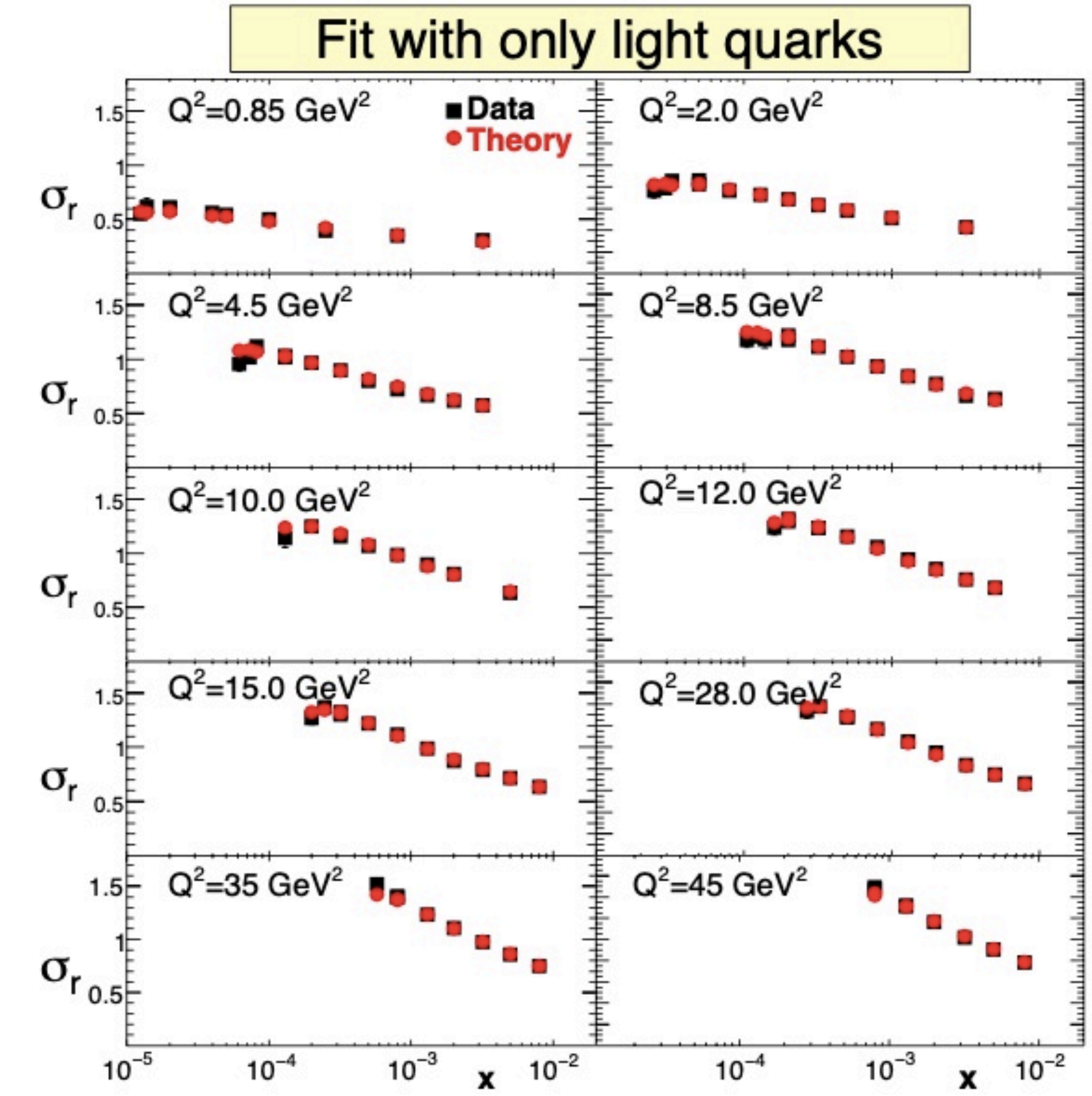

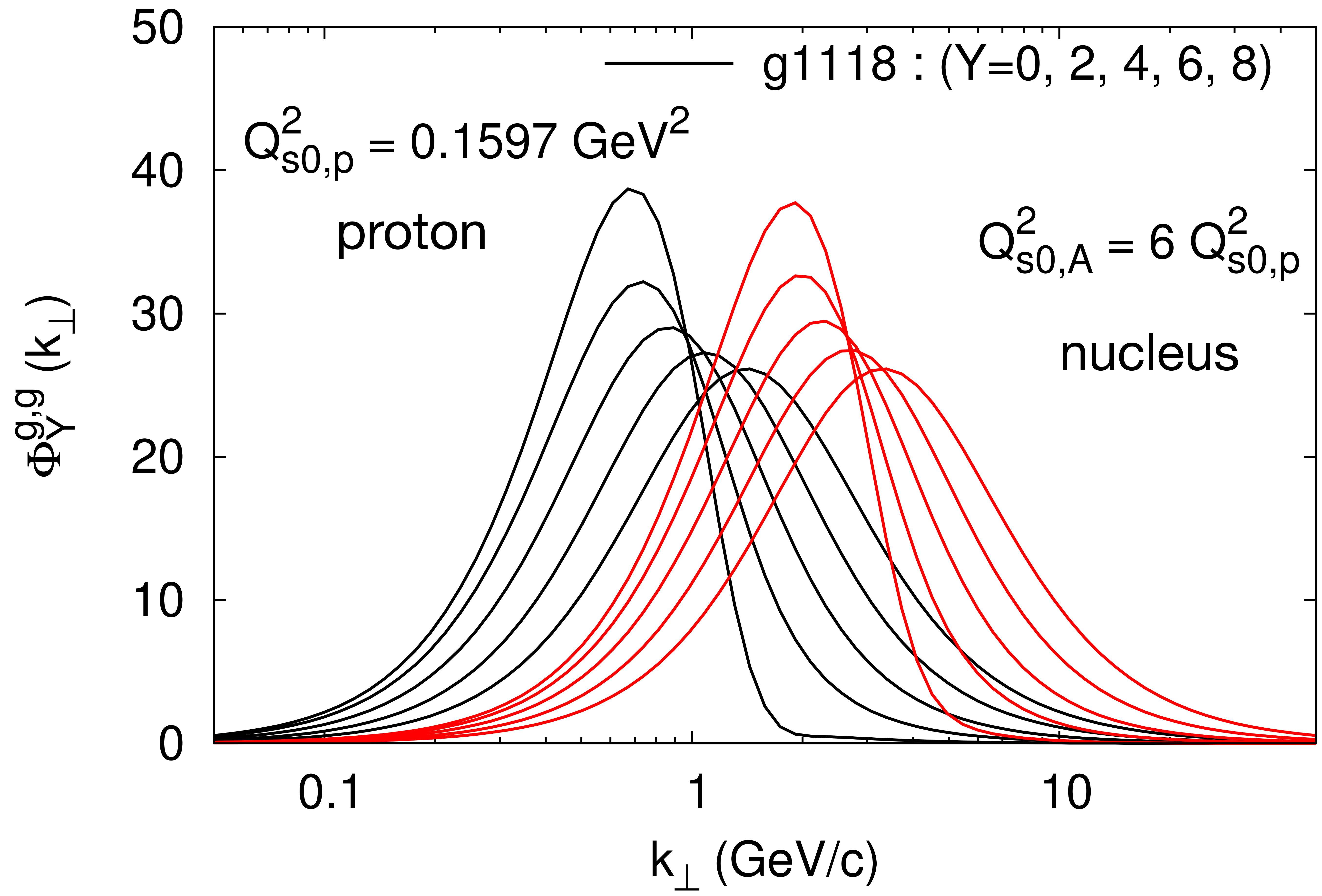

The rapidity dependence of Q_s^2

Gluon's intrinsic momentum: $\langle k_T^2 \rangle \sim Q_s^2$

Geometric Scaling from HERA DIS

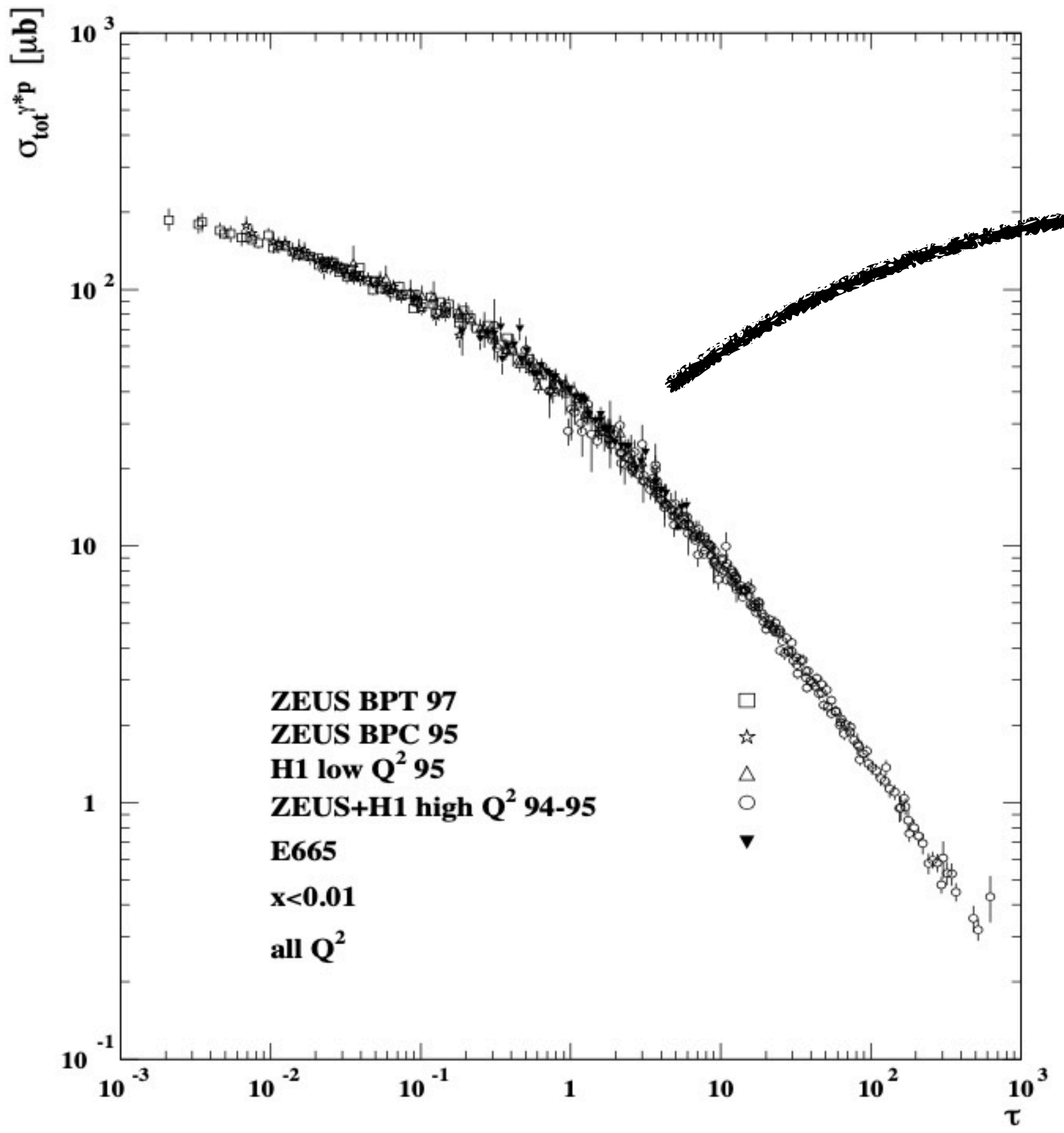

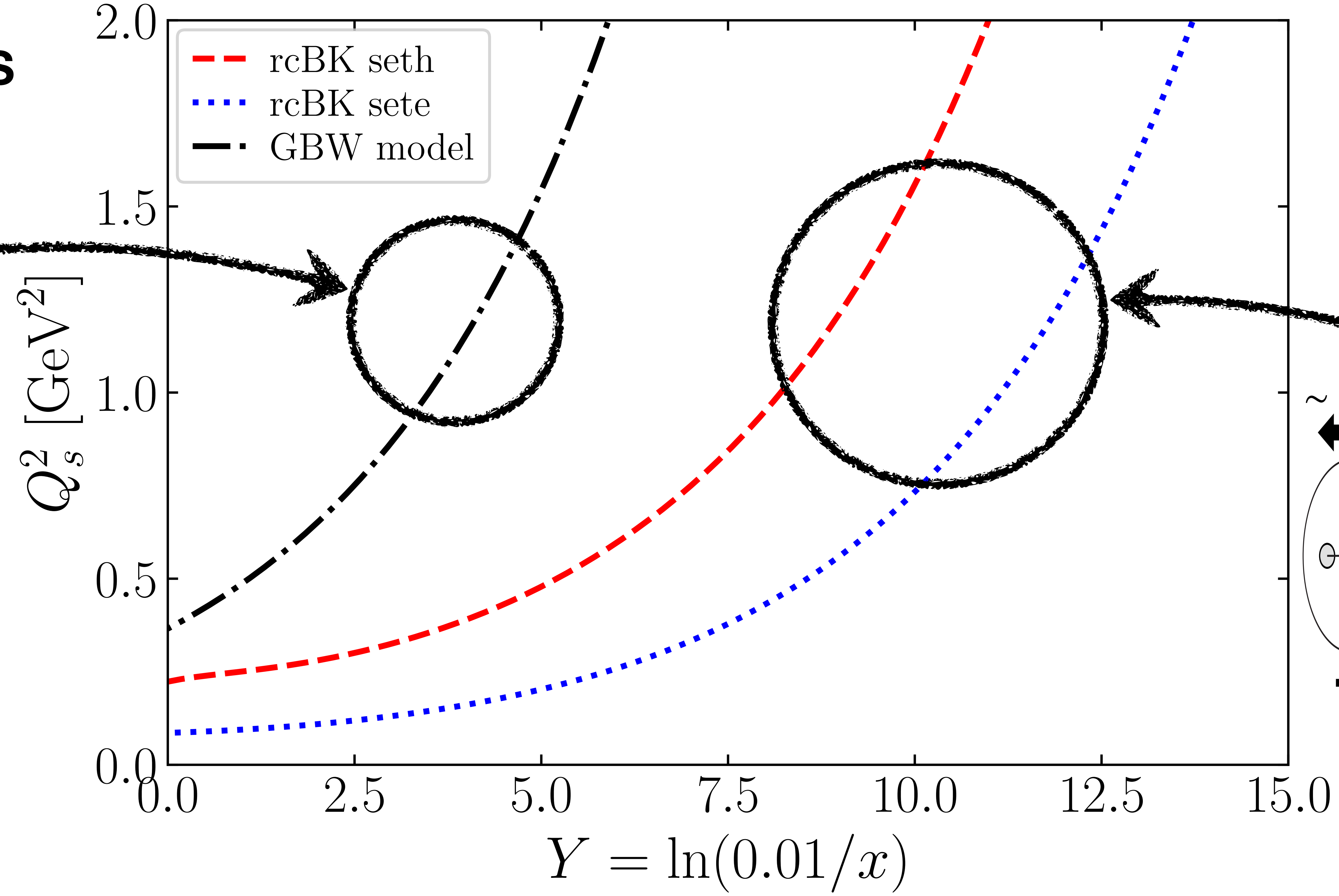

JIMWLK/BK evolution

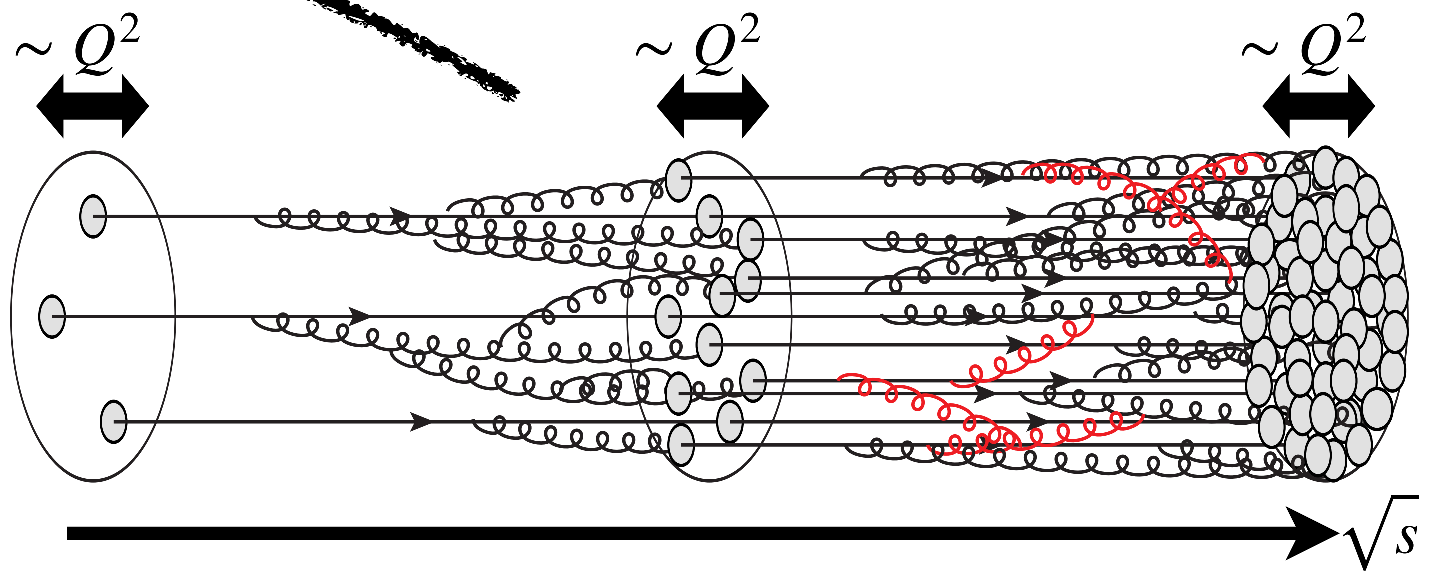

- ❖ Solving BK equation for the dipole amplitude numerically: $N_Y(r_\perp = 1/Q_s) = 0.5$
- ❖ Uncertainty about the shape of the dipole amplitude at $Y = 0$.

Forward experiments probe:

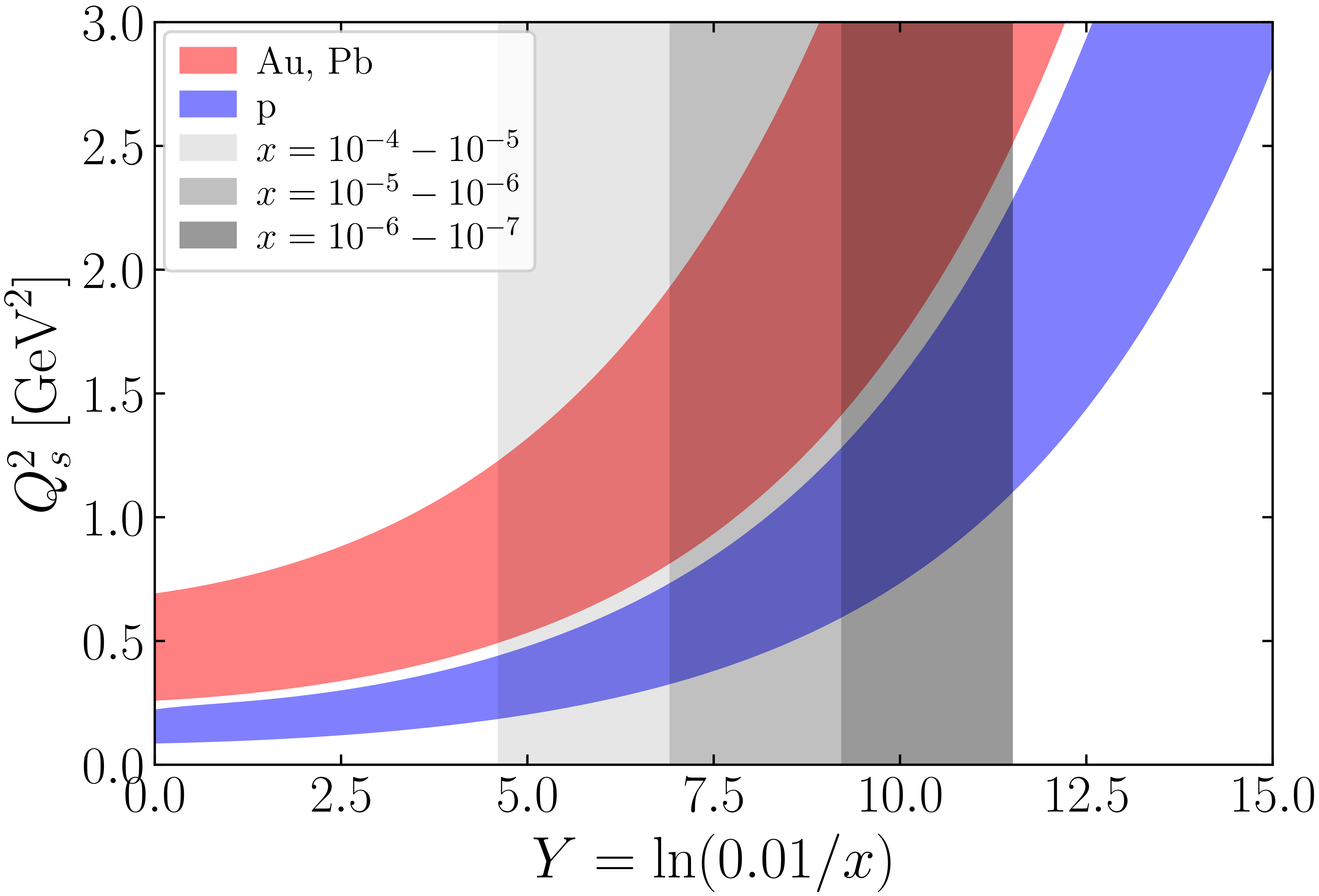

NB: There is further uncertainty about the definition of Q_s^2.

A strategy for saturation hunting at EIC

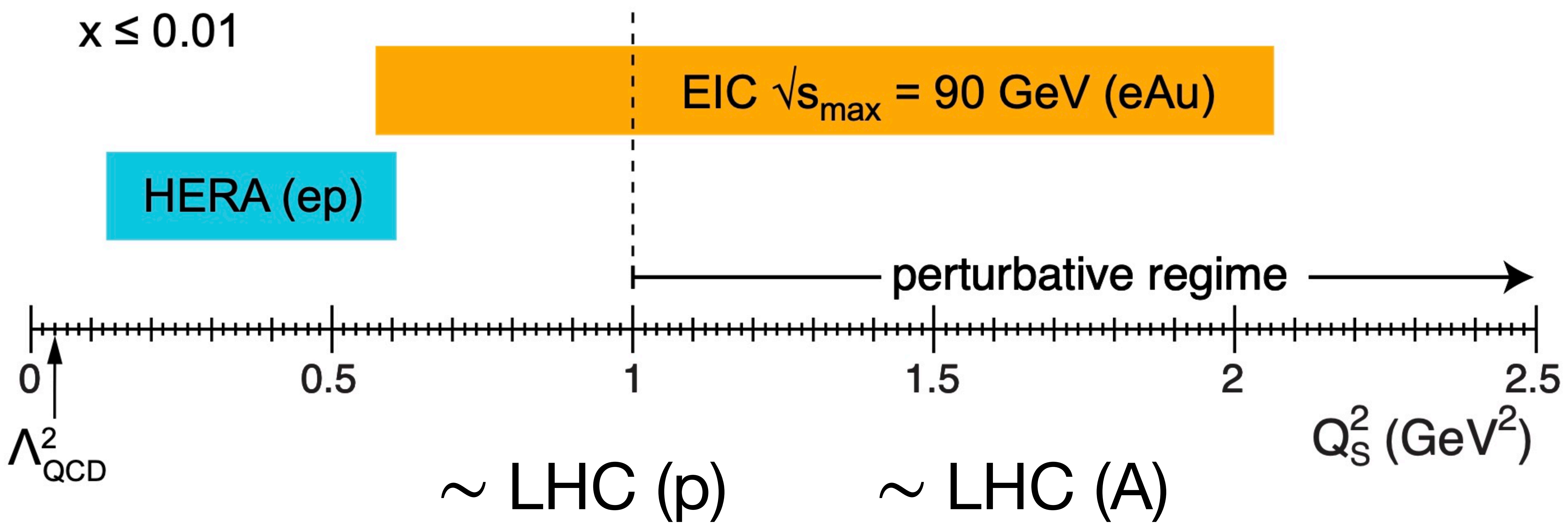

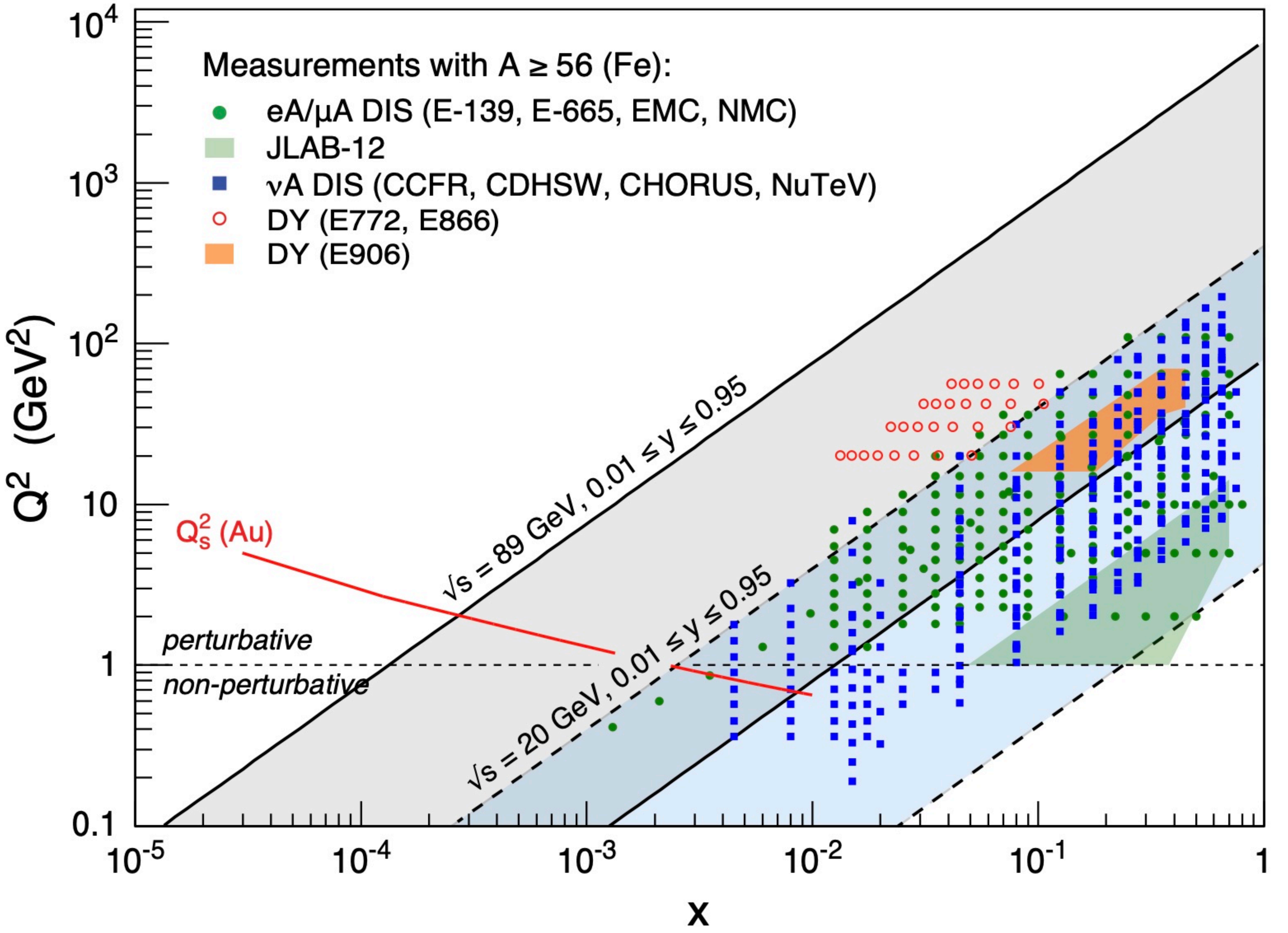

Nuclear enhanced saturation scale

$$Q_{sA}^2 \propto A^{1/3} x^{-0.3}$$

- ❖ The gluon saturation scale depends on the gluon density per transverse plane.
- ❖ Even if x is not extremely small, Q_s^2 can be a perturbative scale and affects various observables.
- ❖ EIC provides an important opportunity to examine $x = 10^{-4} - 10^{-2}$.

Extended geometrical scaling

E. Iancu, K. Itakura and L. McLerran, Nucl. Phys. A 708, 327-352 (2002)

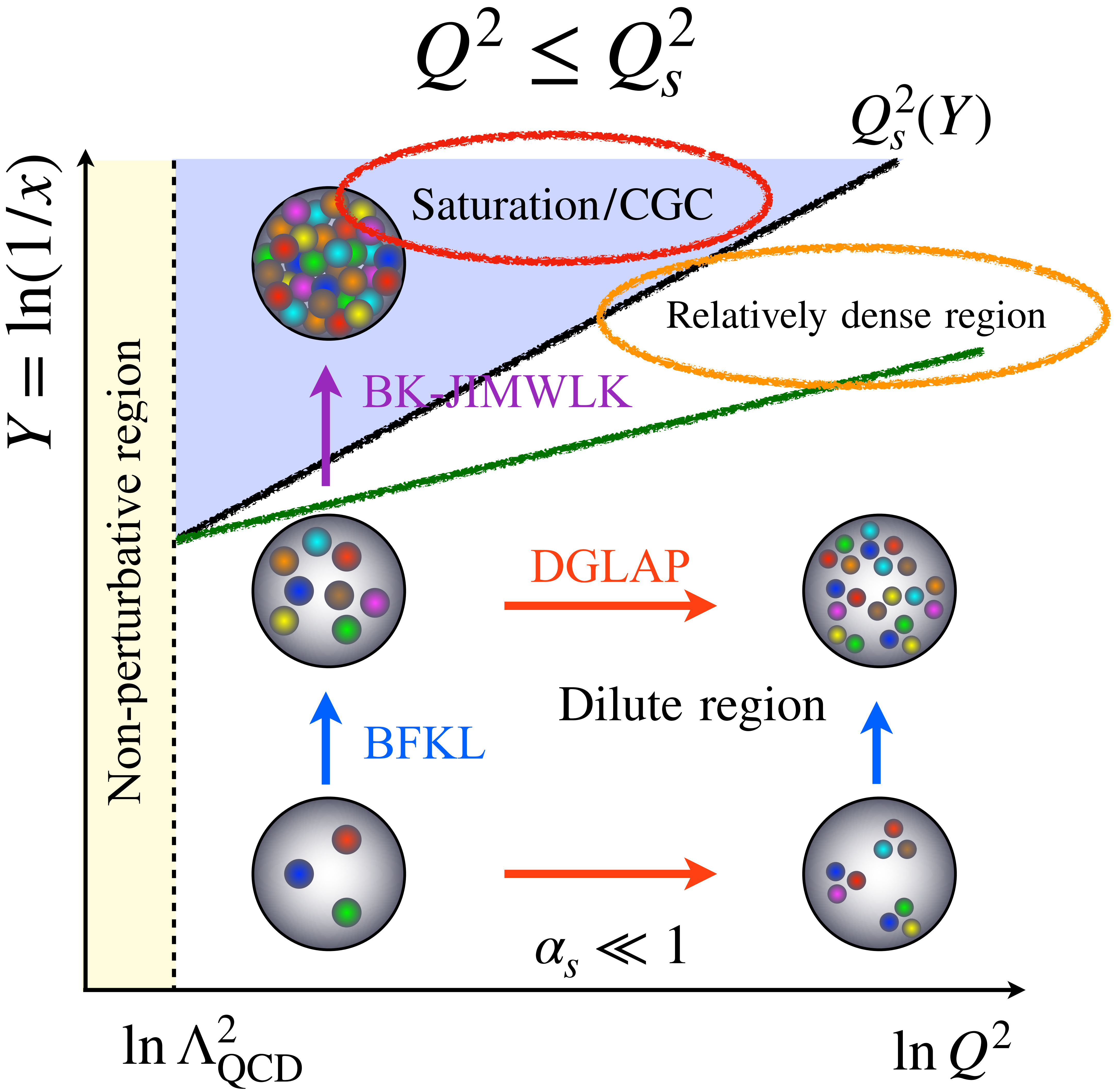

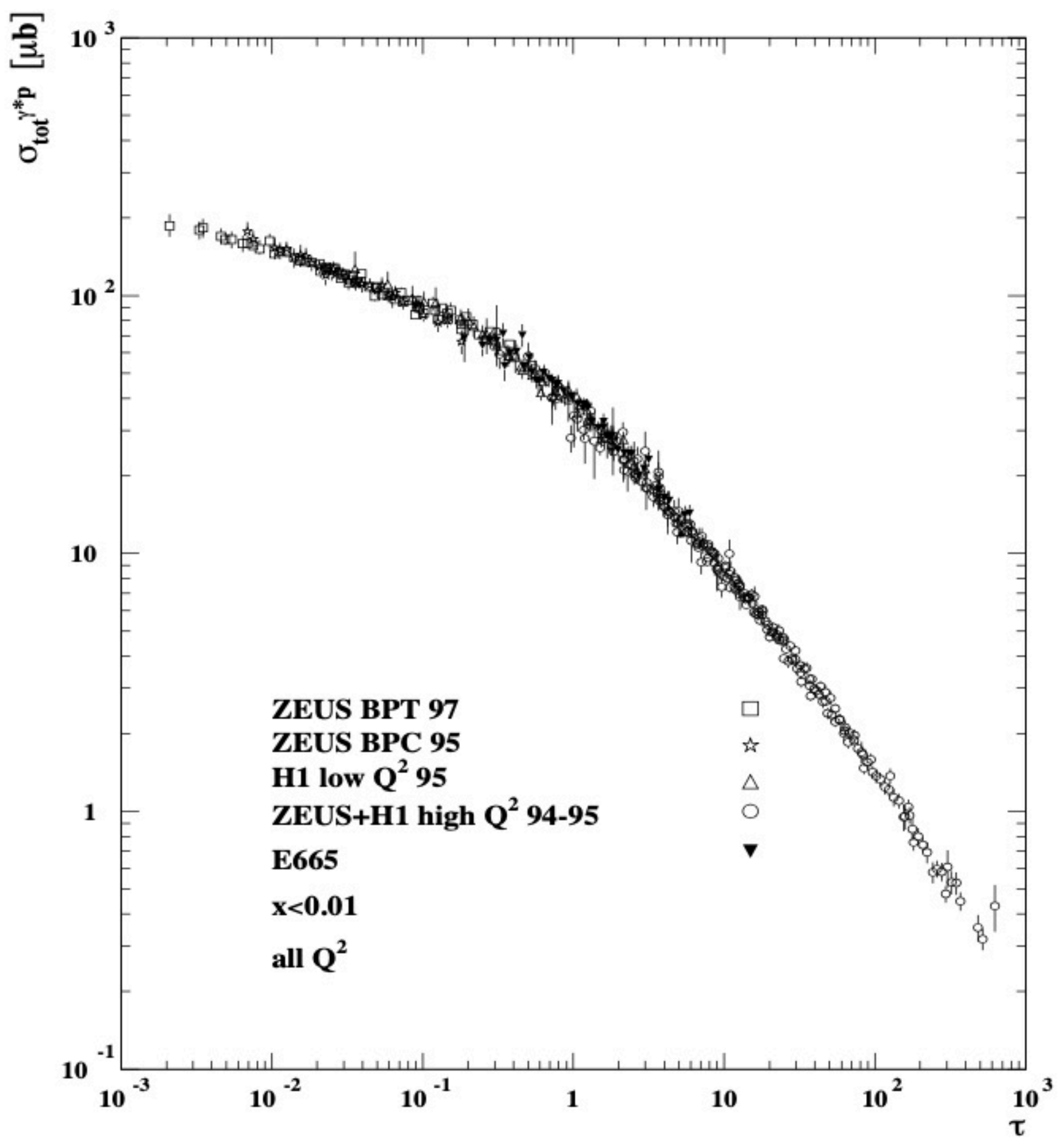

$$Q^2 \leq Q_s^4/\Lambda^2_{\rm QCD}$$

The linear BFKL equation should be applicable outside the deep saturation regime. However, the solution of the BFKL equation shows geometric scaling under the influence of CGC.

Particle production of $p_T \gtrsim Q_s$ could carry out information on CGC!

Kinematics to be considered

(i) Mid rapidity region:

- ❖ $x_1 \sim x_2 < 1$

(ii) Forward rapidity region:

- ❖ $x_1 \sim \mathcal{O}(1),\ x_2 \ll 1$

(iii) Backward rapidity region:

- ❖ $x_2 \sim \mathcal{O}(1),\ x_1 \ll 1$

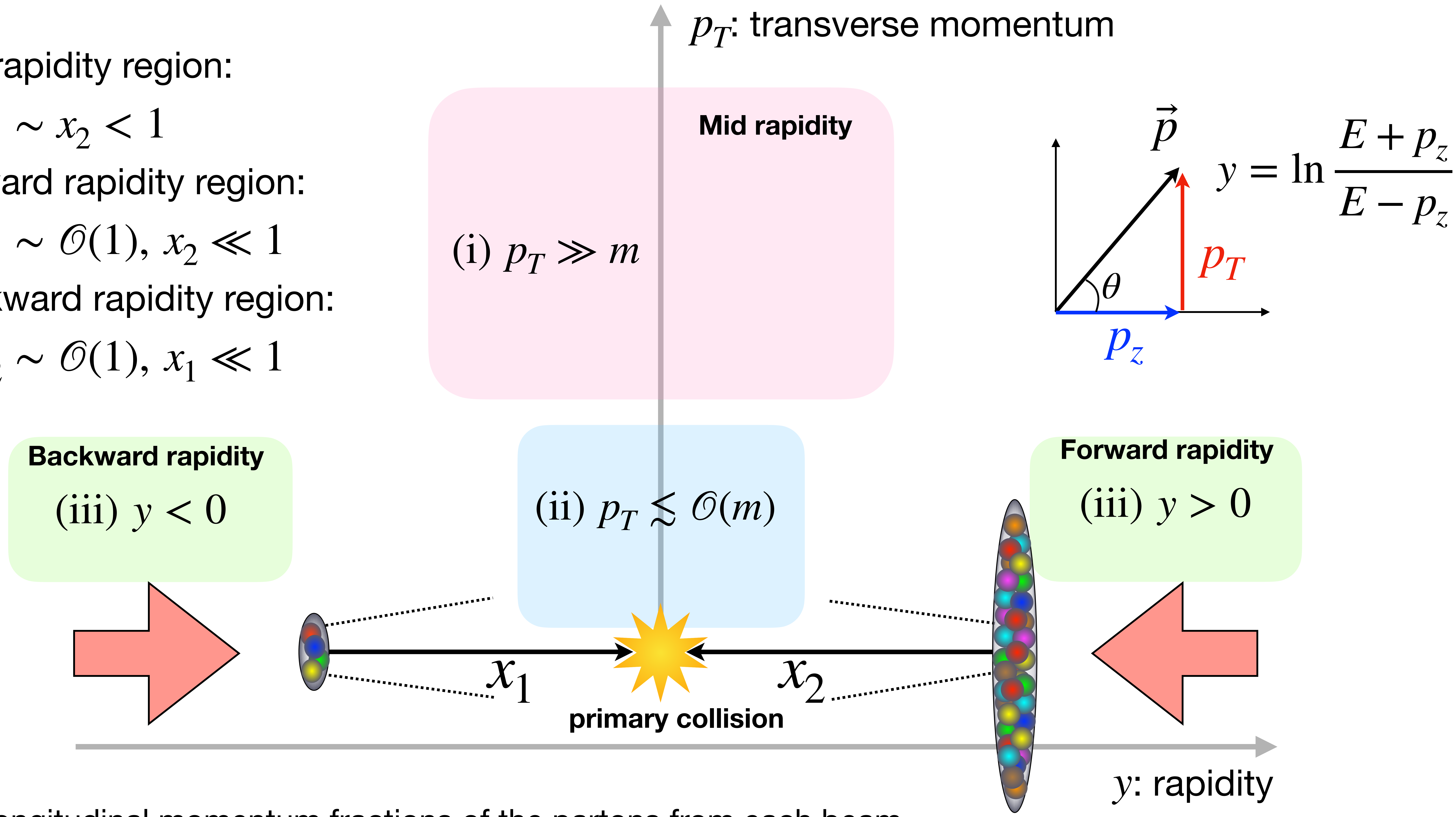

$x_{1,2}$: the longitudinal momentum fractions of the partons from each beam.

Inclusive particle production in hadronic collisions

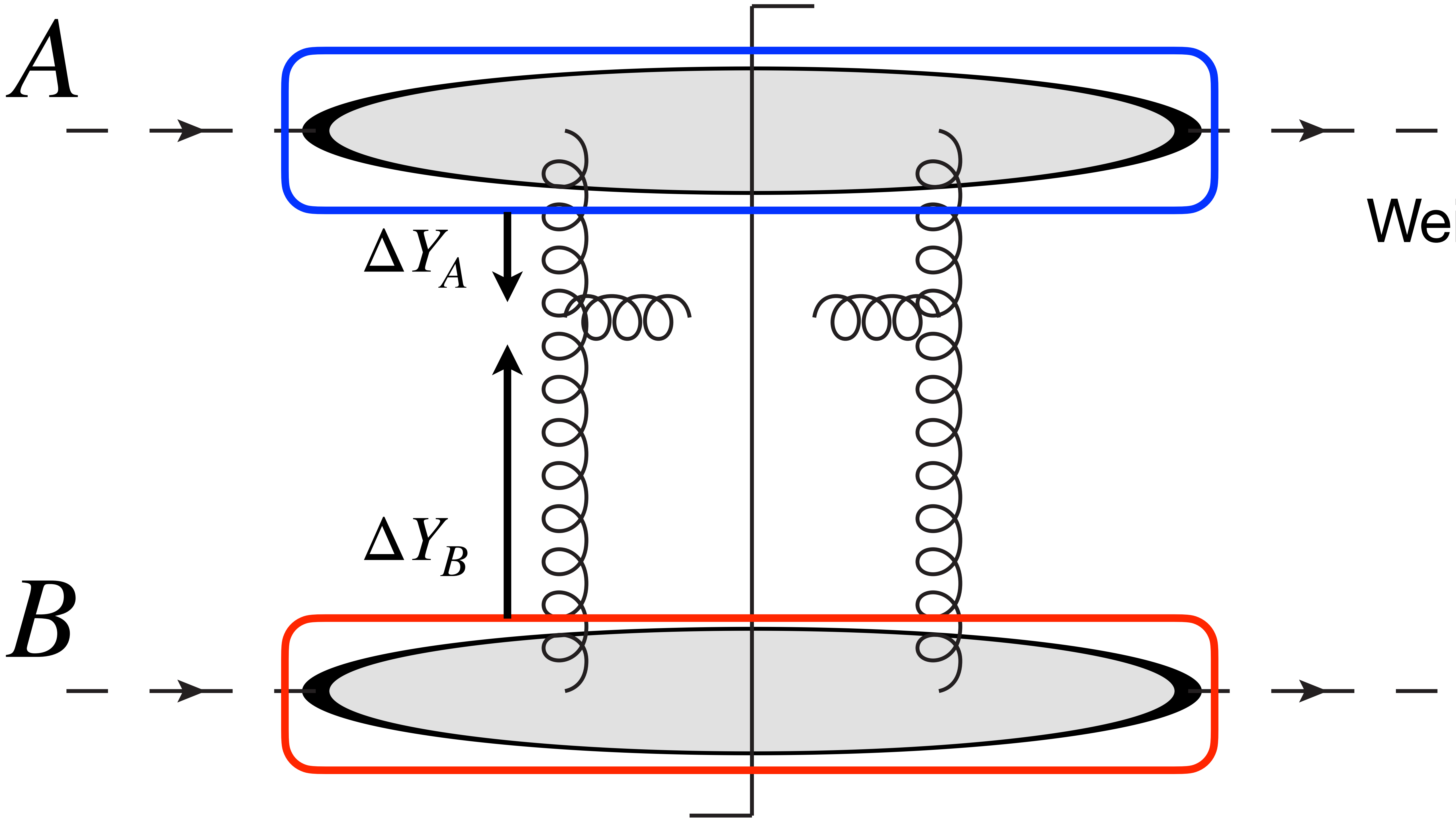

Weight functionals are universal.

$$J^\nu = \delta^{+\nu}\rho_A + \delta^{-\nu}\rho_B$$

pp vs. pA vs. AA
→ different combinations
of Q_A^2 and Q_B^2

$$\langle \mathcal{O} \rangle = \int [\mathcal{D}\rho_A] W_{Y_A}[\rho_A][\mathcal{D}\rho_B] W_{Y_B}[\rho_B] \mathcal{O}[\rho_A, \rho_B]$$

- ❖ If $\Delta Y_A \ll \Delta Y_B$ such as particle production in pp/pA at forward rapidity, $Q_{s,A}^2 \ll Q_{s,B}^2$
- ❖ Hybrid factorization ansatz: collinear factorization with PDFs describes projectile.

Charged hadron multiplicity in pA collisions

A. Dumitru, D. E. Kharzeev, E. M. Levin and Y. Nara, PRC85, 044920 (2012)

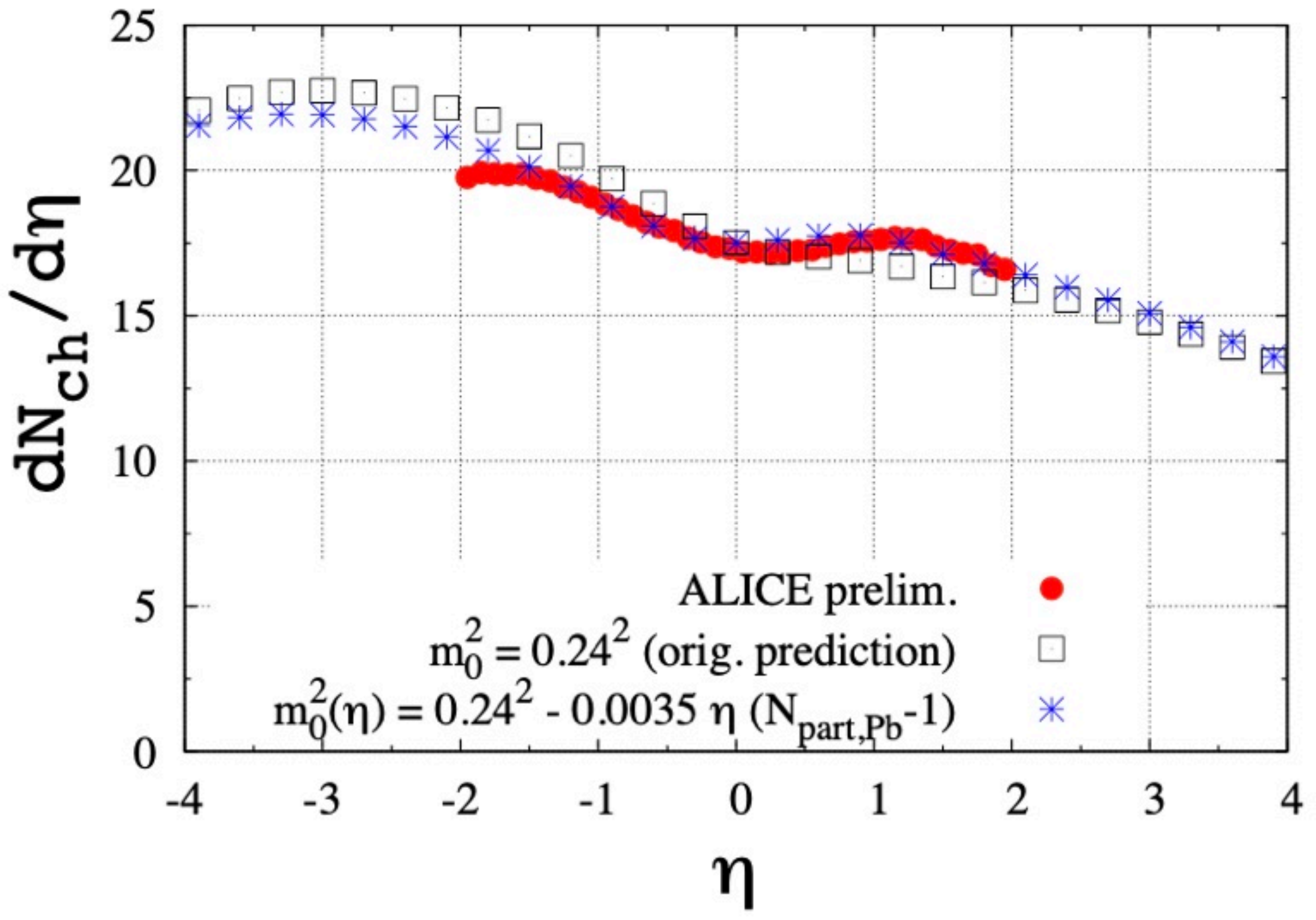

KLN saturation model

J. L. Albacete, A. Dumitru, H. Fujii and Y. Nara, NPA897, 1-27 (2013)

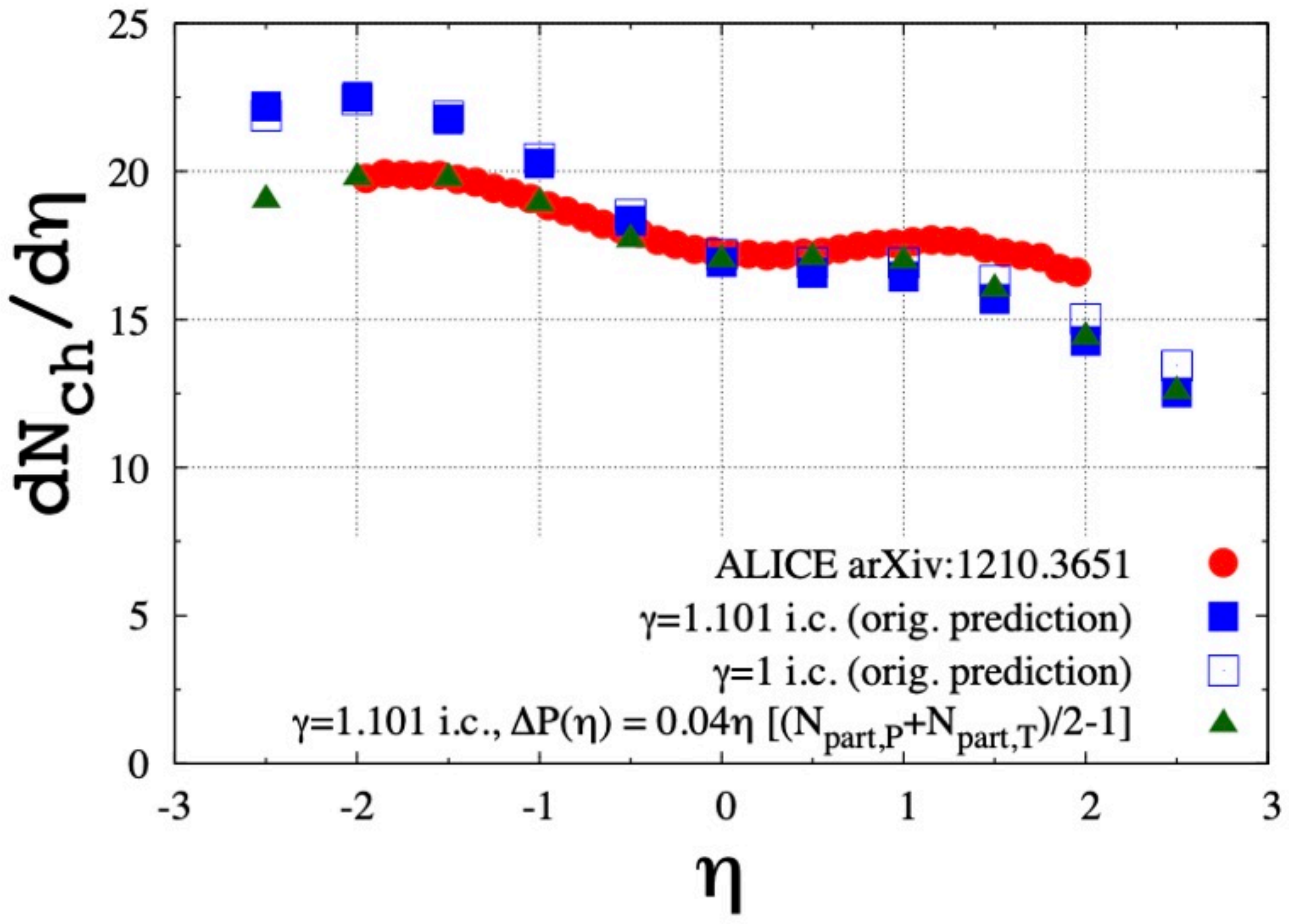

rcBK equation

P. Tribedy and R. Venugopalan, PLB710, 125-133 (2012) [erratum: PLB718, 1154-1154 (2013)]

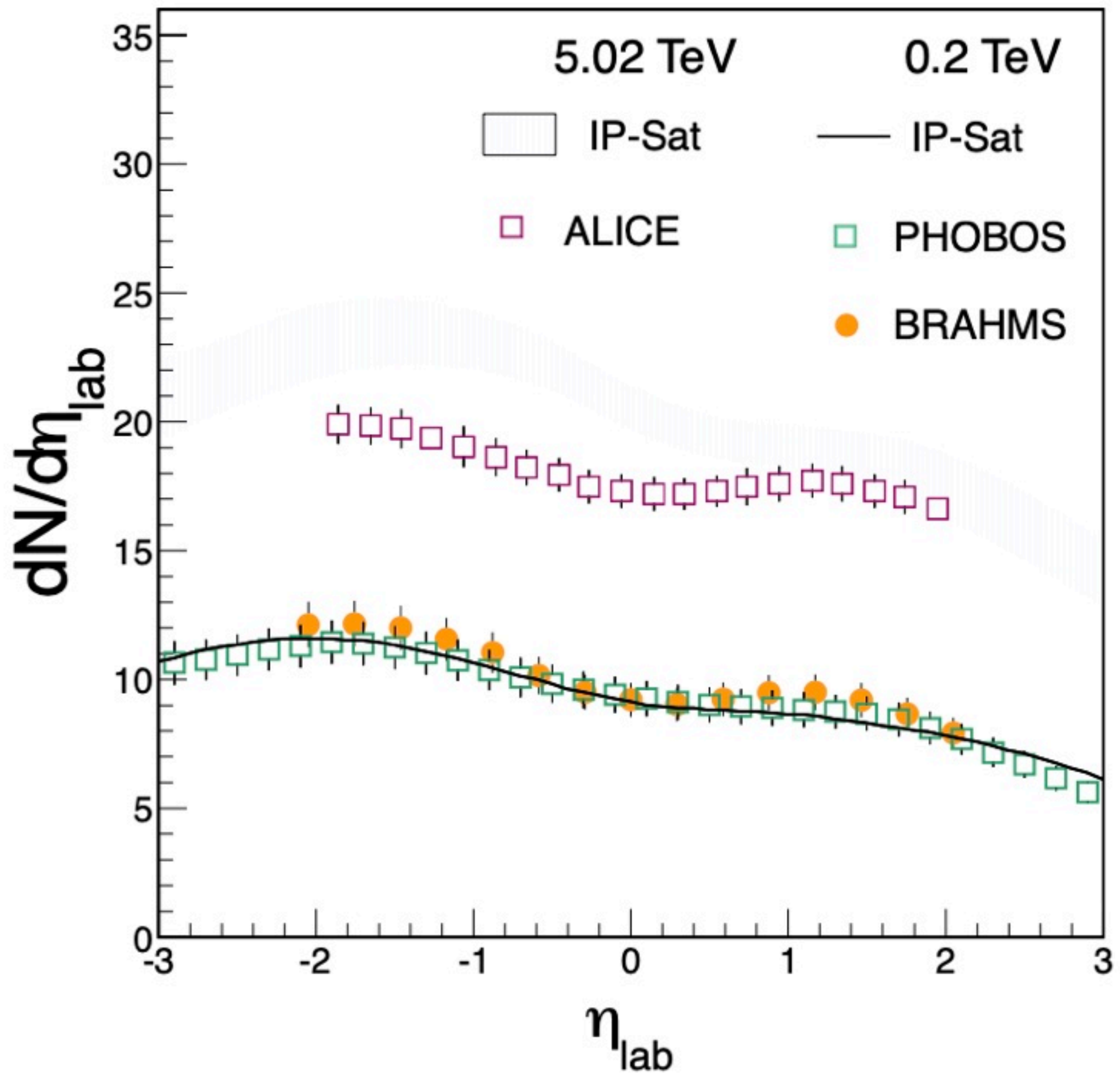

IP-Sat

Caution: Hadronization (Fragmentation) dynamics is blinded.

Impact parameter dependence

❖ b-CGC model

Iancu, Itakura, Munier (2003)
Watt, Motyka, Kowalski(2006)
Watt, Kowalski (2008)

- Linear gluon bremsstrahlung at small-x: BFKL solution.
- Nonlinear recombination in the dense regime: BK solution.
- b-dependence introduced in the saturation scale Q_s.

Since the b-dependence models also confinement, it cannot be constrained by saturation physics alone.

❖ IP-Sat model

Kowalski, Teaney (2003)

- Glauber-Mueller dipole picture: Multiple scattering.
- Each dipole scattering xsection follows DGLAP evolution.
- b-dependence in a gluon profile function in hadrons/nuclei.

❖ BK model

Balitsky (2006)

- NLO running coupling evolution kernel available. (stable numerically)
- MV model is an input distribution.
- b-dependence is not taken into account.

* Input parameters in each model are well constrained by precise HERA data.

Hadron production at mid-rapidity

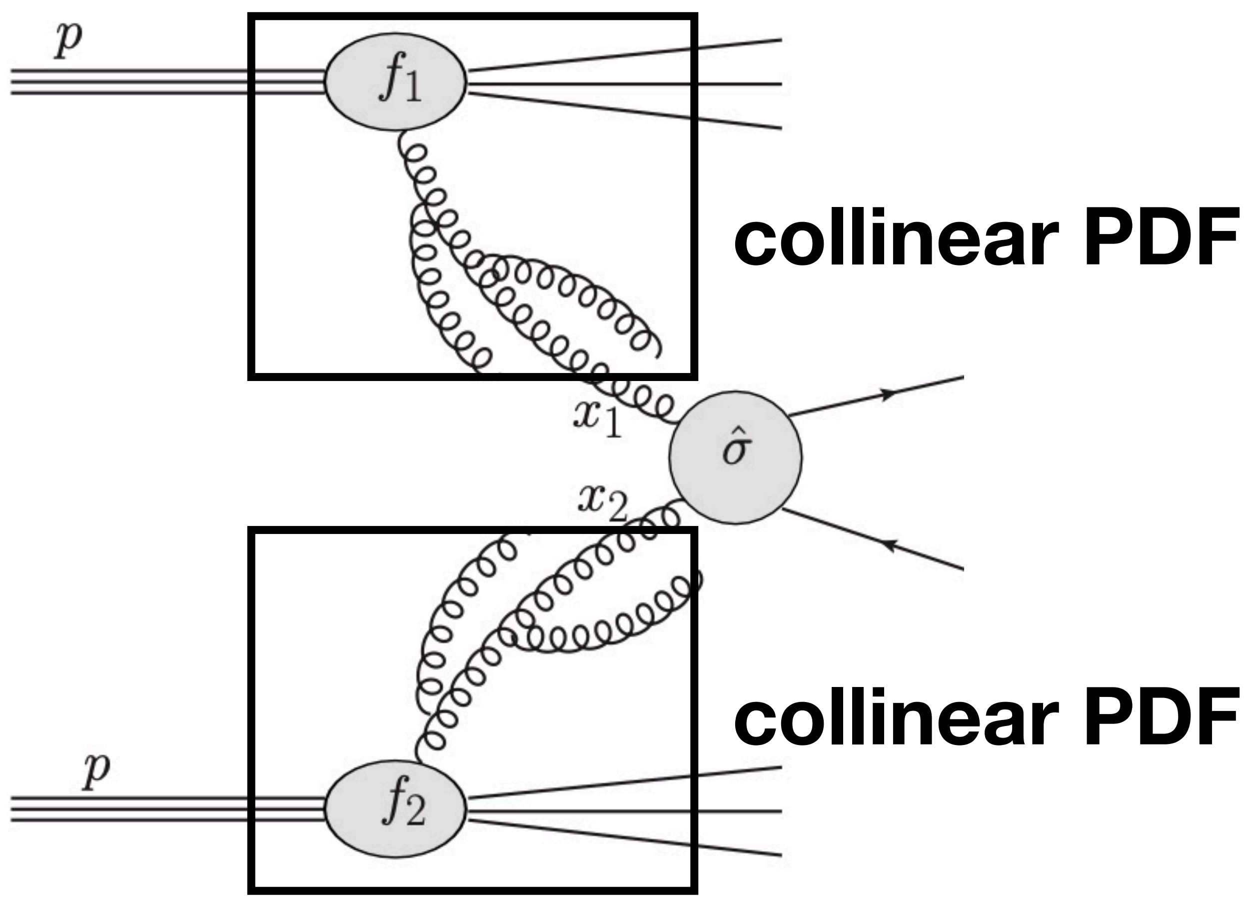

QCD factorization for high-p_T hadron production

Perturbatively calculable coefficients

$$\frac{d\sigma_{p+p\to h+X}}{dp_T} \approx f_{i/p} \otimes f_{j/p} \otimes D_k^D \otimes C_{ij\to k}$$

Universal functions: PDFs, FFs

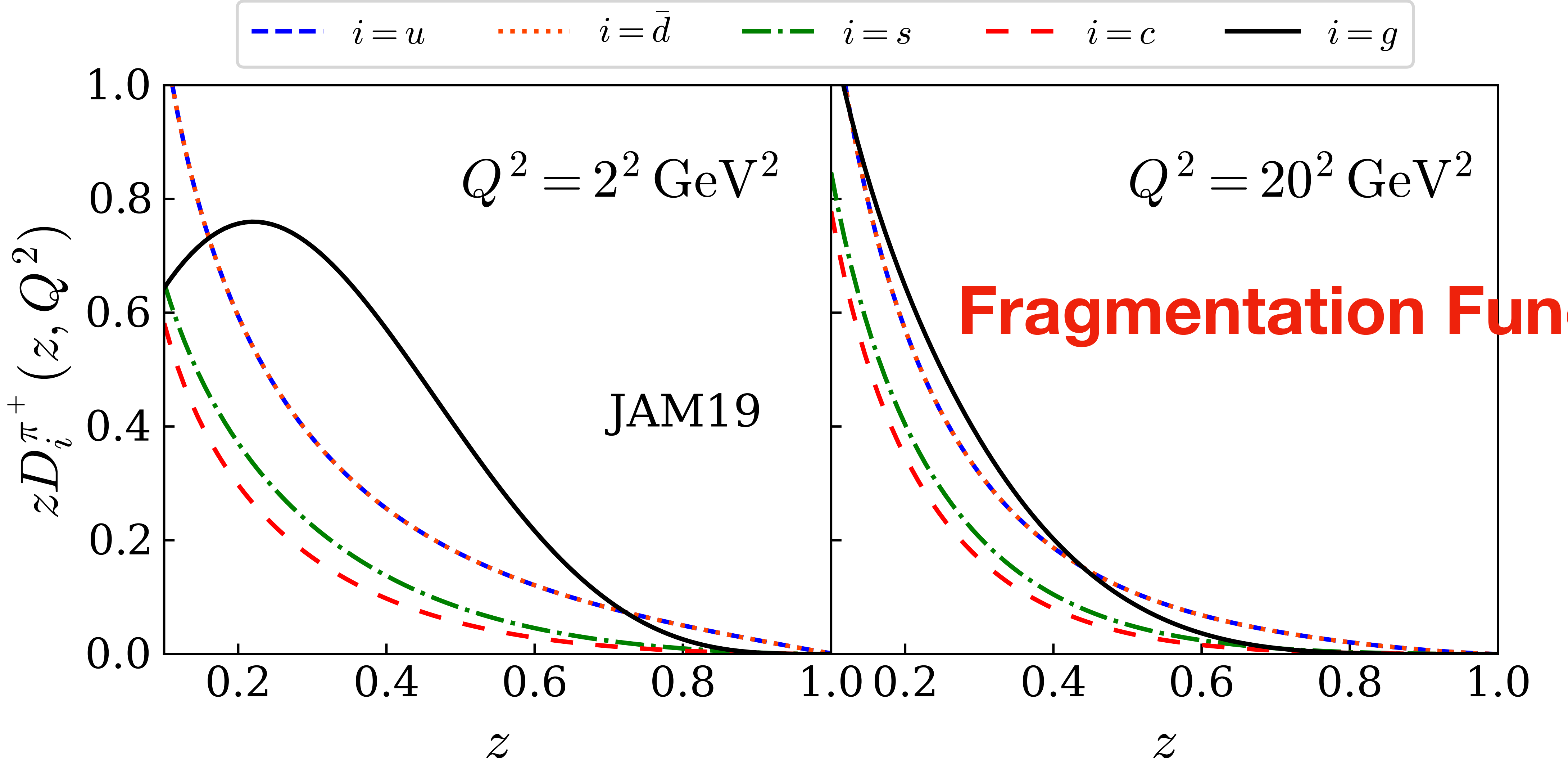

Fragmentation Functions

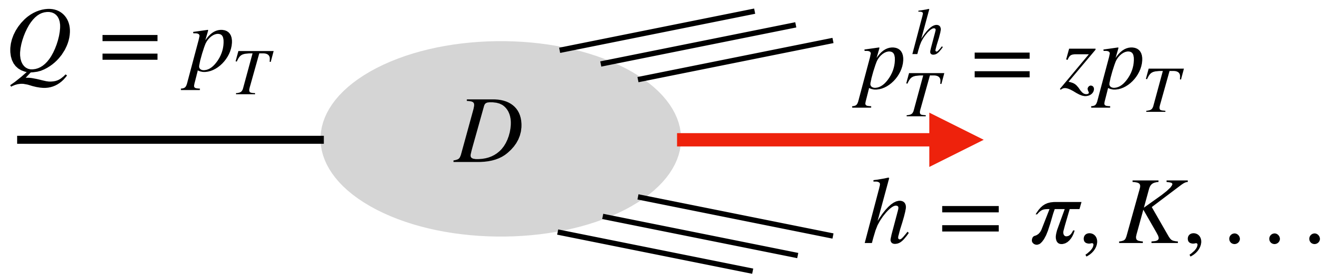

Lee, Qiu, Sterman, **KW**, 2108.00305 [hep-ph]

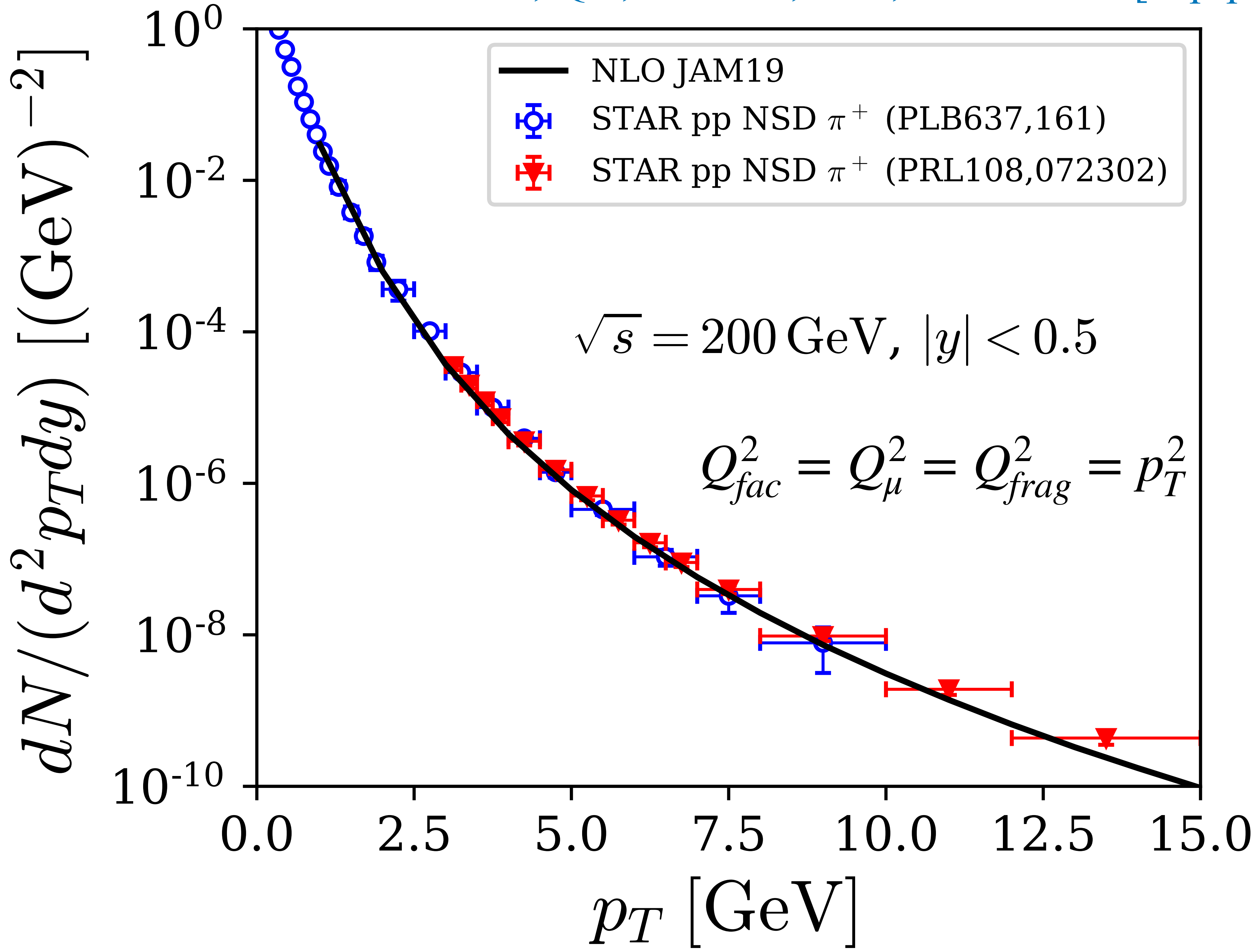

Hadron production at forward-rapidity

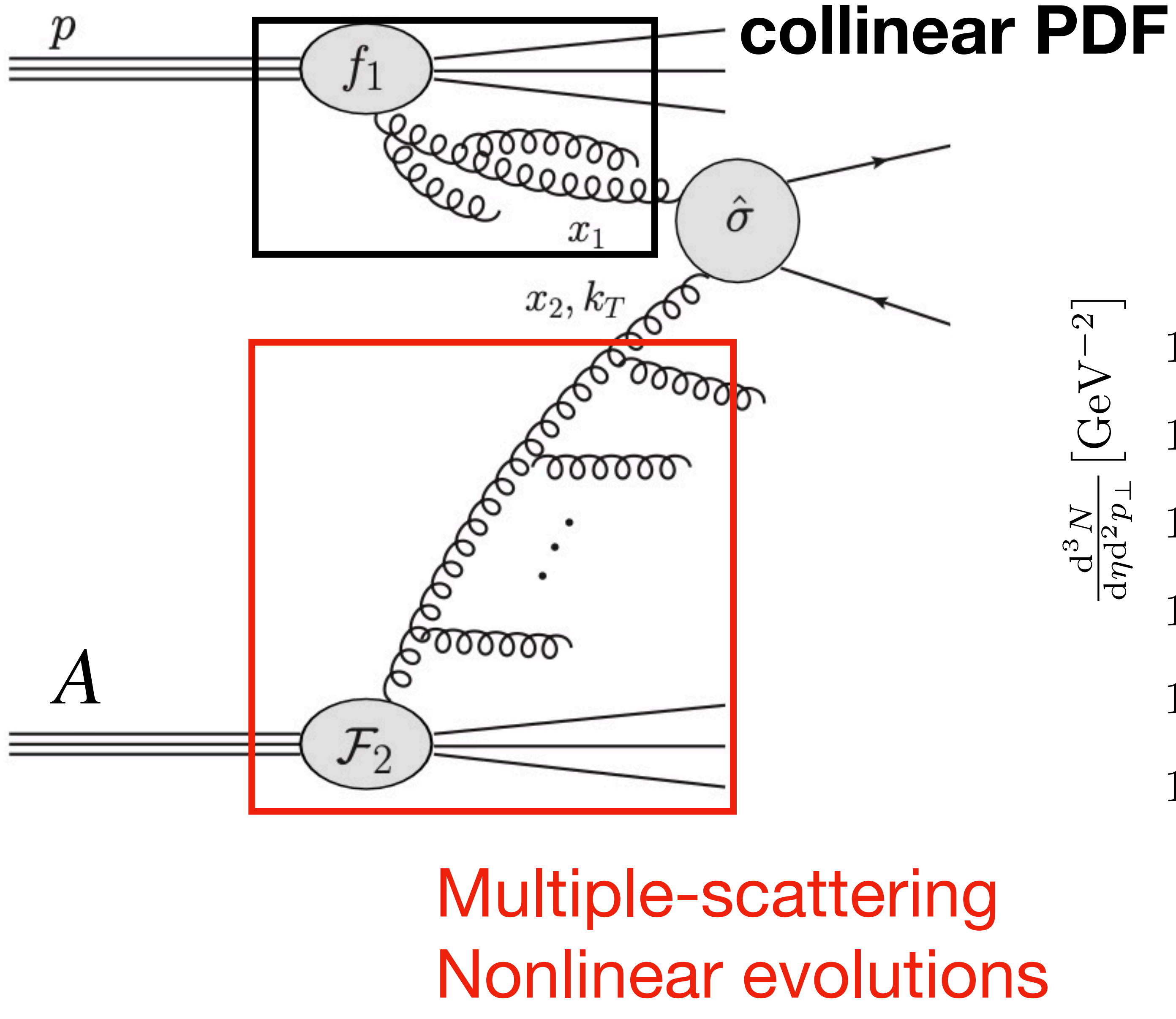

KW, Xiao, Yuan and Zaslavsky, PRD92, no.3, 034026 (2015)

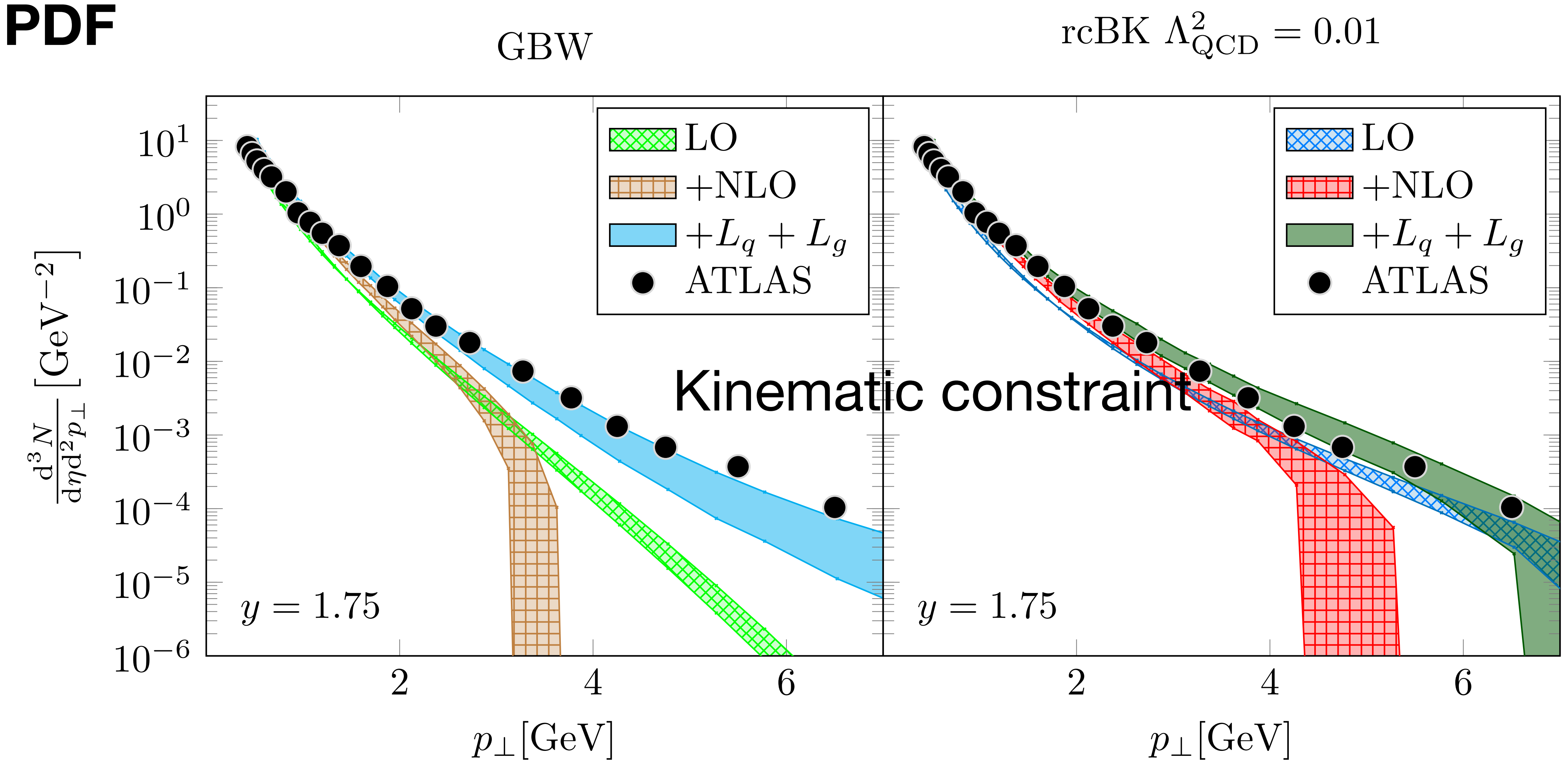

Y. Shi, L. Wang, S.Y. Wei and B.W. Xiao, PRL128, no.20, 202302 (2022)

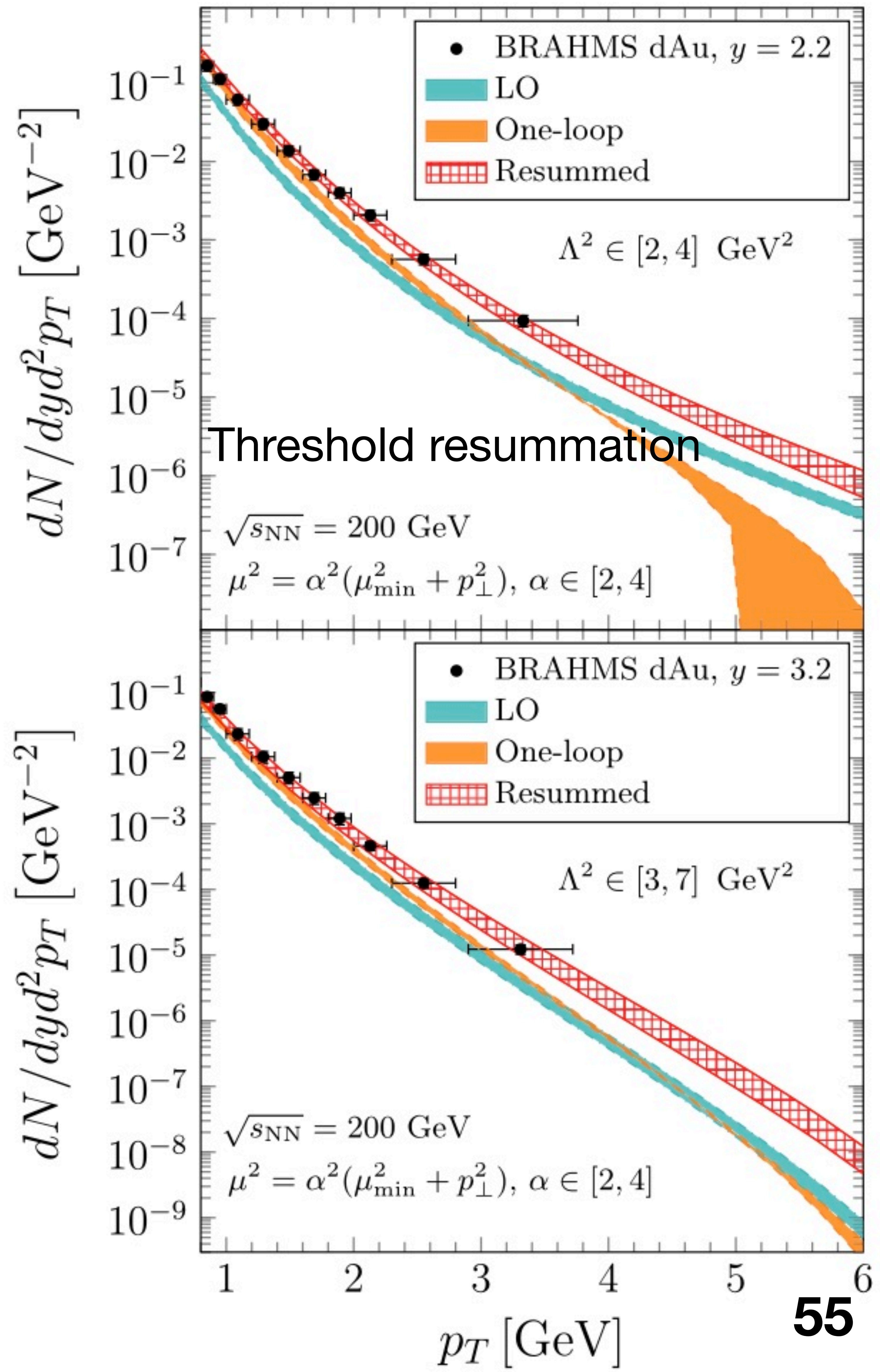

Liu, Ma and Chao, PRD100, no.7, 071503 (2019)

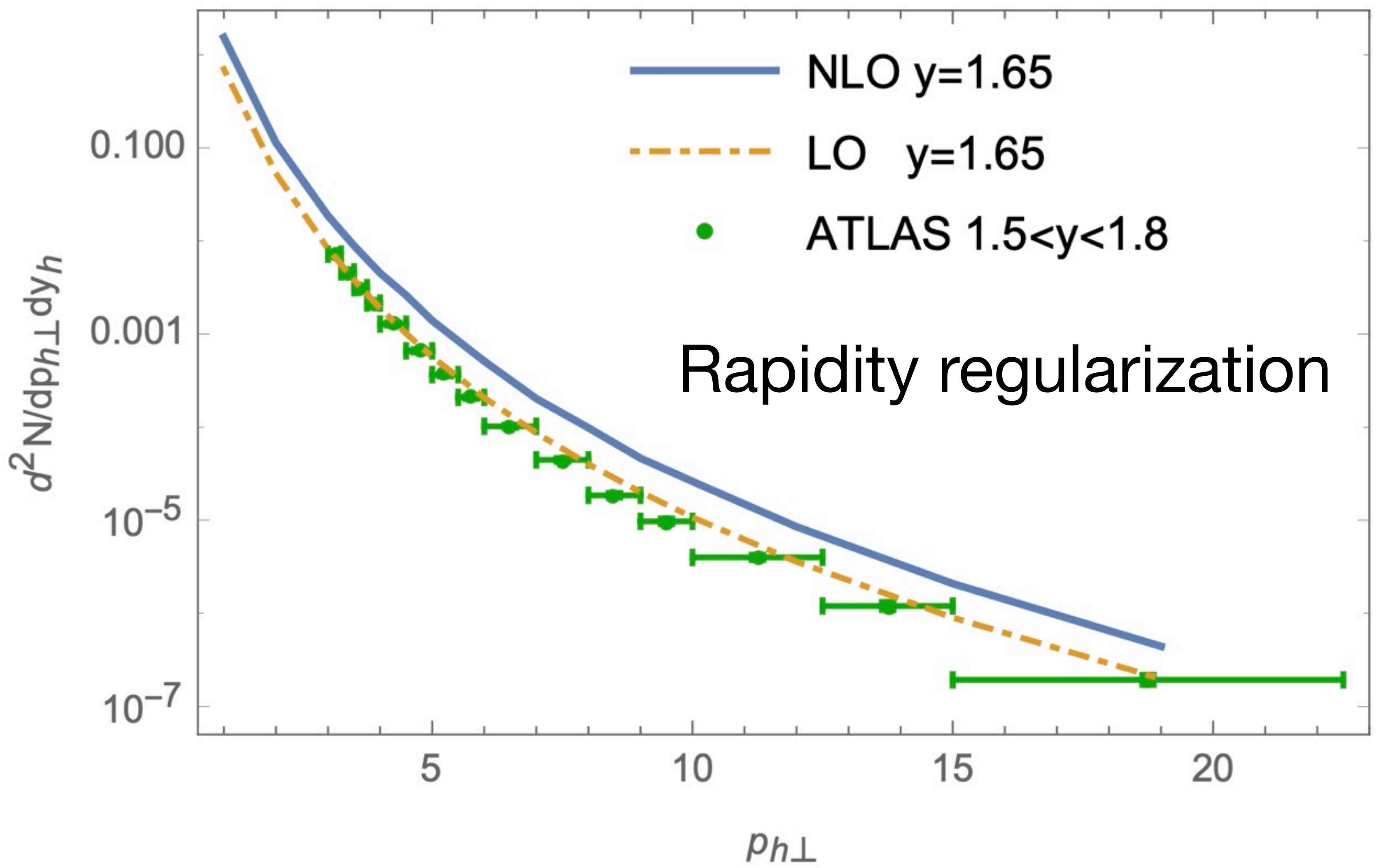

Liu, Kang and Liu, PRD102, no.5, 051502 (2020)

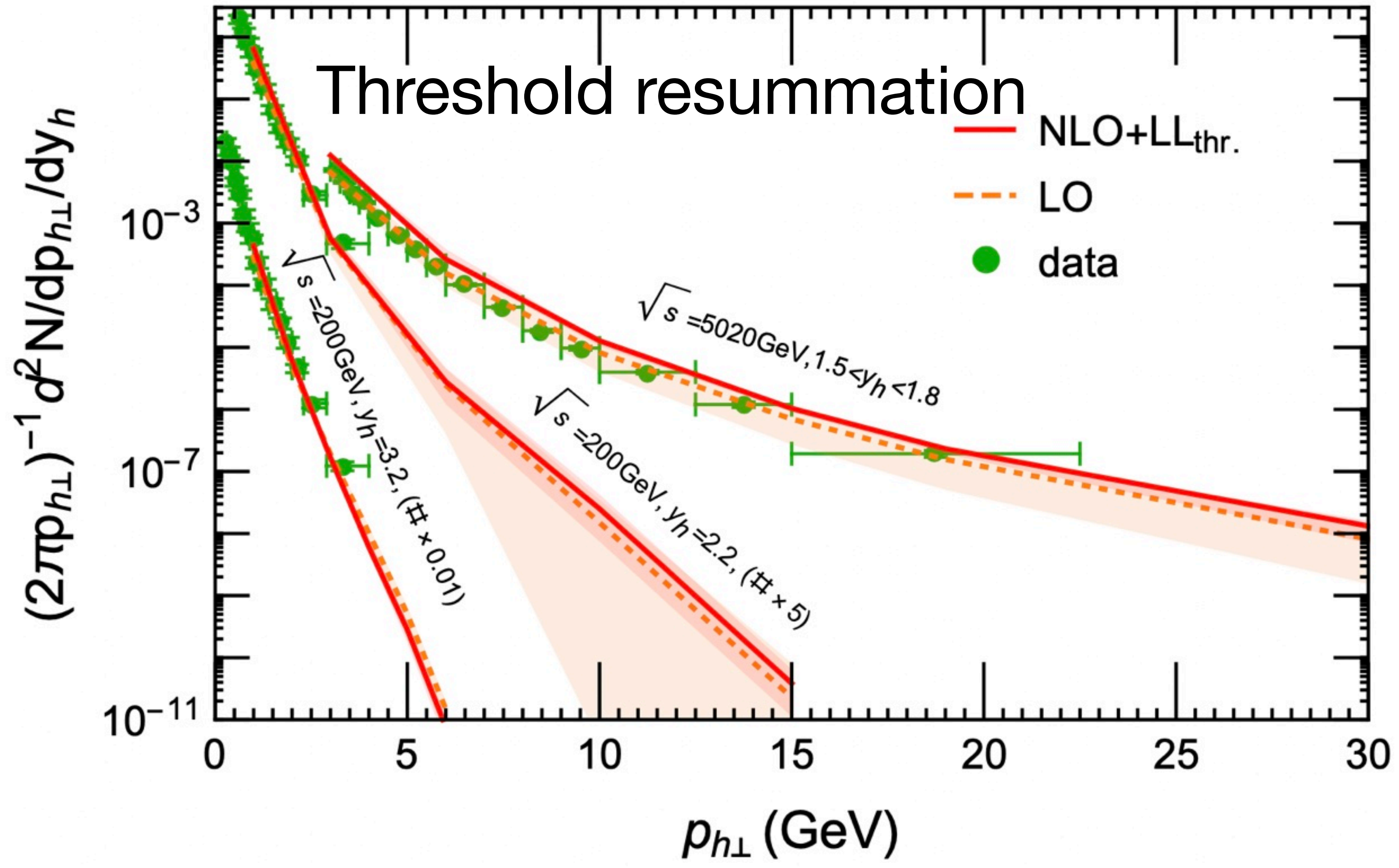

Hadronization model revisited

FFs should be applicable in high-momentum regions, i.e., $p_T \gtrsim 1\,\mathrm{GeV}$. Below that, we need a hadronization model, which is crucial for phenomenology.

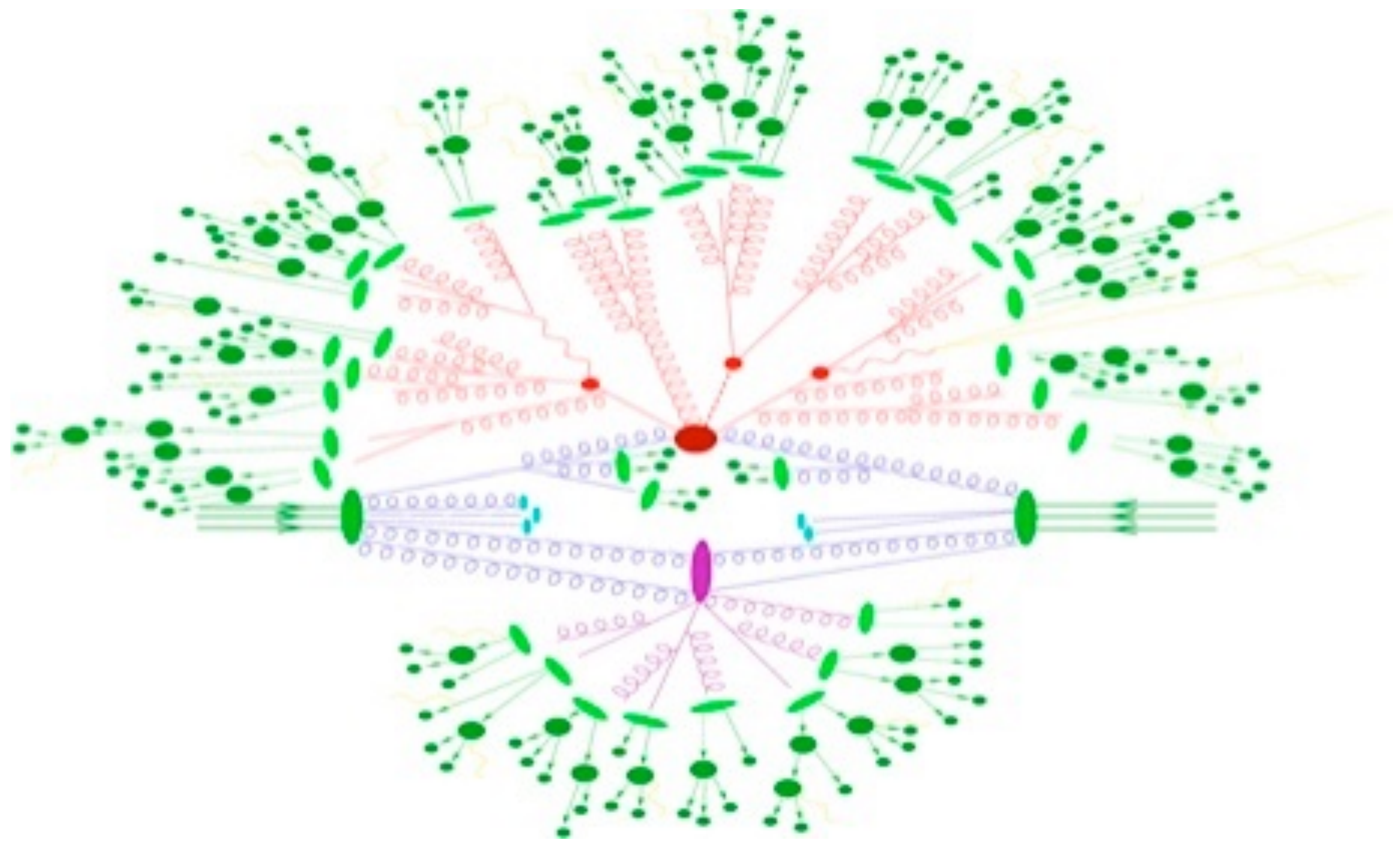

Local Parton Hadron Duality (LPHD) Hypothesis

- Parton's momentum does not change : $p_\perp^g \langle z \rangle = p_\perp^h$.
- Bulk particles do not depend on $\langle z \rangle$: $dN_{ch}/d\eta \sim dN_g/d\eta$.
- Good description of multiplicity dependence in e^+e^-.

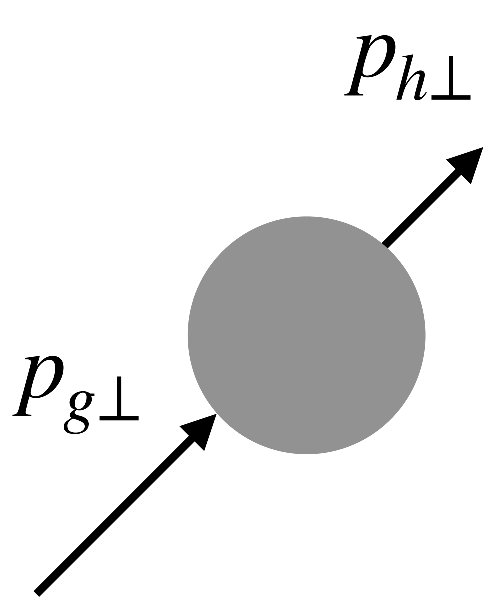

Dokshitzer, Khoze and Troian, J. Phys. G 17, 1585-1587 (1991)
Dokshitzer, Khoze, Mueller and Troian, ``Basics of perturbative QCD,'' (1991)
Khoze and Ochs, Int. J. Mod. Phys. A12, 2949-3120 (1997)

Lund String Fragmentation model

- Hadron production from the breaking of a string between $q\bar{q}$.
- Implemented in PYTHIA.

Bierlich et al. SciPost Phys. Codebases 8 (2022)

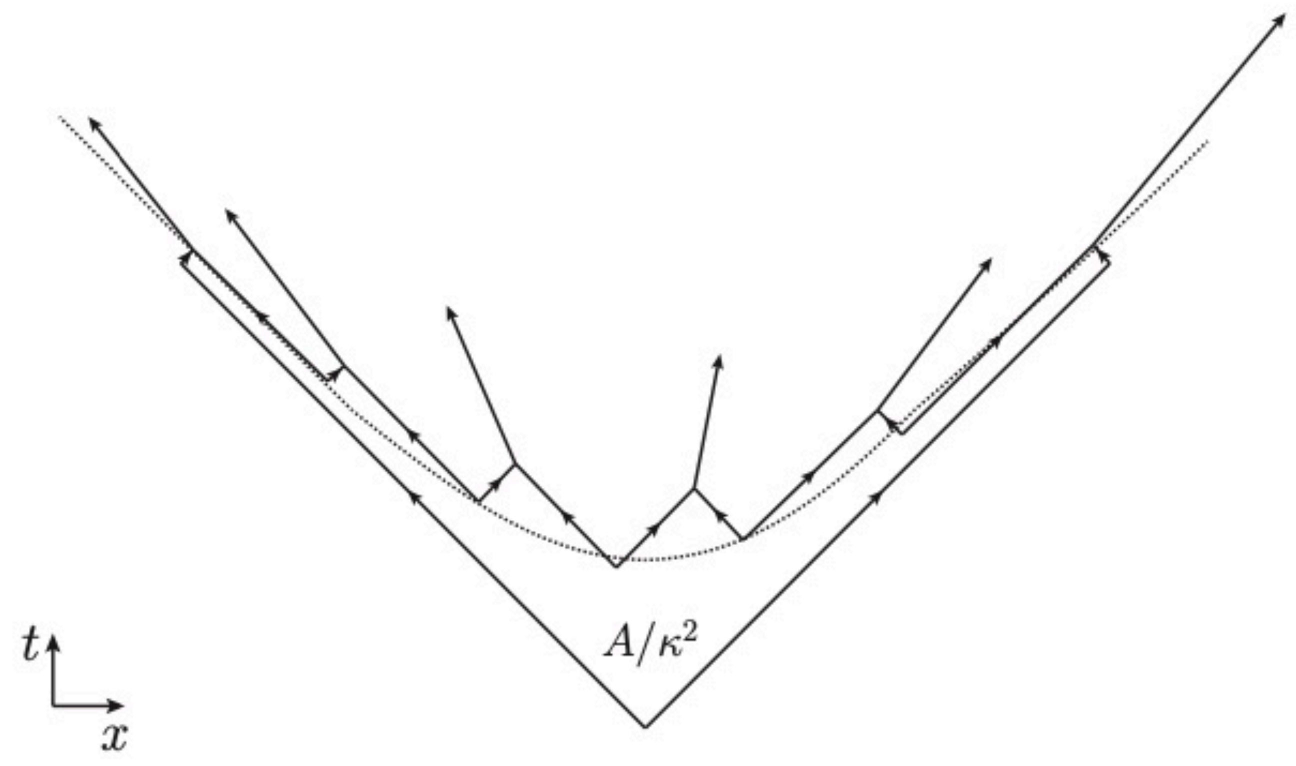

FF vs. LPHD vs. String

Deng, Fujii, Itakura and Nara, PRD91, no.1, 014006 (2015)

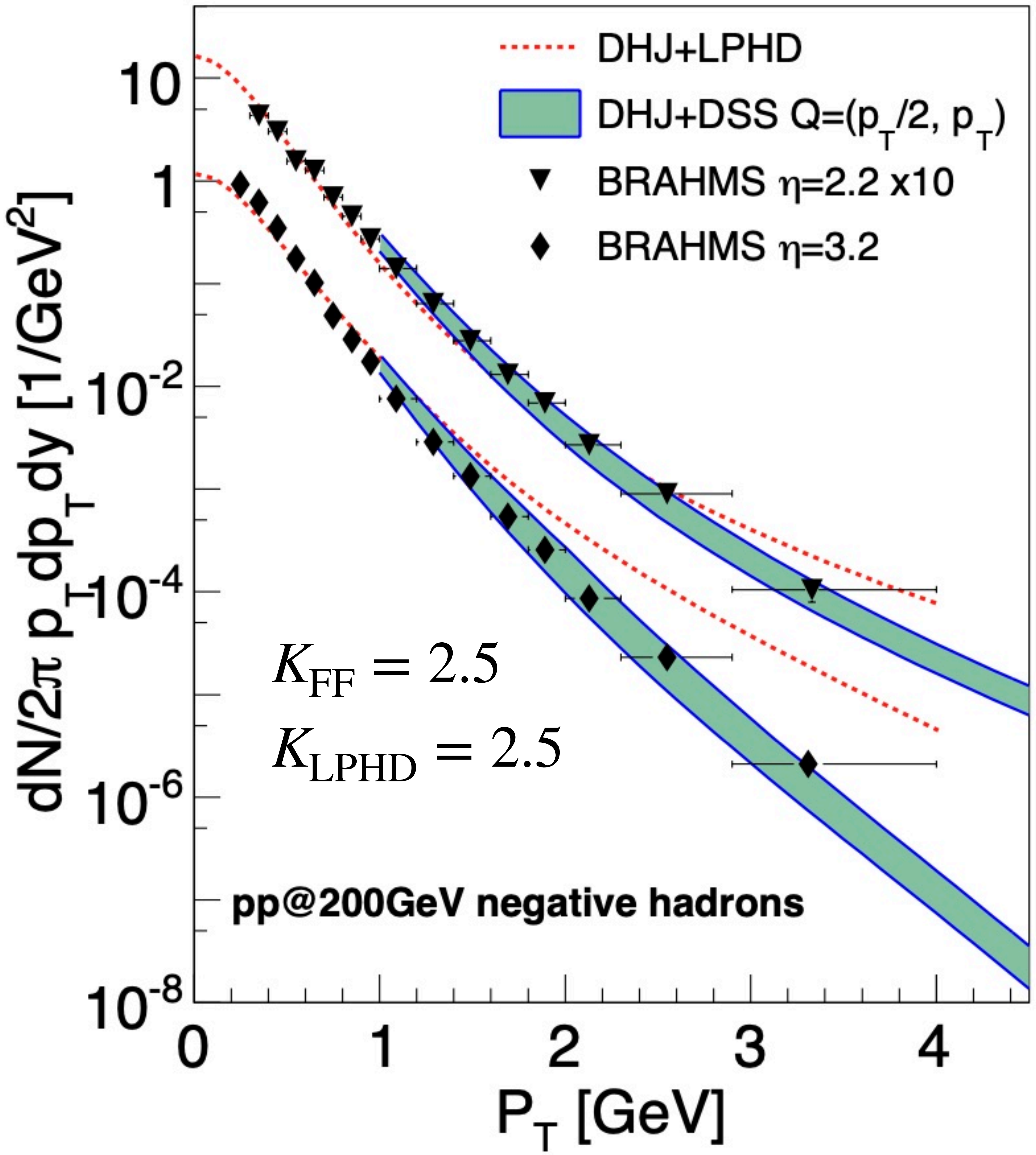

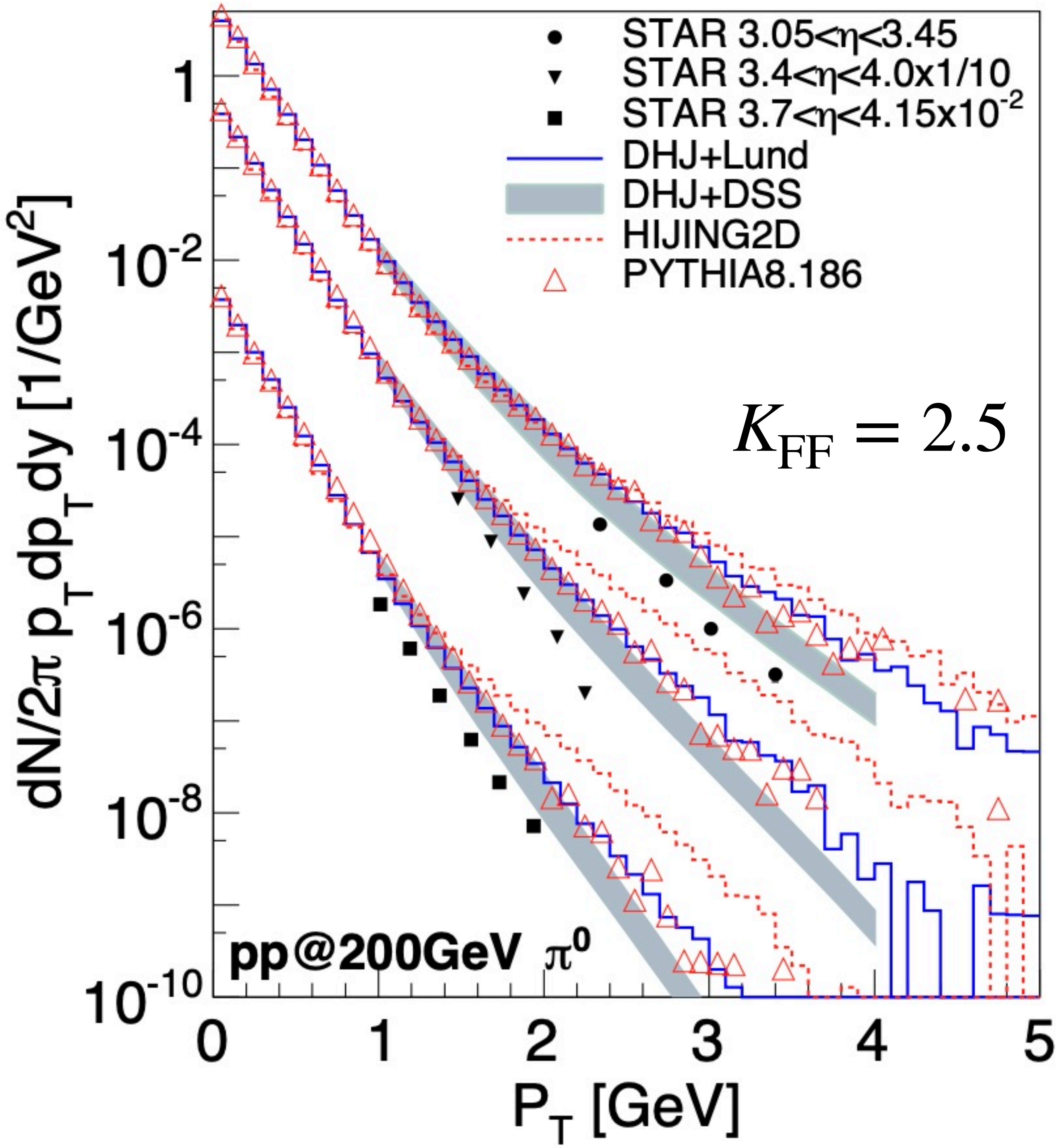

CGC vs. LHCf data on π^0

Deng, Fujii, Itakura and Nara, PRD91, no.1, 014006 (2015)

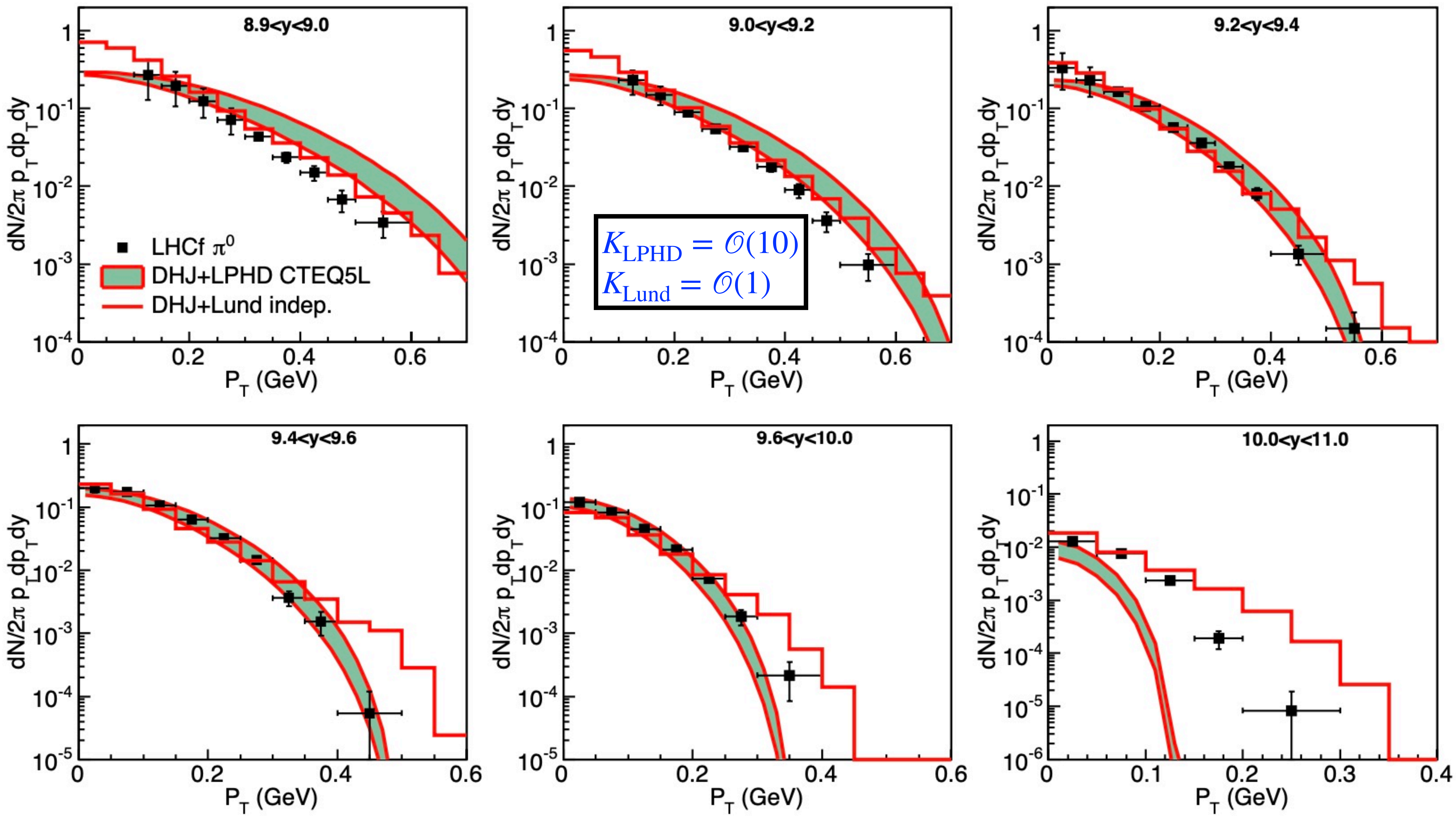

CGC+FF vs. LHCb data on D_0

Based on [Ma, Tribedy, Venugopalan, **KW**, PRD98, no.7, 074025 (2018)]

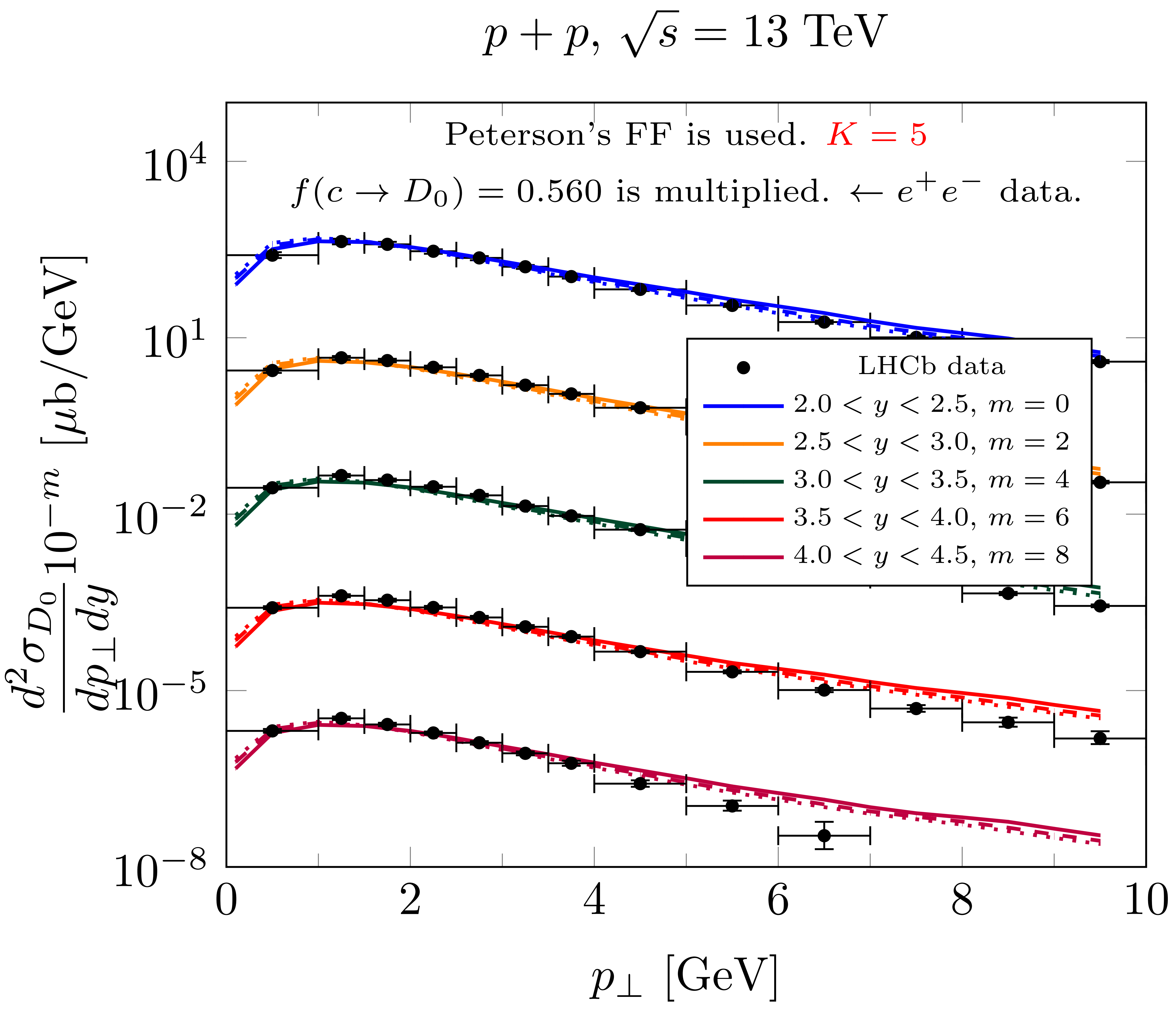

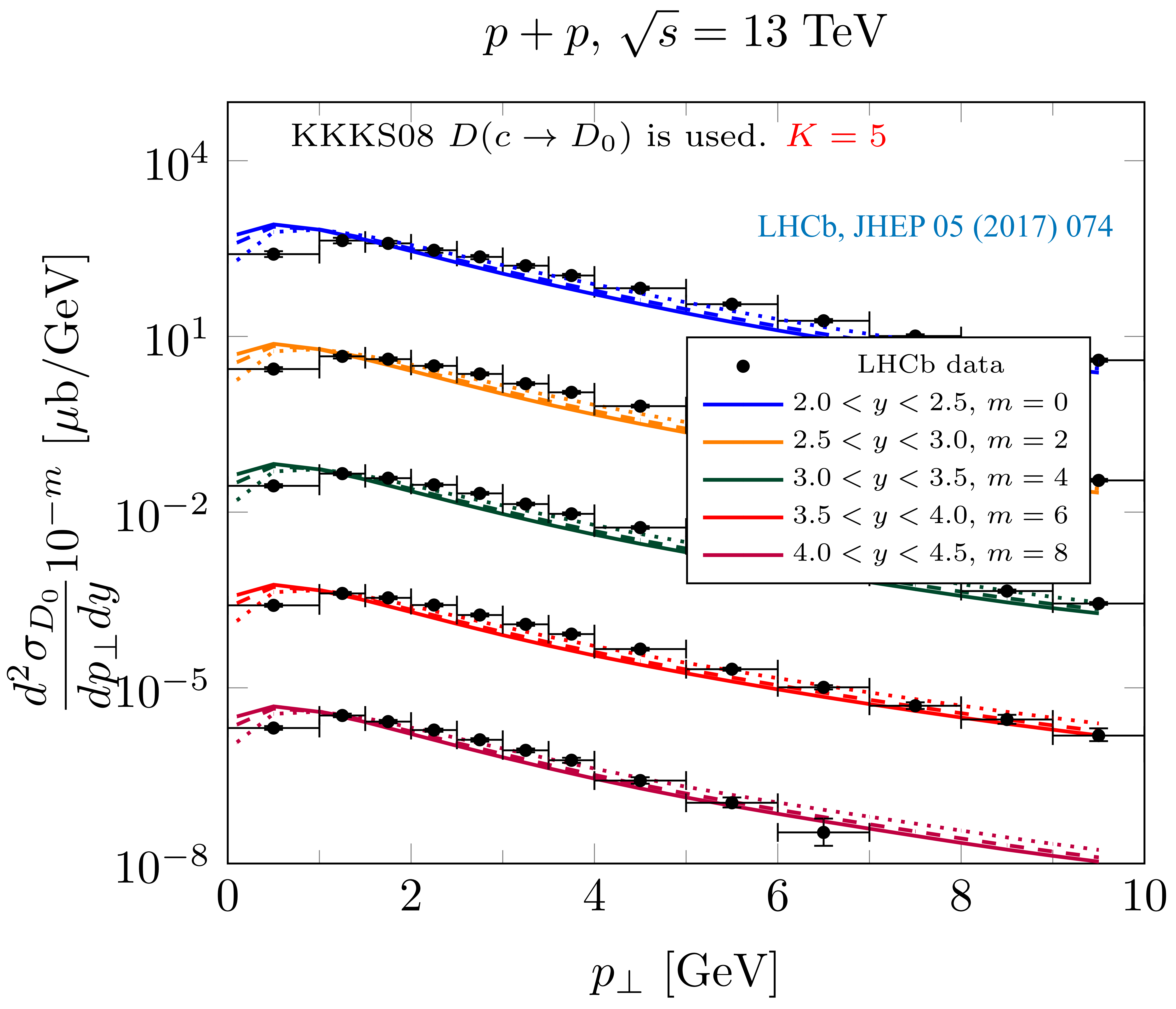

More on theoretical results

Bhattacharya, Kling, Sarcevic and Stasto, [arXiv:2306.01578 [hep-ph]].

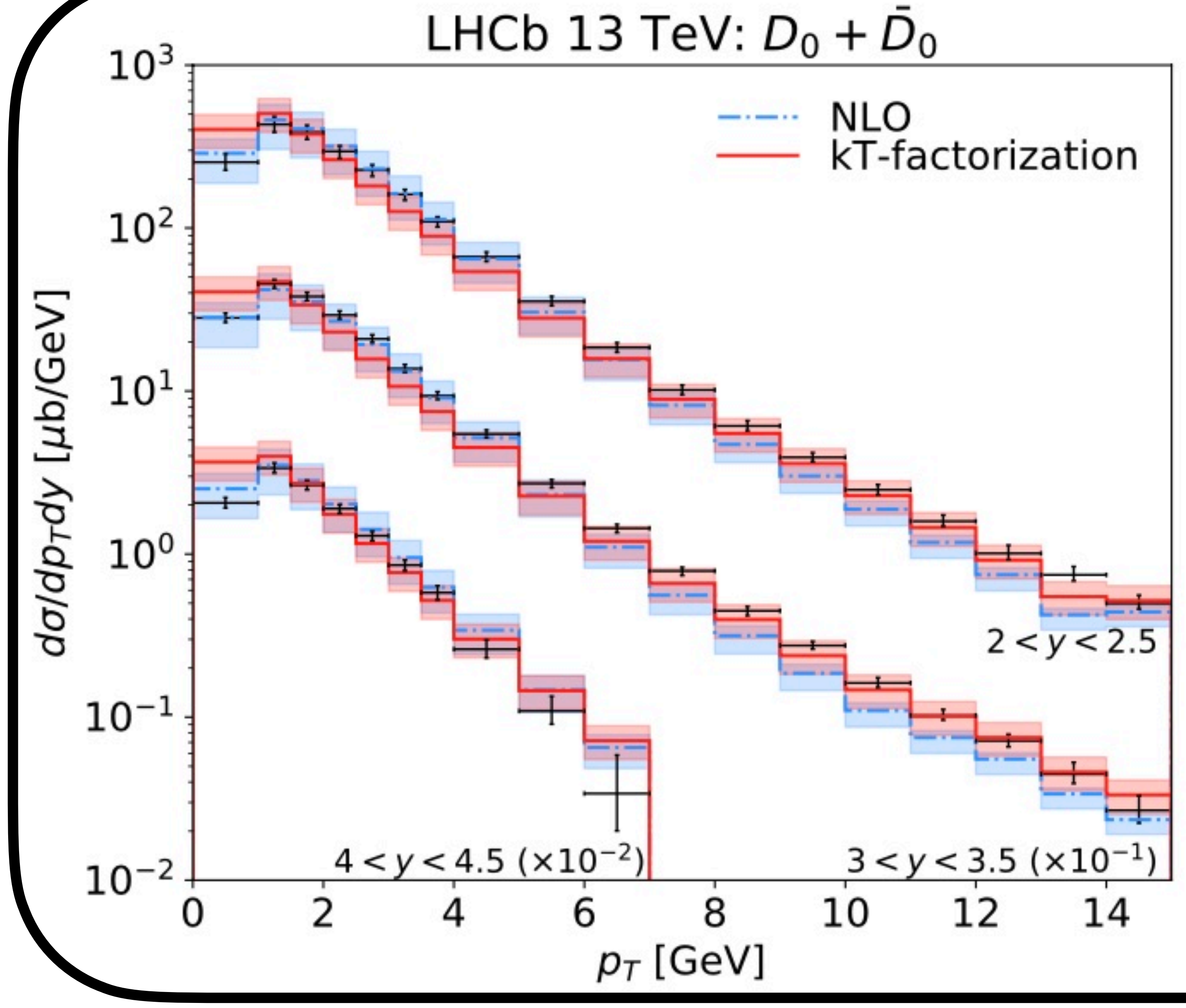

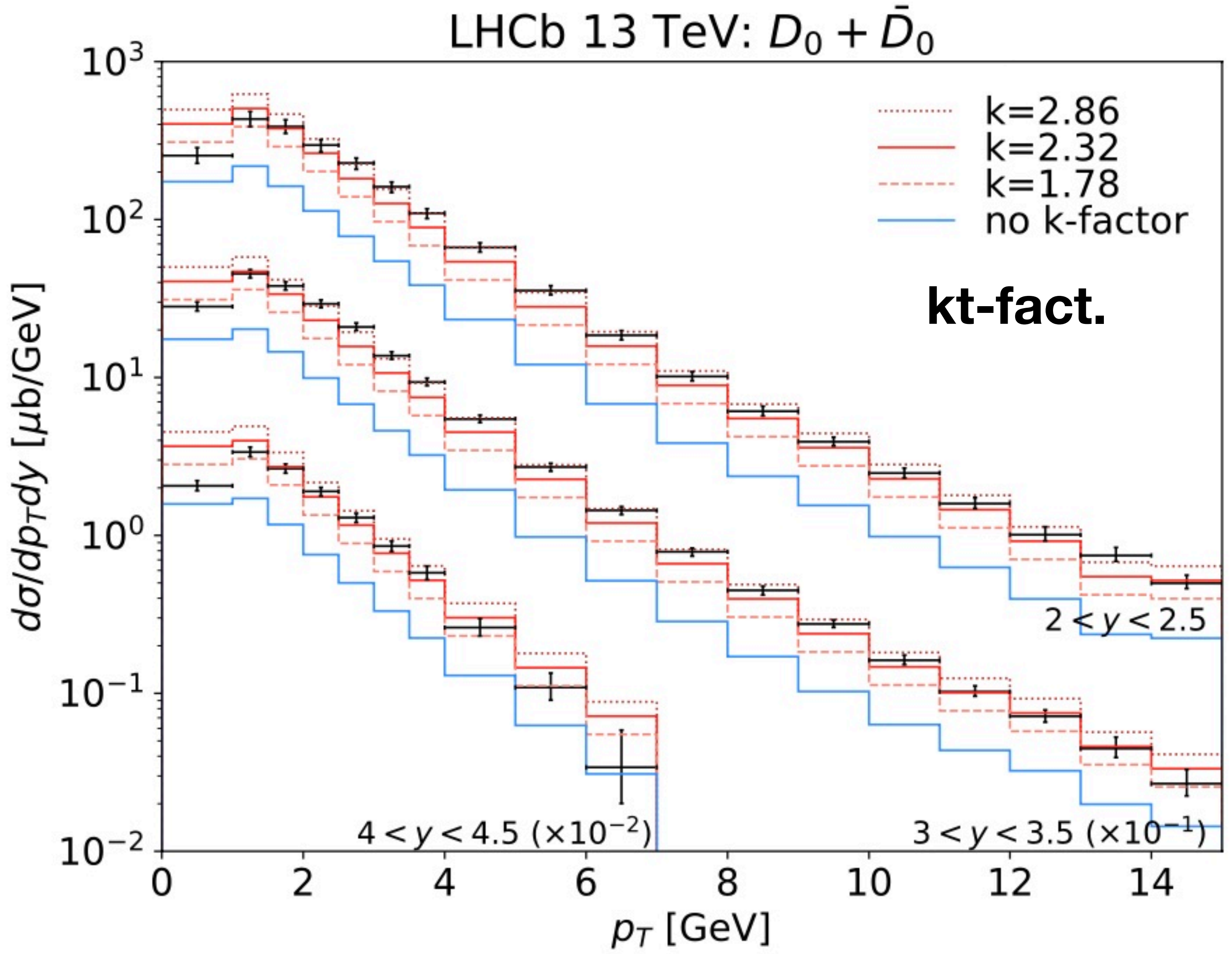

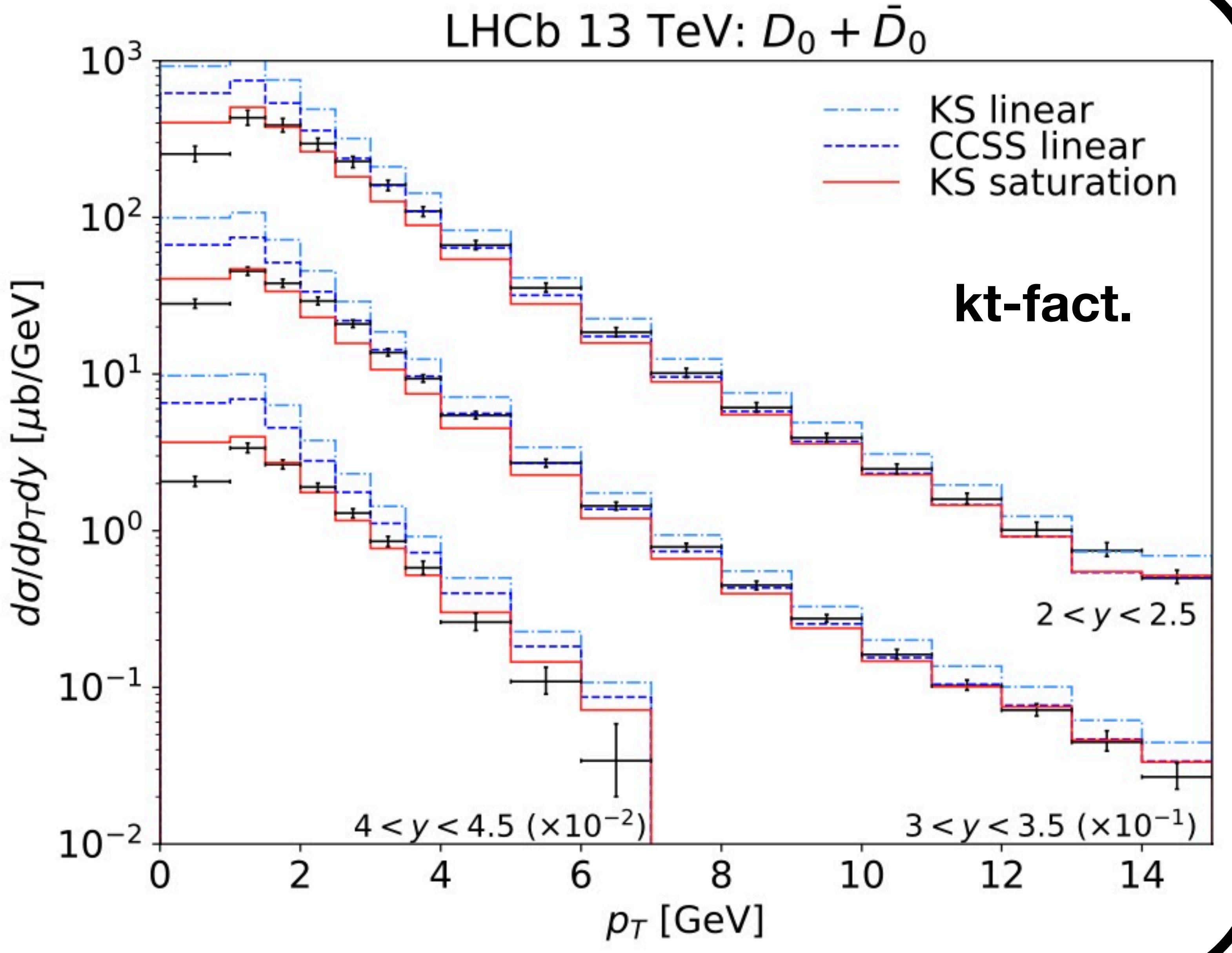

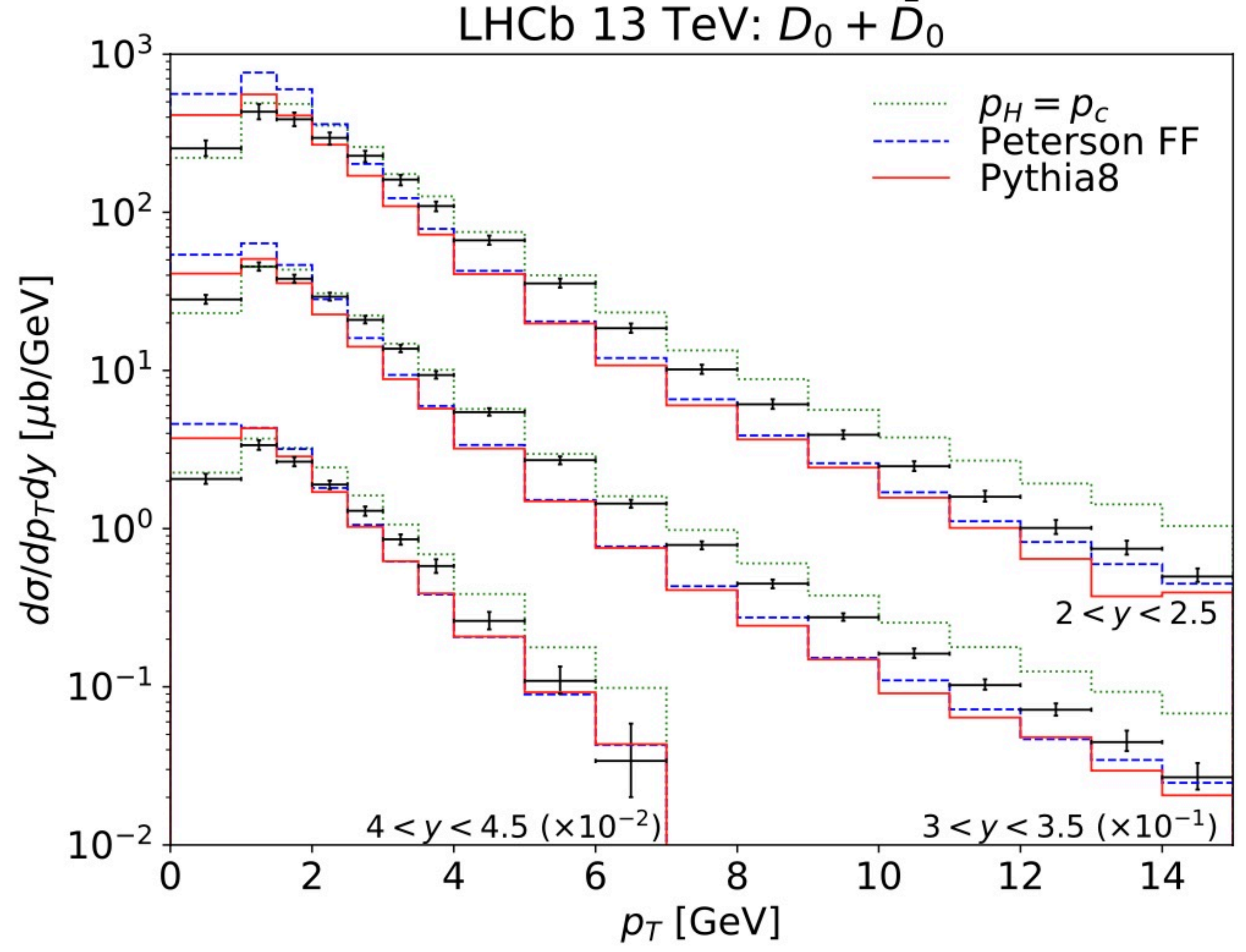

Pythia 8 with the QCD-inspired color reconnection scheme

Two large theoretical uncertainties:

❖ Hadronization model and scheme dependence

❖ No NLO calculations in k_t-factorization

From charm hadrons to neutrinos

Bhattacharya, Kling, Sarcevic and Stasto, [arXiv:2306.01578 [hep-ph]].

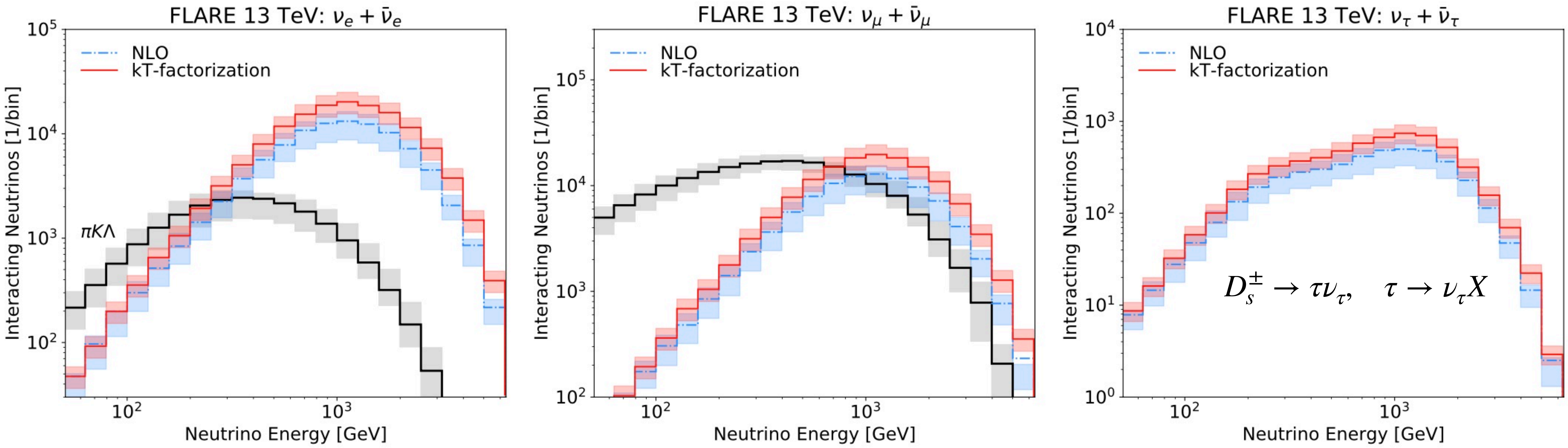

- High-energy electron neutrinos are mostly produced via charm-semileptonic decay.
- **Caution:** If global data fitting is to be done in the future, various factorization issues need to be considered.
- How accurately can information on gluon saturation be extracted? How much impact is there from **the beam remnant**? Parton shower effects….

Appendix
Diffraction and UPC

Coherent diffractive production

Fig. from Toll and Ullrich, PRC87, no.2, 024913 (2013)

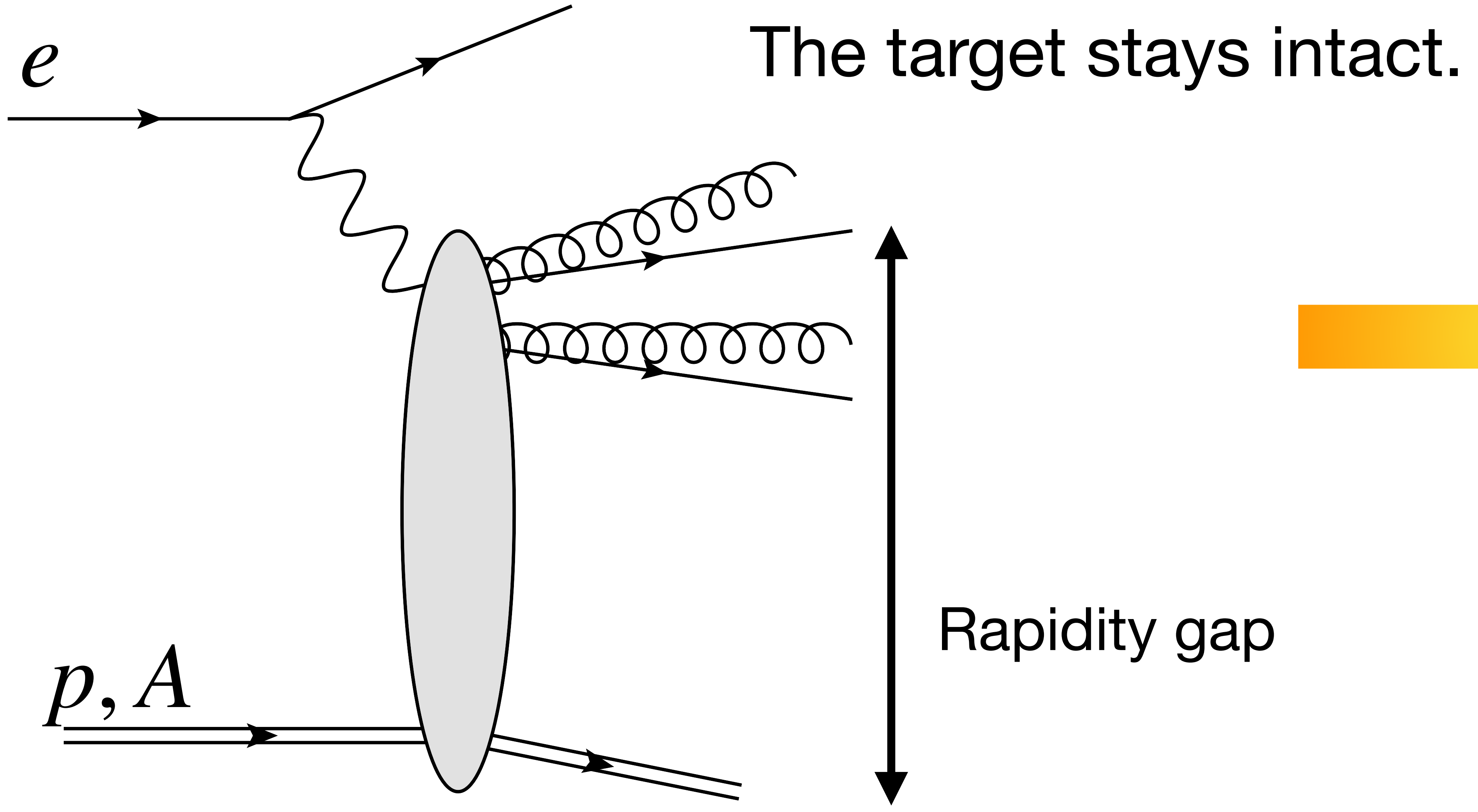

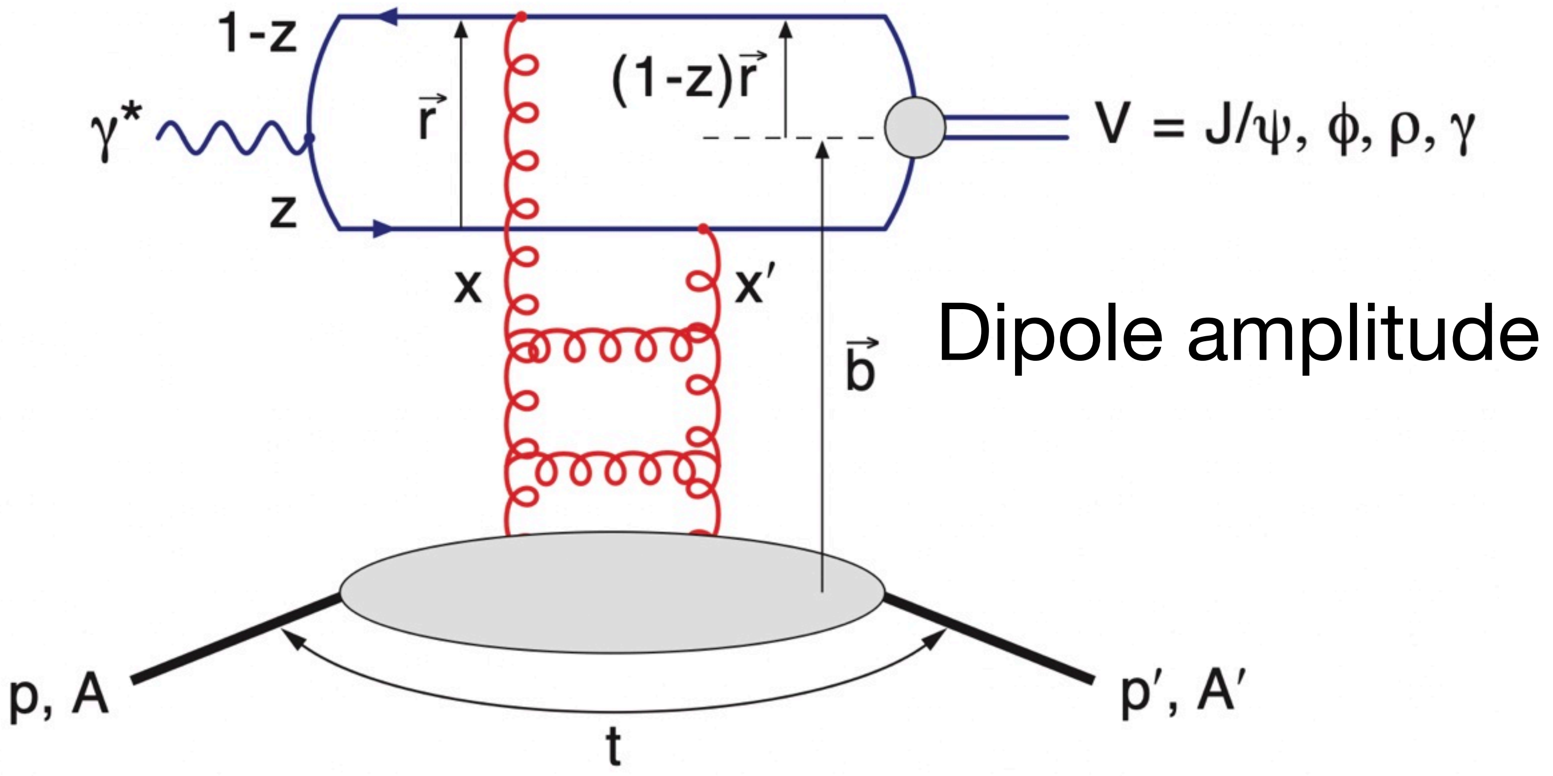

$$\frac{d\sigma^{\gamma^* A \to VA}_{coherent}}{dt} \propto \left| \langle \mathscr{A} \rangle \right|^2$$

Armesto and Rezaeian, PRD90, no.5, 054003 (2014)

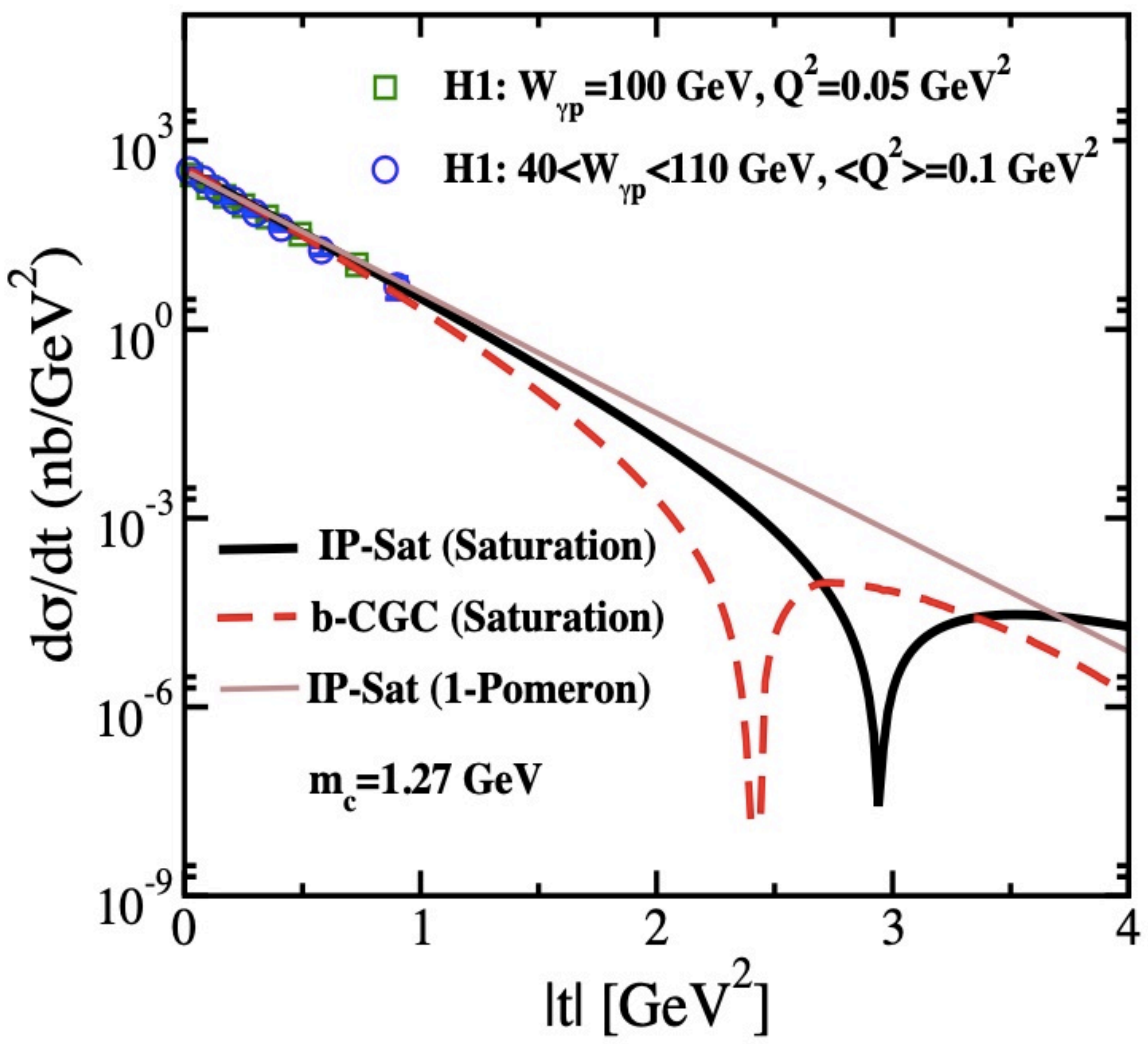

- ❖ t: the momentum transfer between a vector meson V and the target,
- ❖ $\mathscr{A}$: the production amplitude of the meson V, proportional to the gluon distribution function.
- ❖ $\langle \cdot \rangle$: the average due to the nuclear wavefunction

Incoherent diffractive production

Mantysaari and Schenke, PRL117, no.5, 052301 (2016)

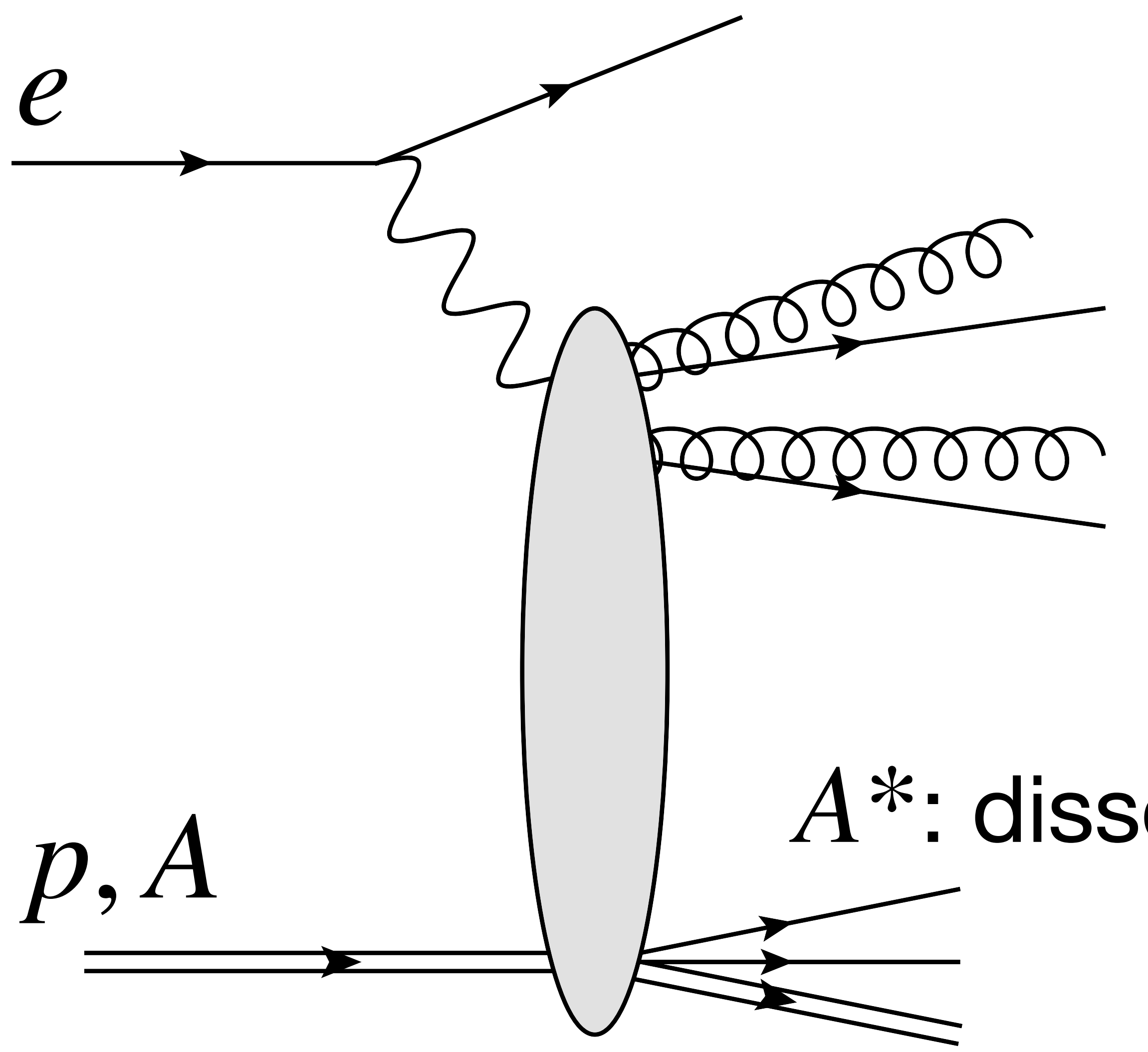

The target breaks, but still, a rapidity gap presents.

$$\frac{d\sigma^{\gamma^* A \to V A^*}_{incoherent}}{dt} \propto \langle |\mathscr{A}|^2 \rangle - |\langle \mathscr{A} \rangle|^2$$

Offers a direct measure of the lumpiness of gluons

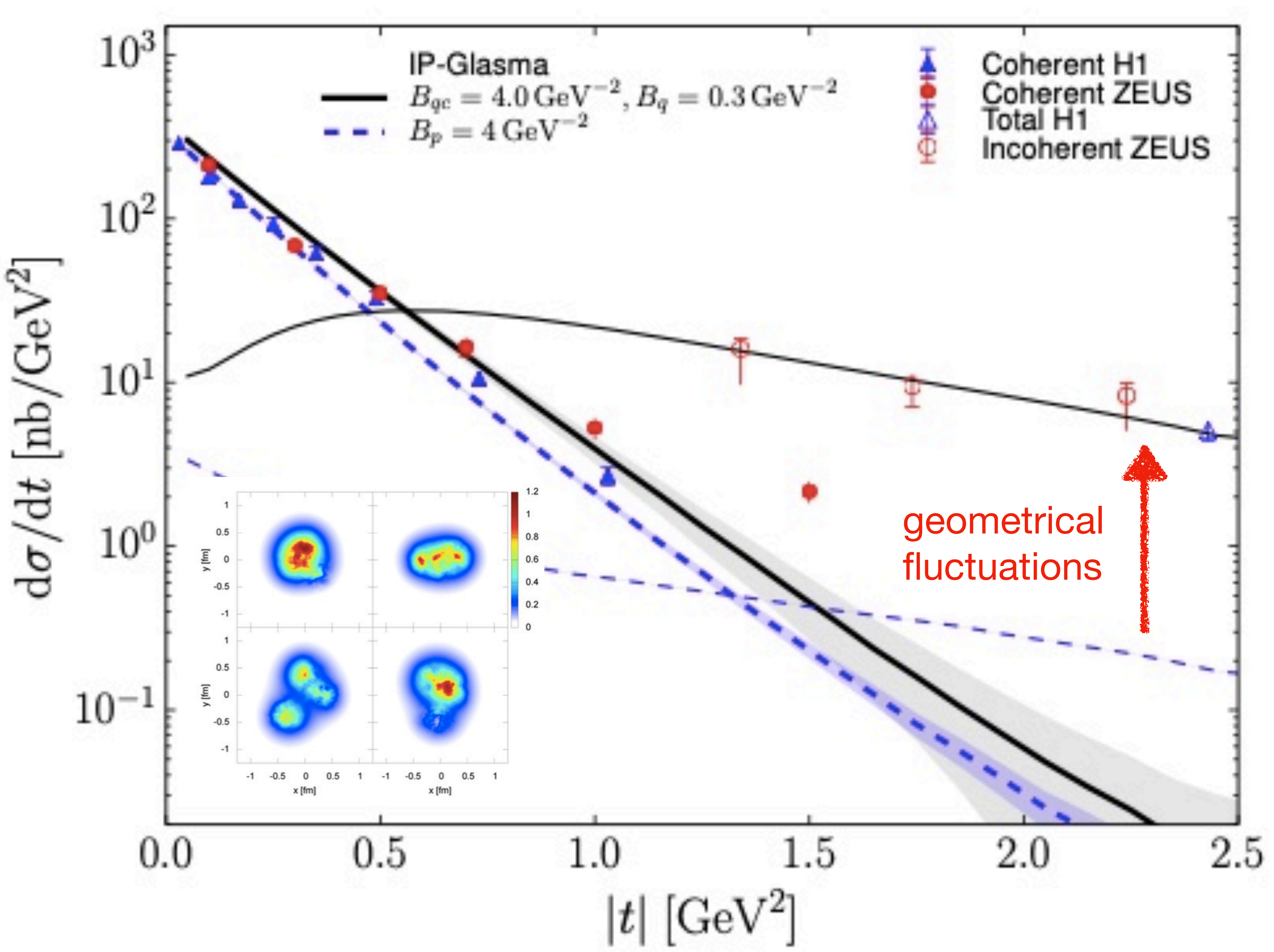

❖ Theoretical uncertainty in the production of vector mesons arises from the description of their light-cone wave function and the dipole amplitude.

Exclusive diffraction on nuclei

Toll and Ullrich, PRC87, no.2, 024913 (2013)

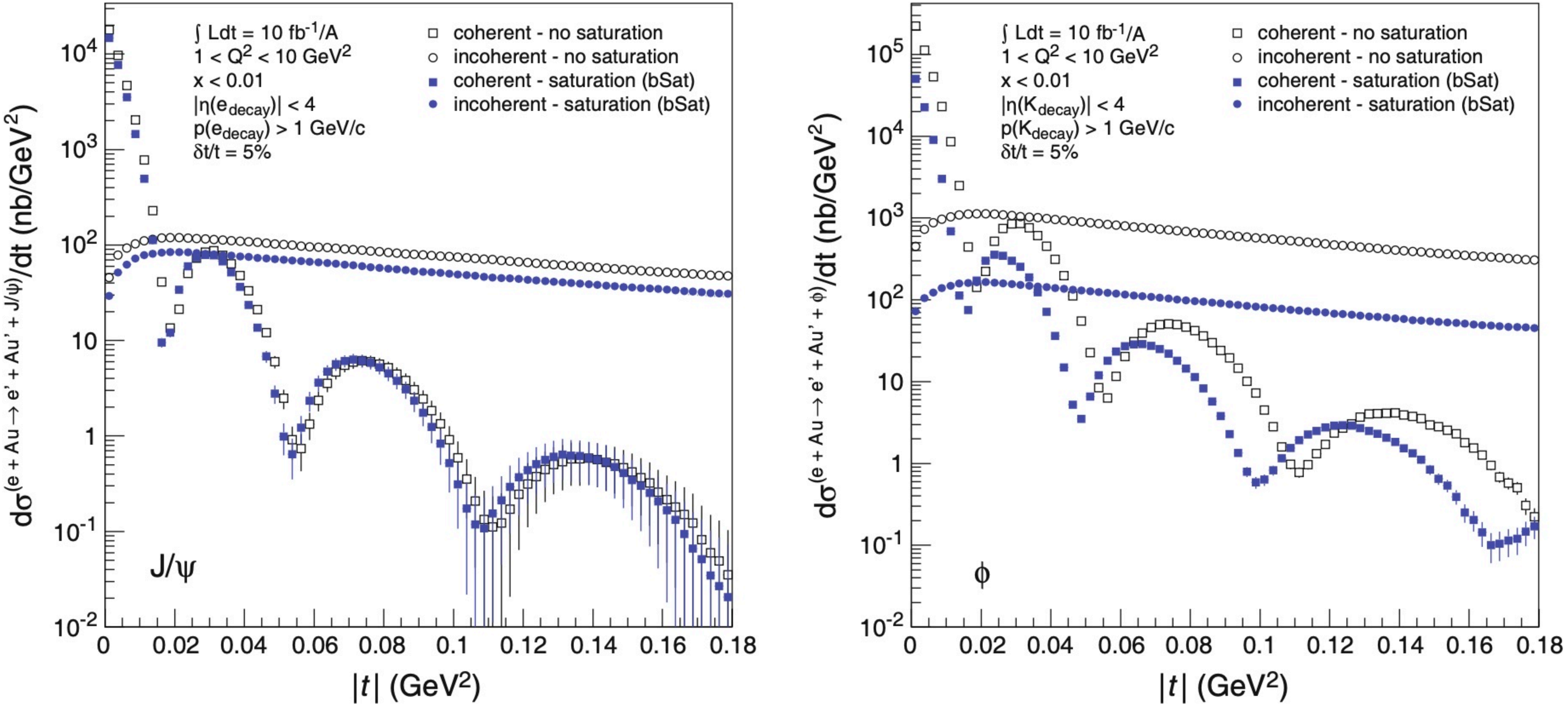

Light vector meson is more sensitive to saturation, and dips could be seen.

Ultra-Peripheral Collisions

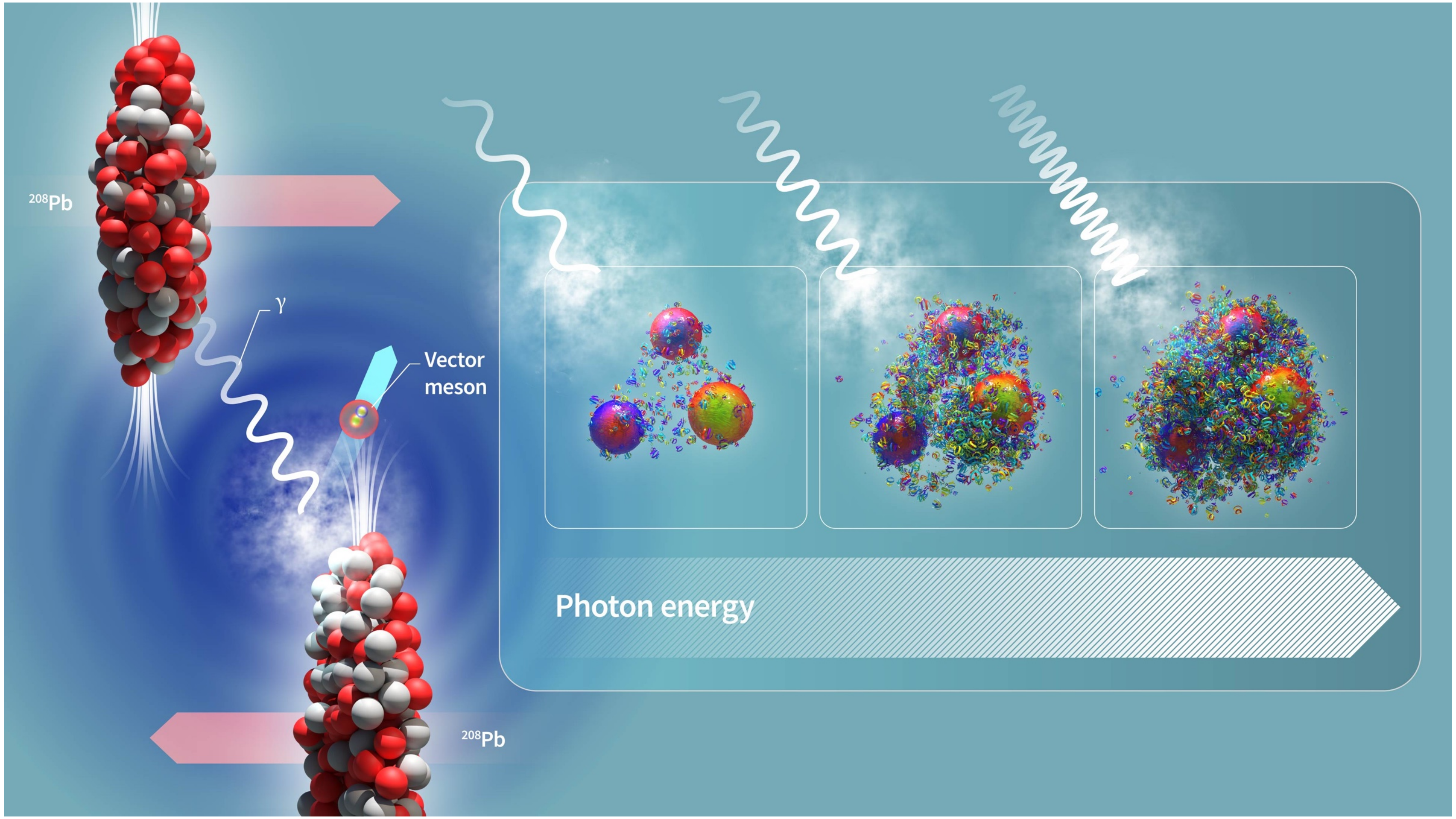

❖ Nuclei are strong sources of electromagnetic fields (Weizsäcker-Williams photon distribution).

❖ Photon virtuality is low: $Q^2 \sim 0$, so that exchanges photons are quasi-real.

Coherent J/ψ production in UPC

Eskola, Flett, Guzey, Löytäinen, Paukkunen, [arXiv:2203.11613 [hep-ph]].

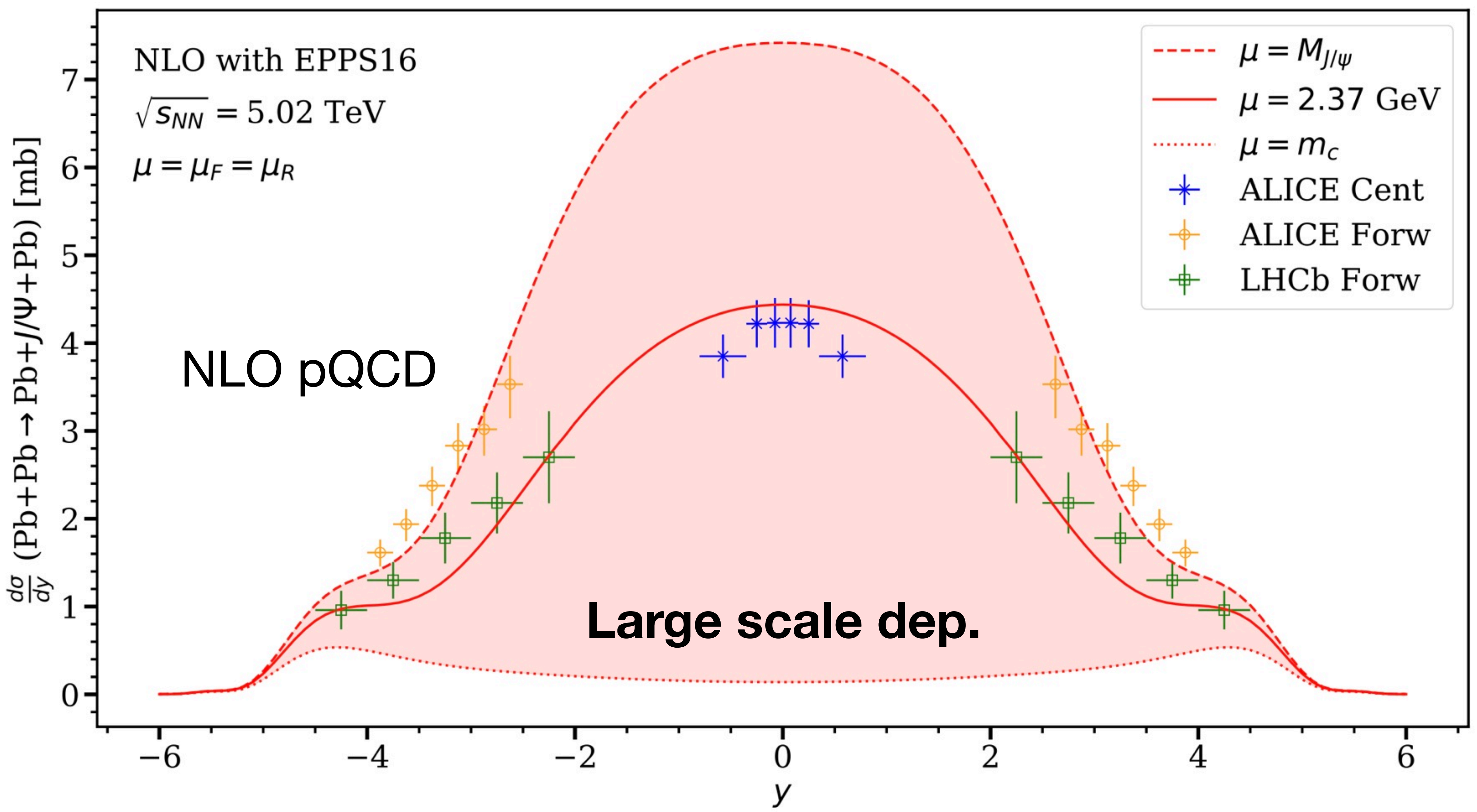

LHCb collaboration, [arXiv:2206.08221 [hep-ex]].

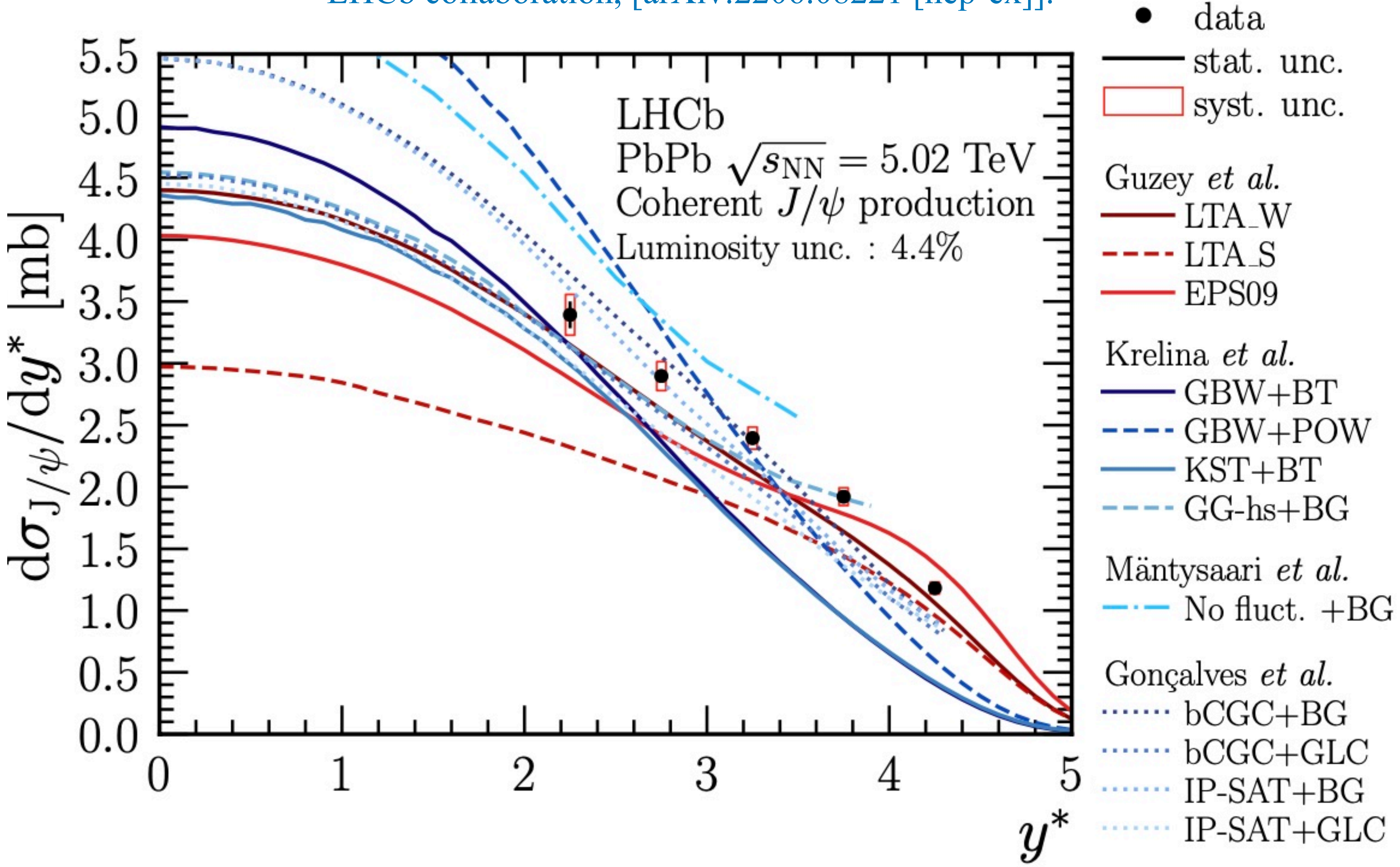

- ❖ Large theoretical uncertainties about GPDs, LF wave function, and so forth.
- ❖ Any model calculations cannot be ruled out by data comparison.

Energy dependence of quarkonium photo-production

Arroyo Garcia, Hentschinski and Kutak, PLB795, 569 (2019)

$x \simeq M_V^2/W^2$

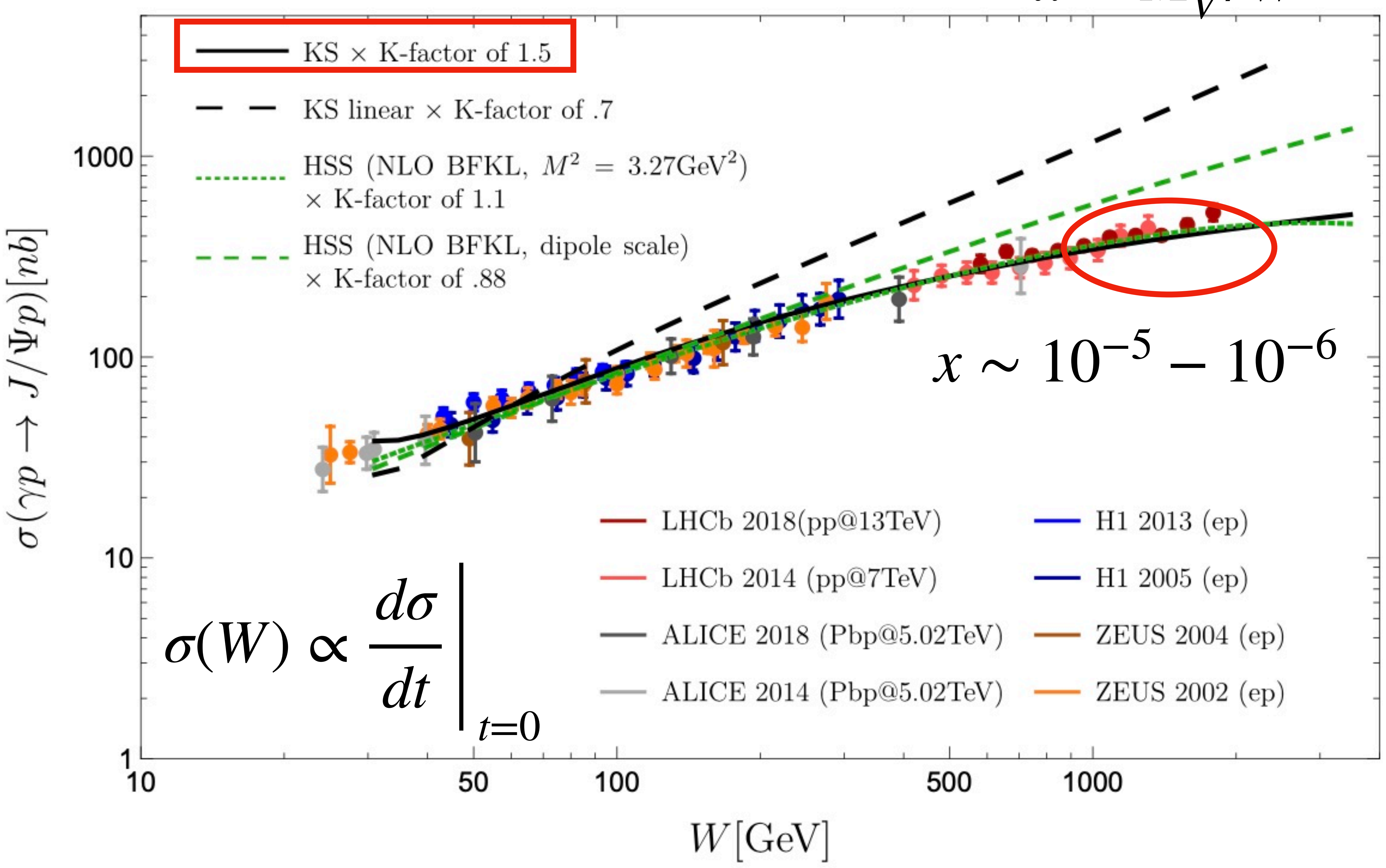

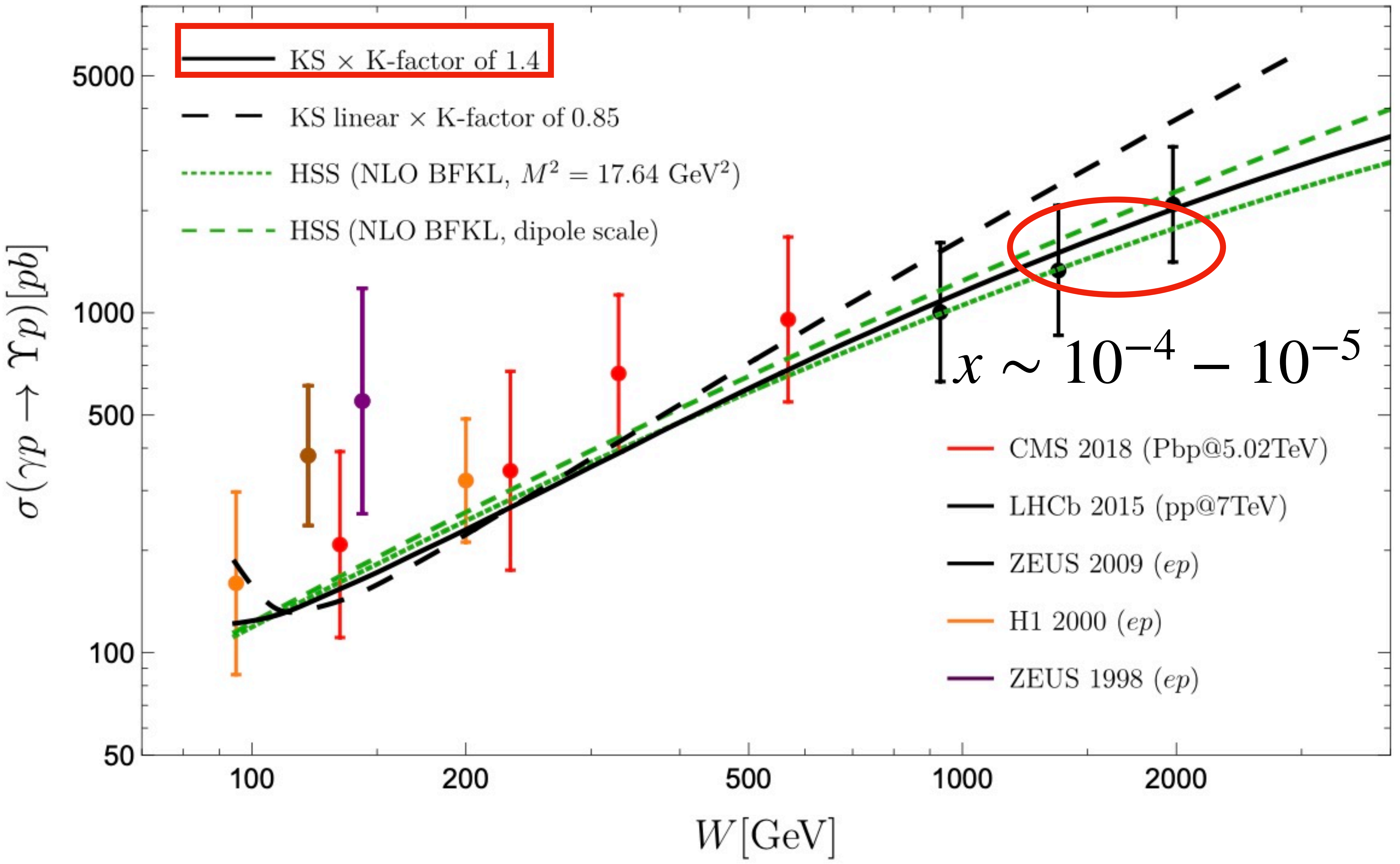

❖ Without the nonlinear recombination effect, the rapid growth of the gluon density in W results in the worse description of data.

❖ NLO BFKL evolution can also describe data, but it involves very large perturbative corrections.

Appendix
TMD and CGC

Two distinct approaches

❖ TMD approach

✓ TMD factorization is valid for all x.

✓ Leading twist (+ subleading power)

✓ On-shell hard scattering parts with transverse-momentum-dependent PDFs.

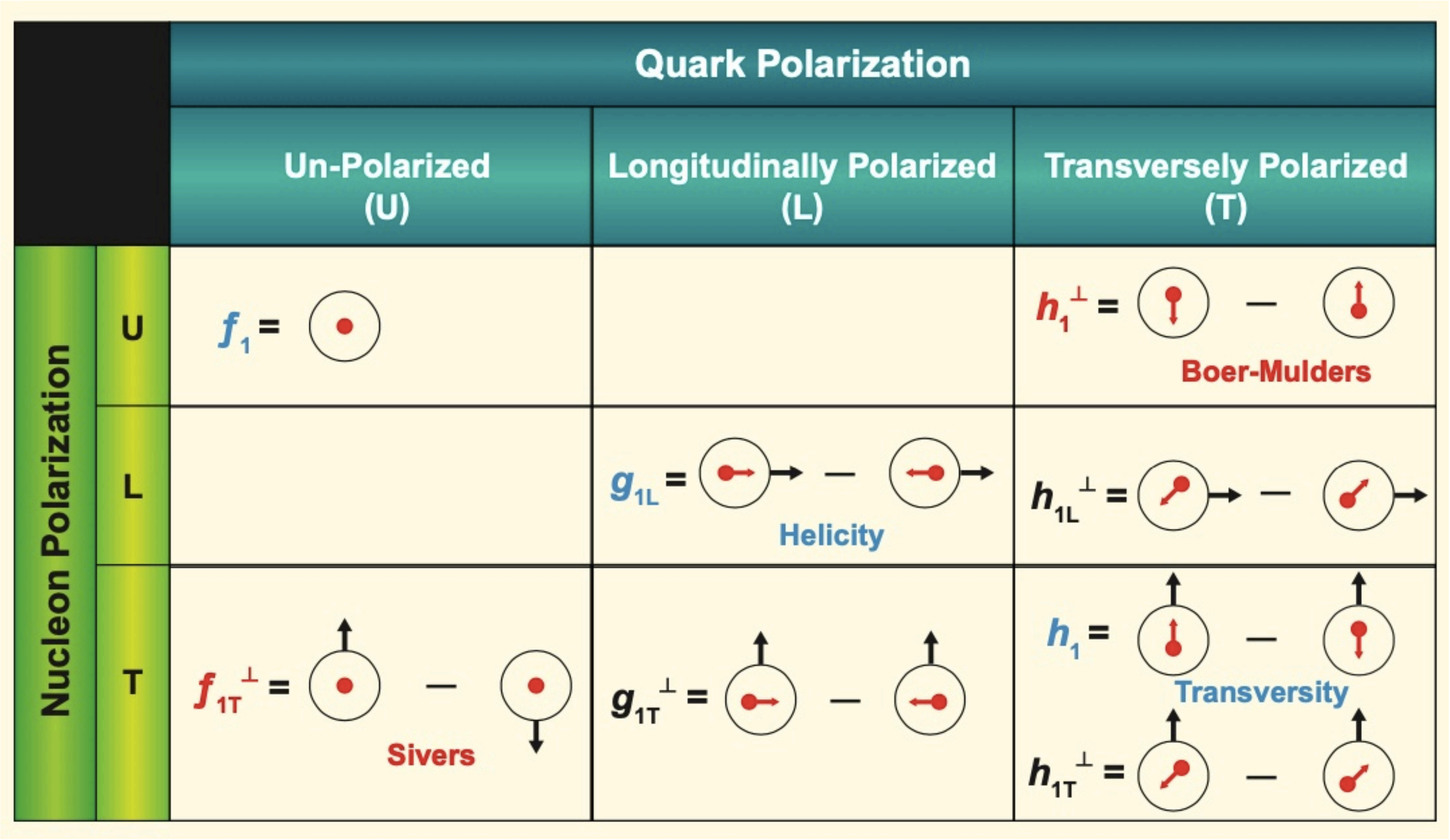

❖ CGC approach

✓ Only valid at $x \ll 1$.

✓ Higher twist contributions are included.

✓ Off-shellness of hard parts is taken into account.

✓ Multi-point Wilson line correlators

NAS report

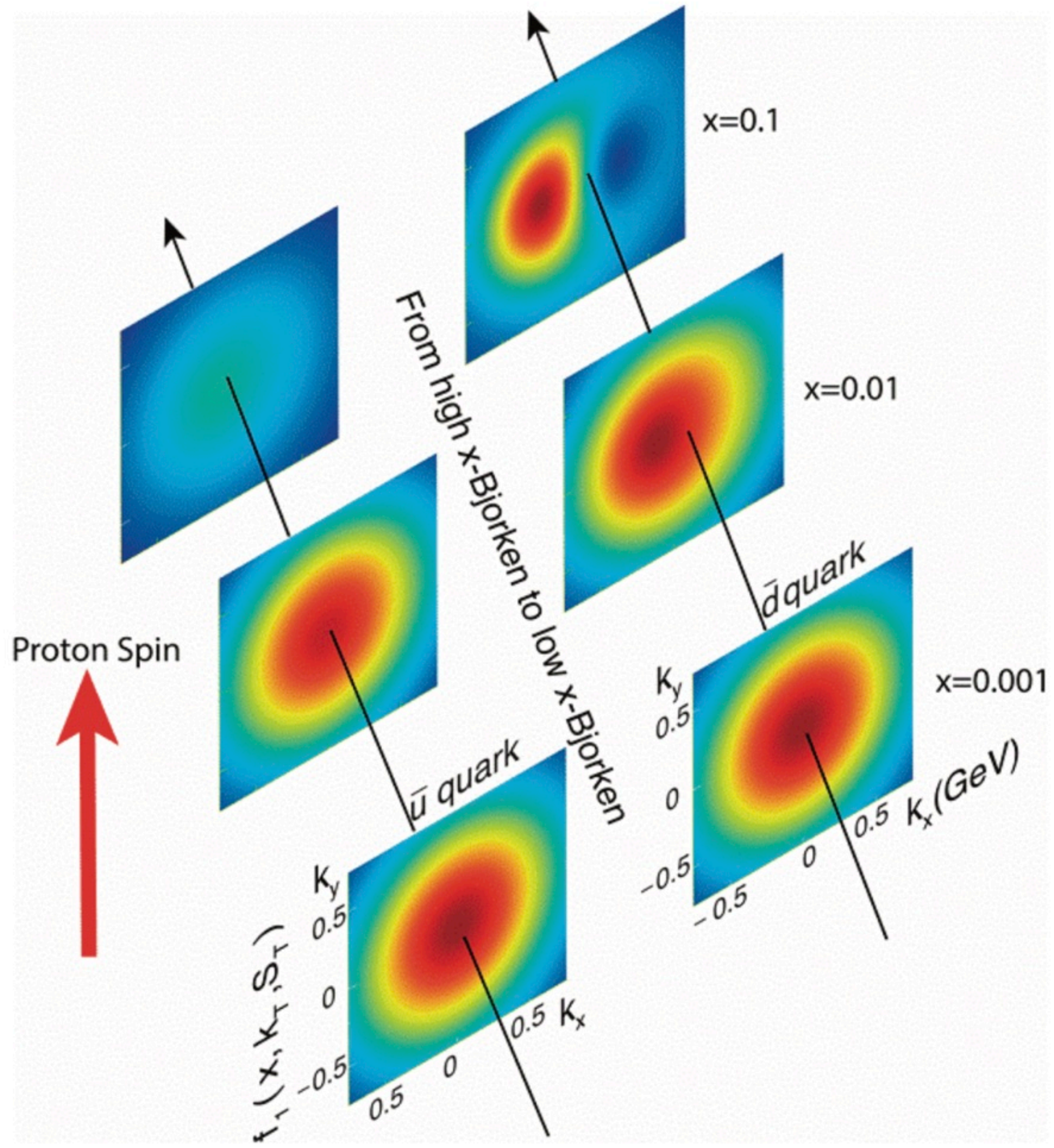

Process dependent gluon distributions

F. Dominguez, C. Marquet, B.-W. Xiao and F. Yuan, PRD83, 105005 (2011)

	DIS and DY	SIDIS	hadron in pA	photon-jet in pA	Dijet in DIS	Dijet in pA
$G^{(1)}$ (WW)	×	×	×	×	√	√
$G^{(2)}$ (dipole)	√	√	√	√	×	√

Weizsäcker-Williams gluon distribution function (Number density of gluon)

$$xG^{(1)}(x,k_\perp) = \int \frac{2d\xi^- d^2\xi_\perp}{(2\pi)^3 P^+} e^{ixP^+\xi^- - ik_\perp\cdot\xi_\perp} \left\langle P \left| \mathrm{Tr}\left[F^{+i}(\xi^-,\xi_\perp)\mathcal{U}^{[+]\dagger}F^{+i}(0)\mathcal{U}^{[+]}\right] \right| P \right\rangle$$

Unintegrated dipole gluon distribution function (Not clear partonic picture)

$$xG^{(2)}(x,k_\perp) = \int \frac{2d\xi^- d^2\xi_\perp}{(2\pi)^3 P^+} e^{ixP^+\xi^- - ik_\perp\cdot\xi_\perp} \left\langle P \left| \mathrm{Tr}\left[F^{+i}(\xi^-,\xi_\perp)\mathcal{U}^{[-]\dagger}F^{+i}(0)\mathcal{U}^{[+]}\right] \right| P \right\rangle$$

Process dependent gauge links:

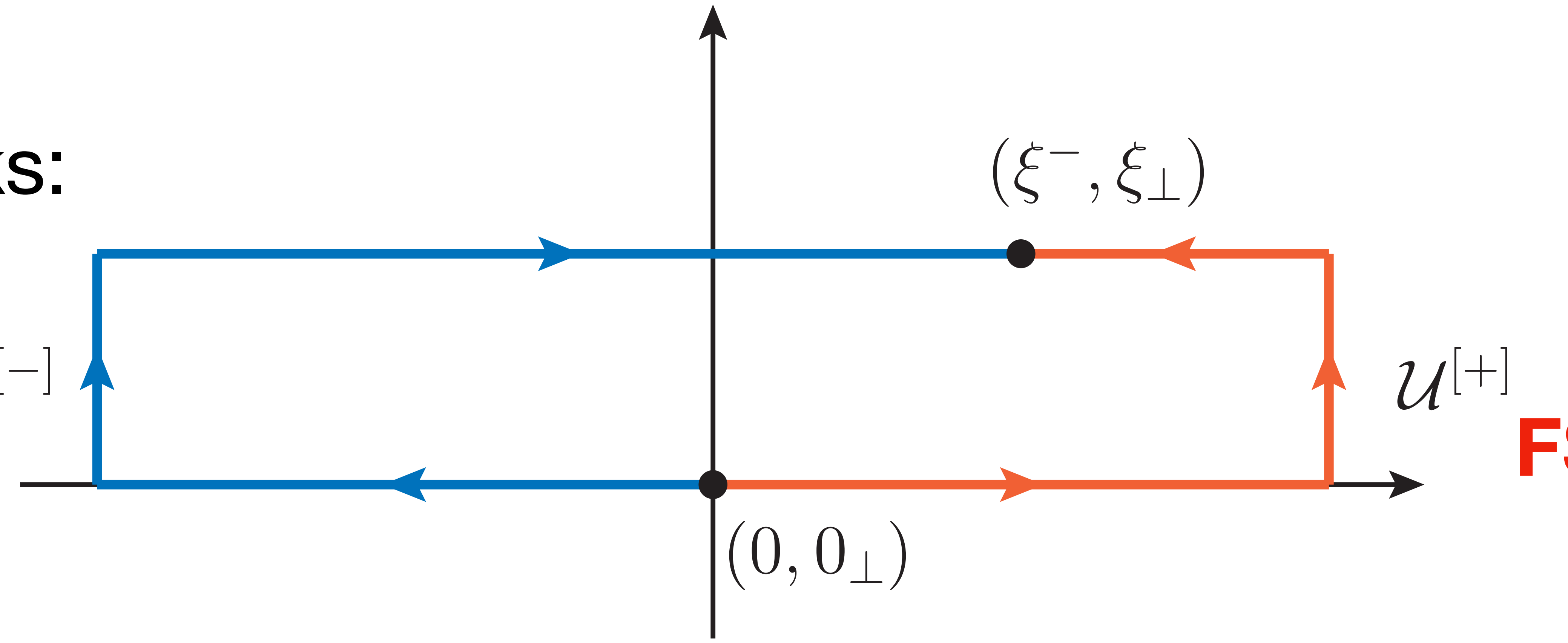

IS interactions

FS interactions

Universality at small-x

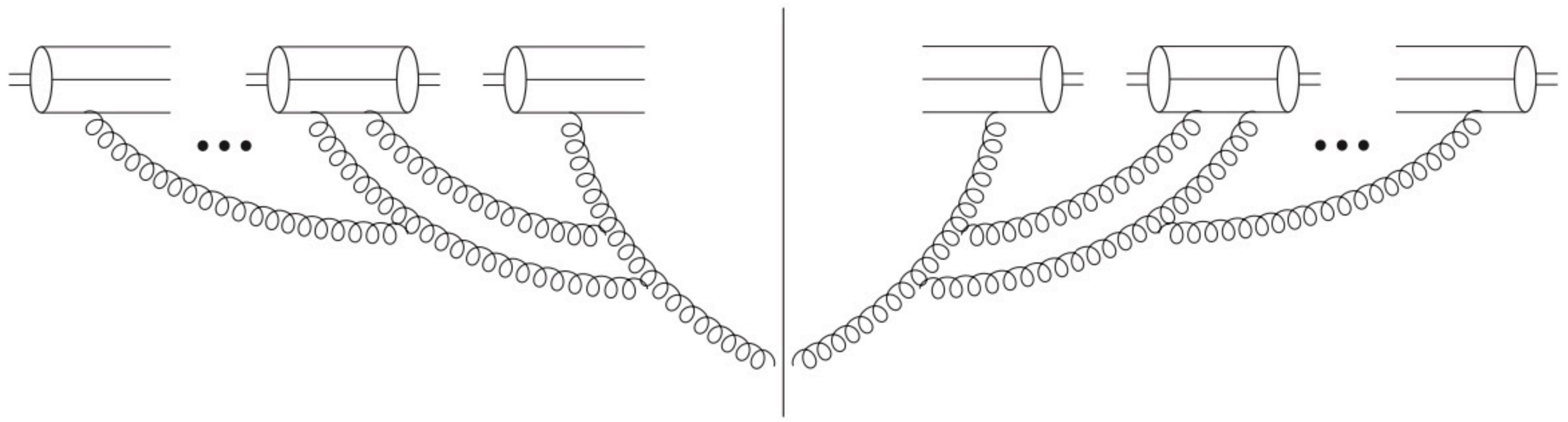

WW distribution can be evaluated using MV model at small-x and for a large nucleus only when a Gaussian distribution of ρ is used.

$$xG^{(1)}(x,k_\perp) \simeq \frac{2C_F S_\perp}{\pi^2\alpha_s}\int \frac{d^2r_\perp}{(2\pi)^2}\frac{e^{-ik_\perp\cdot r_\perp}}{r_\perp^2}\left[1-e^{-\frac{1}{4}r_\perp^2 Q_s^2}\right]$$

Dipole distribution can be naturally related to the color-dipole cross-section in CGC:

$$xG^{(2)}(x,k_\perp) \simeq \frac{N_c S_\perp k_\perp^2}{2\pi^2\alpha_s}\int \frac{d^2r_\perp}{(2\pi)^2}\frac{e^{-ik_\perp\cdot r_\perp}}{r_\perp^2}\frac{1}{N_c}\langle \mathrm{Tr}\left[U(0)U^\dagger(r_\perp)\right]\rangle$$

Things get more complicated when considering processes involving more gluons.

Some remarks on TMD and CGC

➢ Process dependent gluon TMDs: different gauge link structures

$$\mathcal{F}_{gg}^{(1)}(x_2,k_t) = 2\int \frac{d\xi^+ d^2\boldsymbol{\xi}}{(2\pi)^3 p_A^-} e^{ix_2 p_A^- \xi^+ - ik_t\cdot\boldsymbol{\xi}} \frac{1}{N_c}\left\langle A \left| \mathrm{Tr}\left[F^{i-}(\xi)\,\mathcal{U}^{[-]\dagger} F^{i-}(0)\,\mathcal{U}^{[+]}\right] \mathrm{Tr}\left[\mathcal{U}^{[\square]\dagger}\right] \right| A\right\rangle ,$$

$$\mathcal{F}_{gg}^{(2)}(x_2,k_t) = 2\int \frac{d\xi^+ d^2\boldsymbol{\xi}}{(2\pi)^3 p_A^-} e^{ix_2 p_A^- \xi^+ - ik_t\cdot\boldsymbol{\xi}} \frac{1}{N_c}\left\langle A \left| \mathrm{Tr}\left[F^{i-}(\xi)\,\mathcal{U}_\xi^{[\square]\dagger}\right] \mathrm{Tr}\left[F^{i-}(0)\,\mathcal{U}_0^{[\square]}\right] \right| A\right\rangle ,$$

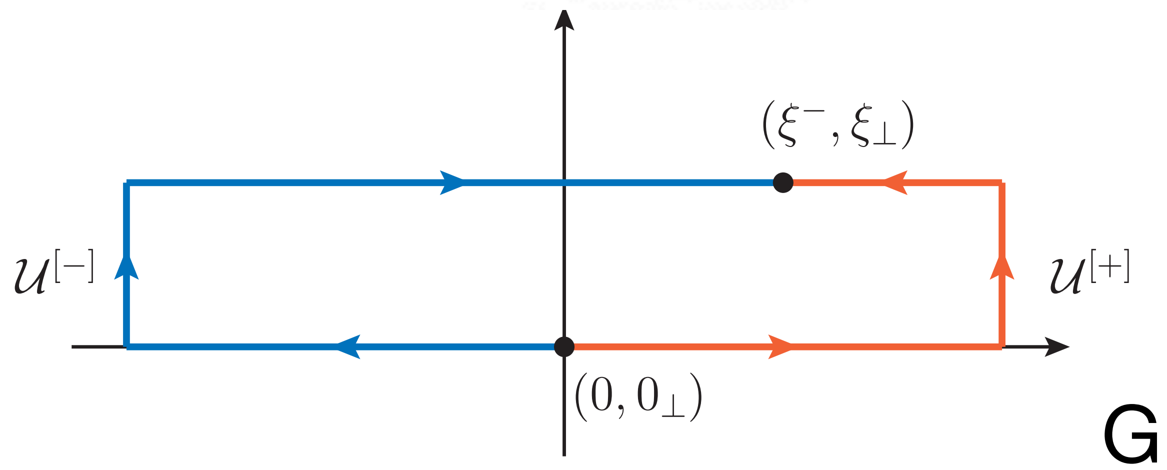

Dominguez, Marquet, Xiao and Yuan, PRD83, 105005 (2011)
Marquet, Petreska and Roiesnel, JHEP10, 065 (2016)
…

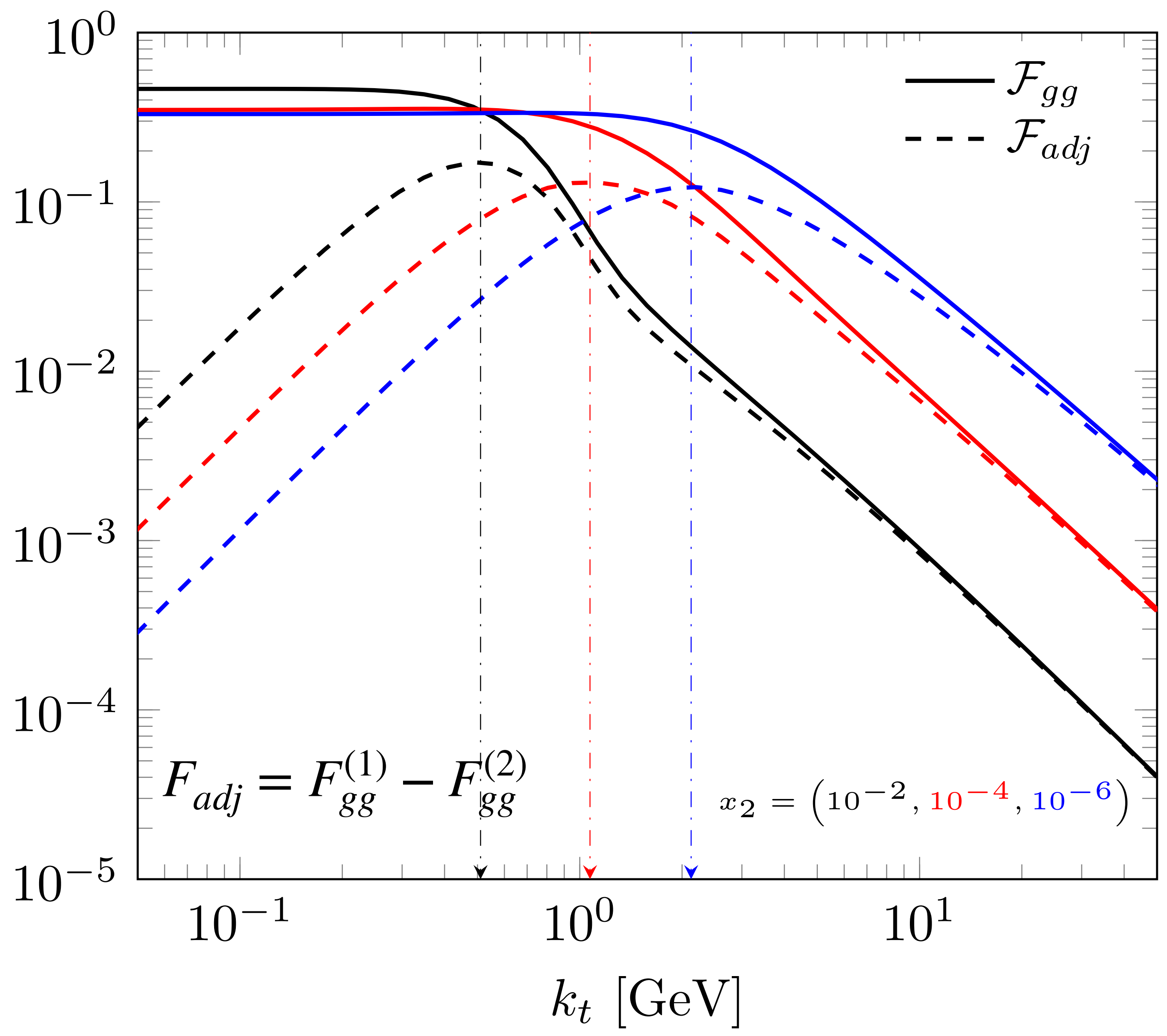

Gluon TMDs in small-x limit can be obtained from CGC

➢ From TMD framework to CGC framework

TMD + kinematic twist $\mathcal{O}(k_t/Q)$ = Improved TMD

Improved TMD + higher-body genuine twist $\mathcal{O}(Q_s/Q)$ = CGC

k_t : off-shellness in short distance parts

Q : a hard scale.

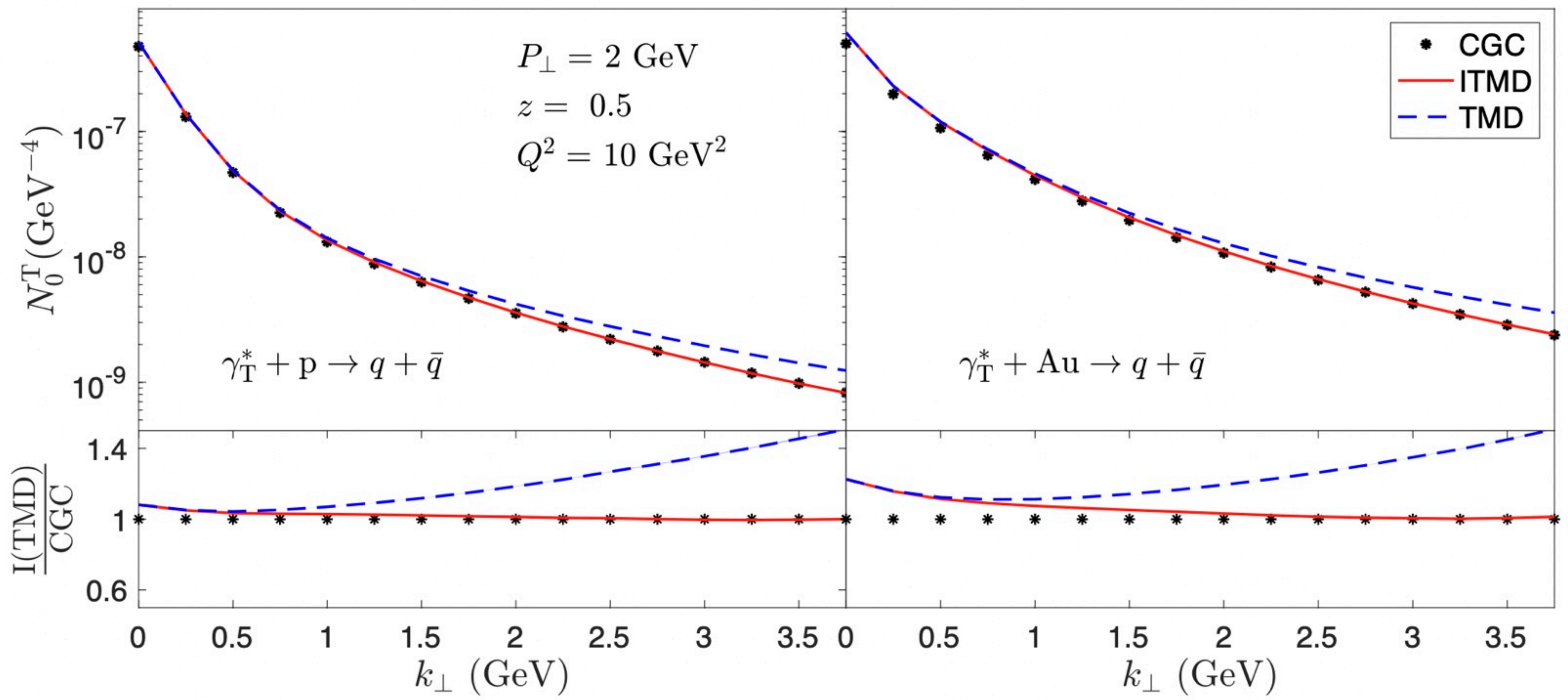

Altinoluk, Boussarie and Kotko, JHEP05, 156 (2019).
Mantysaari, Mueller, Salazar and Schenke, PRL124, no.11, 112301 (2020).
Fujii, Marquet and **KW**, JHEP12, 181 (2020).
Altinoluk, Marquet and Taels, JHEP06, 085 (2021).
Boussarie, Mantysaari, Salazar and Schenke, [arXiv:2106.11301 [hep-ph]].
…

From TMD to CGC

k_t : off-shellness in short distance parts

Q : a hard scale.

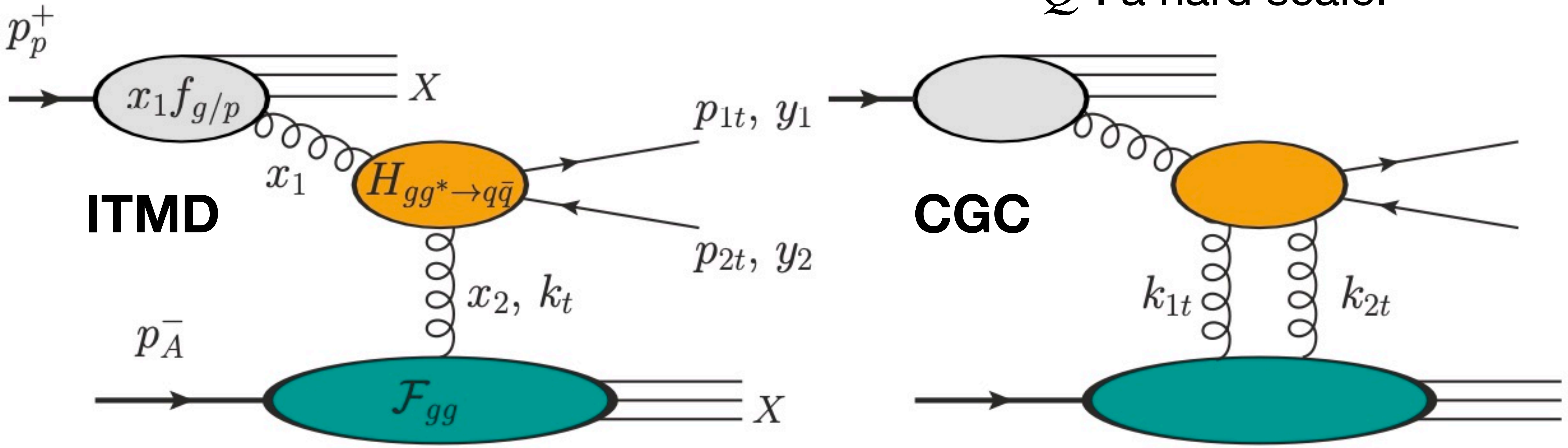

- σ_{BFKL} + power correction $\mathcal{O}\left(\frac{Q_s}{k_t}\right)$ = Improved TMD (ITMD)
- σ_{TMD} + power correction $\mathcal{O}\left(\frac{k_t}{Q}\right)$ = Improved TMD (ITMD)
- σ_{ITMD} + power correction $\mathcal{O}\left(\frac{Q_s}{Q}\right)$ = CGC

Altinoluk, Boussarie and Kotko, JHEP05, 156 (2019).
Mantysaari, Mueller, Salazar and Schenke, PRL124, no.11, 112301 (2020).
Fujii, Marquet and **KW**, JHEP12, 181 (2020).
Altinoluk, Marquet and Taels, JHEP06, 085 (2021).
Boussarie, Mantysaari, Salazar and Schenke, [arXiv:2106.11301 [hep-ph]].
…

Twist effects in forward dijet production (1/2)

H. Fujii, C. Marquet and **KW**, JHEP12, 181 (2020)

LHC

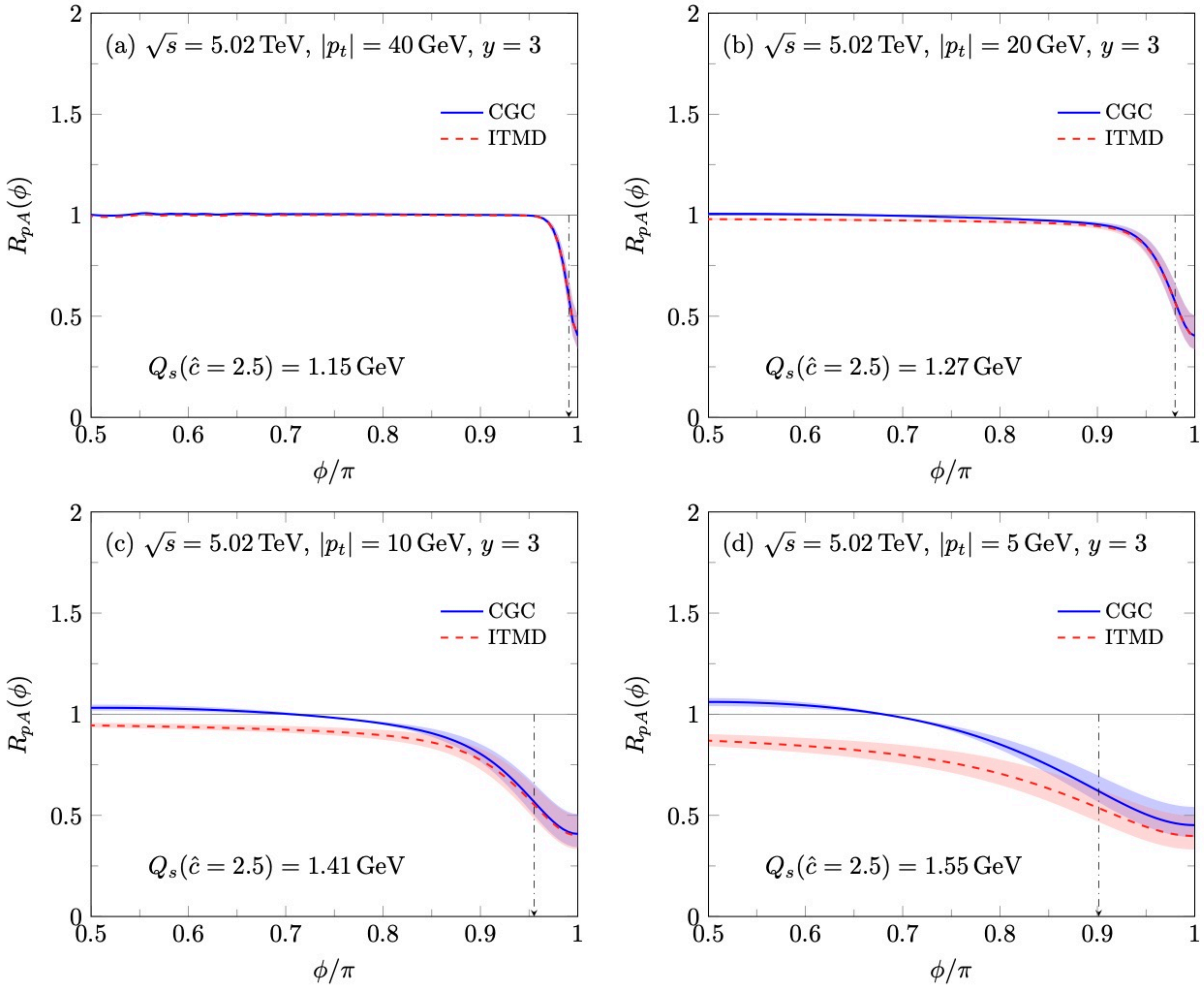

RHIC

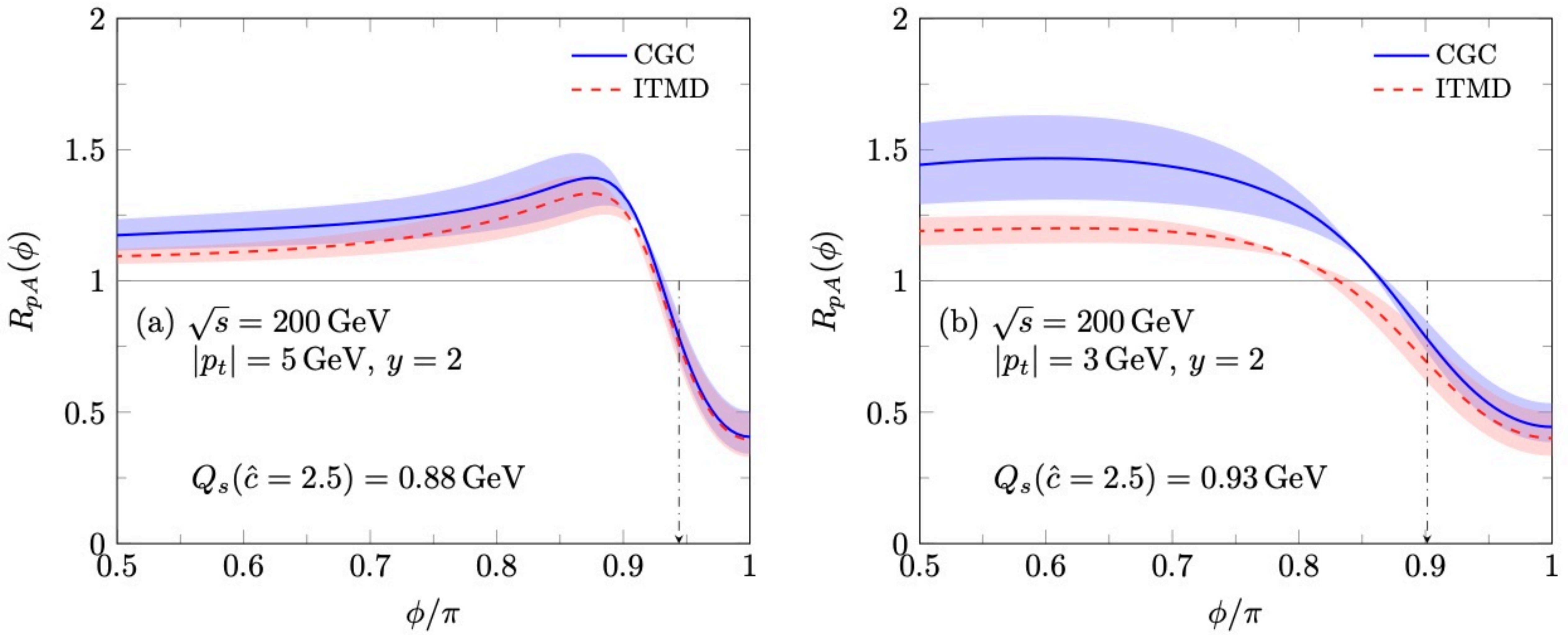

Dijet correlation is a good playground for studying the twist effects.

- ❖ Near-side: large intrinsic k_t
- ❖ Away-side: large genuine-twist

Twist effects in forward dijet production (2/2)

R. Boussarie, H. Mantysaari, F. Salazar and B. Schenke, JHEP 09, 178 (2021)

EIC

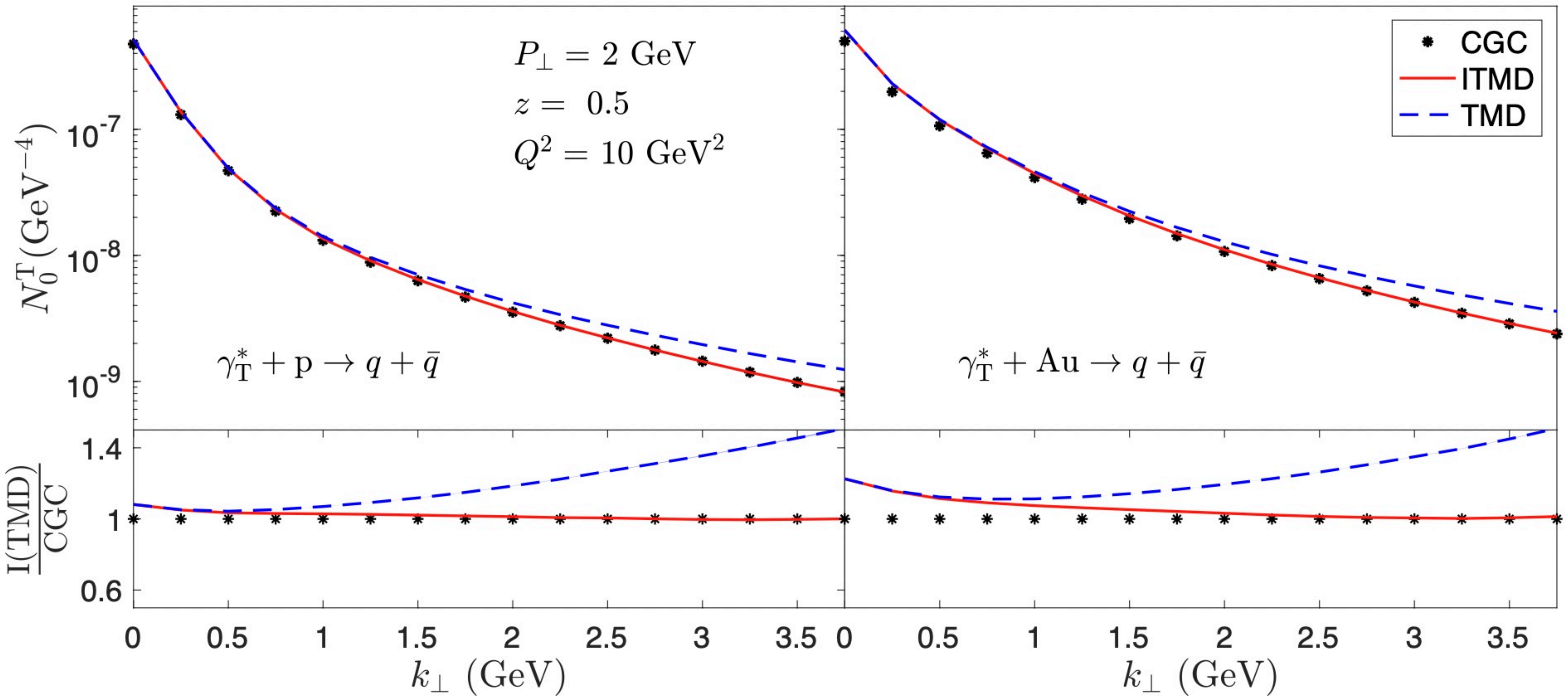

momentum imbalance of dijet: $k_\perp = k_{1\perp} + k_{2\perp}$

Genuine twist is sizeable for heavier targets.

Appendix:
Other Cold Nuclear Effects

Ratios: pA vs. pp

Nuclear modification factor: $R_{pA} = \frac{1}{A}\frac{d\sigma_{pA}}{d\sigma_{pp}}$

LHCb collaboration, [arXiv:2205.03936 [nucl-ex]].

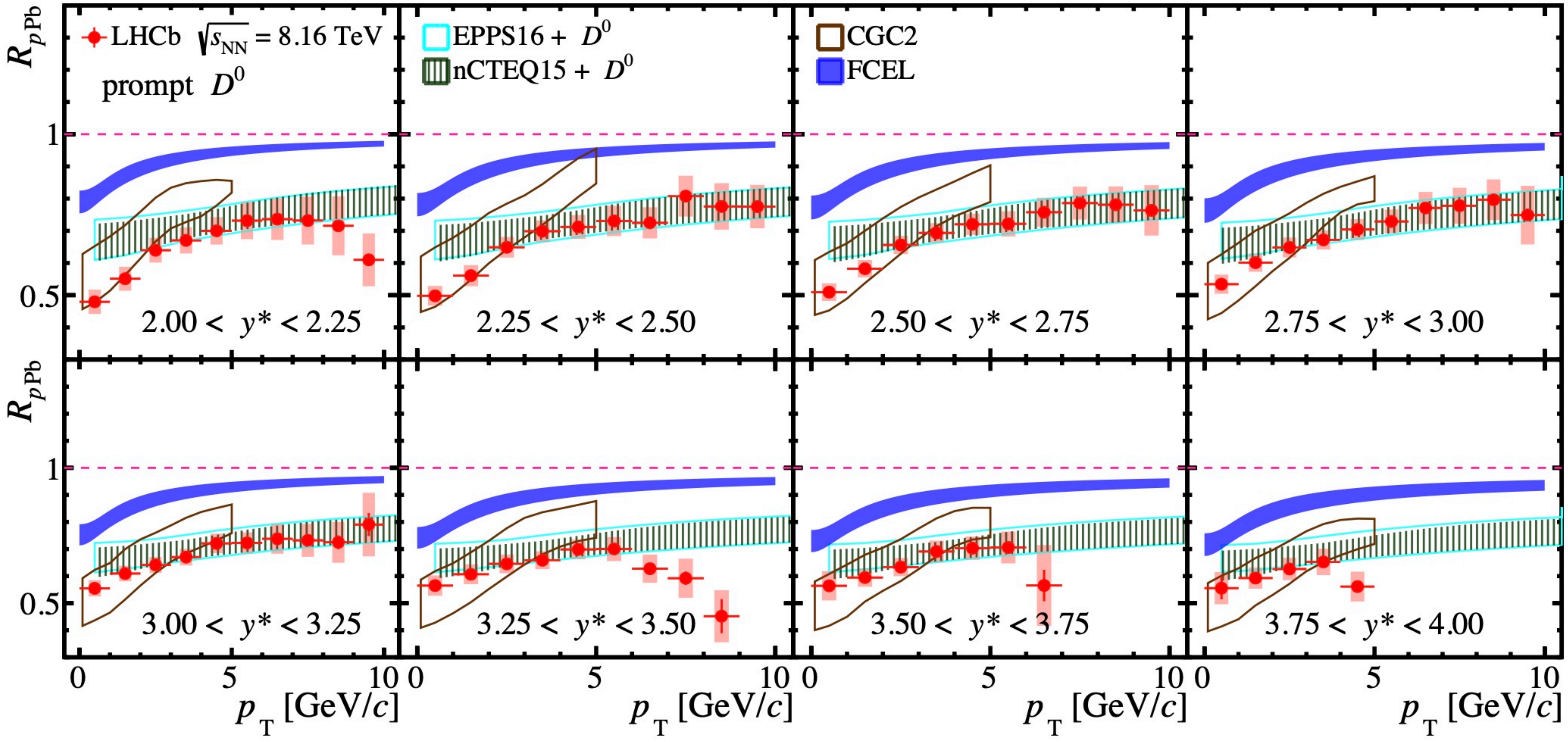

Both CGC EFT and non-CGC calculations describe data.

Nuclear PDFs

$$R_i^A(x, Q^2) = \frac{f_i^{p/A}(x, Q^2)}{f_i^p(x, Q^2)}$$

- $R^A > 1$ for $x \gtrsim 0.8$: Fermi motion
- $R^A < 1$ for 0.25 or $0.3 \lesssim x \lesssim 0.8$: EMC effect
- $R^A > 1$ for $0.1 \lesssim x \lesssim 0.25$ or 0.3: antishadowing
- $R^A < 1$ for $x \lesssim 0.1$: shadowing

Low scattering energies: incoherent sum

$$\sigma^A = A\sigma^n$$

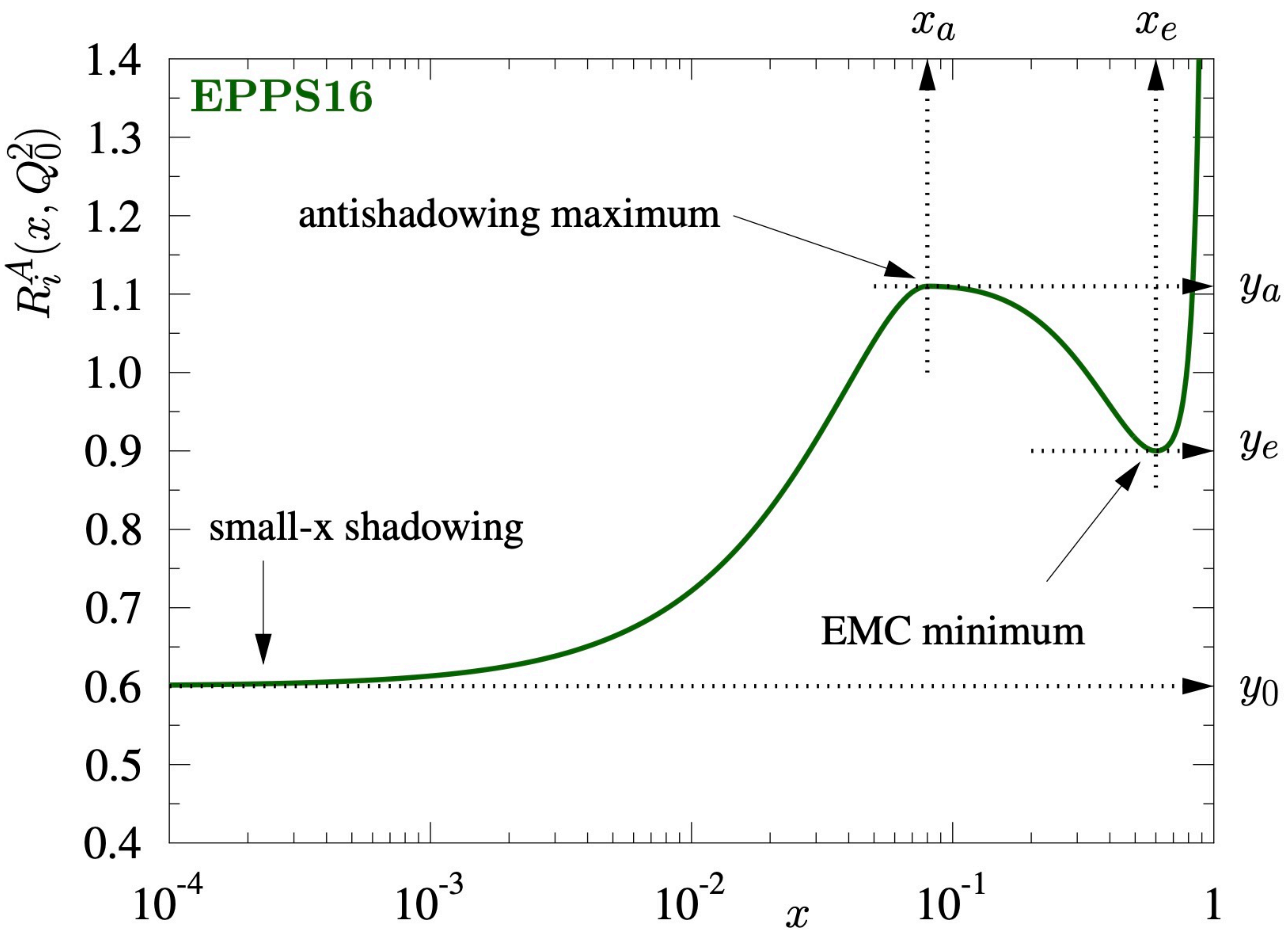

High scattering energies: coherent multiple scatterings play a role

The impact of forward D-meson on nPDFs

R. Abdul Khalek, *et al.* [NNPDF], Eur. Phys. J. C 82, no.6, 507 (2022)

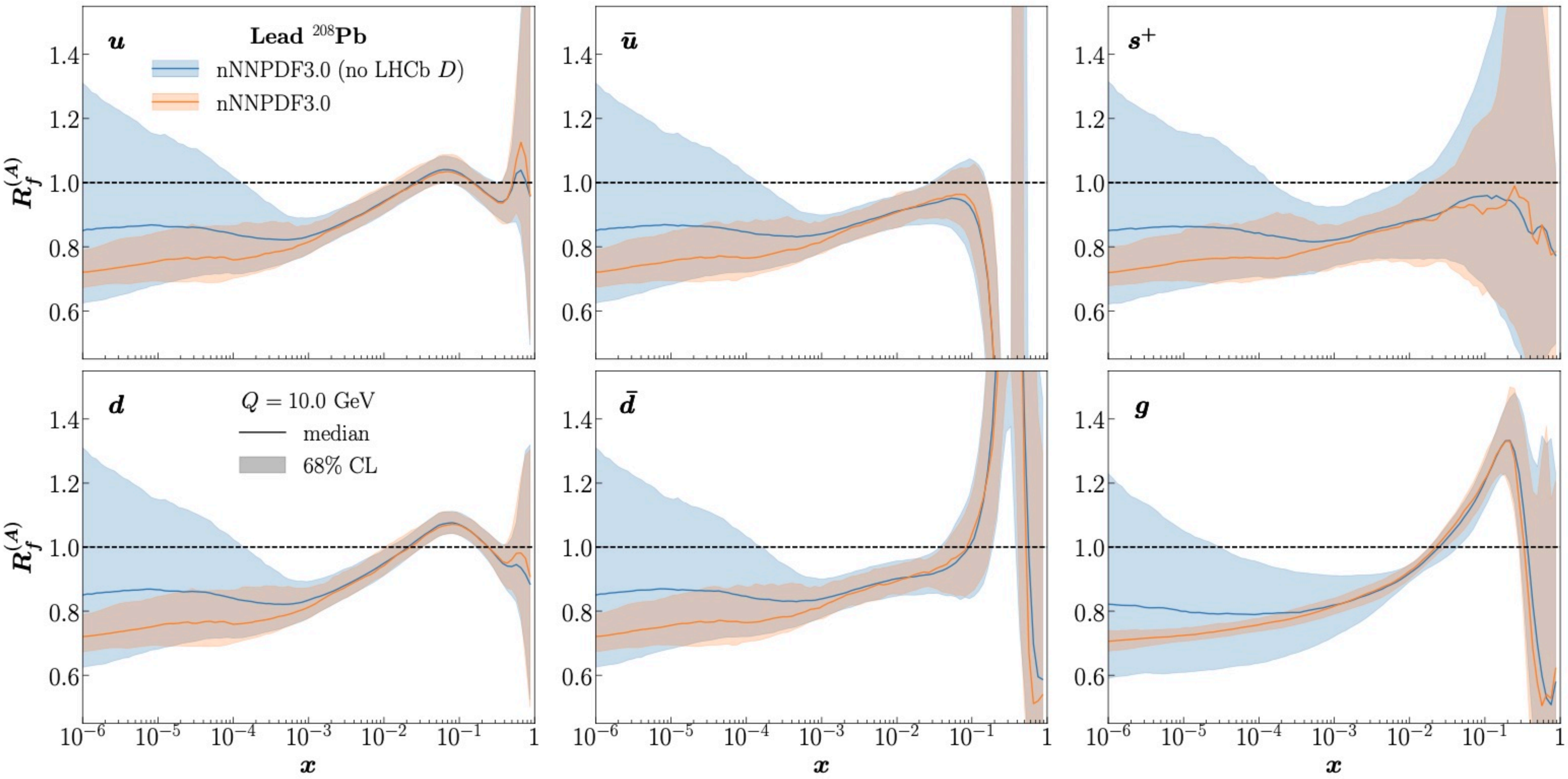

Parton energy loss in medium

J. D. Bjorken, FERMILAB-PUB-82-059-THY (1982)
M. Gyulassy and X. N. Wang, NPB420, 583-614 (1994)

E-loss happens via scattering with medium or induced gluon radiation:

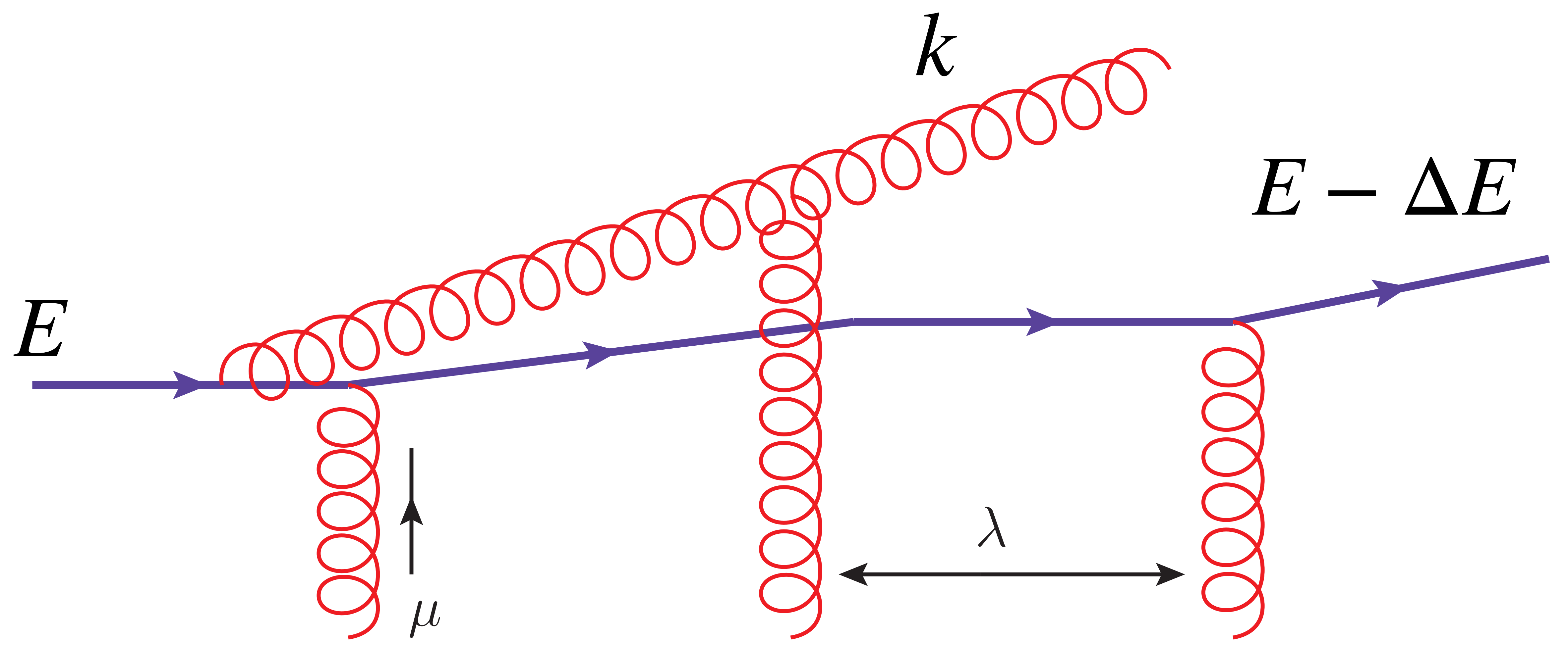

E-loss is characterized by transport (diffusion) coefficient $\hat{q} = \mu^2/\lambda$:

- ✓ λ: parton's mean-free path in the medium.
- ✓ μ: typical momentum transferred from 1 soft scattering.
- ✓ $\langle k_\perp^2 \rangle \sim \hat{q}\, t_f$ with $t_f \sim k^+/k_\perp^2$: transverse momentum broadening in the medium.

E-loss in three distinct regimes

Depending on the gluon formation time t_f :

➡ **Bethe-Heitler regime ($t_f \ll \lambda$)**: each scattering center acts as an indep. source.

➡ **Landau-Pomeranchuk-Migdal regime ($\lambda \ll t_f \ll L$)**: a group of t_f/λ scattering centers acts as a single radiator.

➡ **Fully coherent (Long formation time or factorization) regime ($L \ll t_f$)**: all scattering centers in the medium act coherently as a source of radiation.

The gluon radiation spectrum:

$$dI = \frac{d\sigma_{\rm rad}}{d\sigma_{\rm el}} = \frac{\sum |M_{\rm rad}|^2}{\sum |M_{\rm el}|^2} \frac{dk^+ dk_\perp^2}{2k^+(2\pi)^3}$$

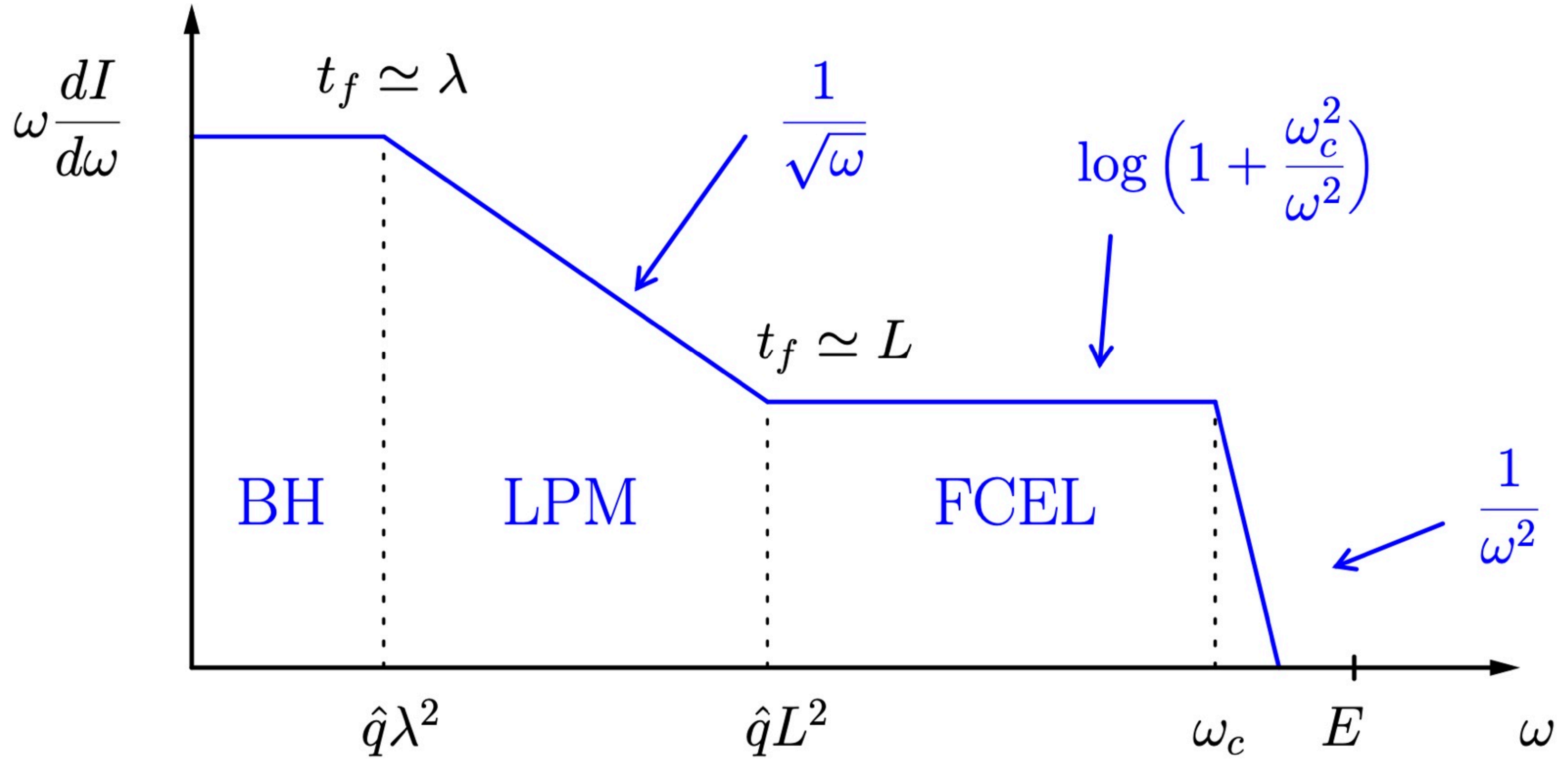

Parametric dependence of LPM and FCEL

❖ **LPM E-loss (initial state or final state):**

Baier, Dokshitzer, Mueller, Peigne, Schiff, NPB484, 265 (1997)
Zakharov, JETP Lett.63, 952 (1996)
Wang and Guo, NPA696, 788-832 (2001)
Gyulassy, Levai and Vitev, NPB 571, 197 (2000)
…

$$\Delta E^{\text{BDMPS}}_{\text{LPM}} = \langle \epsilon \rangle \sim \alpha_s \hat{q} L^2$$

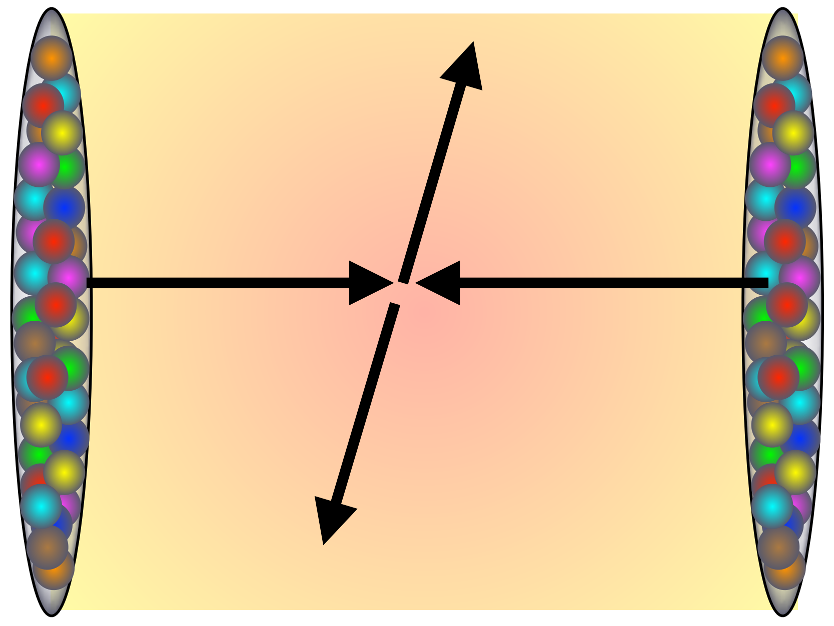

✓ Important for hadron production in nuclear DIS, and jet in QGP.

✓ The fractional E-loss: $\Delta E/E \to 0$ as $E \to \infty$.

❖ **Fully Coherent E-loss (initial state & final state):**

$$\Delta E_{\text{FCEL}} \sim \alpha_s \frac{\sqrt{\hat{q}L}}{Q_{\text{hard}}} E$$

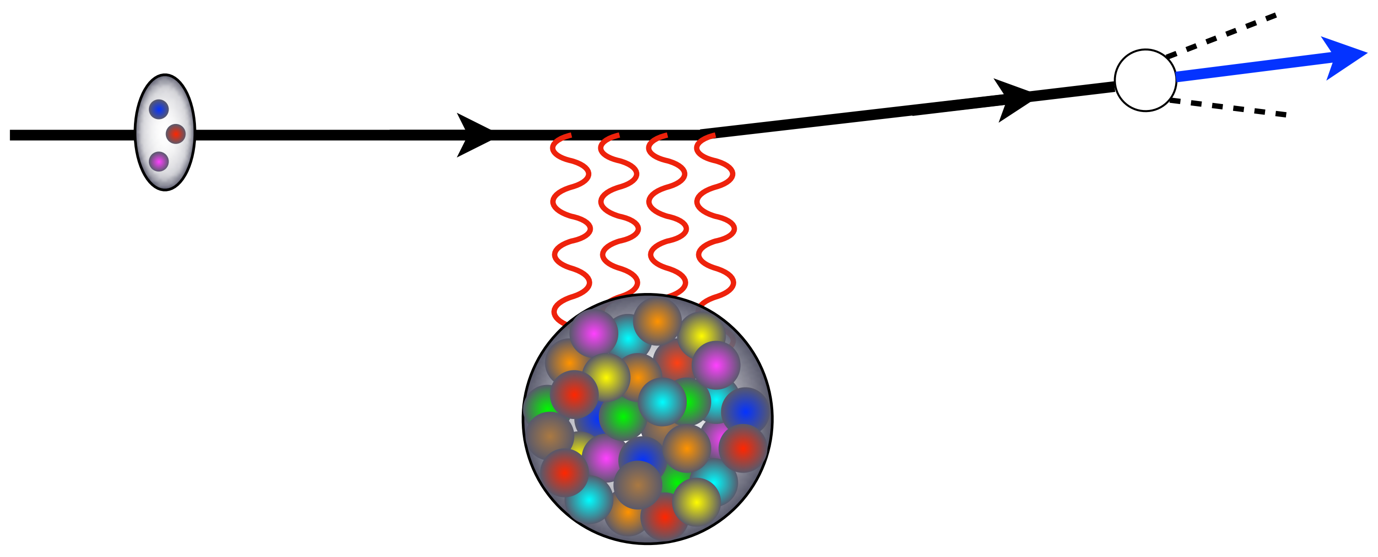

✓ Important for hadron production in pA collisions.

✓ $\Delta E/E$ cannot vanish as $E \to \infty$: important at all energies.

Phenomenology in LLA

$$E\frac{d\sigma_{pA\to h+X}}{d^3p} = A\int_0^{\epsilon_{\max}} d\epsilon\ \mathscr{P}(\epsilon)\ E\frac{d\sigma_{pp\to h+X}}{d^3p}\Bigg|_{E\to E+\epsilon}$$

Energy (rapidity) shift

Probability distribution (**quenching weight**) in double-log approx. (DLA): Baier, Dokshitzer, Mueller, Schiff, JHEP09, 033 (2001)

$$\mathscr{P}(\epsilon) \simeq \frac{dI}{d\epsilon}\exp\left\{-\int_\epsilon^\infty d\omega \frac{dI}{d\omega}\right\}$$

Arleo and Peigne, PRL109, 122301 (2012), JHEP03, 122 (2013)

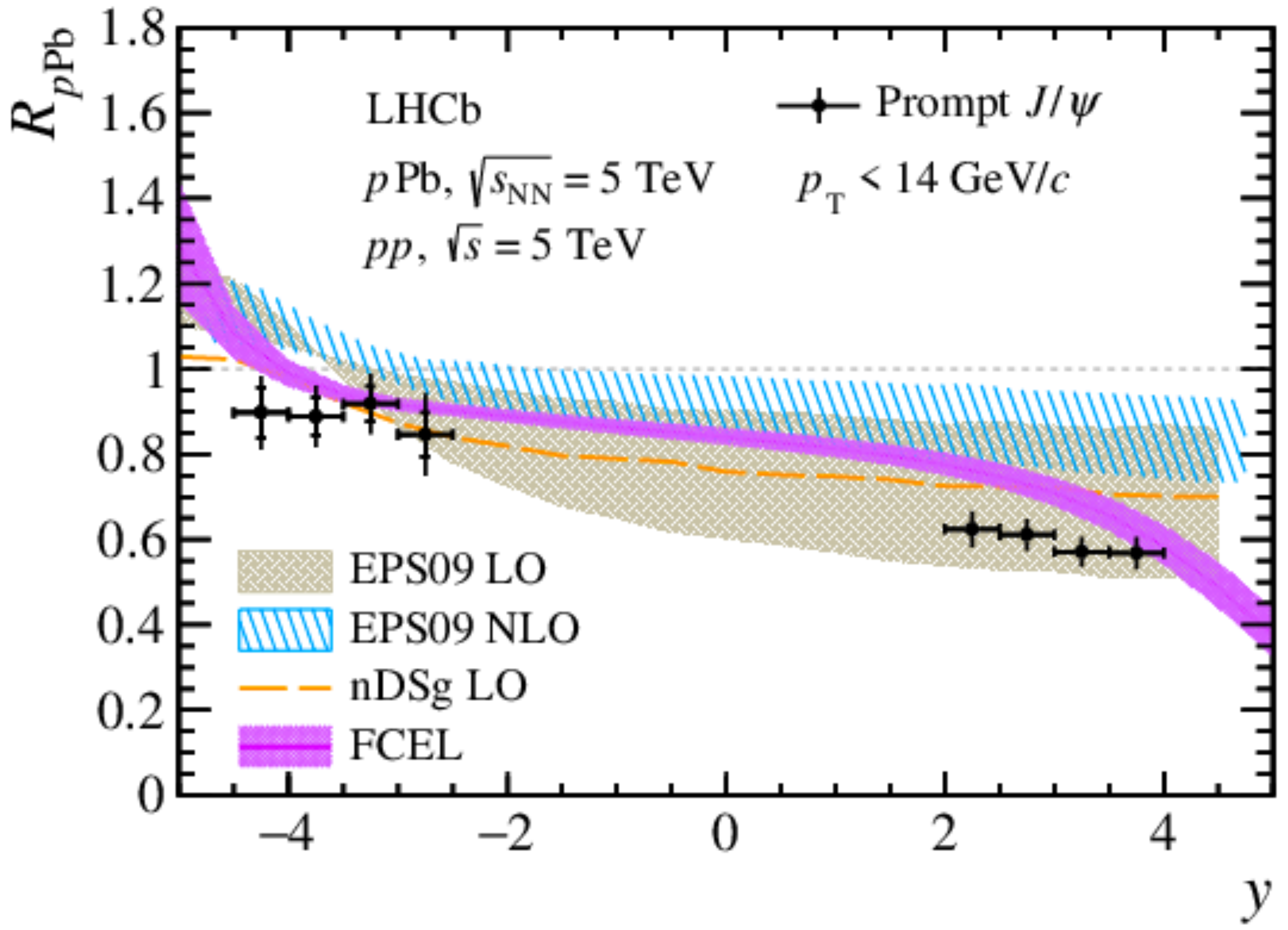

Arleo, Jackson, Peigne, JHEP01, 164 (2022)

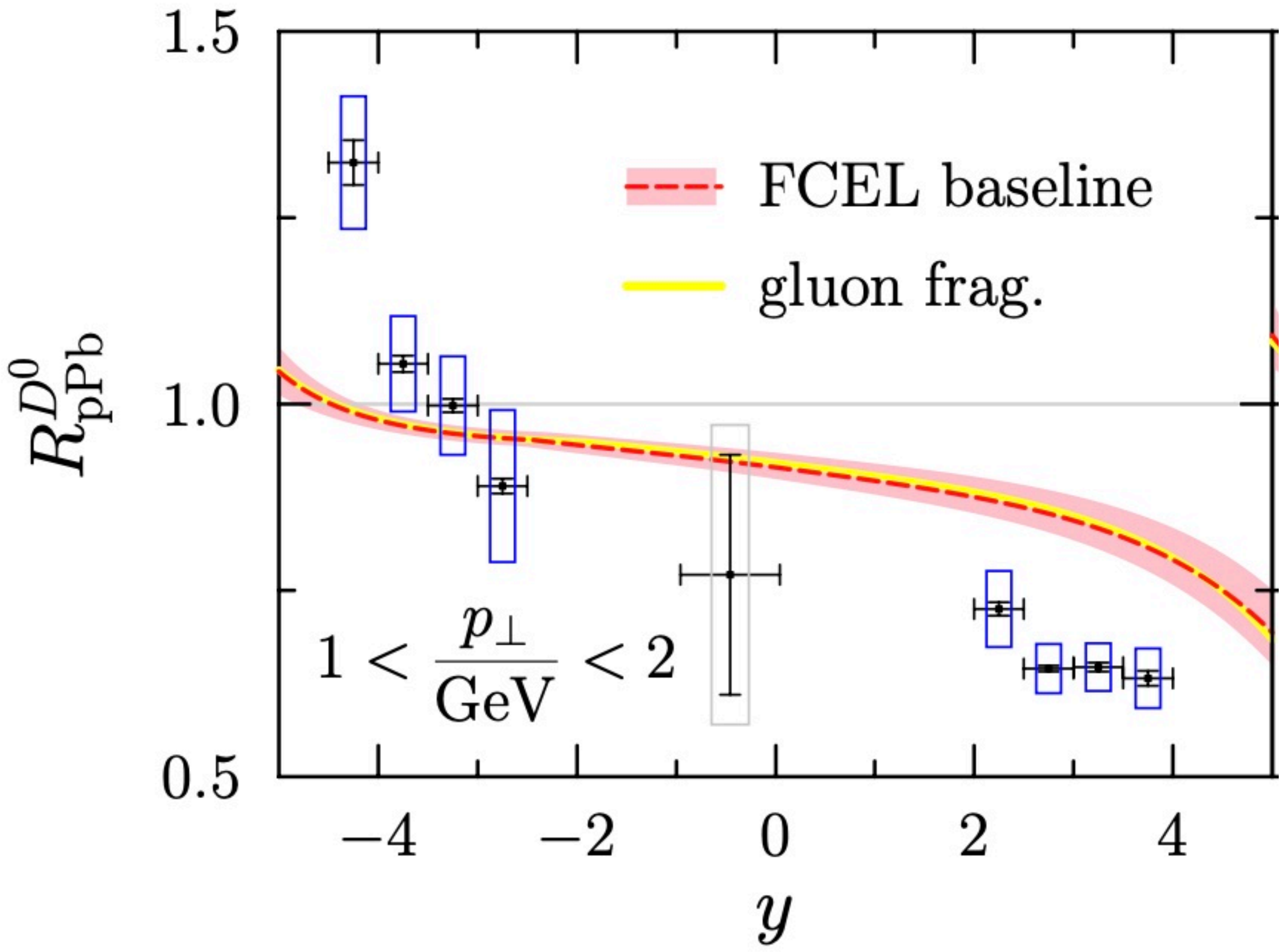

Suppression of atmospheric neutrino fluxes

initial CR flux: $\Phi_p(E) \propto E^{-\gamma}$

$$R_\nu(E) = \int dz z^\gamma \mathscr{P}(z), \quad z = 1/(1+x)$$

F. Arleo, G. Jackson and S. Peigne, Phys. Lett. B 835, 137541 (2022)

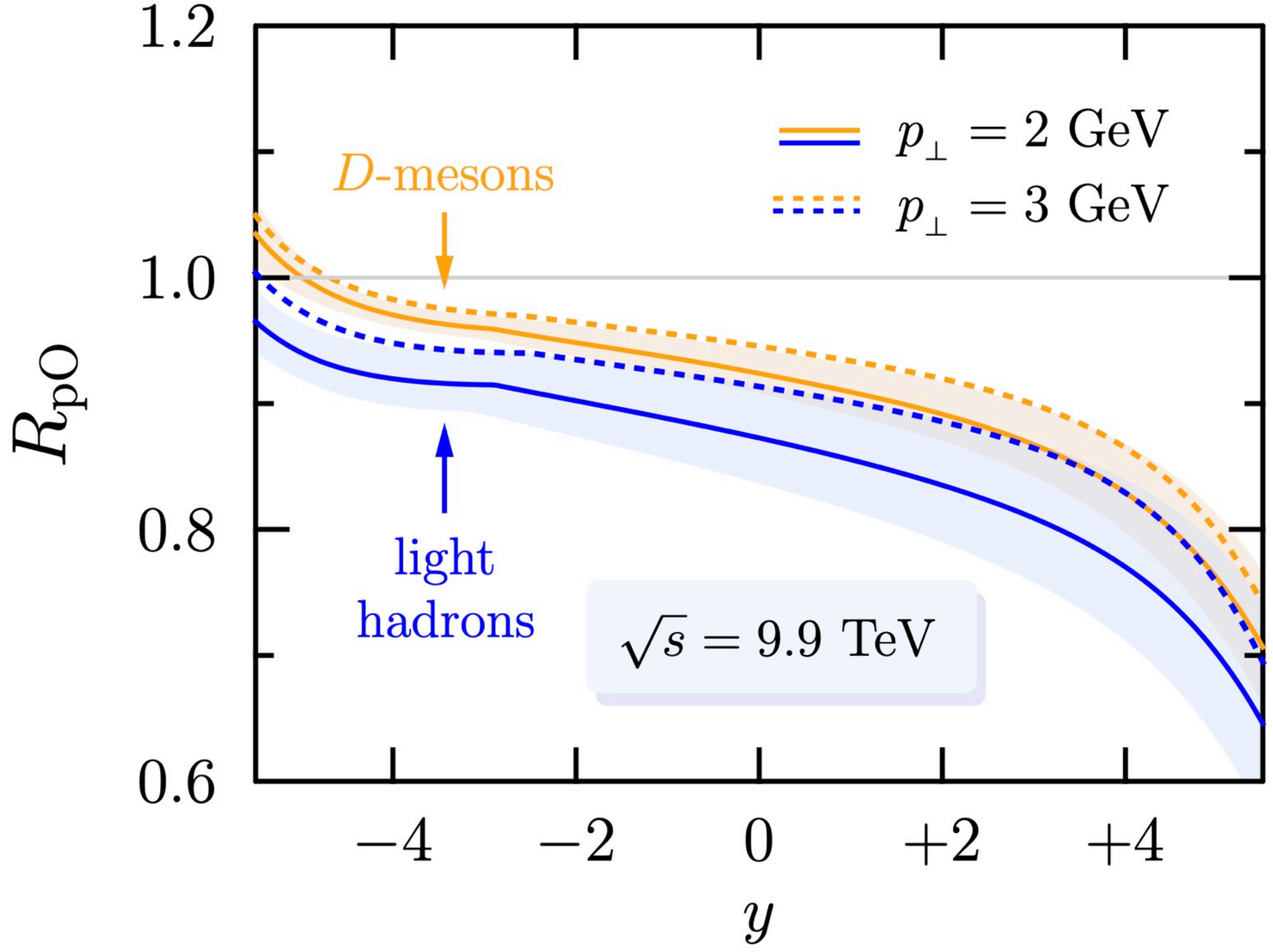

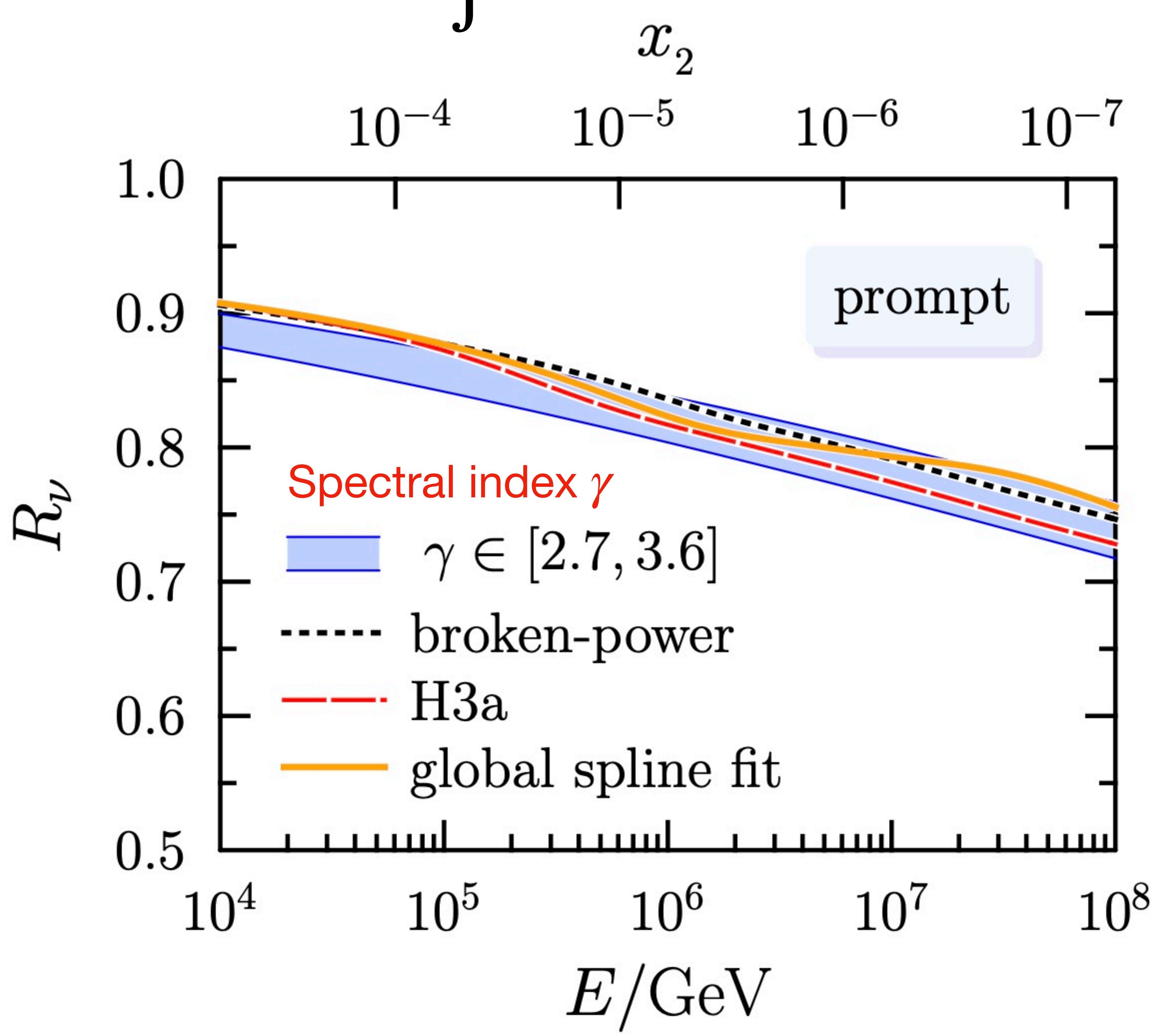

❖ Background atmospheric ν flux is suppressed by $\sim 10 - 25\ \%$ in IceCube energy ranges.

Appendix:
CGC calculations at NLO

Hybrid factorization for a dilute-dense system

$$\frac{d\sigma_{p+A\to h+X}}{dyd^2p_T} = \int x_p f_{a/p}(x_p) \otimes \mathscr{F}_a(k_\perp) \otimes D_a^h(z) \otimes \mathscr{H}^{(0)}$$

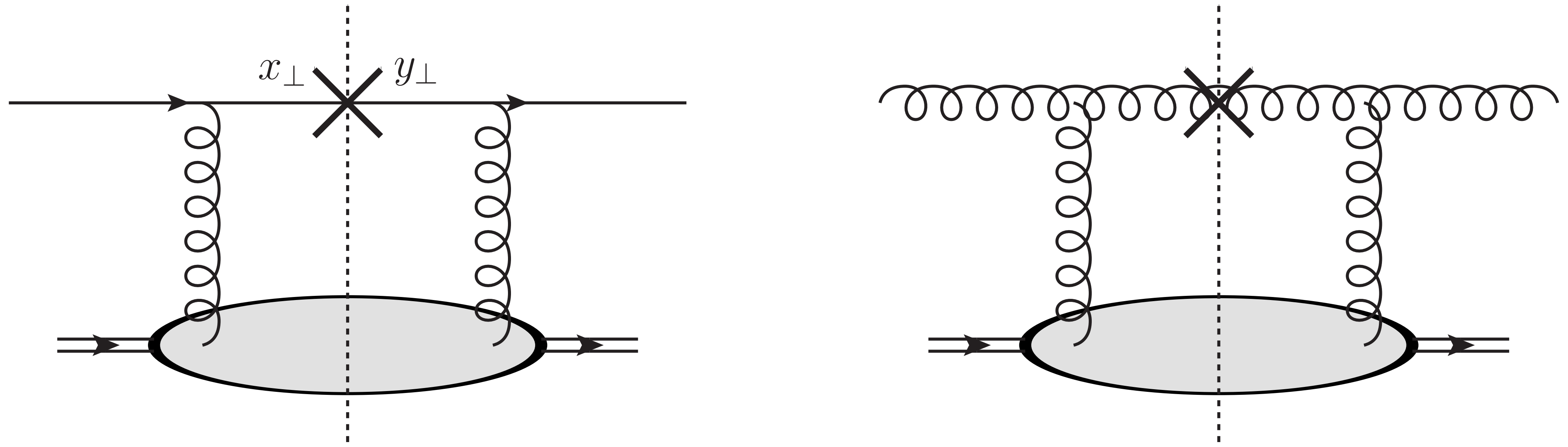

A. Dumitru, A. Hayashigaki and J. Jalilian-Marian, NPA765, 464-482 (2006)

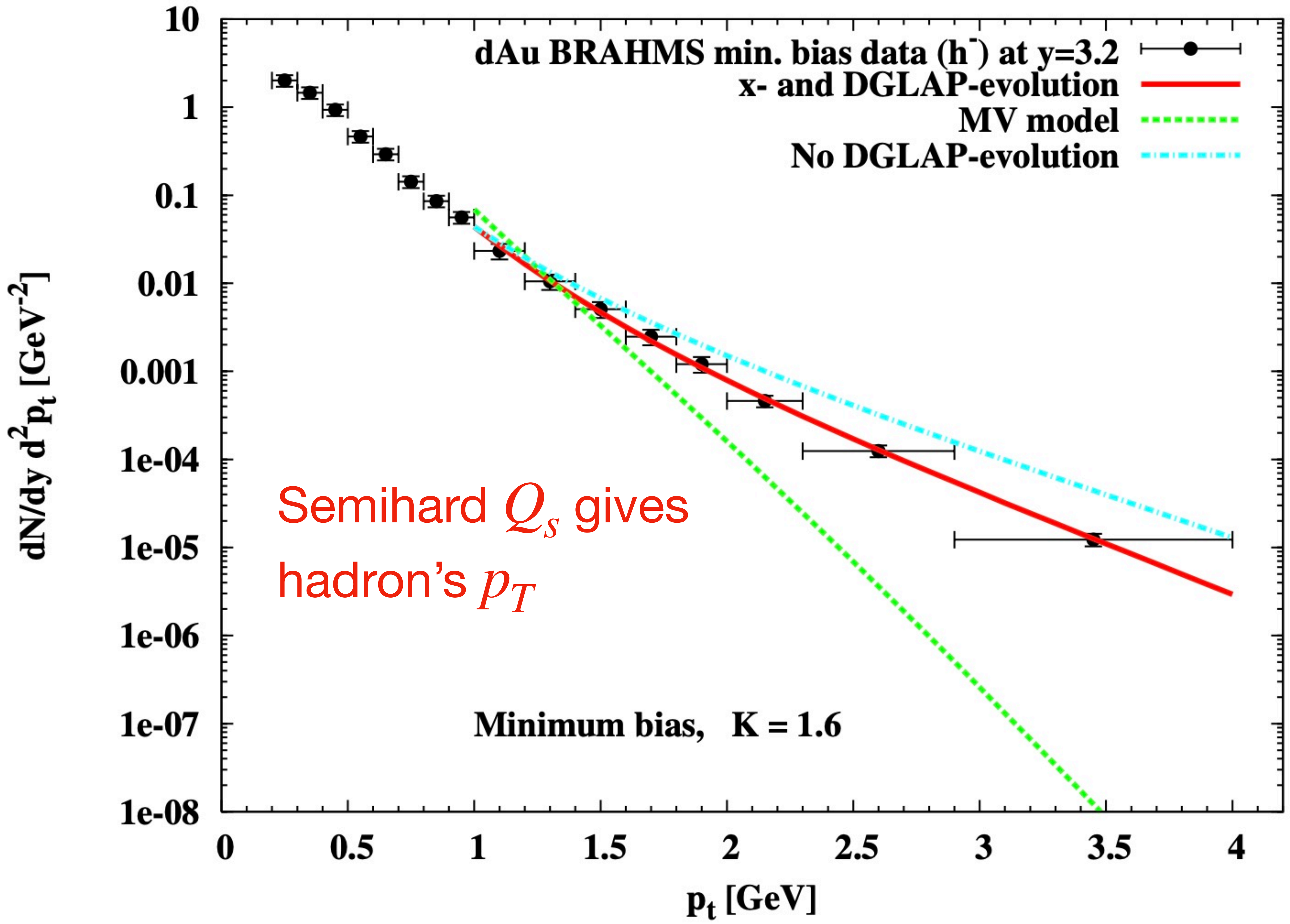

- ❖ Dilute projectile: collinear PDFs
- ❖ Dense target: Wilson line correlators $\mathscr{F}$ (not standard parton densities)
- ❖ Room for NLO corrections

NLO corrections

$$\frac{d\sigma_{p+A\to h+X}}{dyd^2p_T} = \int x_p f_{a/p}(x_p) \otimes \mathscr{F}_a(k_\perp) \otimes D_a^h(z) \otimes \mathscr{H}^{(0)}$$

$$+\frac{\alpha_s}{2\pi}\int x f_{a/p}(x) \otimes \mathscr{F}_{ab}(k_\perp) \otimes D_b^h(z) \otimes \mathscr{H}^{(1)}$$

Real

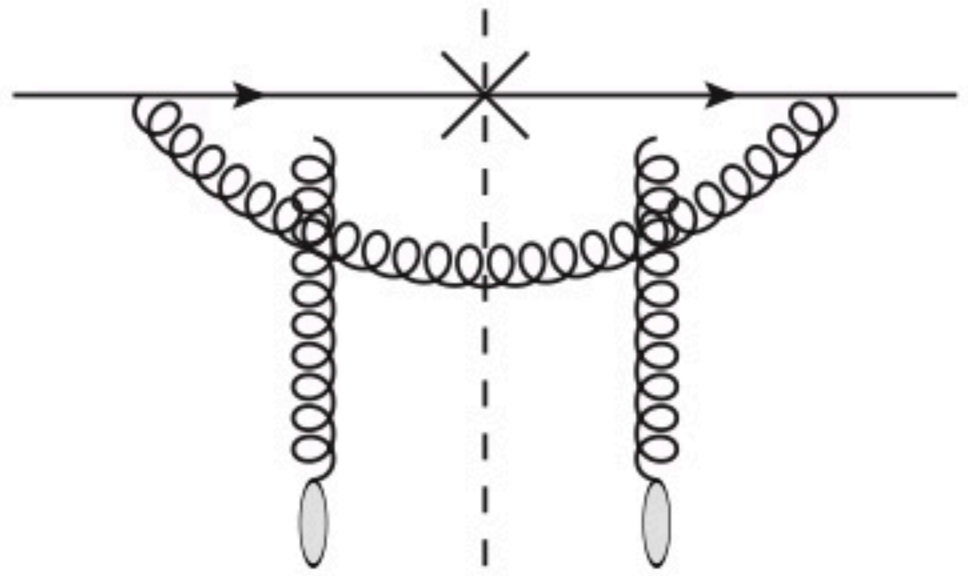

(a)

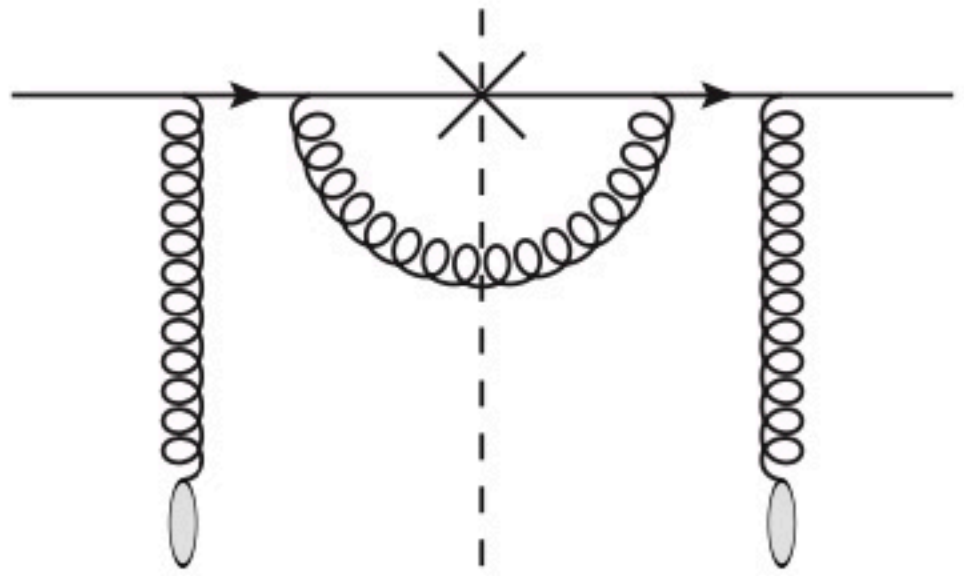

(b)

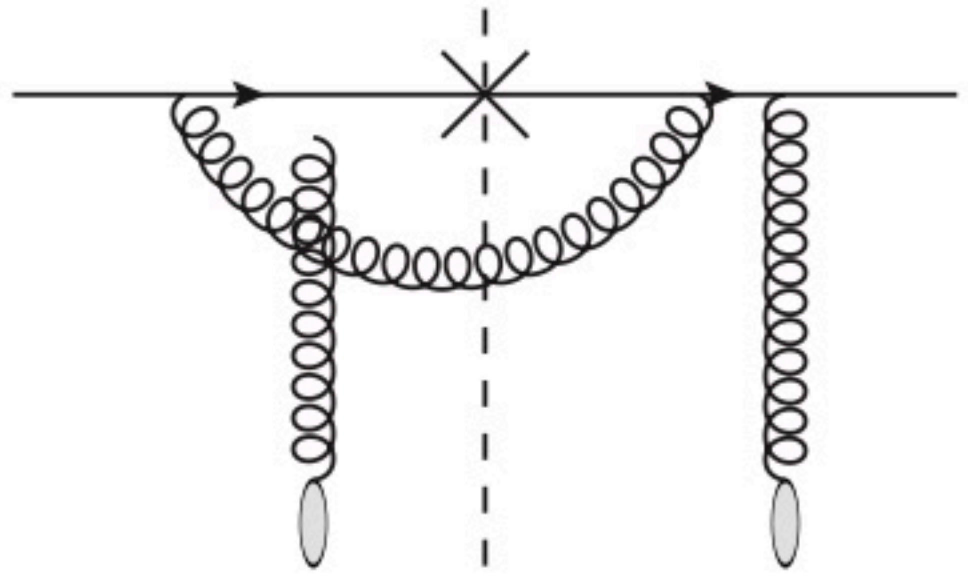

(c)

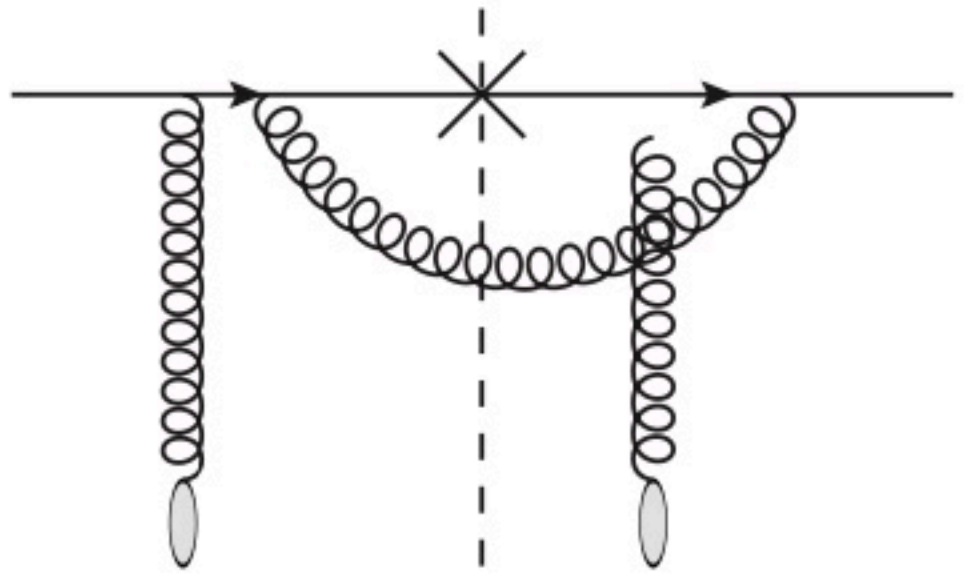

(d)

Virtual

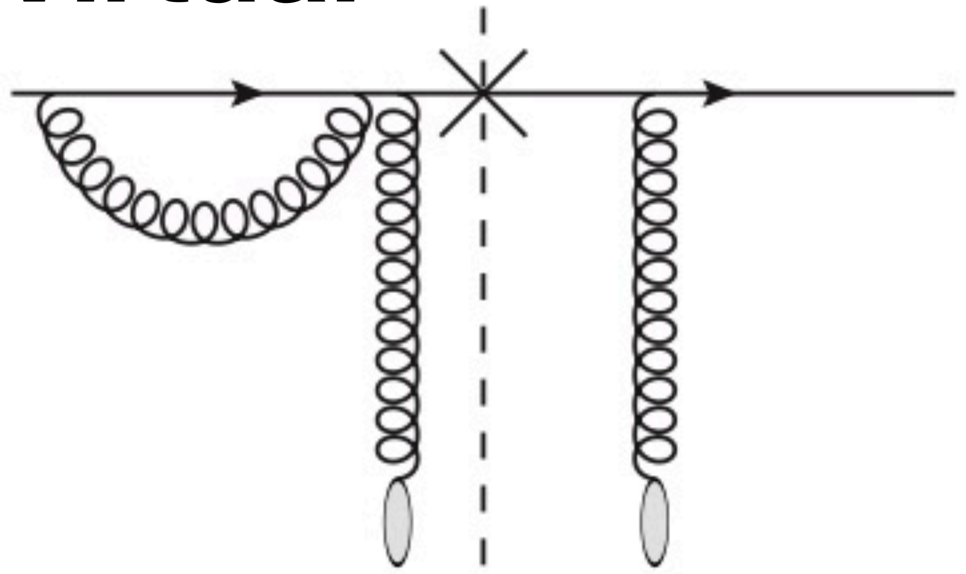

(a)

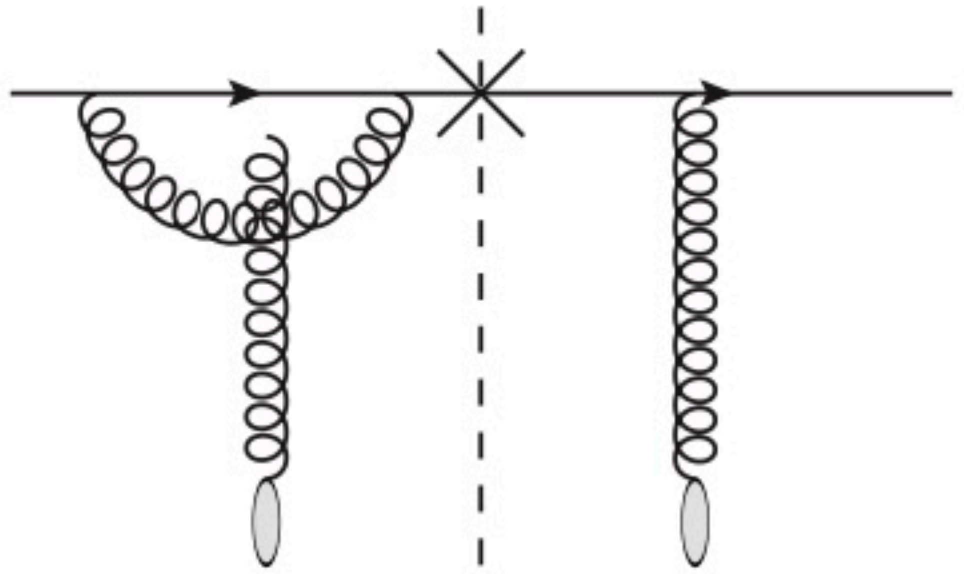

(b)

Relevant channels:

$$qg \to qg, \quad gg \to gg, \quad gg \to q\bar{q}$$

A set of master equations at NLO

G. A. Chirilli, B.W. Xiao and F. Yuan, PRD86, 054005 (2012)

$$\frac{d\sigma^{p+A\to h+X}}{d^2p_{h\perp}dy} = \sum_f \int_\tau^1 \frac{dz}{z^2}\int_{x_p}^1 \frac{dx}{x}\xi\left(xq_f(x,\mu), xG(x,\mu)\right)\begin{pmatrix} S_{qq}^{(0)}+\frac{\alpha_s}{2\pi}S_{qq} & \frac{\alpha_s}{2\pi}S_{gq} \\ \frac{\alpha_s}{2\pi}S_{qg} & S_{gg}^{(0)}+\frac{\alpha_s}{2\pi}S_{gg}\end{pmatrix}\begin{pmatrix} D_{h/q}(z,\mu) \\ D_{h/g}(z,\mu)\end{pmatrix}$$

$$\begin{pmatrix} q_f(x,\mu) \\ G(x,\mu)\end{pmatrix} = \begin{pmatrix} q_f^{(0)}(x) \\ G^{(0)}(x)\end{pmatrix} - \frac{1}{\hat{\epsilon}}\frac{\alpha_s(\mu)}{2\pi}\int_z^1 \frac{d\xi}{\xi}\begin{pmatrix} C_F\mathscr{P}_{qq}(\xi) T_R\mathscr{P}_{qg}(\xi) \\ \sum_f C_F\mathscr{P}_{gq}(\xi) N_c\mathscr{P}_{gg}(\xi)\end{pmatrix}\begin{pmatrix} q_f(x/\xi) \\ G(x/\xi)\end{pmatrix}$$

$$\begin{pmatrix} D_{h/q}(z,\mu) \\ D_{h/g}(z,\mu)\end{pmatrix} = \begin{pmatrix} D_{h/q}^{(0)}(z) \\ D_{h/g}^{(0)}(z)\end{pmatrix} - \frac{1}{\hat{\epsilon}}\frac{\alpha_s(\mu)}{2\pi}\int_z^1 \frac{d\xi}{\xi}\begin{pmatrix} C_F\mathscr{P}_{qq}(\xi) C_F\mathscr{P}_{gq}(\xi) \\ \sum_f T_R\mathscr{P}_{qg}(\xi) N_c\mathscr{P}_{gg}(\xi)\end{pmatrix}\begin{pmatrix} D_{h/q}(z/\xi) \\ D_{h/g}(z/\xi)\end{pmatrix}$$

$$\mathscr{F}(k_\perp) = \mathscr{F}^{(0)}(k_\perp) - \frac{\alpha_s N_c}{2\pi^2}\int_0^1 \frac{d\xi}{1-\xi}\int \frac{d^2x_\perp d^2y_\perp d^2b_\perp}{(2\pi)^2} e^{-ik_\perp\cdot(x_\perp-y_\perp)}\frac{(x_\perp-y_\perp)^2}{(x_\perp-b_\perp)^2(y_\perp-b_\perp)^2}\left[S_Y^{(2)(x_\perp,y_\perp)} - S_Y^{(4)(x_\perp,b_\perp,y_\perp)}\right]$$

❖ Colliner divergences → PDFs and FFs.

❖ Rapidity divergence → Wilson line correlators.

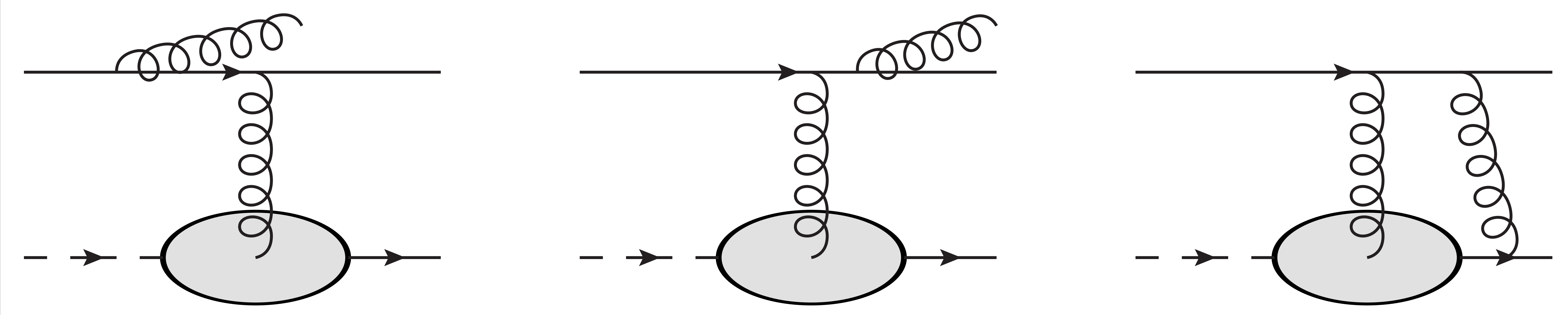

First numerical computations: LO + NLO

A. M. Stasto, B. W. Xiao and D. Zaslavsky, PRL112, no.1, 012302 (2014)

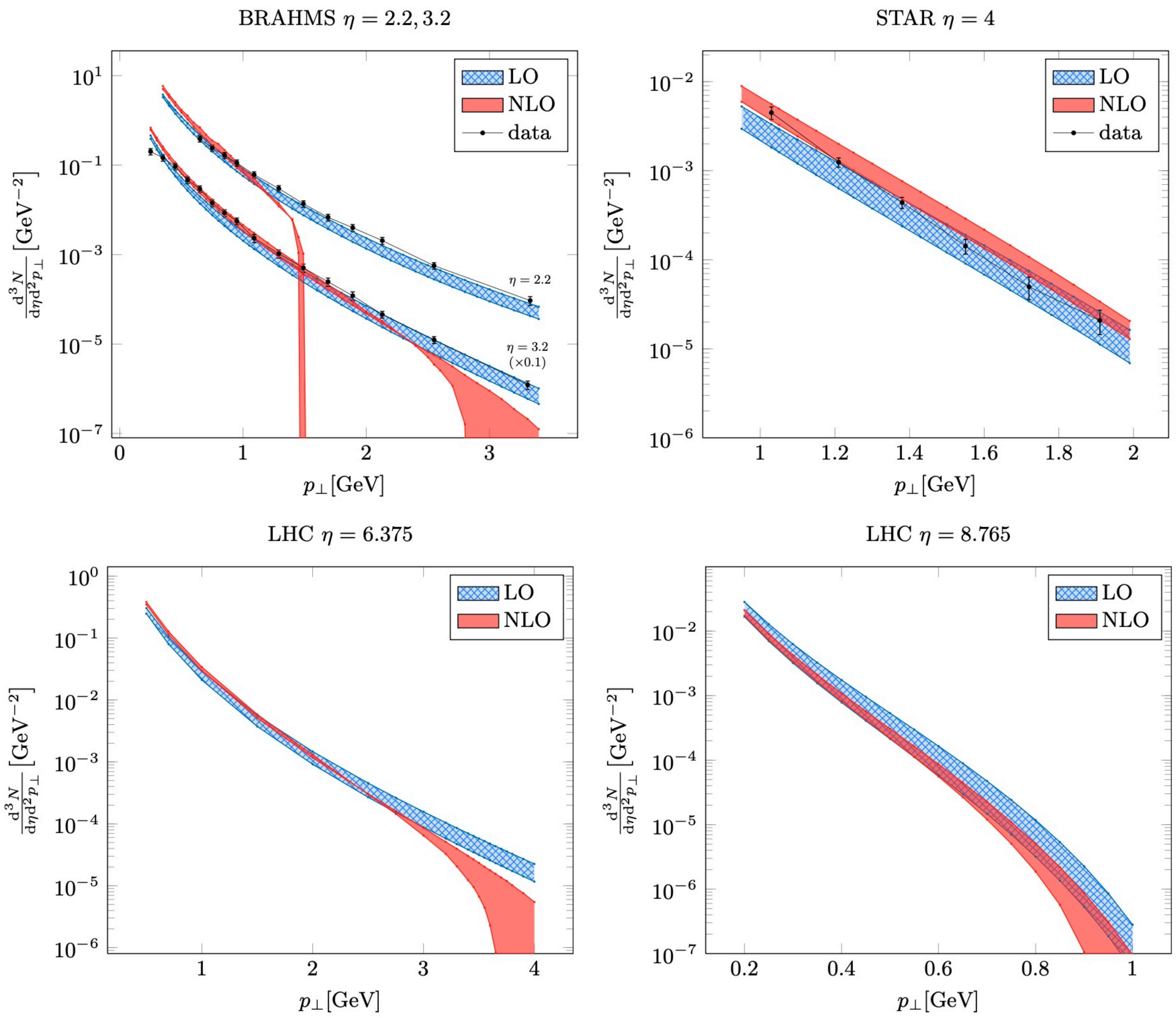

Toward the precision era

KW, Xiao, Yuan and Zaslavsky, PRD92, no.3, 034026 (2015)

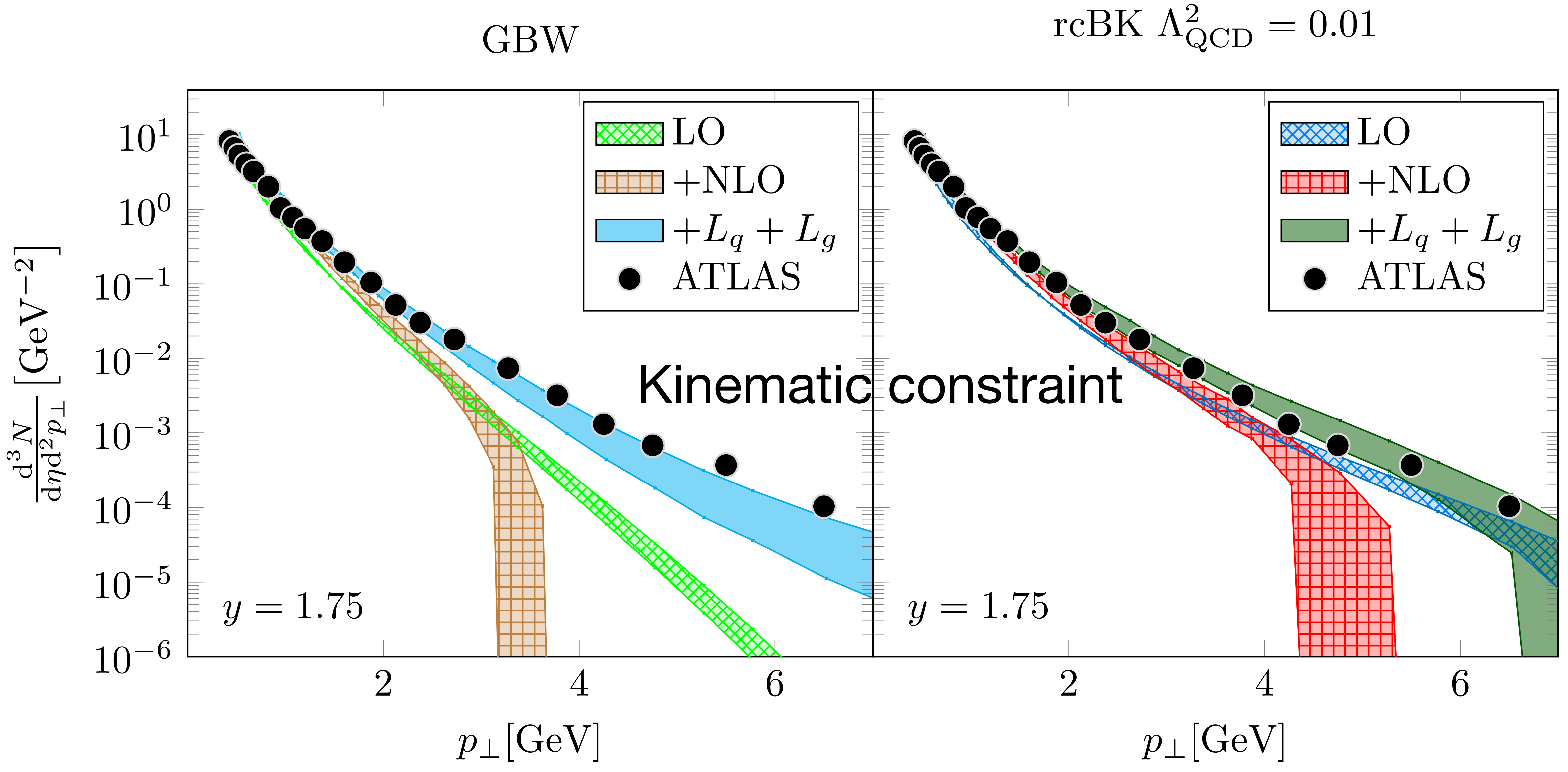

Y. Shi, L. Wang, S.Y. Wei and B.W. Xiao, PRL128, no.20, 202302 (2022)

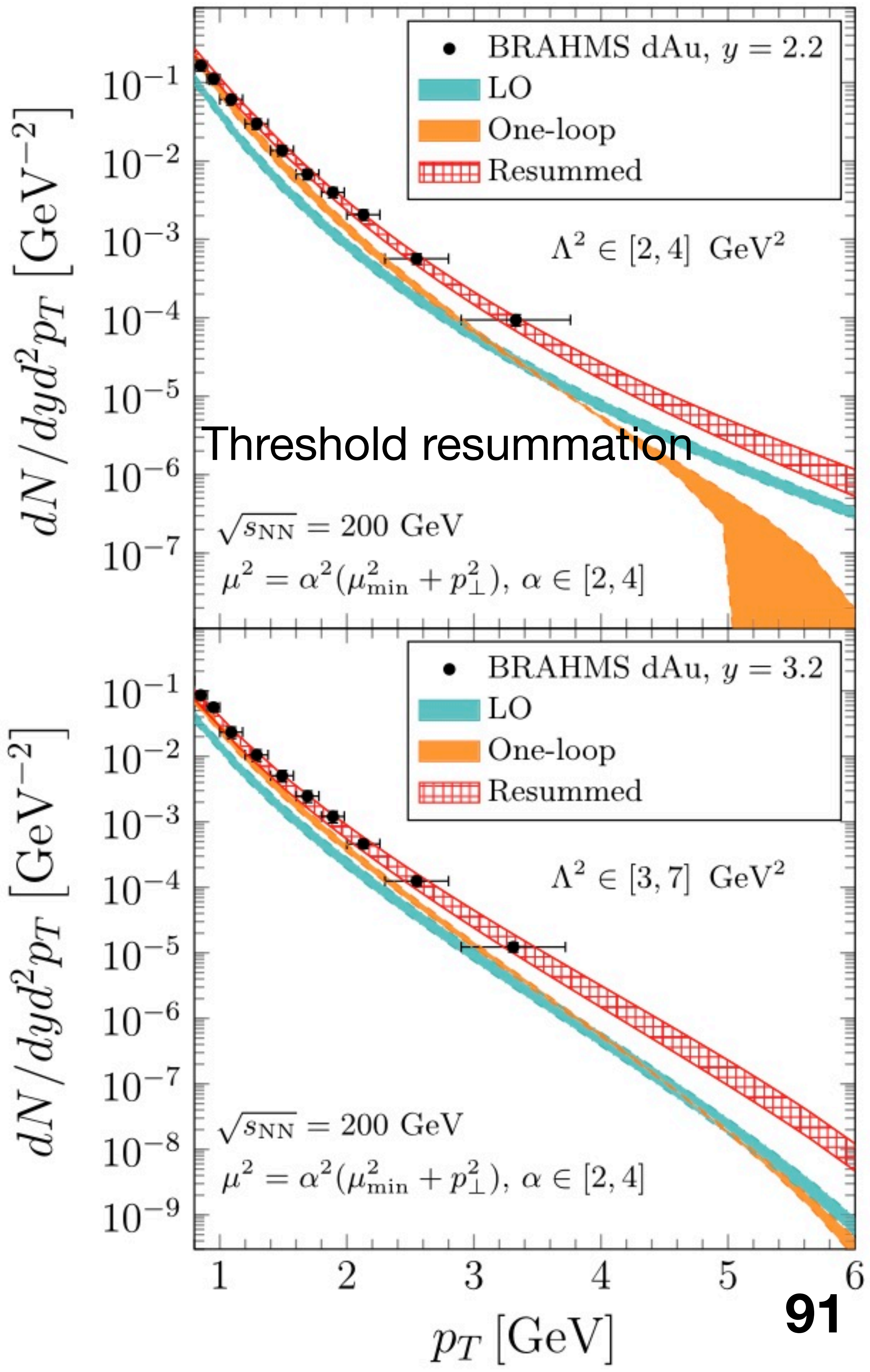

Liu, Ma and Chao, PRD100, no.7, 071503 (2019)

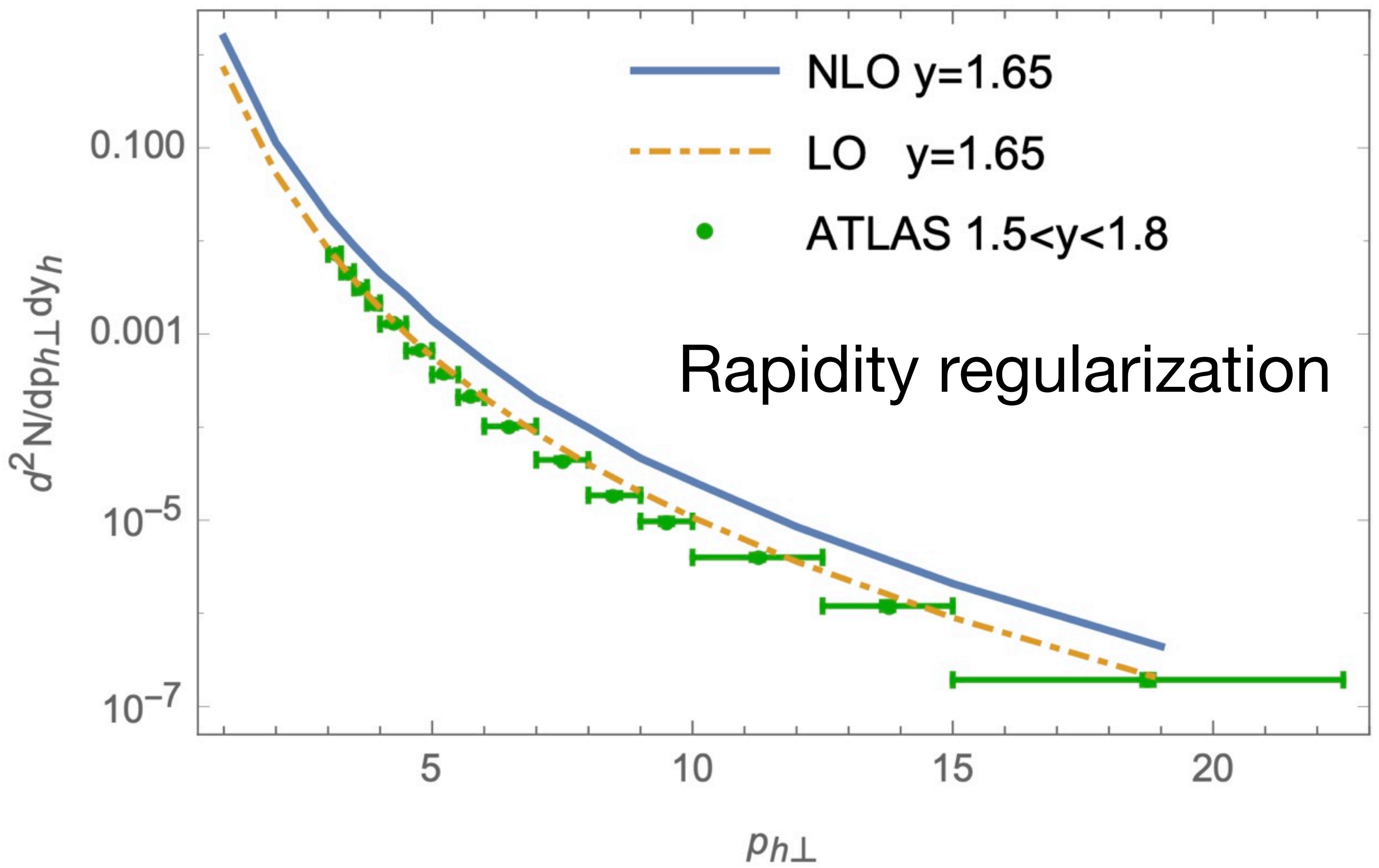

Liu, Kang and Liu, PRD102, no.5, 051502 (2020)

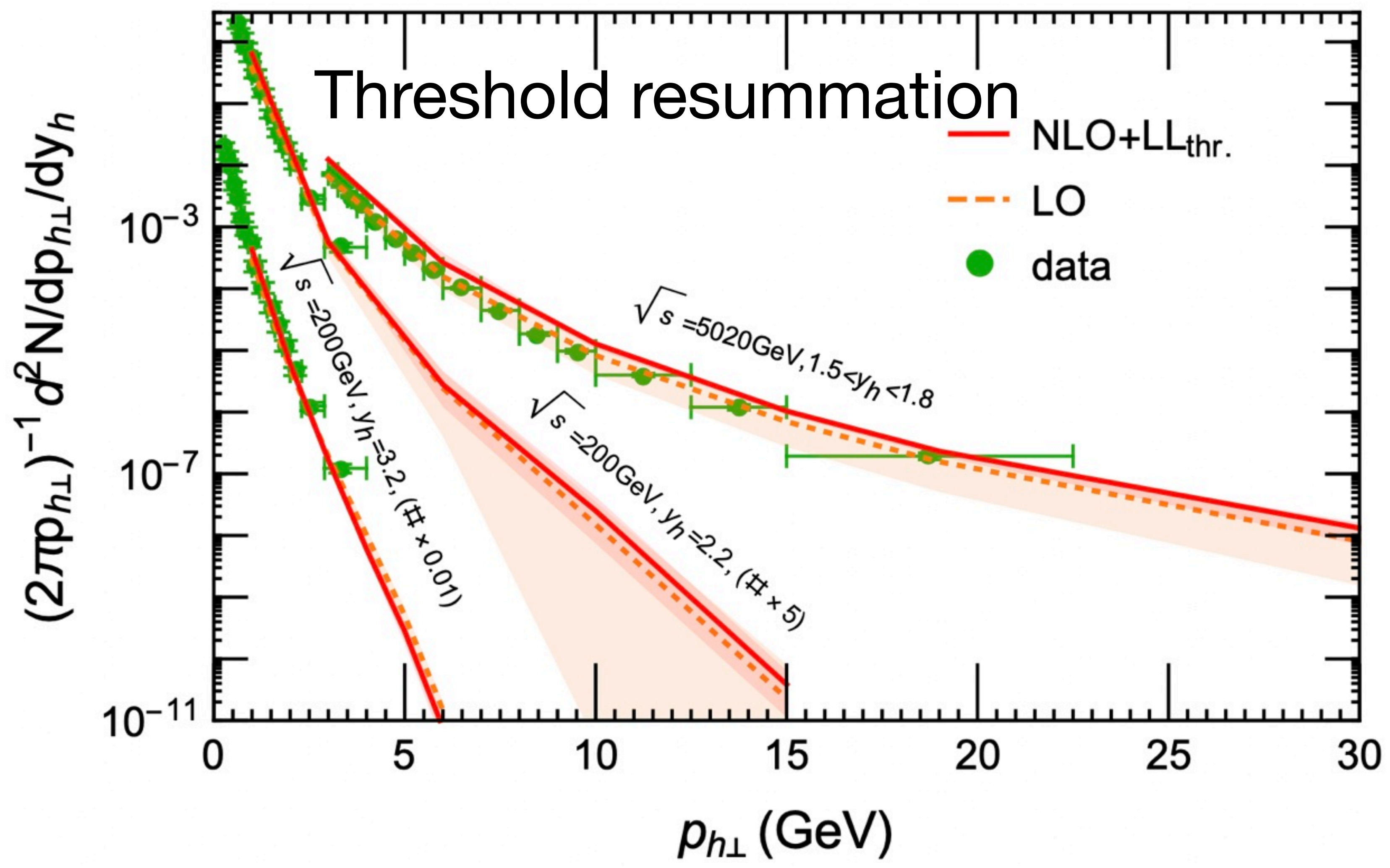

Dijet production in DIS at NLO: cutting-edge

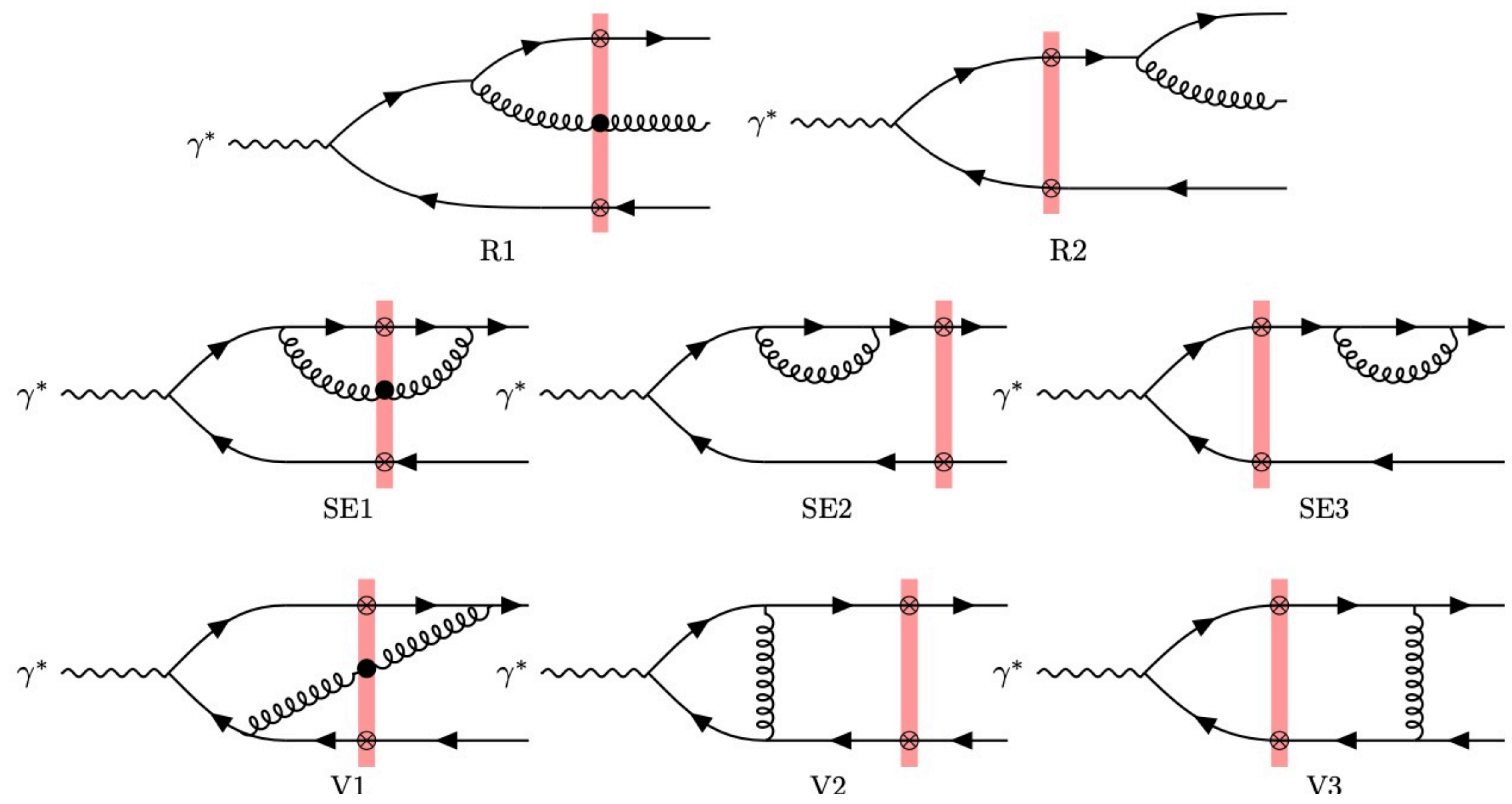

P. Caucal, F. Salazar, B. Schenke, T. Stebel and R. Venugopalan, JHEP08, 062 (2023)

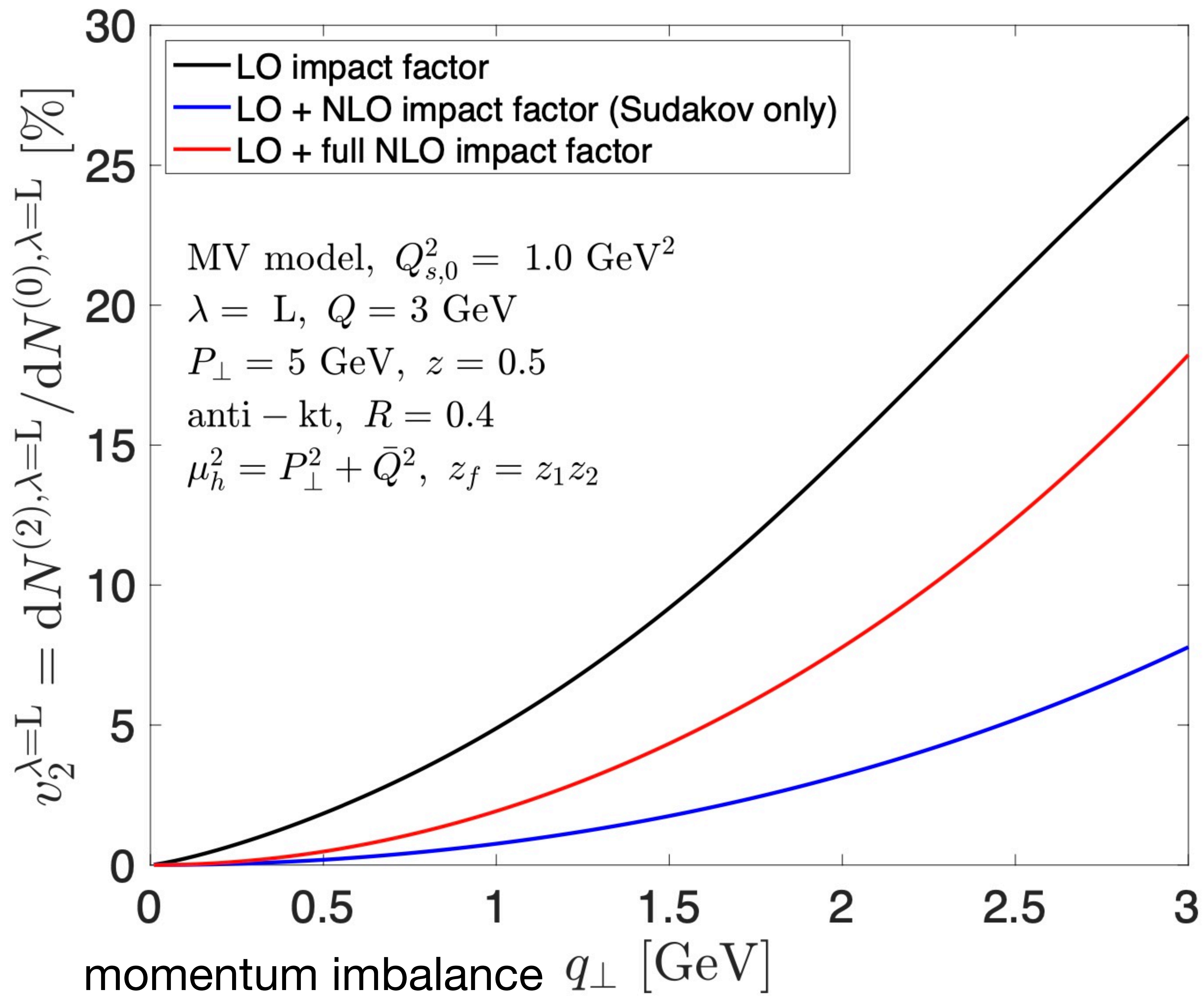

To define jets, k_t algorithm, anti-k_t algorithm, and the Cambridge/Aachen algorithm are applicable. → NLO hard factors.

Pushing business towards the NLO frontier

- ➢ Phenomenology of quarkonium production in pp/pA collisions in the CGC framework have been performed at LO level with leading logarithmic small-x evolution.
- ➢ Efforts are being made to push the precision to NLO level.
  - inclusive hadron production in pA
  - inclusive dijet (+ photon) in eA
  - exclusive dijet in eA
- ➢ NLO calculations for exclusive J/ψ production have been performed recently.
- ➢ Extensive NLO calculations for inclusive quarkonium production in pA/eA collisions are exciting tasks to complete in the next decade.

Chirilli, Xiao and Yuan, PRD86, 054005 (2012)
Altinoluk, Armesto, Beuf, Kovner, Lublinsky, PRD91, no.9, 094016 (2015)
KW, Xiao, Yuan and Zaslavsky, PRD92, no.3, 034026 (2015)
Ducloué, Lappi and Zhu, PRD93, no.11, 114016 (2016)
Liu, Ma and Chao, PRD100, no.7, 071503 (2019)
Liu, Kang and Liu, PRD102, no.5, 051502 (2020)
…
Roy and Venugopalan, PRD101, no.3, 034028 (2020)
Caucal, Salazar and Venugopalan, [arXiv:2108.06347 [hep-ph]]
Boussarie, Grabovsky, Ivanov, Szymanowski and Wallon, PRL119, no.7, 072002 (2017)
…

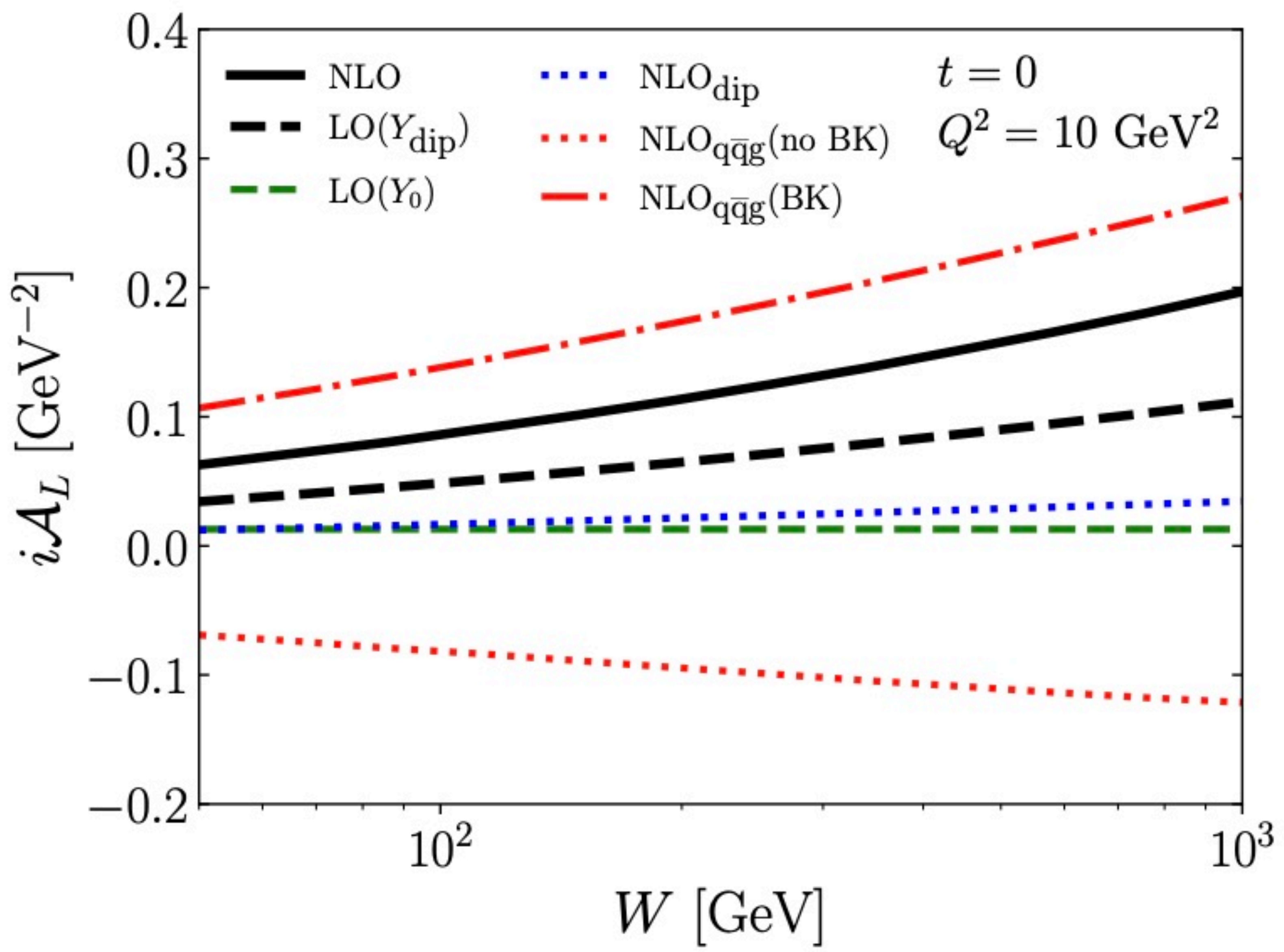

Mäntysaari and Penttala, PLB823, 136723 (2021)

Appendix:
Introduction to EIC physics

U.S. Electron-Ion Collider @ BNL

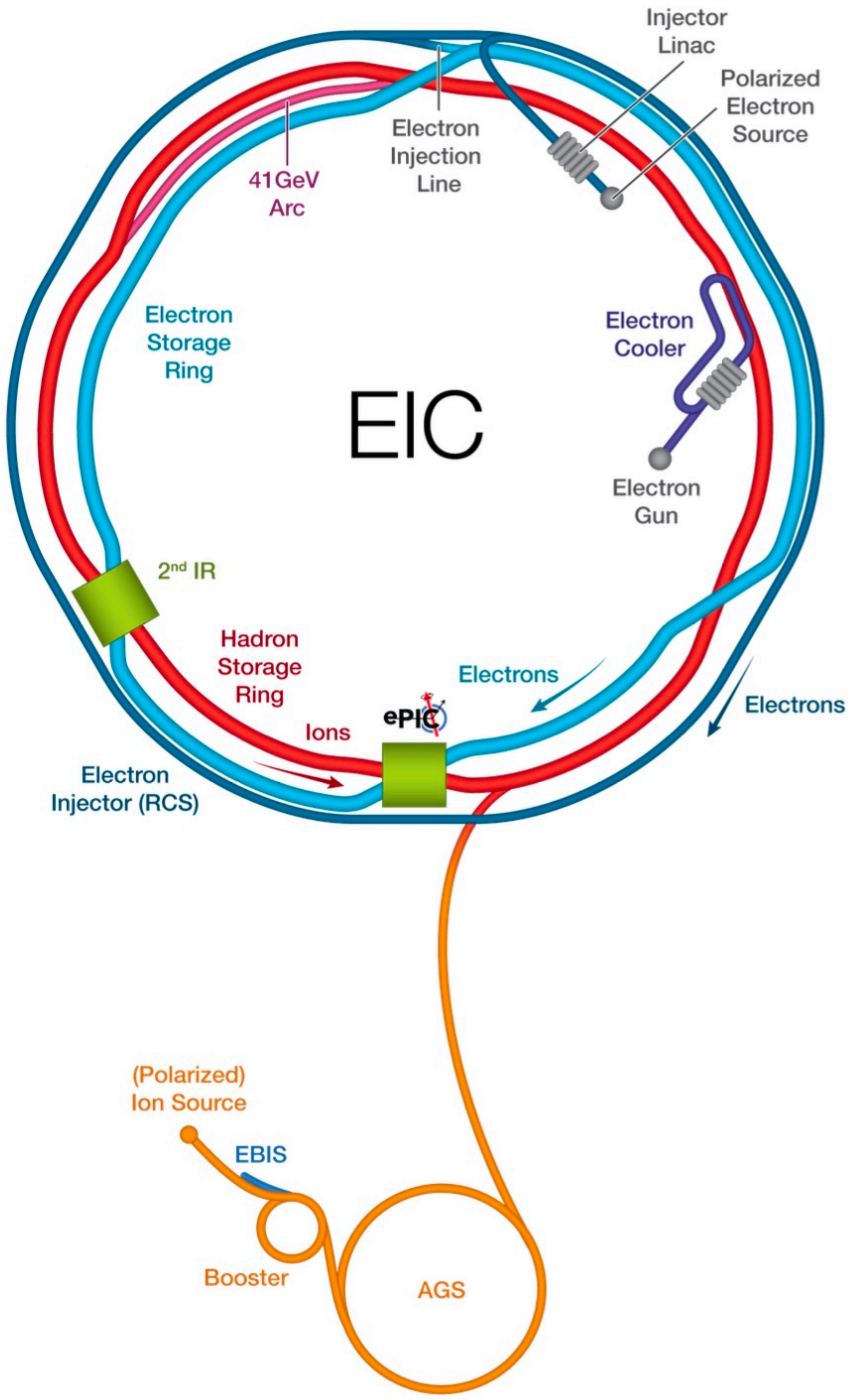

The world's first collider for polarized electron and polarized proton and electron-nucleus collision.

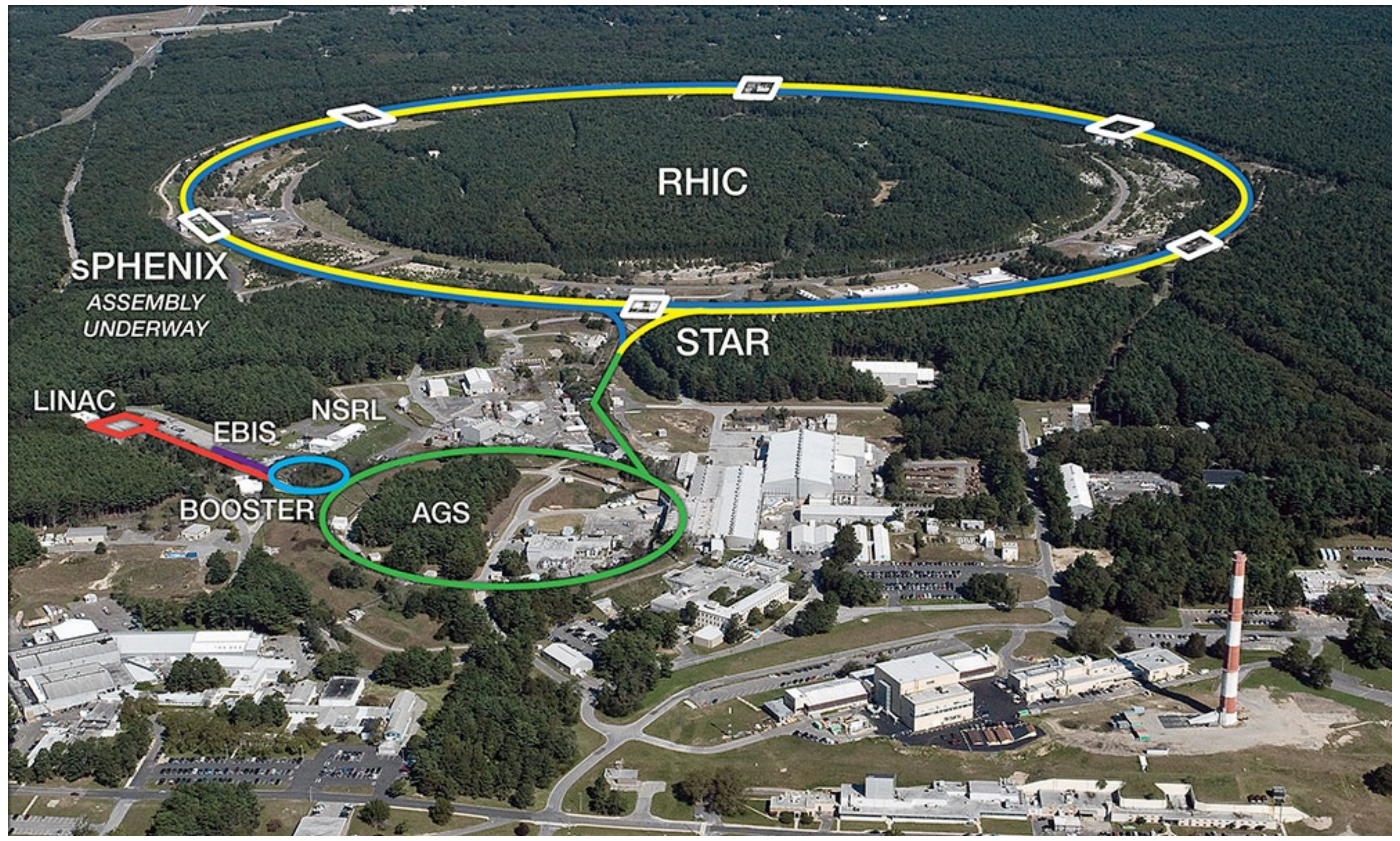

Machine properties :

- ❖ 80% polarized electron beam : 5 -18 GeV
- ❖ 70% polarized proton beam : 40 - 275 GeV
- ❖ Ion available for target: 40 - 110 GeV
- ❖ CM energy : $\sqrt{s_{ep}} = 20 - 140\,\mathrm{GeV}$
- ❖ Luminosity (100 - 1000 × HERA): $\mathscr{L} = 10^{33} - 10^{34}\,\mathrm{cm}^{-2}\mathrm{s}^{-1}$

Kinematic distributions

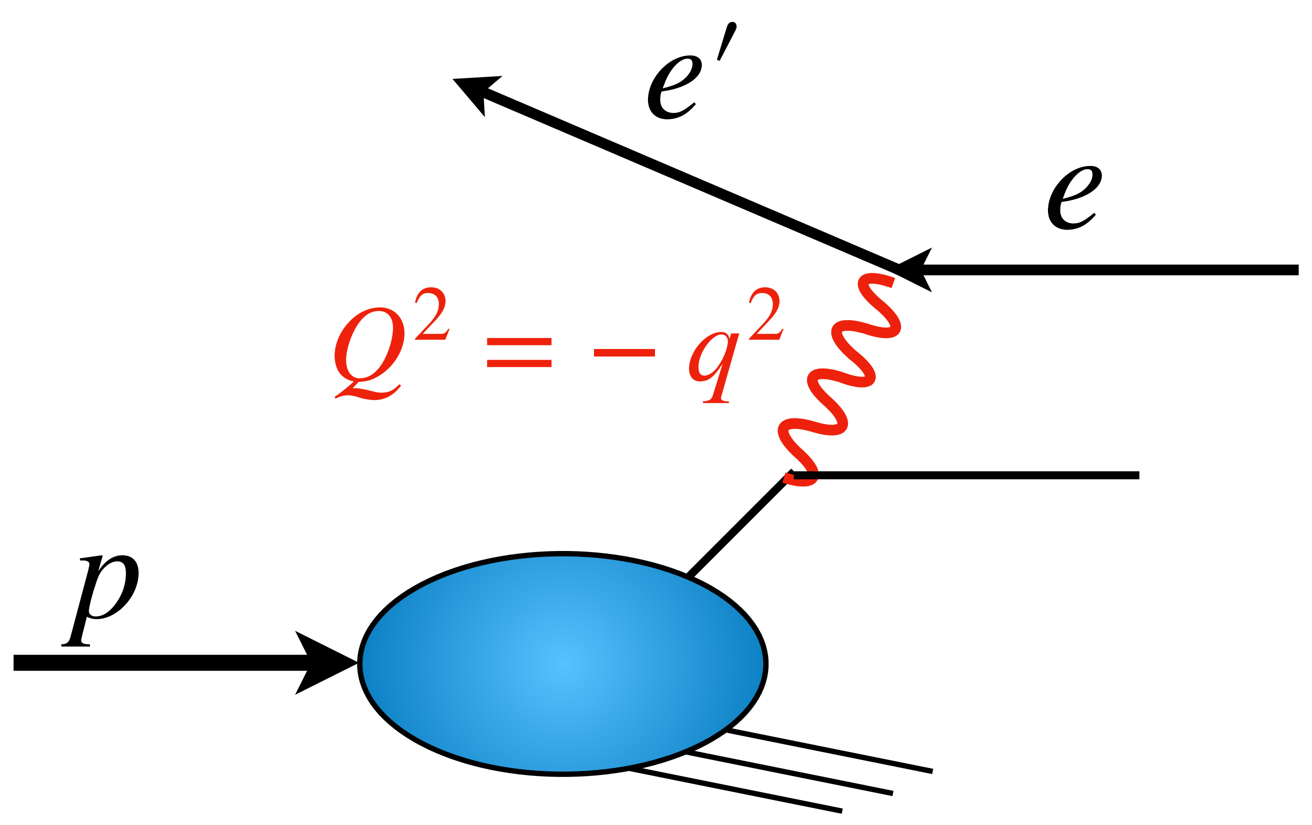

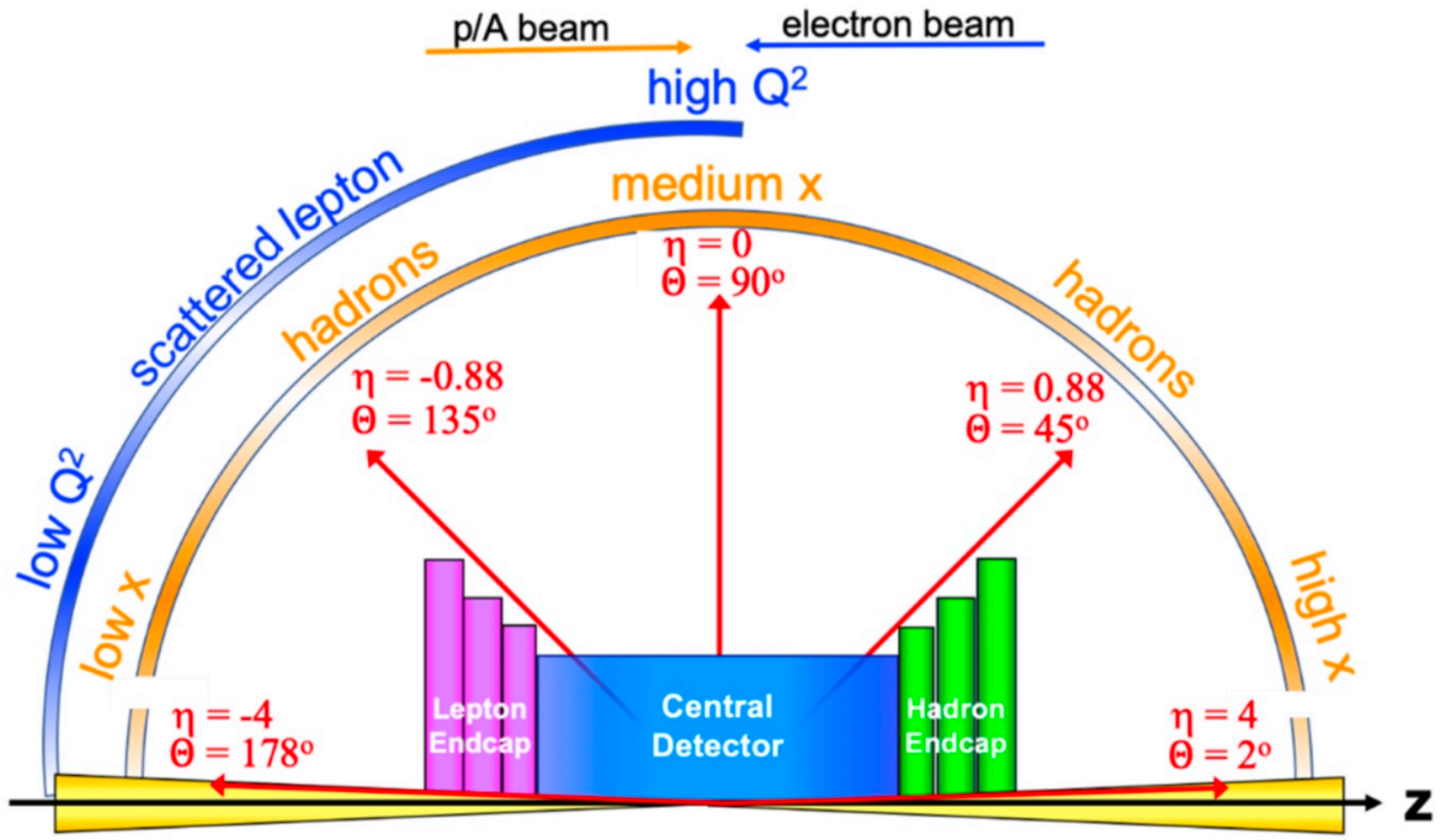

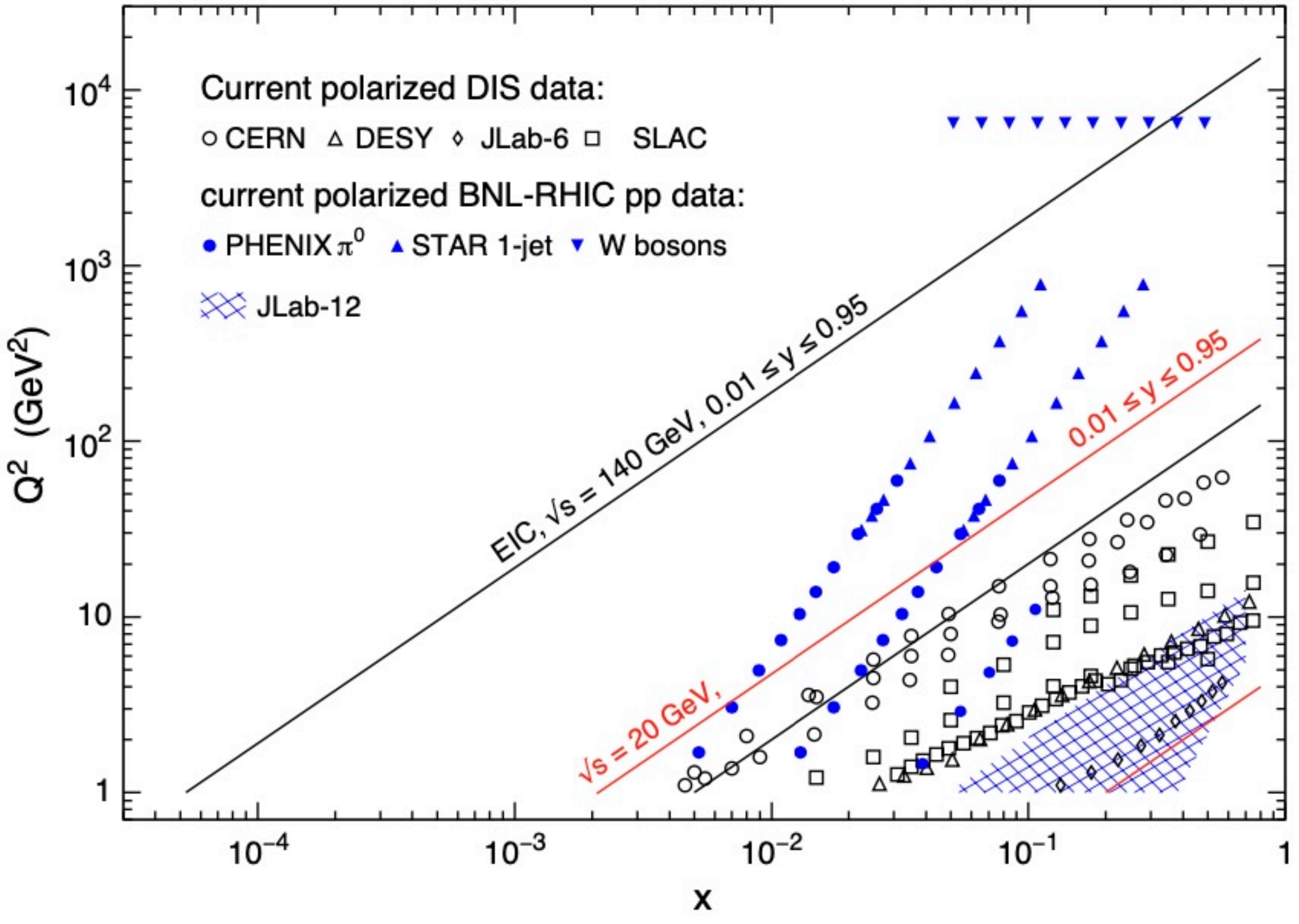

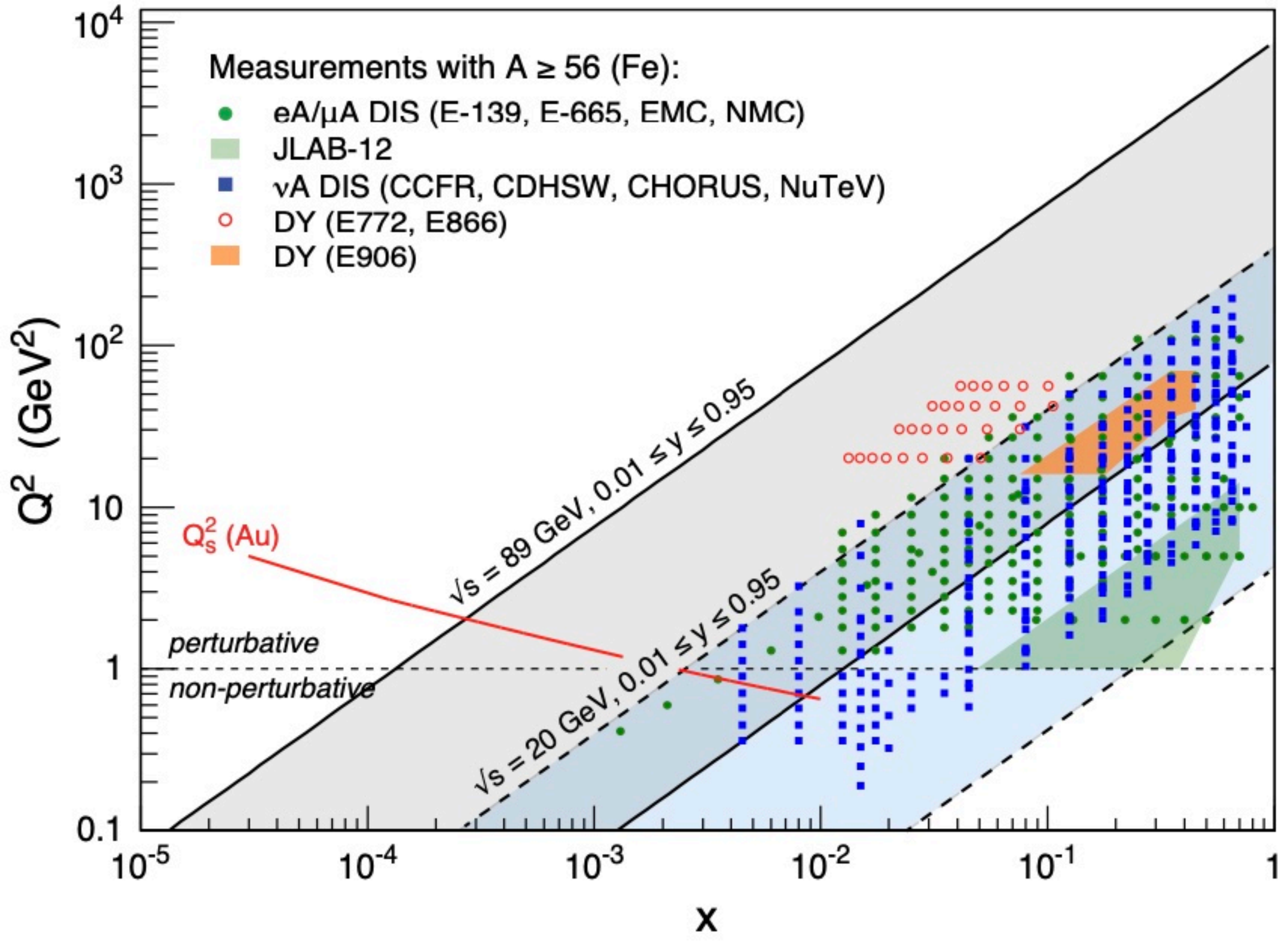

Key Science Question I: Properties of Proton

How do the nucleonic properties such as mass and spin emerge from partons and their underlying interactions?

❖ The origin of the proton's spin (1/2):

$$\frac{1}{2} = \frac{1}{2}\Delta\Sigma + \Delta G + L_{\mathrm{quark}} + L_{\mathrm{gluon}}$$

Quark spin (~30%) Gluon helicity Orbital angular momenta (less known)

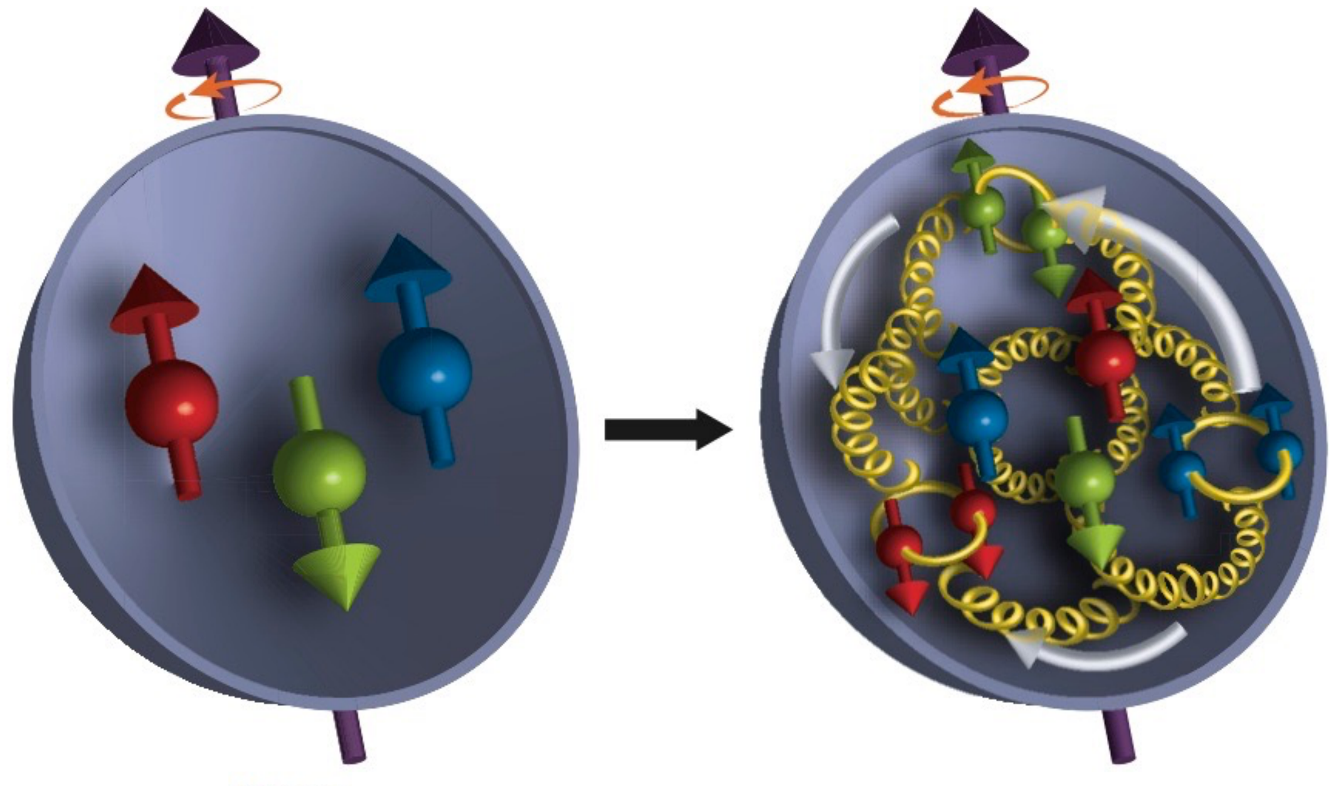

→ A polarized proton beam is needed.

❖ The origin of the proton's mass:

✓ Quarks (Higgs mechanism) contribute to only 1%.

✓ Gluon is massless but dynamically provides 99% contribution.

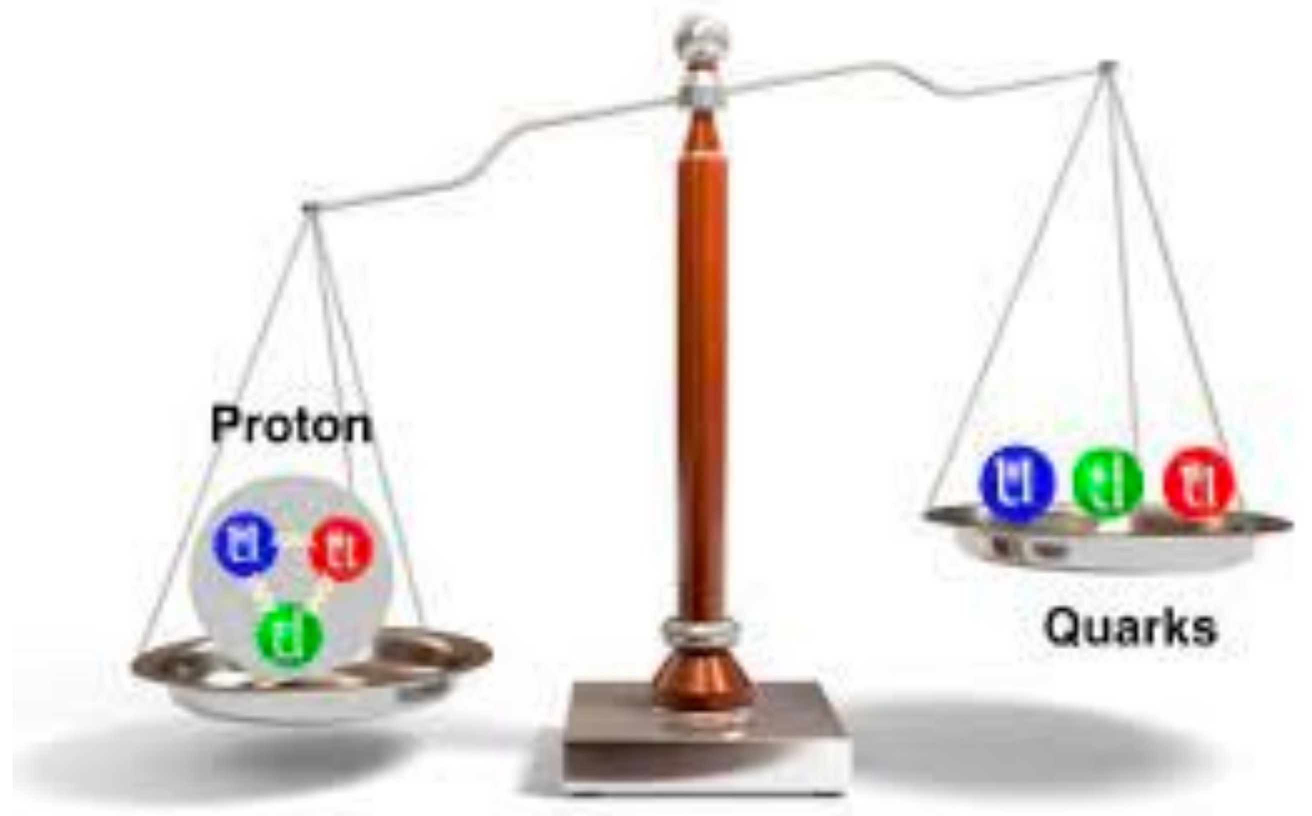

Key Science Question II: Color Confinement

How are partons inside the nucleon distributed in both momentum and position space?

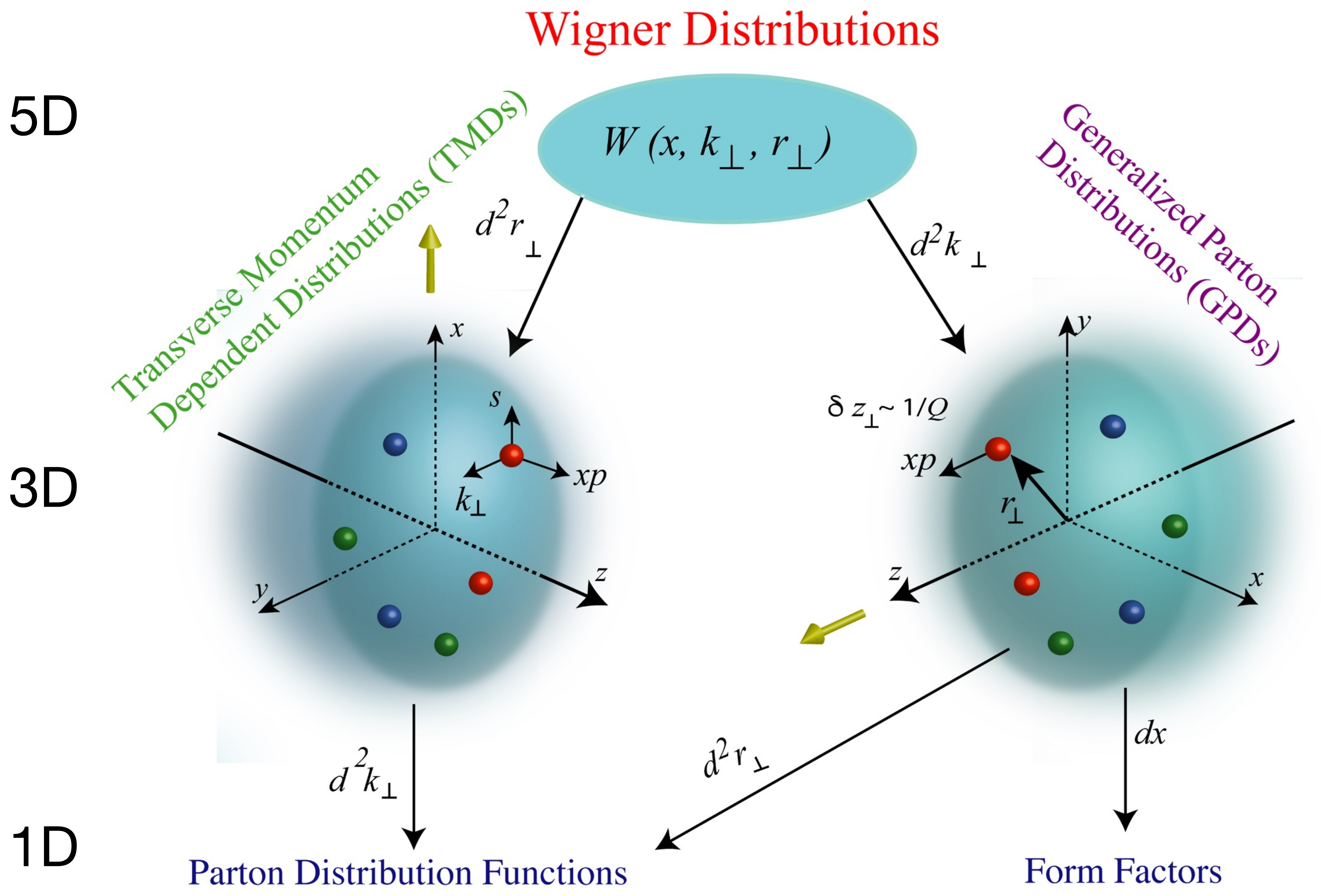

3D partonic structure of a proton is related to the proton's spin: classically $L_z = (\vec{k}_T \times \vec{b}_T)_z$

Key Science Question III: New Form of Matter

How does a dense nuclear environment affect the gluon density in nuclei? Does it saturate at high energy, giving rise to gluonic matter (Color Glass Condensate) or a gluonic phase with universal properties in all nuclei and even in nucleons?

Proton

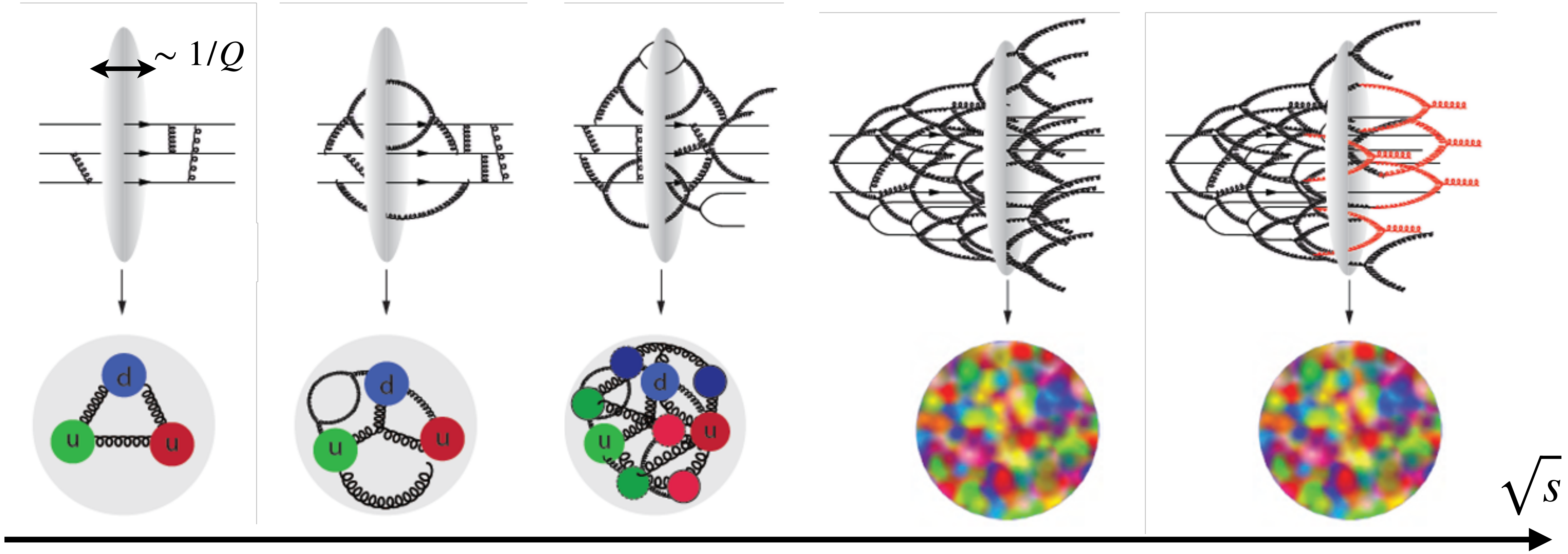

Nucleus

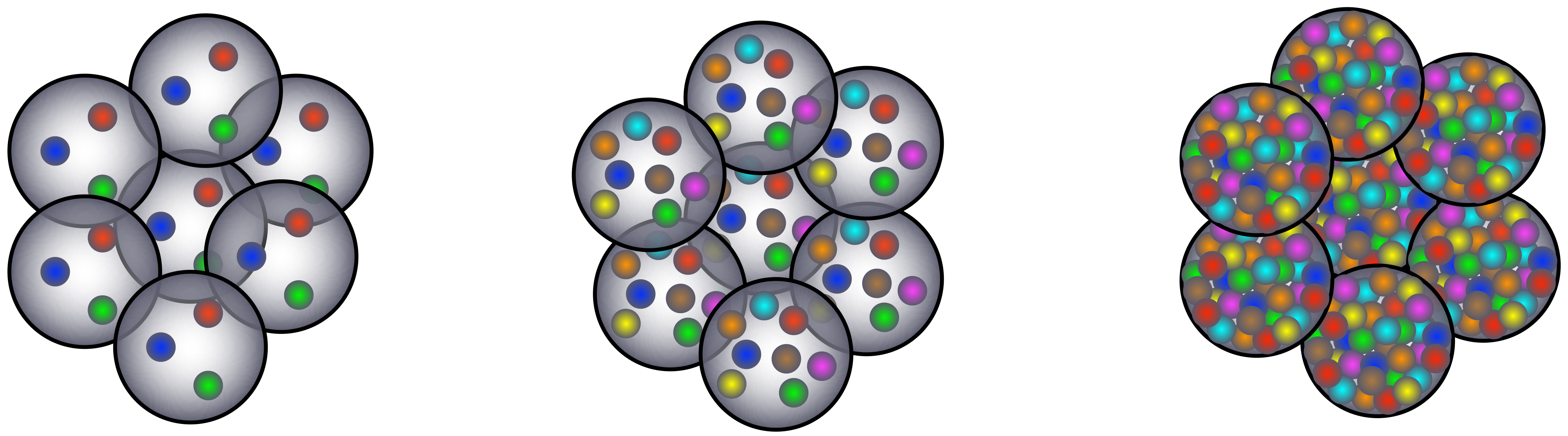

Heavy nuclei could become CGC rapidly.

→ Nuclear beams are needed.

Key Science Question IV: Neutralization of Color

How do color-charged quarks and gluons, and jets, interact with a nuclear medium?
How do the confined hadronic states emerge from these quarks and gluons?
How do the quark-gluon interactions create nuclear binding?

Hadronization has been actively studied in e^+e^- and pp collisions.

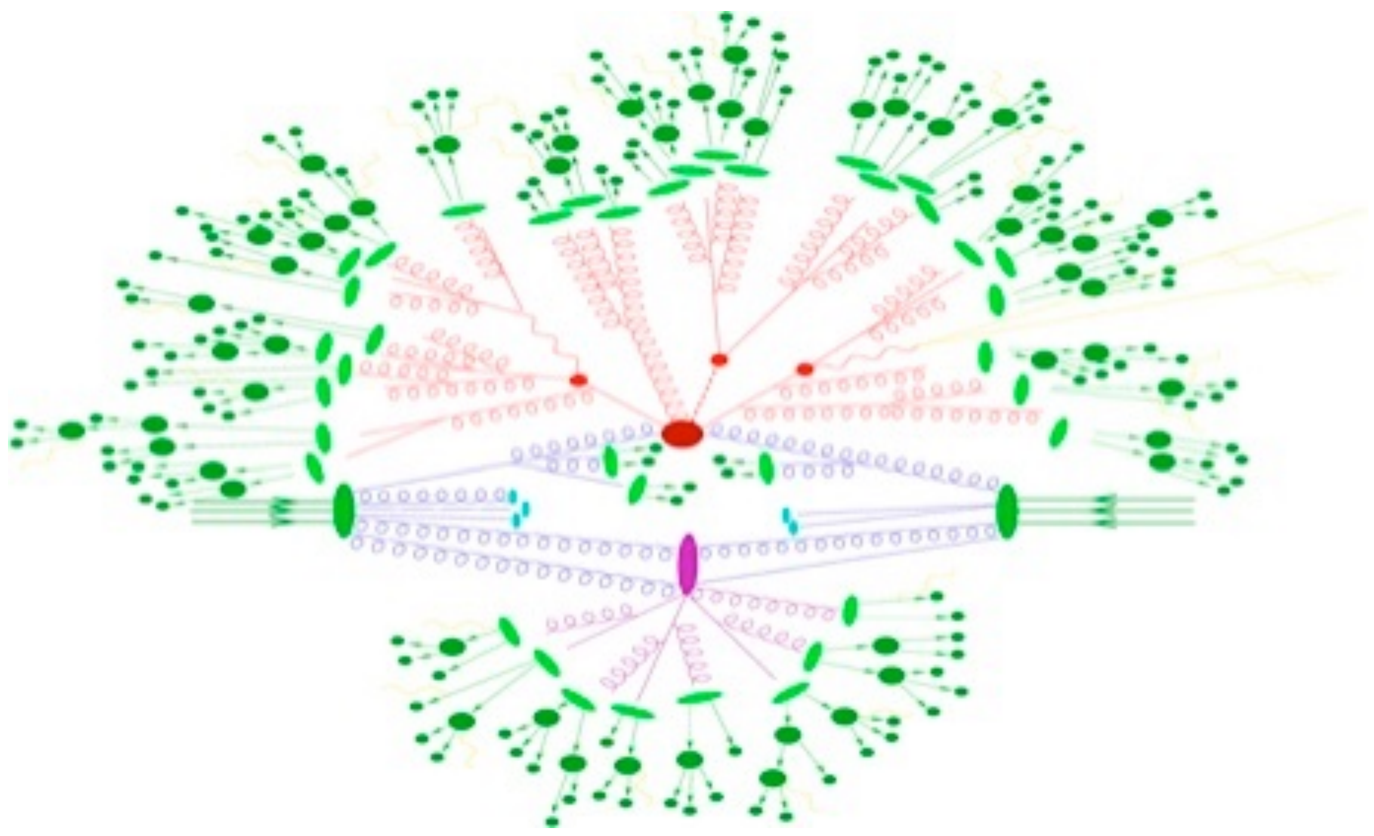

The nuclear target is a femto-scope to explore hadronization in the medium.

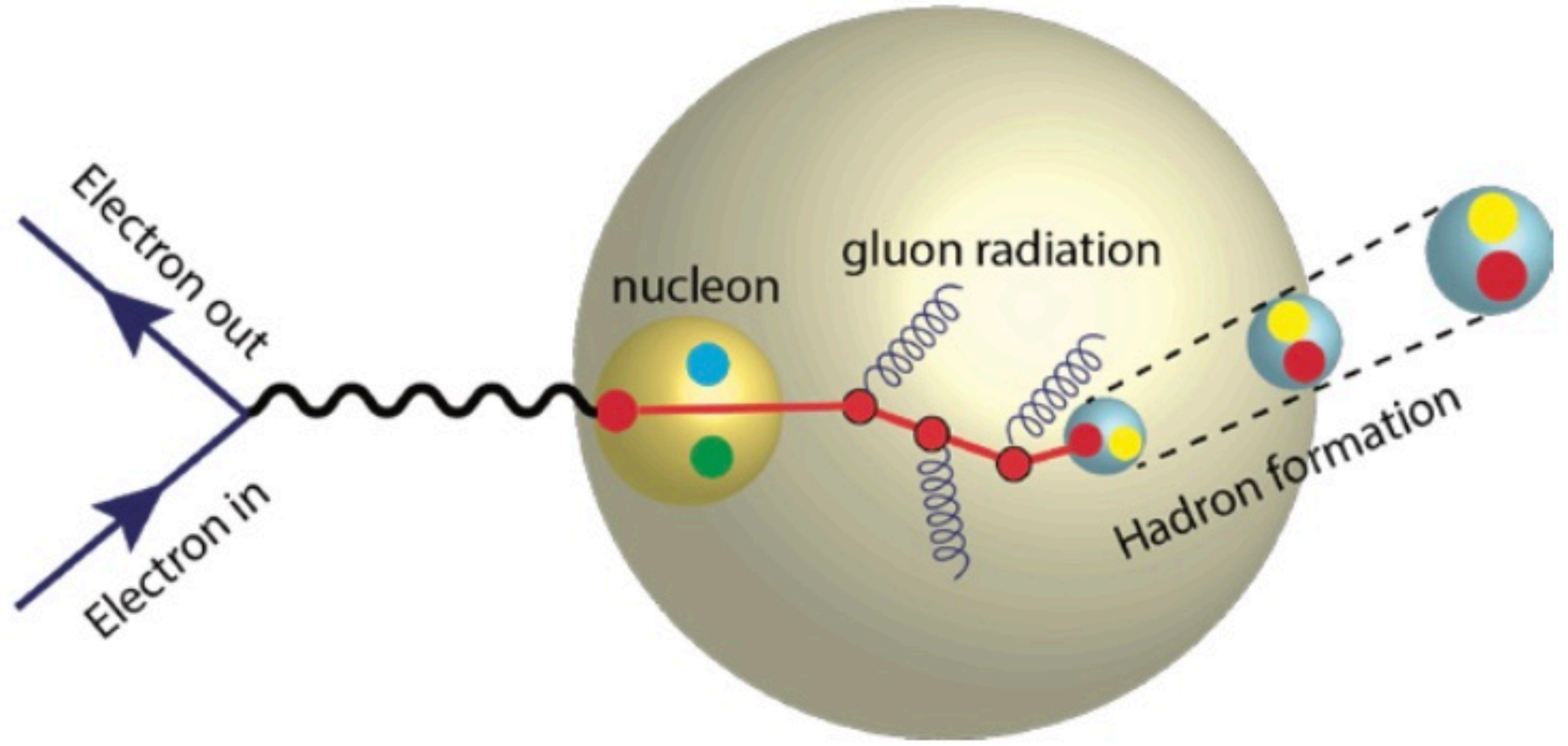

filter to diagnose hadronization dynamics

→ An electromagnetic probe is needed to control the initial condition for hadronization precisely.

Hard processes and hadron structure

❖ Lepton-Lepton collisions

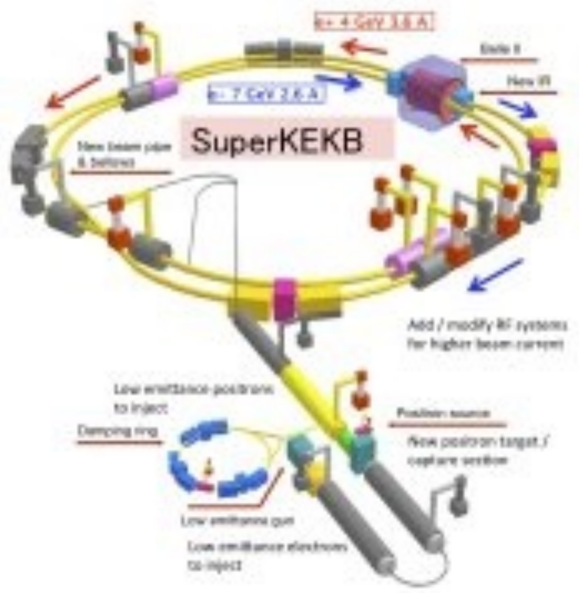

$e^+ + e^- \rightarrow h + X$

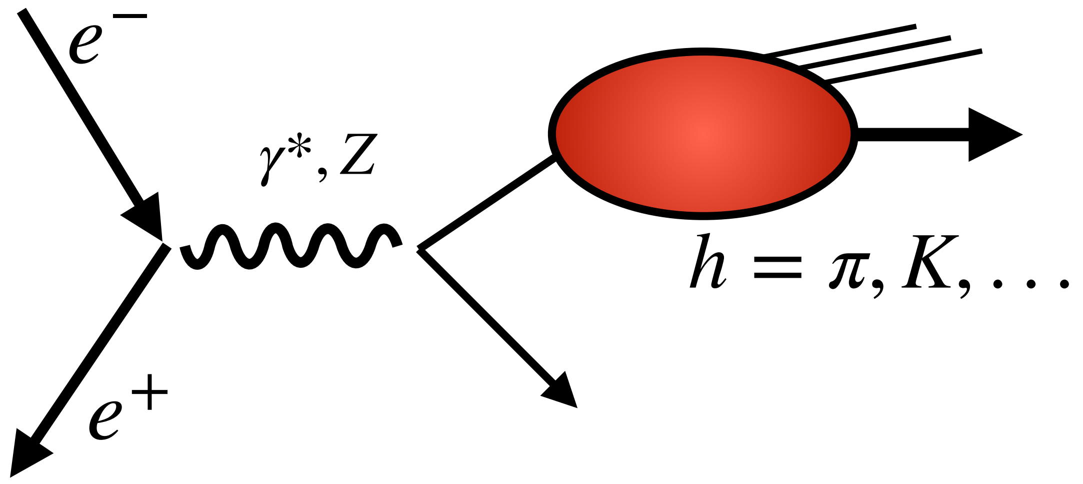

- No hadron in the initial state.
- Hadrons emerge from energetic particles in vacuum.
- Not ideal to explore hadron structure.

❖ Hadron-Hadron collisions

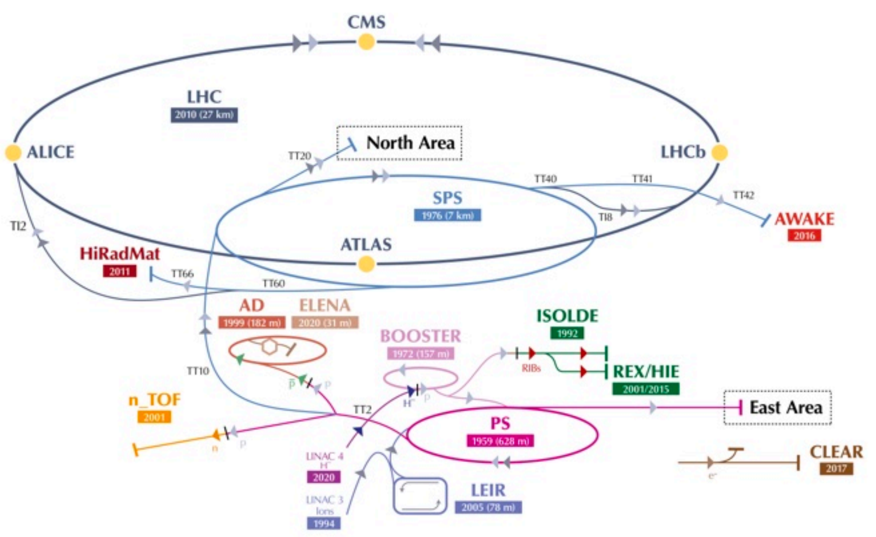

$p + p \rightarrow h + X$

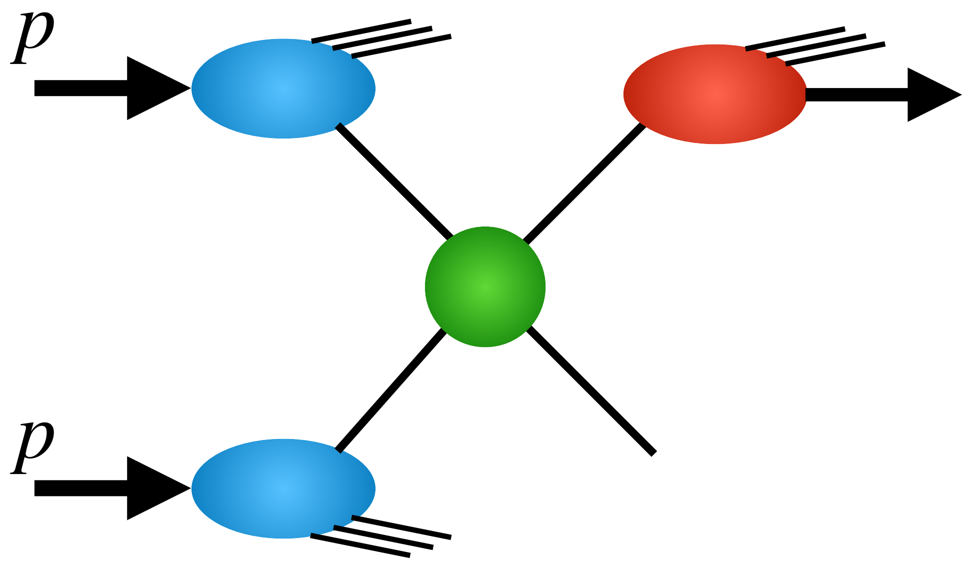

- Hadron structure in the initial state can be studied, but hadrons can be produced.
- Nuclear targets and polarized proton are available.
- There are collision-induced effects.

❖ Lepton-Hadron collisions

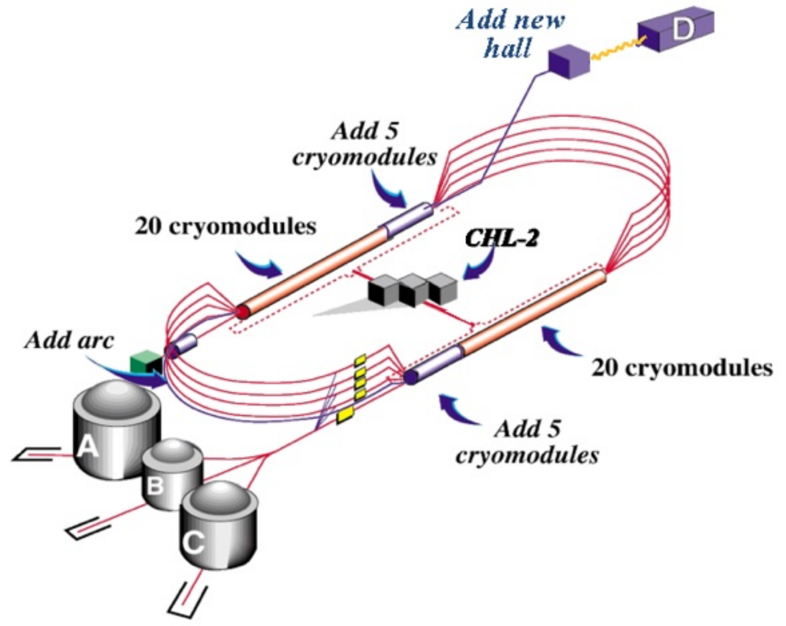

$e + p \rightarrow e' + h + X$

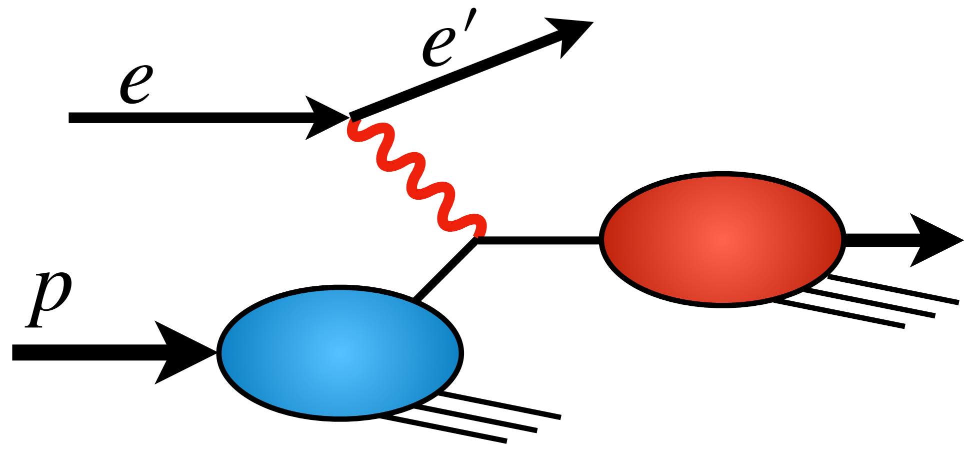

- Beam hadron can be broken or stay intact.
- Hadron tomography with high precision.
- Nuclear and polarized targets are available.
- Cleaner than hadron-hadron.

Luminosity: EIC vs. Other experiments

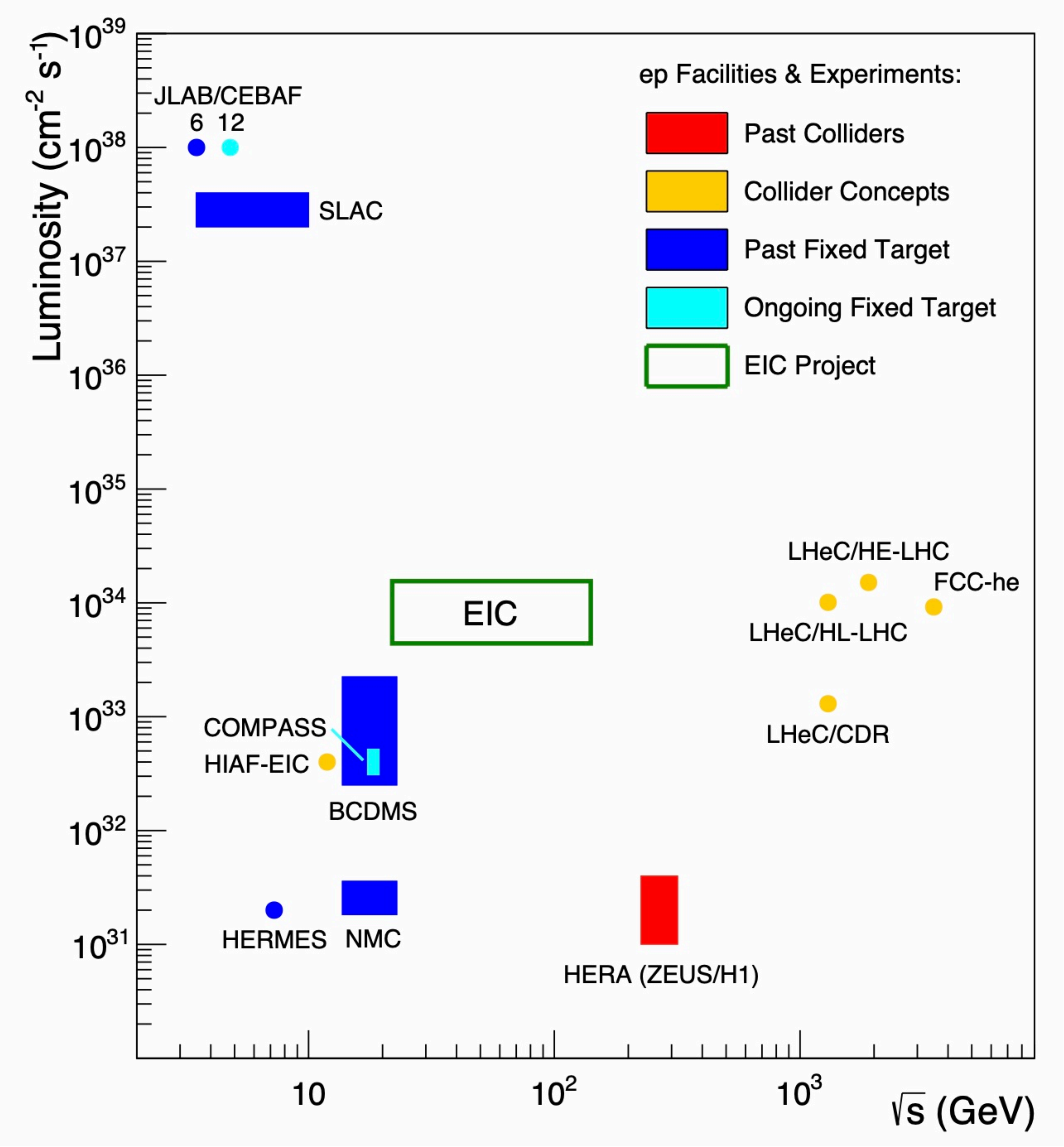

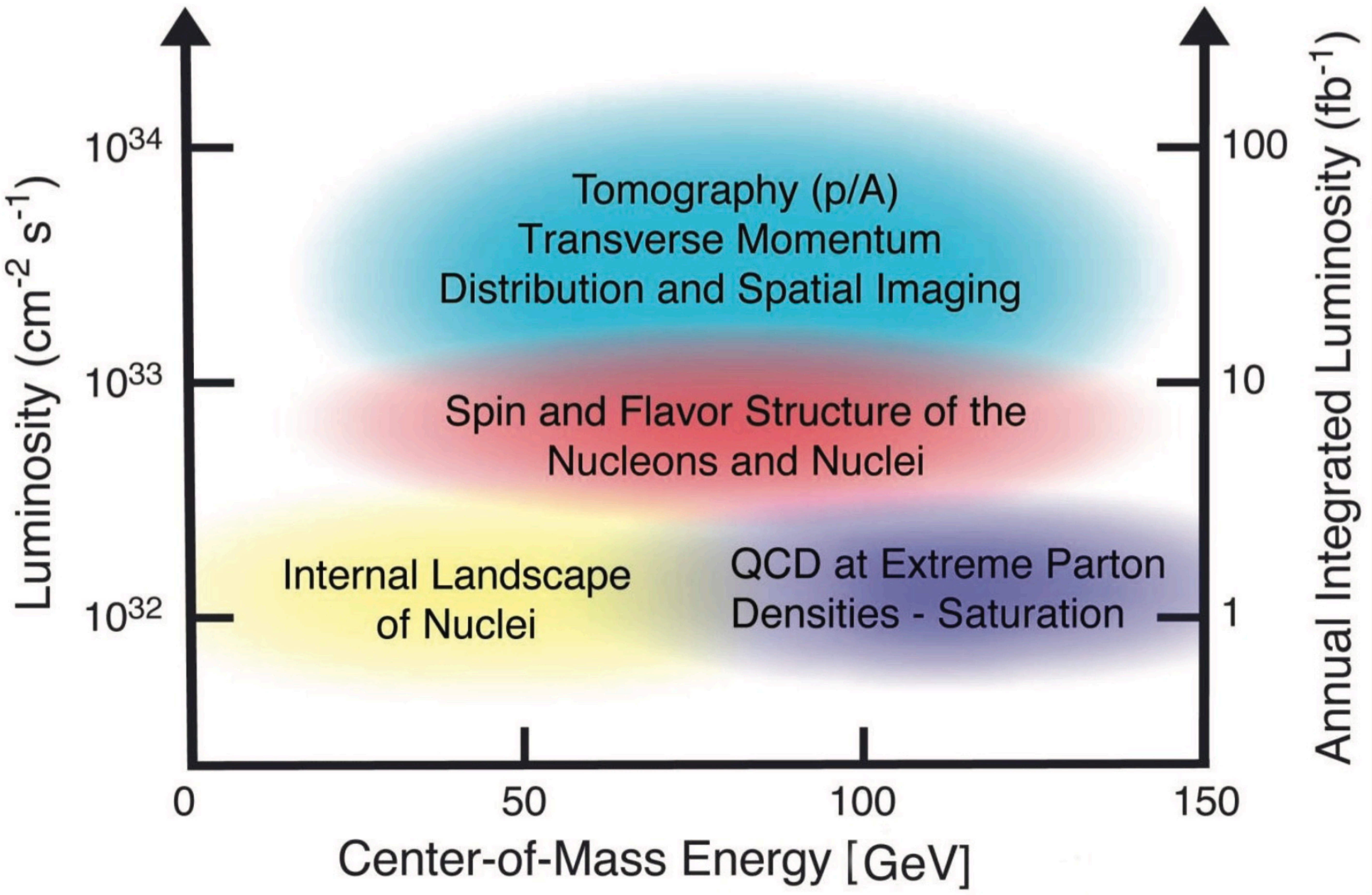

Different categories of processes at EIC

Neutral-current Inclusive DIS: $e + p/A \longrightarrow e' + X$; for this process, it is essential to detect the scattered electron, e', with high precision. All other final state particles (X) are ignored. The scattered electron is critical for all processes to determine the event kinematics.

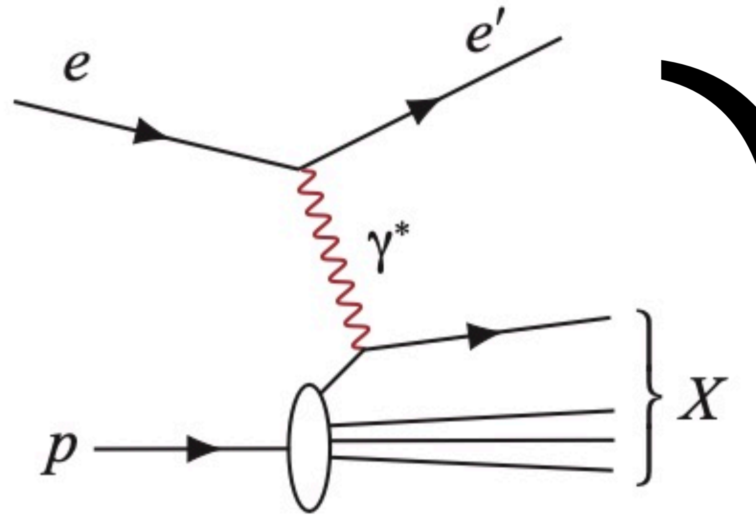

Charged-current Inclusive DIS: $e + p/A \longrightarrow \nu + X$; at high enough momentum transfer Q^2, the electron-quark interaction is mediated by the exchange of a $W^{\pm}$ gauge boson instead of the virtual photon. In this case the event kinematic cannot be reconstructed from the scattered electron, but needs to be reconstructed from the final state particles.

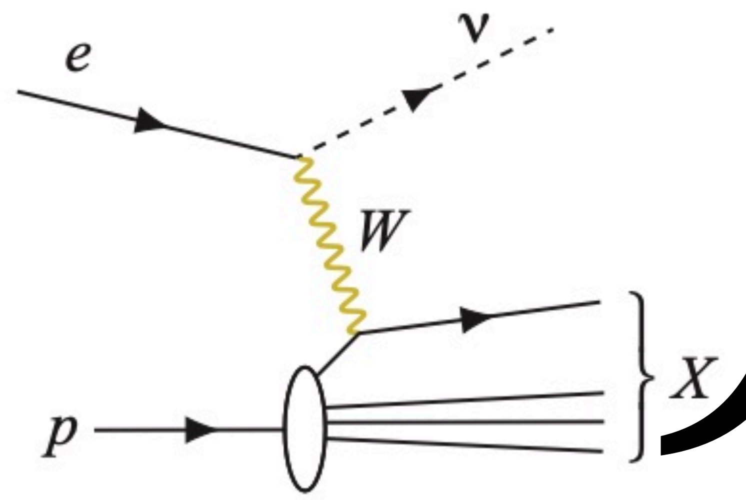

Modern Rutherford's scattering

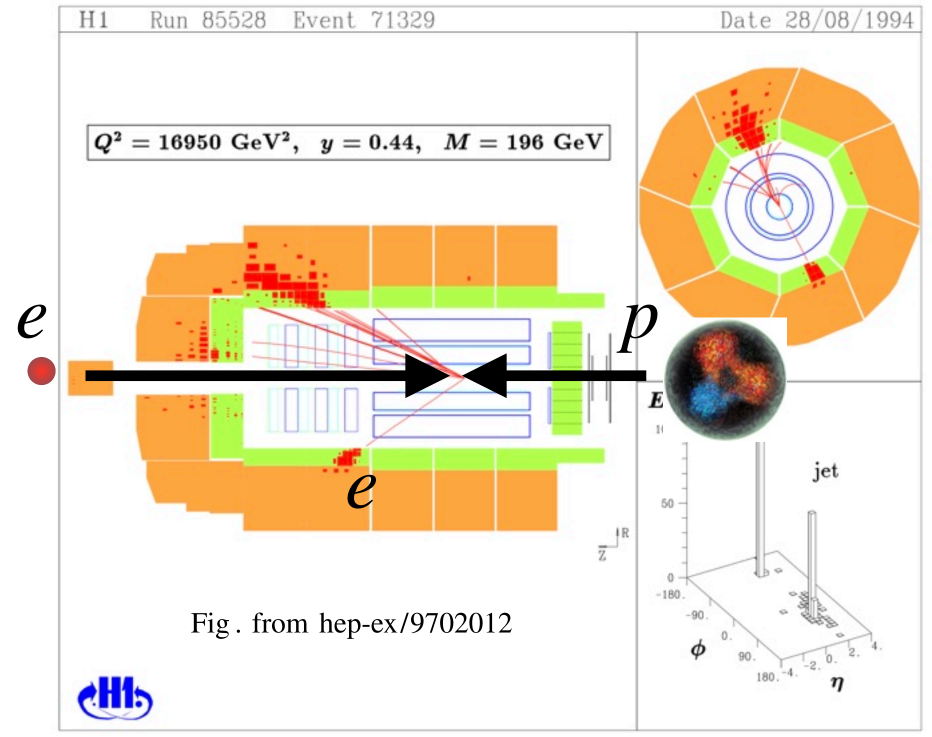

1D momentum distribution

Semi-inclusive DIS: $e + p/A \longrightarrow e' + h^{\pm,0} + X$, which requires measurement of *at least one* identified hadron in coincidence with the scattered electron.

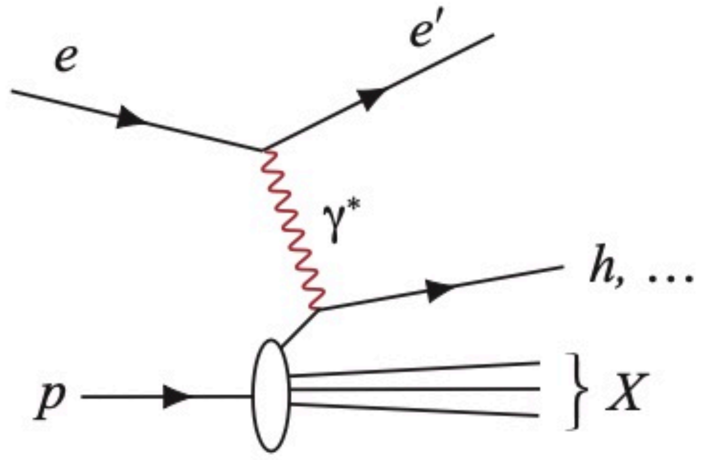

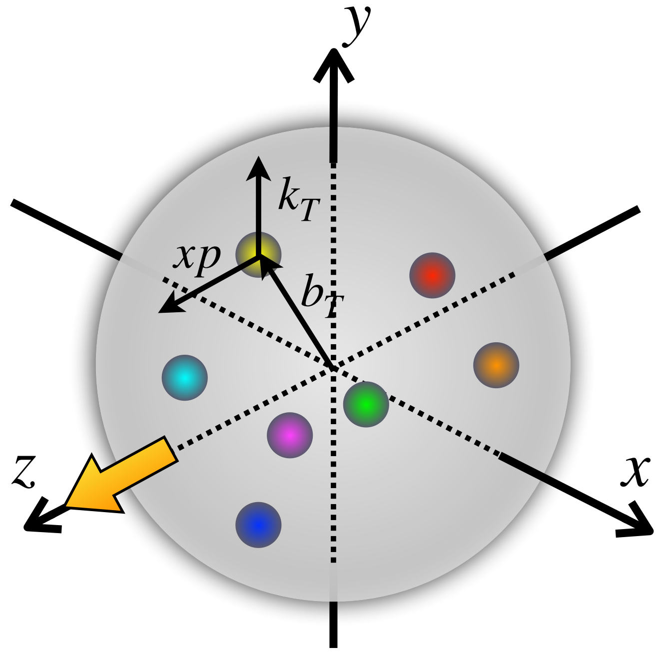

Parton's confined motion

Exclusive DIS: $e + p/A \longrightarrow e' + p'/A' + \gamma/h^{\pm,0}/VM$, which require the measurement of *all* particles in the event with high precision.

J/ψ, Υ

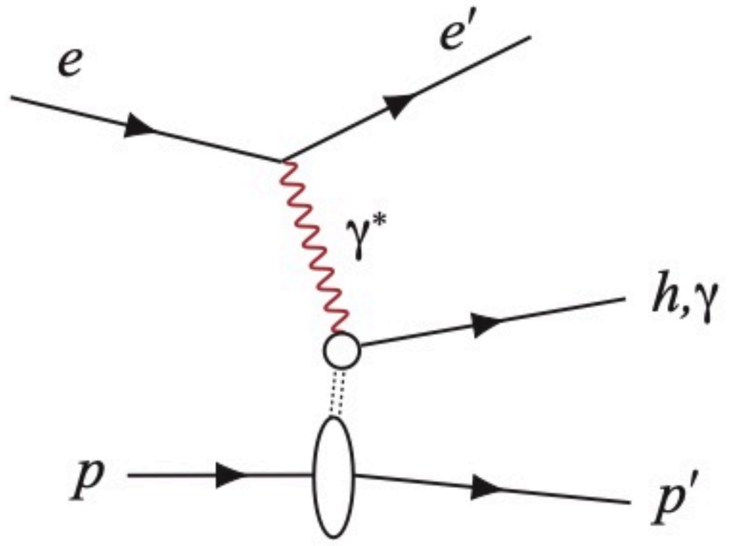

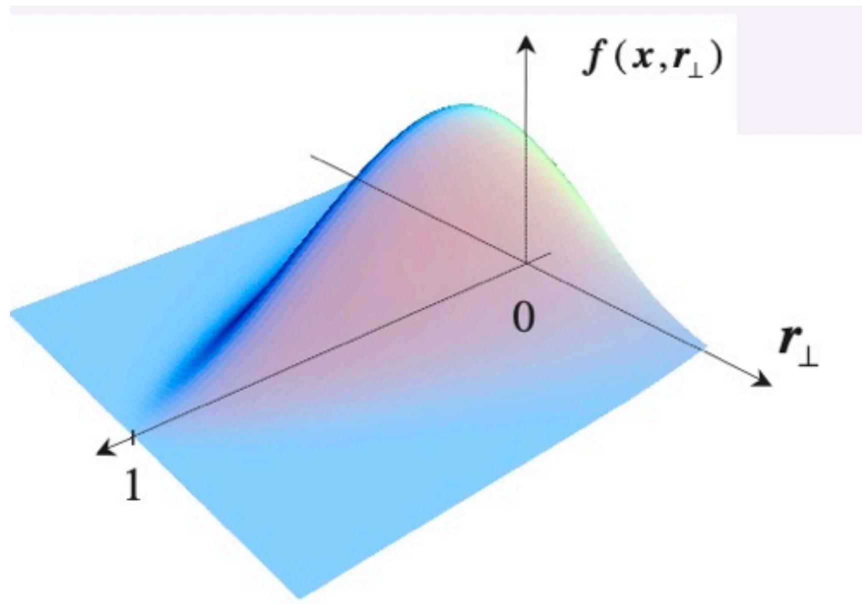

Parton's spatial distribution